Studies on Transition Metal Macrocyclic Complexes

Alan J. Holder

Ph.D. Thesis

University of Edinburgh

1987

To my Mother and Father

Acknowledgements

I would deeply like to thank my supervisor, Dr. M. Schroder for his invaluable help and encouragement throughout the project. I would also like to thank Dr. T.I. Hyde for his assistance in the running of esr spectra and electrochemical data. I am very grateful to Dr. A.J. Blake and Dr. R.O. Gould who performed all the crystallographic work in the project. I would like to thank Drs. S.G.D. Henderson, A.J. Lavery and all who have contributed advice and encouragement throughout the project. Additionally I would like to thank Mr. J. Millar and Mr. L. Bell for running ^{1}H n.m.r. spectra, Mr. A. Taylor and Miss E. Stevenson for mass spectra and Mrs. E. McDougall for elemental analyses. I am indebted to the University of Edinburgh for the use of facilities and to S.E.R.C. for financial support. I would also like to thank Mrs. Christian Ranken for typing the thesis.

Finally I am deeply indebted to Dr. Tony Stephenson who, as my supervisor before his tragic early death last year, was the source of my inspiration in Chemistry. Tony's qualities of enthusiasm and humanity were a byword both within and outside the University, and his loss is irreplaceable. Hopefully the spirit by which he lived and worked will remain with those of us who knew him for the rest of our lives.

Abstract

Chapter 1

The general aims of the project are introduced and a survey of the relevant background literature to the project given.

Chapter 2

The synthesis, structure and electrochemistry of the homoleptic thioether macrocyclic complex cation $[Pt(L^1)_2]^{2+}$ (L^1 = 1,4,7-trithiacyclononane) are described. A single crystal X-ray diffraction study of $[Pt(L^1)_2](PF_6)_2$ reveals an unusual pentaco-ordinate geometry for $[Pt(L^1)_2]^{2+}$ due to an apical interaction of one of the sulphur atoms ($Pt\text{-}S_{ax}$ = 2.885Å) to the 'PtS_4' equatorial plane ($Pt\text{-}S_{eq}$ = 2.25-2.30Å). Electrochemical studies upon $[Pt(L^1)_2]^{2+}$ in acetonitrile reveal a chemically reversible one electron oxidation ($E_{\frac{1}{2}}$ = +0.385V vs Fc/Fc^+). Either controlled potential electrolysis or chemical oxidation (70% $HClO_4$) leads to the formation of the d^7 $[Pt(L^1)_2]^{3+}$ cation which is characterised by esr and electronic spectroscopy. Further oxidation of $[Pt(L^1)_2]^{3+}$ to $[Pt(L^1)_2]^{4+}$ in 70% $HClO_4$ occurs over an extended time.

The synthesis and electrochemistry of the related macrocyclic thioether systems $[Pt(L^2)]^{2+}$ and $[Pt(L^3)]^{2+}$ (L^2 = 1,4,8,11-tetrathiacyclotetradecane; L^3 = 1,4,7,10,13,16-hexathiacyclooctadecane) are reported. The preparation and reactions of $[Pt(L^1)Cl_2]$ are also described.

Chapter 3

The synthesis, structure and electrochemistry of $[Pd(L^1)_2]^{2+}$ are described. A single crystal X-ray diffraction study of $[Pd(L^1)_2](PF_6)_2$ reveals a novel distorted octahedral geometry for $[Pd(L^1)_2]^{2+}$ due to significant apical interactions of two sulphur donors (Pd-S_{ax} = 2.952Å) to the 'PdS_4' square plane (Pd-S_{eq} = 2.311, 2.332Å). Electrochemical studies upon $[Pd(L^1)_2]^{2+}$ in acetonitrile reveal a chemically reversible one electron oxidation ($E_{\frac{1}{2}}$ = +0.605V). Either controlled potential electrolysis or chemical oxidation (70% $HClO_4$) yields the stable d^7 $[Pd(L^1)_2]^{3+}$ cation which is characterised by esr and electronic spectroscopy. A single crystal X-ray diffraction study of $[Pd(L^1)_2](H_3O)$-$(ClO_4)_4 . {}^3H_2O$ shows the $[Pd(L^1)_2]^{3+}$ cation to exhibit a Jahn Teller distorted octahedral geometry (Pd-S_{ax} = 2.5448Å, Pd-S_{eq} = 2.3558, 2.3692Å), in accord for a low spin d^7 species.

Both $[Pd(L^1)_2]^{2+}$ and $[Pd(L^2)]^{2+}$ show reduction chemistry to give the transient d^9 species $[Pd(L^1)_2]^{+}$ and $[Pd(L^2)]^{+}$ respectively. The chemistry of $[Pd(L^3)]^{2+}$ and $[Pd(L^1)Cl_2]$ is also described, and the single crystal X-ray structures of $[Pd(L^2)](PF_6)_2$ and $[Pd(L^1)Cl_2]$ reported.

Chapter 4

The synthesis, structure and electrochemistry of $[Rh(L^1)_2]^{3+}$ are described. A single crystal X-ray diffraction study of $[Rh(L^1)_2](PF_6)_3$ shows the expected

octahedral geometry for the complex cation (Rh-S = 2.3329Å). Electrochemical studies upon $[Rh(L^1)_2]^{3+}$ in acetonitrile reveals two chemically reversible one electron reductions ($^1E_{\frac{1}{2}}$ = -0.71V, $^2E_{\frac{1}{2}}$ = -1.08V) assigned as Rh(III)/Rh(II) and Rh(II)/Rh(I) couples respectively. The $[Rh(L^1)_2]^{2+}$ cation is investigated by esr spectroscopy. Reactions of $[Rh_2(CO)_4Cl_2]$ and $[Rh_2(C_2H_4)_4Cl_2]$ with L^1 are also described.

Chapter 5

A reinvestigation of the electrochemistry of $[Ni(L^1)_2]^{2+}$ is undertaken and the $[Ni(L^1)_2]^{3+}$ and $[Ni(L^1)_2]^{+}$ species, obtained via controlled potential electrolysis, are characterised by esr spectroscopy.

The preparation of $[Cu(L^1)(CH_3CN)]^{+}$ is described. The complex cation gives stable adducts with PPh_3 and $AsPh_3$ and the single crystal X-ray structure of $[Cu(L^1)(AsPh_3)](ClO_4)$ is reported.

Chapter 6

The preparation of exodendate macrocyclic complexes of dirhodium carboxylates $[Rh_2(O_2CR)_4]$ are described. The 1:1 adducts $[Rh_2(O_2CR)_4(cyclam)]_n$, 3:2 adducts $[(Rh_2(O_2CR)_4)_3(L)_2]_n$ (L = L^1, L^4, L^5) and 2:1 adducts $[(Rh_2(O_2CR)_4)_2(L)]_n$ (L = L^2, tmc) have been characterised for a variety of carboxylates (L^4 = 1,4,7-triazacyclononane, L^5 = 1,4,7-trimethyl-1,4,7-triazacyclononane, tmc = tetramethylcyclam). These structures are in accord for exodentate co-ordination

of the macrocycles to two, three and four separate metal centres respectively.

Chapter 7

Reactions of the tetraaza macrocycles cyclam and H_2L (tetramethyldibenzotetraaza-annulene) with the binuclear multiply metal-metal bonded species $[Mo_2Cl_8]^{4-}$ $[Mo_2(O_2CMe)_4]$, $[Ru_2(O_2CMe)_4Cl]$ and $[Os_2(O_2CR)_4Cl_2]$ are described.

A reinvestigation of the reaction of $Mo(CO)_6$ and H_2L to give $[Mo(CO)_4(H_2L')]$ is undertaken. The single crystal X-ray diffraction study of $[Mo(CO)_4(H_2L')]$ confirms that migration of a proton from an amine to one of the diiminato rings has occurred.

Contents

List of Tables and Figures

CHAPTER 1

Introduction

1 Introduction

1.1 Background to project

Macrocyclic systems are characterised by their high degree of kinetic and thermodynamic stability,[1] and by their ability to stabilise a wide range of transition metal oxidation states.[2] Macrocyclic systems based on the tetrapyrrole unit are widely distributed in nature and are of substantial importance in life.[3] In such systems four of the co-ordination sites of the metal are bound by the macrocyclic ligand, leaving one or two axial sites to participate in substrate binding and activation, often involving a redox process. Examples of the role of macrocyclic complexes *in vivo* include oxygen uptake and transport (Fe-haemoglobin and myoglobin)[4], election carrier systems (Fe-cytochromes)[5], substrate modification (Co-vitamin B_{12})[6] and light harvesting (Mg-chlorophyll).[7] In these and other natural systems the efficiency of these systems is due not only to the metal/tetrapyrrole unit, but also the tertiary protein structure around the macrocyclic unit.[8]

Since the 1960's considerable effort has been made to mimic the behaviour of these natural macrocyclic systems by synthetic macrocyclic systems.[9] Such systems are of greatest potential applicability as catalysts in the activation and rearrangement of small molecule substrates.[10] Synthetic macrocyclic complexes are also ideal in the study of a range of transition metal oxidation states over which the macrocyclic unit remains intact.[11] In addition to substantial

work upon synthetic porphyrin and related systems (eg H_2OEP,[12] etioporphyrin,[12] phthalocyanines[13]), a large amount of work has now been carried out upon non porphyrin saturated or unsaturated tetraaza systems such as cyclam (1)[14] and the diimine system (2).[15]

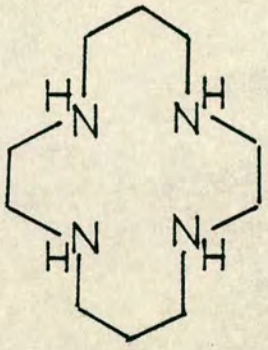

(1)

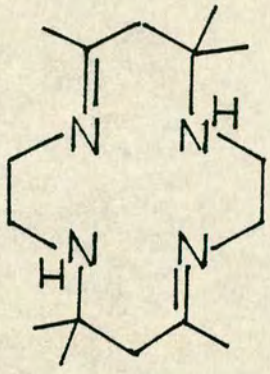

(2)

The observation of both a higher kinetic and thermodynamic stability of macrocyclic complexes relative to analogous non macrocyclic systems was first described by Margerum and Cabbiness,[1] and termed the 'Macrocyclic Effect'. The origin of this effect has excited much study and controversy. The kinetic stability of macrocyclic complexes relative to non macrocyclic analogues has been well characterised in both tetraaza[16] and tetrathia systems.[17] Formation rate constants and particularly dissociation rate constants are found to be substantially depressed in macrocyclic systems, as illustrated in the kinetic study of the Cu^{2+} systems below (3).[16]

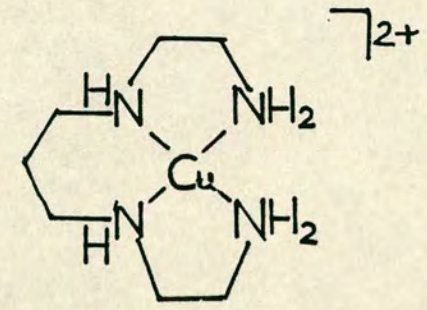

$K_f(M^{-1}s^{-1})$ $K_d(s^{-1})$

8.9×10^4 4.1

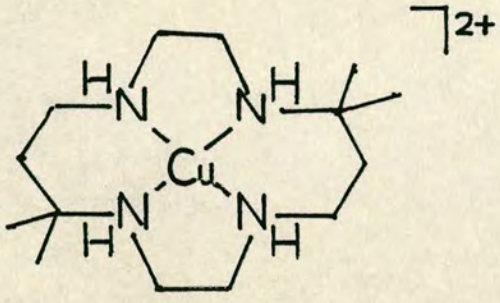

5.8×10^{-2} 3.6×10^{-7}

(3)

The most cogent explanation of the kinetic macrocyclic effect has been proposed by Busch.[18] According to Busch, the rate of detachment of a macrocyclic ligand from a metal centre is substantially depressed since a strain must occur in the ring system upon weakening of a co-ordinative bond. By contrast such a weakening can occur in an open chain ligand without this strain, as a consequence of the distortion not being transmitted to the rest of the ligand. The ligand thus can simply unzip from the metal centre, starting at one end and finishing at the other. In the macrocyclic system the constraining influence of the ring was termed as 'multiple juxtapositional fixedness' (MJF) and is illustrated below (4).

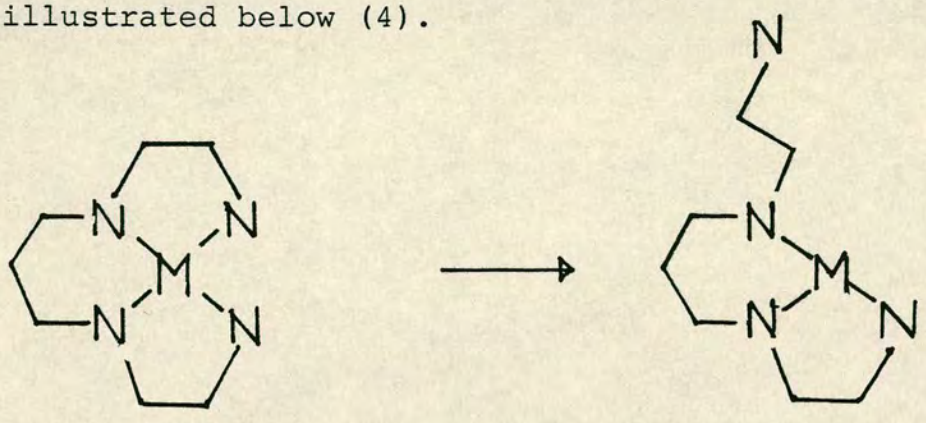

(4)

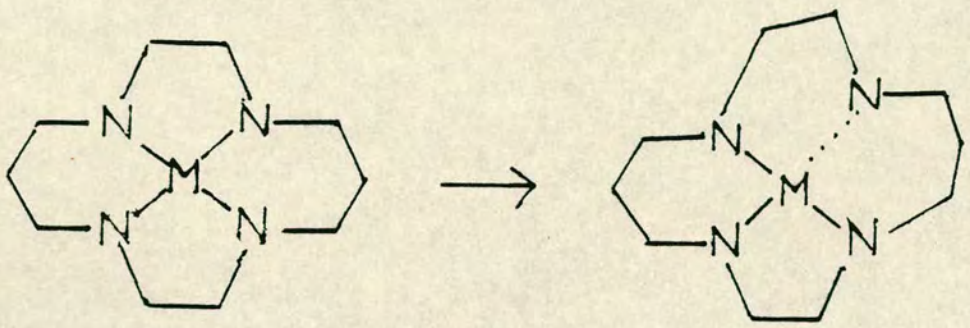

(4)

By consideration of the equilibrium (5).

$$M^{2+}(aq) + L \rightleftharpoons ML^{2+} \qquad (5)$$

the forward rate, $K_f[M^{2+}][L]$ equals the reverse rate, $K_d[ML^{2+}]$ and the stability constant $K_1 = K_f/K_d$. Depression in K_d leads then to higher thermodynamic stability constants for macrocyclic complexes, and typically these are of six to seven orders of magnitude larger than for analogous non macrocyclic systems.[19]

A purely thermodynamic approach in explaining the larger values of stability, or formation constants for macrocyclic systems is more challenging than an explanation of thermodynamic stability as a consequence of kinetic inertness.

The stability constant K for a macrocyclic complex is related to $\Delta G_f = \Delta H_f - T\Delta S_f$. For the macrocyclic system, the additional stability relative to the non macrocyclic system

has been ascribed primarily to either an entropic or enthalpic term, or to a combination of these.[20]

Common to both macrocyclic and related n dentate open chain systems is a stabilising entropy driven 'chelate' term[21] (6) as a consequence of increasing the number of particles in solution on complexation.

$$M(H_2O)_n^{x+} + L \rightarrow ML^{x+} + nH_2O \qquad (6)$$

However for the favourable metathesis reaction (7) this approach is no longer valid (L_m = macrocyclic ligand L = open chain ligand).

$$ML^{x+} + L_m \rightarrow ML_m^{x+} + L \qquad (7)$$

as the number of particles in solution remains the same.

Studies by Margerum *et al.*[19] upon Ni^{2+} complexes of cyclam (1), Me_2 cyclam (8) and 2-3-2-tet (9) showed that

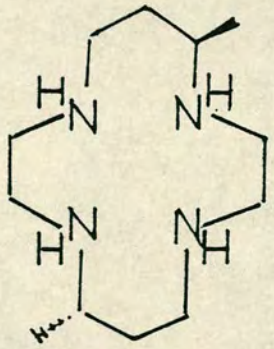

(8)

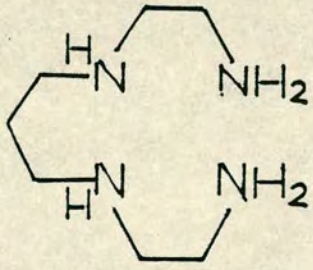

(9)

for the macrocyclic complexes the enthalpy term was dominant in the stabilisation primarily as a consequence of the ligand solvation energies, the free primary amine 2,3,2 tet having a much higher solvation energy than the

secondary macrocyclic amines. Detailed studies by Clay *et al.*[22] evaluated the thermodynamic terms not just for metal complexes but also for free ligands in a wide variety of macrocyclic tetraaza systems led to the conclusion that an additional entropy term contributed to the macrocyclic effect. Although the macrocyclic effect is primarily enthalpy driven (via differences in solvation energies for the ligands in a metathesis reaction), an additional favourable entropy term is also present probably arising via translational factors.

In a constrained macrocycle the internal degrees of freedom are severely restricted relative to a linear system. On binding to metal centre however both systems are now highly restricted so the net loss in translational entropy is substantially greater on binding for the open chain ligand. It is not yet entirely clear whether an enthalpic contribution - via increased metal→ligand bond strength also plays a role in the origin of the macrocyclic effect.[23]

The high kinetic stability of macrocyclic complexes is central to much current work upon these systems. The restriction of certain co-ordination sites about the metal enables substrate uptake and rearrangement to occur at specific labile sites, and may additionally involve redox processes at the metal centre without break up of the metal macrocycle moiety, which forms the basis of the catalytic behaviour of many of these systems. The activation of small molecule substrates such as CO,[24] CO_2,[25] O_2 [26] and H_2 [27], and the potential of a fuel cell based on the four electron

reduction of O_2 to H_2O [28] have been studied with a variety of porphyrin and non porphyrin macrocyclic complexes.

Recently it has been shown that facially co-ordinating tridentate ligands such as 1,4,7-triazacyclononane[29] and 1,4,7-trithiacyclononane[30] also exhibit a high degree of kinetic and thermodynamic stability. It is with these small ring systems, in particular 1,4,7-trithiacyclononane (L^1) with which the majority of this project is concerned.

1.2 Aims of work

The major aim of this work was to synthesise a variety of platinum metal complexes of the trithia macrocycle 1,4,7-trithiacyclonone (L^1) (10).

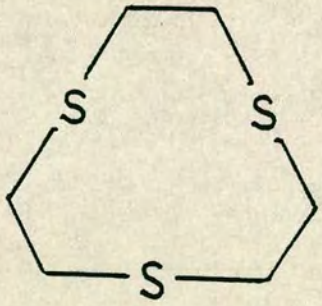

(10)

An investigation of the bis-$[M(L^1)_2]^{n+}$ species, in particular their structural and redox properties, for platinum (Chapter 2), palladium (Chapter 3) and rhodium (Chapter 4) is highly desirable. For these metals, in which a variety of stereochemical modes may occur in different oxidation states, the high degree of co-ordinative flexibility of L^1 coupled with the expected high kinetic stability of the complexes should yield a rich electrochemistry. The ligand L^1 which can formally act as a π acceptor or π donor may enable the stabilisation of both d^7 and d^9 oxidation states, which are

rarely observed in mononuclear platinum metal complexes. A comparative study of $[Pt(L^2)]^{2+}$, $[Pt(L^3)]^{2+}$ (Chapter 2), $[Pd(L^2)]^{2+}$, $[Pd(L^3)]^{2+}$ and $[Pd(L^4)_2]^{2+}$ (Chapter 3) is also made in order to ascertain the importance of stereochemistry in relation to redox behaviour for platinum metal centres. (L^2 = 1,4,8,11-tetrathiacyclotetradecane (11), L^3 = 1,4,7,10,13,16-hexathiacyclooctadecane (12), L^4 = 1,4,7-triaza-cyclonone (13)).

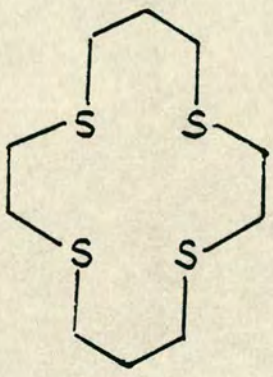

(11)

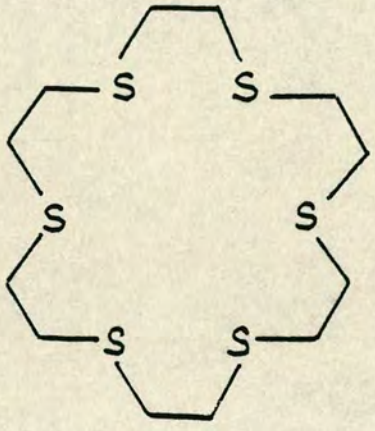

(12)

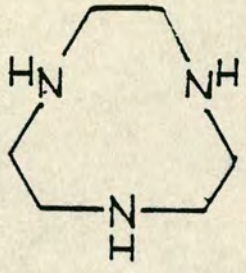

(13)

In Chapter 5 the electrochemistry of $[Ni(L^1)_2]^{2+}$, studied by Wieghardt *et al.*[31] is reinvestigated to determine the nature of the redox processes occurring in this system. Additionally a study is undertaken upon the $[Cu(L^1)]^{+}$ moiety which may mimic the thia co-ordination of the active sites in blue copper proteins such as azurin and plastocyanin.[32] The second main area of study in this project concerns the reaction of binuclear metal-metal bonded complexes with macrocyclic ligands. Binuclear metal-metal bonded species react in three general ways: (a) formation of axial adducts, (b) equatorial exchange, with retention of the metal-metal bond, or (c) exchange leading to disruption of the metal-metal bond.[33]

Reaction of a variety of tri and tetradentate macrocyclic ligands with the $[Rh_2(O_2CR)_4]$ moiety was undertaken to try and obtain axial adducts in which the macrocyclic ligands are bound in an *exo* manner. Information about the stoichiometry and structures of such complexes would be of value in understanding the conformational preferences of the various macrocyclic ligands (Chapter 6).

The synthesis of $[M_2L_2]^{n+}$ systems via equatorial exchange of a variety of multiply metal-metal bonded systems with tetraaza macrocyclic ligands such as cyclam and H_2L (14),

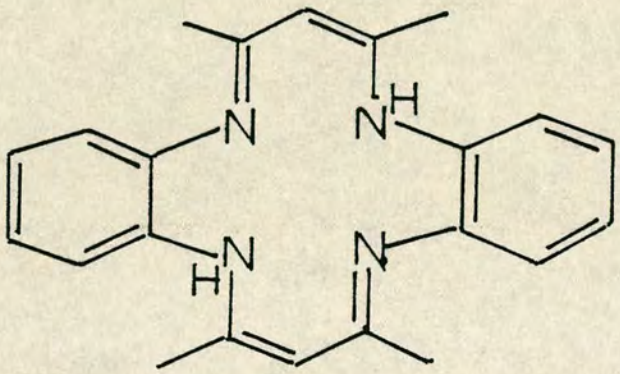

(14)

may result in significant structural, redox and magnetic properties being observed. These systems may give valuable information on the nature of metal-metal bonding, as well as being of potential applicability in catalysis (Chapter 7).

1.3 Recent developments in the study of tridentate macrocyclic ligands

1.3.1 1,4,7-Triazacyclononane

1,4,7-Triazacyclononane (L^4) was first synthesised in 1972 [34] and in subsequent work has been characterised as a

strong, tridentate facially co-ordinating ligand. Subsequent to the initial characterisation of the octahedral complexes $[M(L^4)_2]^{n+}$ (M = Co(III)[34], Ni(II)[35-37], Cu(II)[35]) by Zompa *et al.* a systematic study of the redox properties of a number of first row complexes $[M(L^4)_2]^{n+}$ (M = Cr-Ni) was undertaken by Wieghardt *et al.*[38] These complexes were characteristic by their very high kinetic stability in aqueous solution over a wide pH range, and in the observation of a strong ligand field generated by the triaza ligands. Electrochemical investigations upon these complexes showed reversible (Fe,Co), or quasi reversible (Cr,Mn,Ni) (II)/(III) couples in aqueous solution. In separate studies[39] the $[Cu(L^4)_2]^{2+}$ cation showed a partially reversible (II)/(III) couple, which became increasingly more reversible on lowering the temperature. The kinetic inertness of these systems enables the use of these systems in the study of outer sphere electron transfer reactions.

Many of the first row transition metal complexes $[M(L^4)_2]^{n+}$ have been structurally characterised. Octahedral co-ordination about the metal centre has been observed for Fe(II)[40] Fe(III)[40] Co(II)[41] and Ni(II)[36], but a departure from octahedral geometry was observed for the low spin d^7 $[Ni(L^4)_2]^{3+}$ [43] and d^9 $[Cu(L^4)_2]^{2+}$ [39,44] cations, as a consequence of a Jahn-Teller distortion.

The isolation and characterisation of the $[Ni(L^4)_2]^{3+}$ cation, by both esr spectroscopy,[43,45] and a single crystal X-ray diffraction study demonstrated the facility of the L^4 ligand to stabilise a variety of metal oxidation states, and conform to the stereochemical requirements of the metal centre.

Literature reports of second and third row transition metal complexes of type $[M(L^4)_2]^{n+}$ are less numerous. Both $[Rh(L^4)_2]^{3+}$ [46] and $[Ru(L^4)_2]^{2+}$ [47] have been synthesised by Wieghardt *et al.* and a reversible one electron oxidation (at +0.37V vs NHE) is quoted for the latter.[47] The structure and oxidation chemistry of $[Pt(L^4)_2]^{2+}$ has been reported.[48] The $[Pt(L^4)_2]^{2+}$ cation represented the first structurally characterised complex of L^4, in which the ligand is bidentate, to give overall a square planar geometry at the metal centre. Chemical oxidation of $[Pt(L^4)_2]^{2+}$ yielded the octahedral $[Pt(L^4)_2]^{4+}$ cation.

A large number of mono, and binuclear $M:L^4 = 1:1$ complexes have also been prepared. Both five co-ordinate $[M(L^4)X_2]$ [36,49] (M = Ni(II),Cu(II), X = Hal^-, NCS^-, NO_3^-) and six co-ordinate $[M(L^4)X_3]$ [46,47,50-52] (M = Co(III), Mo(III), Ru(III), Rh(III), X = hal^- $C_5Me_5^-$ NO_2^-) complexes have been reported. Similar complexes can also be obtained in many cases with related triaza macrocyclic ligands of larger ring size eg 1,4,7-triazacyclodecane and 1,5,9-triaza cyclododecane.[53,49] Binuclear complexes incorporating the $[M(L^4)]$ moiety have also been extensively studied. In these complexes the two $[M(L^4)]$ or closely related $[M(L^5)]$ moieties (L^5 = 1,4,7-trimethyl-1,4,7-triazacyclononane) are connected via bridging ligands. These bridging ligands are usually based on oxygen eg: oxo, hydroxyl, sulphate, carbonate or carboxylate. Two general structures (15),(16) usually result in which the bridging ligands may differ.

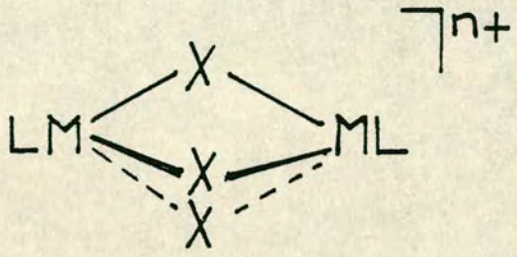

(15)

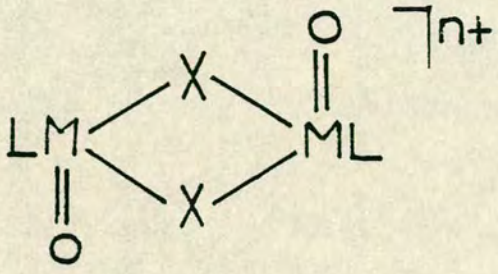

(16)

These complexes are generally redox active, and have been characterised for a variety of transition metal centres M = V[54,55] Cr[56] Mn[57] Fe[58] Co[56,59], Mo[51,60] Ru[47] and Rh[46,56].

Some of these systems are of possible biological significance. For example $[Fe_2(\mu\text{-}O)(\mu\text{-}O_2CMe)_2]^{2+}$ is an accurate model for the spin coupled di-iron centres in the metalloprotein hemerythrin,[162] and possibly in ribonucleotide reductase.[163] The electrochemically active Mn(II) analogue can serve as a model for the water oxidising metalloprotein photo-system II.[164] The bridging ligand need not be based on oxygen, and the complexes $[Ni_2(\mu N_3)_3(L^5)_2]$[61] and $[Cu_2(\mu HNCN)_2(L^5)_2]$[62] represent two recent examples in which the bridging ligand is based on nitrogen.

1.3.2 1,4,7-Trithiacyclononane

Unlike the majority of thio-ether complexes[63] the tridentate macrocycle 1,4,7-trithiacyclononane (L^1) was observed to bind very strongly to metal centres, generating

a high ligand field strength. The octahedral, or nearly octahedral $[M(L^1)_2]^{2+}$ cations (M = Ni(II),Co(II) and Cu(II)) were characterised by X-ray diffraction studies.[64] These complexes were observed to be stable to hydrolysis, in sharp contrast to other thio-ether systems, including complexes of 1,4,8,11-tetrathiacyclotetradecane (L^2)[65] and the larger ring analogue of L^1, 1,5,9-trithiacyclododecane.[66] Work upon L^1 was severely restricted owing to a lack of a high yield synthetic route to the macrocycle. In 1985 however Sellmann and Zapf[67] developed an elegant synthetic route based on a metal template reaction. The availability of the ligand has since spurred further work, notably by Wieghardt *et al.* An electrochemical study upon the bis complexes $[M(L^1)_2]^{2+}$ [31] (M = Fe,Co,Ni) showed a reversible or quasi-reversible one electron oxidation in each case. The oxidation waves (in acetonitrile vs Fc/Fc^+) occurred at a higher potential than for the corresponding $[M(L^4)_2]^{2+}$ systems[38] (in H_2O vs NHE) this being attributed to the softer nature of the thia macrocycle. Indeed doubt was expressed whether the oxidation for the Fe or Ni complexes were metal or ligand based, oxidation occurring at *ca.* +1.0V - the same potential as the (irreversible) oxidation of the free ligand L^1.[31] For $[Co(L^1)_2]^{2+}$ the oxidation however was clearly metal based, with the Co(II)/Co(III) couple occurring at -0.013V. Additionally,a chemically reversible reduction wave was observable, this was also assigned as metal based, to give the $[Co(L^1)_2]^+$ cation at $E_{\frac{1}{2}}$ = -0.86V. The absence of a

similar reduction for $[Co(L^4)_2]^{2+}$ reflects the 'harder' nature of the triaza macrocycle whereas the stabilisation of $[Co(L^1)_2]^{+}$ may indicate some π-acceptor behaviour of L^1. The species $[Co(L^1)_2]^{+}$ represented the first example of a d^8 cobalt complex containing a saturated ligand set.

Magnetic and spectral studies upon $[Co(L^1)_2]^{2+}$ indicated, in contrast to $[Co(L^4)_2]^{2+}$, that the complex was low spin,[31] suggesting an even higher ligand field strength for L^1, relative to L^4. A low spin d^7 complex ($t_{2g}^6 e_g^1$) would be expected to show a Jahn-Teller distortion from octahedral geometry, and this is indeed observed in the single crystal X-ray structure of the complex.[64] Surprisingly however this manifests itself as a tetragonal *compression* with two short, and four longer bonds being observed. This structure has been interpreted[68] in terms of a dynamic averaging, and, significantly, other related complexes showing a Jahn-Teller distortion eg $[Ni(L^4)_2]^{3+}$ [43], $[Cu(L^1)_2]^{2+}$ [64], $[Cu(L^4)_2]^{2+}$ [39,44], $[Co(L^3)]^{2+}$ [69], $[Cu(L^3)]^{2+}$ [70] (17) and $[Co(ttn)_2]^{2+}$ [69] (18) show the expected tetragonal elongation to octahedral geometry.

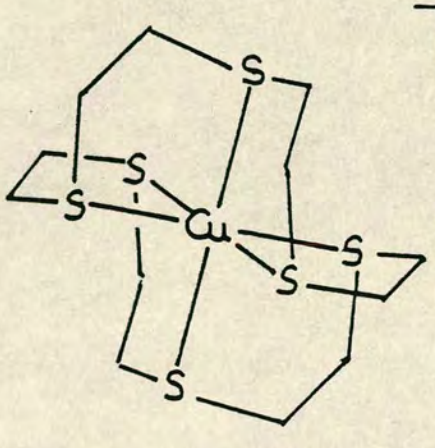

(17)

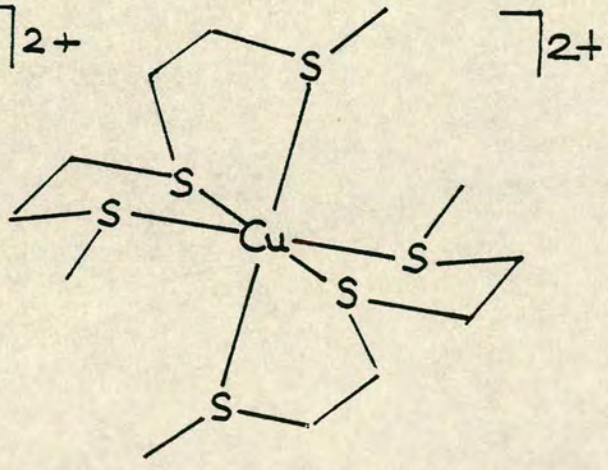

(18)

1.3.3 Other tridentate macrocyclic systems

In the rapidly expanding field of tridentate macrocyclic ligands, much work has centred upon derivatives of 1,4,7-triazacyclononane (L^4) in which the amine protons have been functionalised (19).

(19)

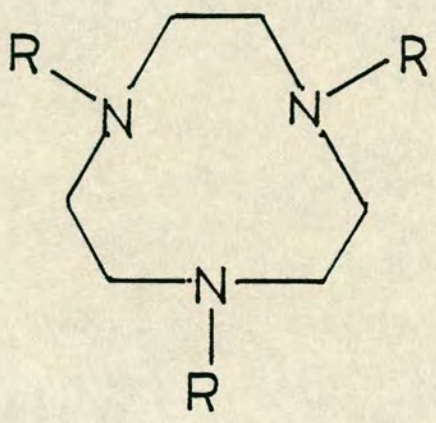

R = CH_3 [54-56,59,71]
CH_2CO_2H [72-76]
$CH_2CO_2C_2H_5$ [77]
$CH_2CH_2SO_3H$ [77]
CH_2CH_2OH [78]
$CH_2CH_2NH_2$ [79,80]
$CH_2PO_3H_2$ [81,82]
$CH_2PO(C_6H_5)_2$ [83-85]
$CH_2(2\text{-}C_6H_4N)$ [86]

1,4,7-Trimethyl-1,4,7-triazacyclononane (L^5) has been characterised in a large variety of both mono and binuclear 1:1 complexes. Mononuclear complexes $[M(L^5)X_3]^{n+}$ (X = hal^- or H_2O) have been characterised for V[55] Cr[56] Mn[71] Co[56] and In[87]. An interesting organometallic $[(C_5Me_5)Rh(L^5)]^{2+}$ [88] has also been recently characterised. Binuclear complexes of L^5 are essentially analogous to the L^4 complexes and have been discussed previously. In contrast both to L^1 and L^4, octahedral complexes of type $[M(L^5)_2]^{n+}$ cannot be synthesised due to the unfavourable steric interactions between methyl groups that would result in such species.

Work with other derivatives of L^4 centres upon their potential to act as hexadentate ligands. The tris (acetato)

derivative of L^4 is a representative example, and has recently been observed to stabilise Ni(III).[75] During the course of our work a square pyramidal Pd(II) complex of 1,4,7-tris(2-pyridylmethyl)-1,4,7-triazacyclononane was characterised.[86] The observed structure of this complex may be as a consequence of the π nature of the pyridyl groups.

Triaza macrocycles of ring size 10→16 have been successfully incorporated into a variety of metal centres (M = Co(III), Ni(II), Cu(II))[49,53,89]. For the 1:1 complexes $[M(L)]^{n+}$ the formation constants were observed to fall upon increasing the macrocycle ring size.[89]

In addition to tridentate macrocycles containing an N_3 or S_3 donor set, mixed donor atom tridentate macrocycles have also recently been synthesised (20).[90]

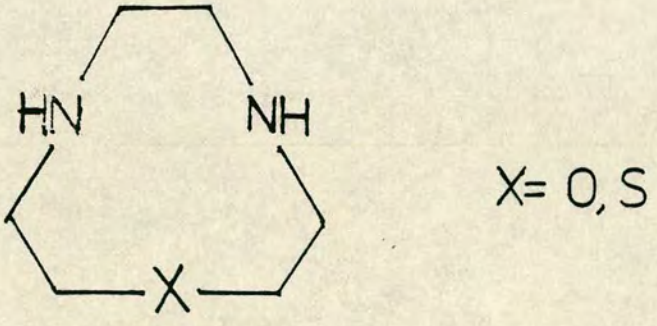

(20)

Extending the number of facially co-ordinating ligand donor sets should enable specific tailoring of complexes so as to optimise their redox and electronic properties.

The aromatic ligand (21) obtained via self condensation of o-aminobenzaldehyde in ethanol in the presence of Ni^{2+} [91] has been characterised in both 1:1 and 2:1 complexes $[M(L)X_3]$, $[M(L)_2]^{n+}$ (M = Co(III), Ni(II)) [92,93].

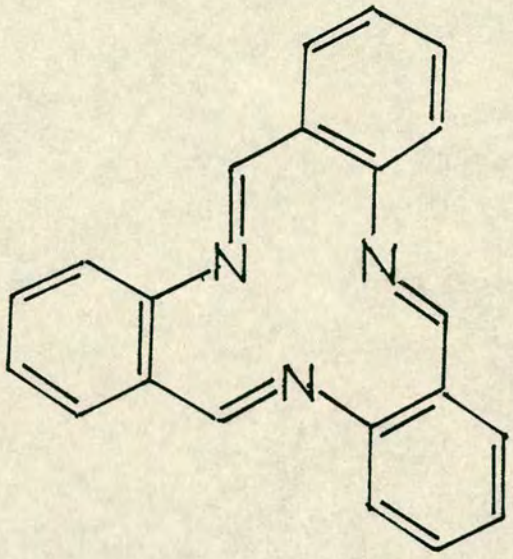

(21)

1.4 Binuclear metal-metal bonded systems

The interaction of tri and tetradentate macrocyclic ligands with binuclear metal-metal bonded systems forms the second part of this project. A variety of both porphyrin, and non porphyrin tetraaza macrocyclic complexes incorporating an unsupported metal-metal bond have been reported in the literature, many acting as precursors for highly reactive monomeric systems. Since the initial characterisation of the $[Re_2Cl_8]^{2-}$ ion,[94] and of $[Mo_2(O_2CMe)_4]$ [95] in which a quadruple bond between the metal atoms is postulated, complexes incorporating a metal-metal bond have rapidly multiplied in number.[96] The formation of a metal-metal multiple bond can be envisaged by overlap of the d orbitals of the metal centres (Figure 1.4.I) to give a σ orbital two π orbitals and two δ orbitals,[97] and the corresponding anti-bonding orbitals. One of the δ orbitals ($\delta d_{x^2-y^2}$) is essentially involved in ligand bonding,[98] so leaving four bonding, and four antibonding orbitals of metal bond character.

Figure 1.4.I Bond orbital scheme for the formation of multiply metal-metal bonded complexes M_2X_8, $M_2(L\text{-}L)_4$.

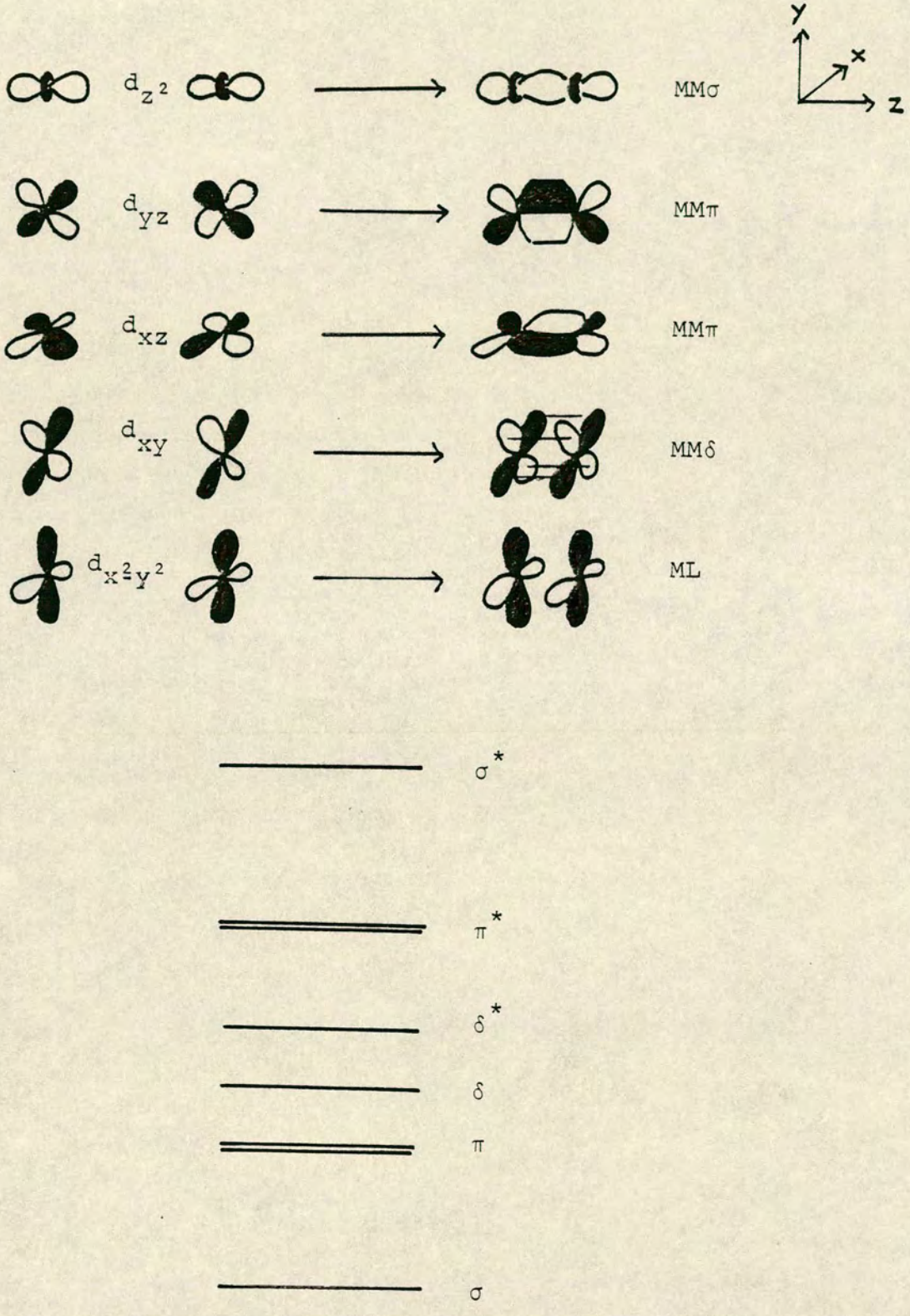

The relative energy of these orbitals is determined by their extent of overlap and on a simple qualitative picture ignoring ligand π bonding an order; $\sigma<\pi<\delta<\delta^*<\pi^*<\sigma^*$ [98] can be established for the metal based orbitals. In both $[Re_2Cl_8]^{2-}$ and $[Mo_2(O_2CMe)_4]$ (22,23) the total of 8 metal based electrons fill the bonding levels to give a quadruple bond.

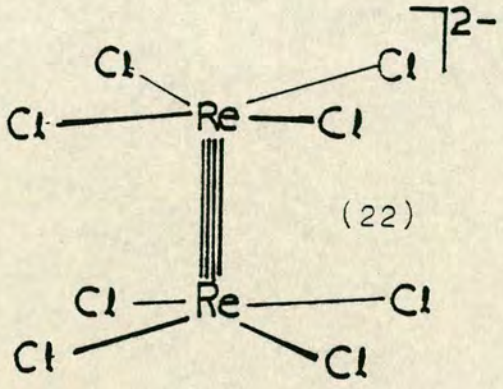

(22)

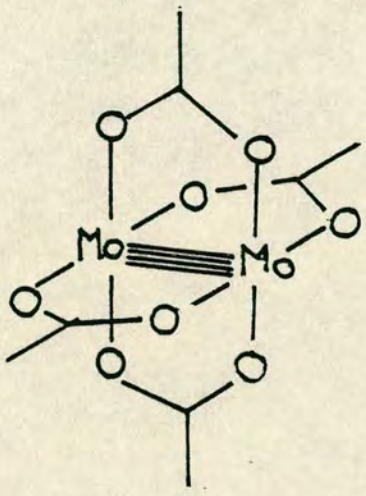

(23)

A reduction in metal-metal bond order is observed on addition or removal of electrons, so that $[Ru_2(O_2CMe)_4Cl]$, [99] an 11 electron system has a metal-metal bond order of 2.5 and $[Rh_2(O_2CMe)_4]$, a 14 electron system has a formal metal-metal bond order of 1. [100] The ordering of metal based orbitals may be influenced by an electronic interaction of the co-ordinating ligand. For instance in $[Ru_2(O_2CMe)_4Cl]$ the δ^* and π^* levels are reversed, and a quartet ground state ($\sigma^2\pi^4\delta^2\pi^*_{xz}{}^1\pi^*_{yz}{}^1\delta^{*1}$) is observed. [101]

Clearly there is the potential of forming complexes of the type $[M_2L_2]^{n+}$ containing an unsupported metal-metal bond where L is a tetradentate macrocyclic ligand, and during the course of this work the number of such systems reported in the literature has grown substantially.

Most extensive studies have centred upon porphyrin complexes $[M_2P_2]$ ($P = OEP^{2-}$, TPP^{2-}) (M = Ru(II)[102,103] Rh(II)[104]); however more recently the Os(II),[105] Mo(II)[106] and Ir(II)[107] systems have been investigated, and show analogous structure and reactivity. $[Ru_2(OEP)_2]$ can be regarded as representative of these systems showing a large number of insertion and binding reactions[103,105] (Figure 1.4.II). The related $[Rh_2P_2]$ systems can be regarded as a source of the [RhP]• free radical which can readily bind, and activate small molecule substrates such as H_2, O_2 and NO.[104,108] $[Ir_2(OEP)_2]$ has recently been shown to undergo alkene insertion and oxidative addition of alkyl C-H bonds.[107] While the porphyrin complexes described above are obtained via monomeric starting materials, the cofacial dimeric systems $[Ru_2L_2]^+$ [109] and $[Rh_2L_2]$ [109,110] (L^{2-} = dianion of (14)) may be generated directly from the metal-metal bonded tetracarboxylate systems via equatorial carboxylate exchange. $[Ru_2L_2]^+$ was observed to show a metal based oxidation to $[Ru_2L_2]^{2+}$ and also a reduction to $[Ru_2L_2]$.[109] Both $[Ru_2L_2]^+$ and $[Ru_2L_2]$ have been structurally characterised[110] with the reduced form showing a longer Ru-Ru bond, as expected on addition of an electron to an antibonding orbital.

The synthesis and characterisation of a variety of $[M_2L_2]^{n+}$ systems via reaction of binuclear metal-metal bonded species with tetraaza macrocyclic ligands such as cyclam (1) and H_2L (14), was undertaken in this project.

Although the predominant reaction mode of the majority of metal-metal bonded systems is equatorial ligand exchange,

Figure 1.4.II A summary of Collman's work on reactions of $Ru_2(OEP)_2$

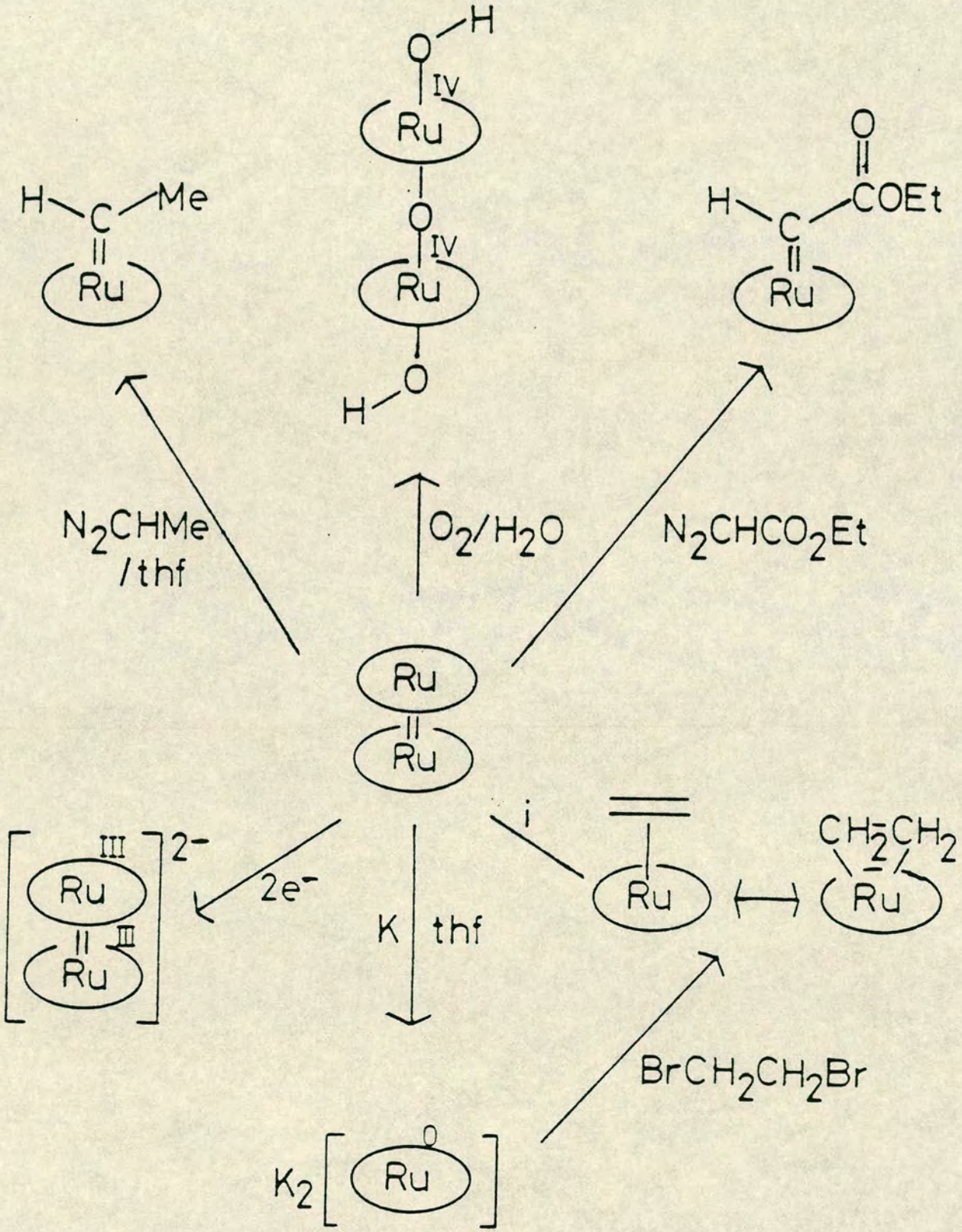

the well characterised $[Rh_2(CO_2R)_4]$ systems react via an axial interaction (24).[100]

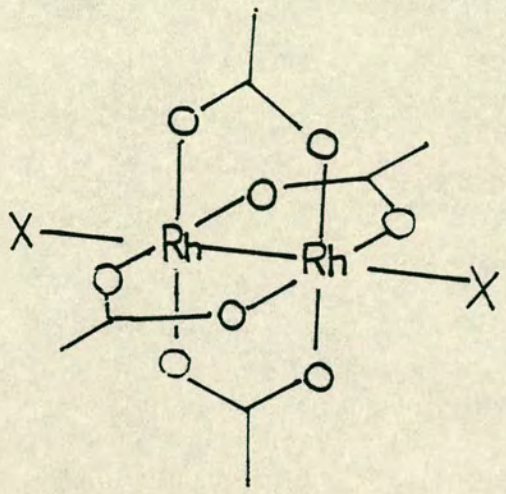

(24)

This leads to the possibility of observing exodentate binding of macrocyclic ligands at the axial sites.

Exodentate co-ordination of macrocyclic ligands is a rarely observed bonding mode in which the macrocycle binds to separate metal centres (25).

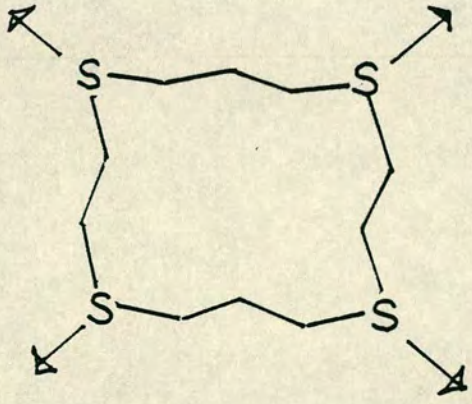

(25)

This mode of co-ordination (Figure 1.4.III) has so far only been reported for thioether macrocycles such as L^2(1,4,8,11-tetrathiacyclotetradecane)[111-113] and L^3(1,4,7,10,13,16-hexathiacyclooctadecane).[114] Significantly, in contrast to tetraaza macrocycles, L^2 shows an exo conformation

Figure 1.4.III Some exodentate-macrocyclic complexes

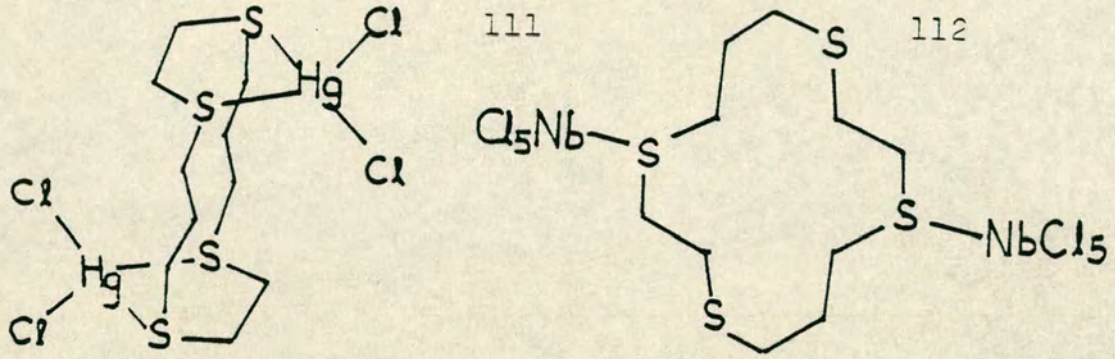

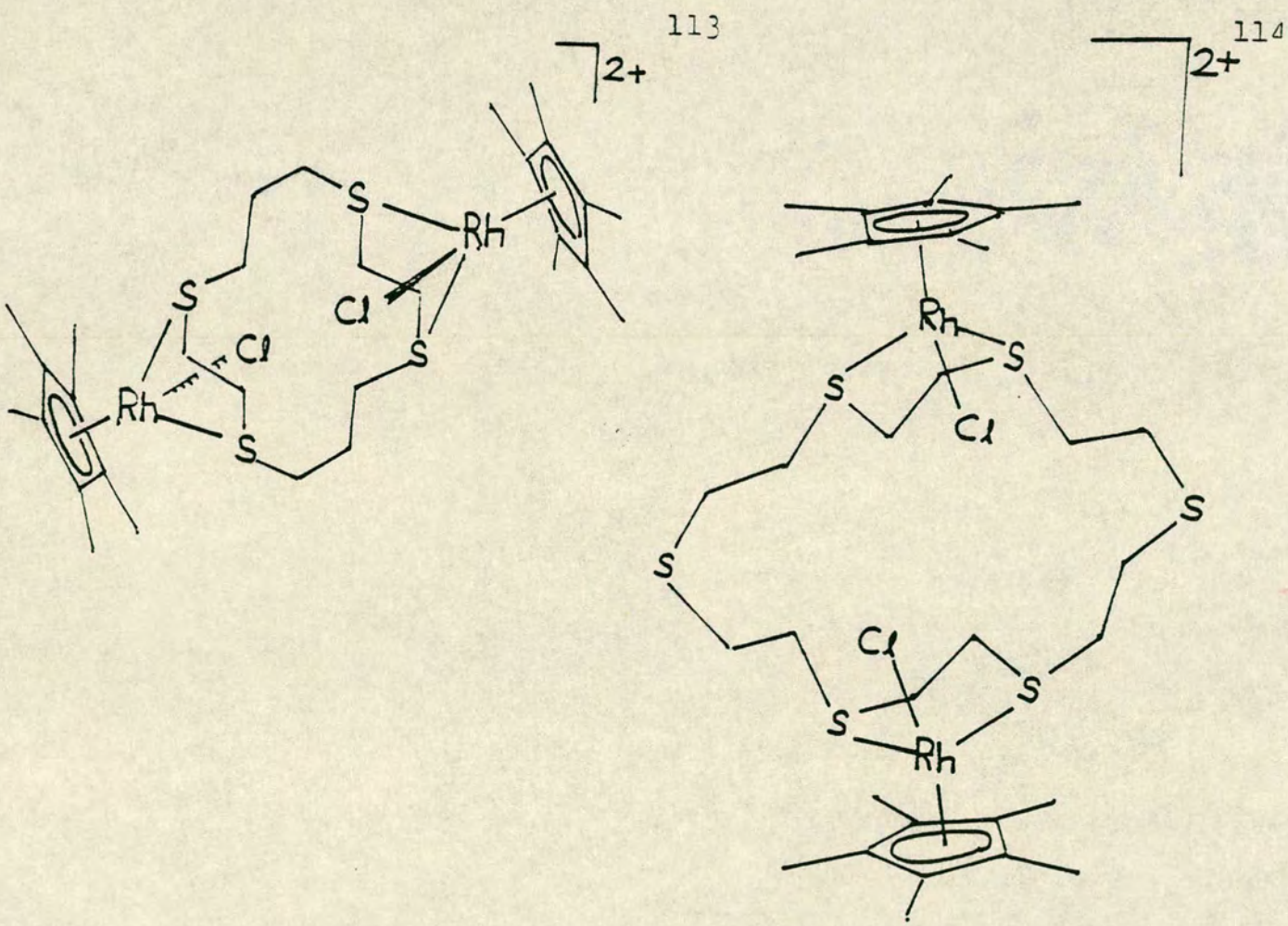

in the free state[115] thus facilitating exo co-ordination to the metal centre. A requirement for exodentate co-ordination appears to be that the metal substrate should have one (or at most two) labile co-ordination sites, under the conditions of the reaction. If all the co-ordination sites about the metal centre are replaced typical endo co-ordination results as in $[Ni(L^2)]^{2+}$ [232] and $[Rh(L^2)]^{+}$.[116]

CHAPTER 2

1,4,7-Trithiacyclononane Complexes of Platinum

2 Platinum complexes of 1,4,7-trithiacyclononane

2.1 Introduction

Mononuclear chemistry of platinum is dominated by the II and IV oxidation states. The d^8 Pt(II) state is characterised by the formation of square planar complexes, whereas the d^6 Pt(IV) state is characterised by octahedral co-ordination. The tridentate ligands L^4 and L^1 (L^4 = 1,4,7-triazacyclononane, L^1 = 1,4,7-trithiacyclononane) appear ideally suited to study a range of oxidation states, for in addition to the high kinetic stability of their complexes, these ligands are able to adjust to the stereochemical demands of the metal centre.

Wieghardt *et al.*[48] have reported, and fully characterised the $[Pt(L^4)_2]^{2+}$ complex cation obtained by reaction of K_2PdCl_4 with an excess of L^4 in hot aqueous solution. The crystal structure of the complex cation (1) shows the expected square planar geometry around the d^8 centre (Pt-N = 2.074(9), 2.077(9) Å) with each macrocycle co-ordinating in a bidentate manner.

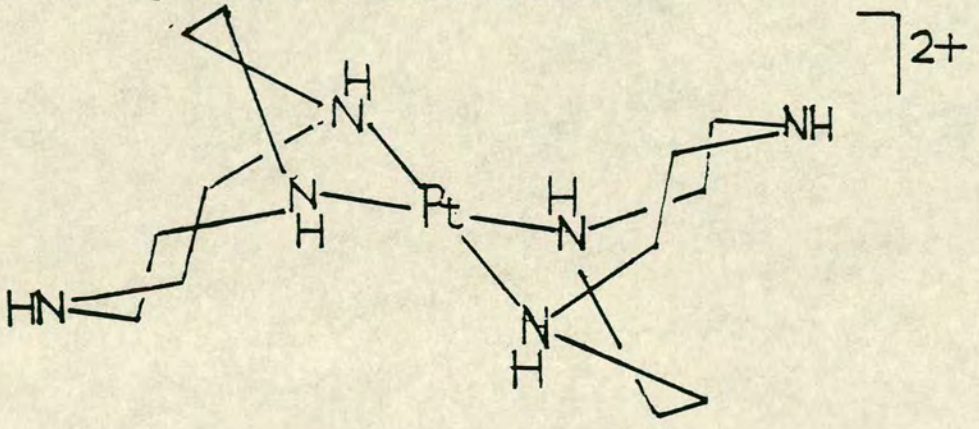

(1)

The remaining nitrogen atoms lie at a significant distance from the metal centre.

The ^1H n.m.r. spectrum of $[Pt(L^4)_2]^{2+}$ in D_2O showed a broad singlet (δ = 3.2 ppm) for the methylene protons, indicating fluxional behaviour of some kind for the triaza ligands. It was postulated that in solution, conformations in which the unco-ordinated nitrogen atoms approach the z axis of the Pt(II) centre quite closely, were present.[48]

This line of evidence was supported by the observed ready oxidation of $[Pt(L^4)_2]^{2+}$ to $[Pt(L^4)_2]^{4+}$, conversion occurring in hot aqueous solution over 20 hrs under a continual stream of air. The ^1H n.m.r. spectrum of the oxidised product closely resembled the spectra for other octahedral $[M(L)_2]^{n+}$ d^6 species (L = L^1,L^4) e.g. $[Co(L^4)_2]^{3+}$ [34,41] with a well defined symmetrical multiplet being observed for the methylene protons. Presumably octahedral co-ordination to the Pt(IV) centre is effected by a change in bonding mode of the macrocycle from bidentate, to tridentate co-ordination.

In exploring the $[Pt(L^1)_2]^{n+}$ system, some similarities, but also some significant differences in behaviour, may be expected. The binding of the soft thio ether L^1 to a soft Pd(II) centre should be highly favoured and a study of the electrochemistry of the $[Pt(L^1)_2]^{2+}$ cation is a clear priority. In contrast to L^4, L^1 may act as either a π acceptor or π donor. The softer nature of the ligand would be expected to lead to relative stabilisation of lower oxidation states, as illustrated in the electrochemistry of $[Co(L^1)_2]^{2+}$ [31,68] relative to $[Co(L^4)_2]$, with only the former showing a reversible (II)/(I) couple. The $[Pt(L^1)_2]^{4+}$ cation

would be expected to be significantly destabilised relative to the $[Pt(L^4)_2]^{4+}$ cation, yet this need not necessarily preclude electrochemical activity for the $[Pt(L^1)_2]^{2+}$ system. The co-ordinative flexibility and high kinetic stability observed for complexes of L^1 should optimise the observation of d^7 or d^9 oxidation states, which for monomeric Pd or Pt are usually transient,[117] and susceptible to rapid disproportionation. This, and the general paucity of work upon platinum metal thio-ether complexes makes study of the $[Pt(L^1)_2]^{n+}$ and related systems highly desirable.

Results and Discussion

2.2 Synthesis and characterisation of $[Pt(L^1)_2]^{2+}$

Reaction of K_2PtCl_4 with two molar equivalents of 1,4,7-trithiacyclononane (L^1) in water/methanol (v.v = 1:1) for 30 minutes under reflux led to the formation of a yellow orange solution of the $[Pt(L^1)_2]^{2+}$ complex cation. Addition of excess NH_4PF_6 and recrystallisation of the resulting solid from water gave orange crystals of $[Pt(L^1)_2](PF_6)_2$. The BF_4^- and BPh_4^- salts could also be prepared, the BPh_4^- salt obtained as red efflorescent crystals upon recrystallisation from nitromethane/diethyl ether. These crystals analysing for $[Pt(L^1)_2](PBh_4)_2.2CH_3NO_2$ became desolvated, and turned yellow over a number of weeks.

The $[Pt(L^1)_2]^{2+}$ cation was characterised by f.a.b. mass spectroscopy using a glycerol/dmf matrix. A strong signal was observed at $M^+ = 555$ assigned to $[Pt(L^1)_2]^+$, with the correct isotopic distribution.

$[Pt(L^1)_2](PF_6)_2$ dissolved readily in acetonitrile or nitromethane to give yellow orange solutions. The electronic spectra of these solutions (Figure 2.2.I) shows an absorption maxima in the visible region (λ_{max} = 432 nm (ε = 95 $M^{-1}cm^{-1}$) CH_3CN). This observation can be contrasted with the electronic spectrum for the tetrathia macrocyclic complex $[Pt(L^2)](PF_6)_2$ (L^2 = 1,4,8,11-tetrathia cyclotetradecane) which shows no absorption in the visible region. This observation suggested that simple square planar co-ordination around Pt(II) in $[Pt(L^1)_2](PF_6)_2$ might not be occurring.

The ^1H n.m.r. spectrum of $[Pt(L^1)_2](PF_6)_2$ run in acetonitrile at room temperature (Figure 2.2.II) shows a central singlet and two slightly broadened platinum satellites due to ^{195}Pt (I = ½ 33.8%). The outer resonances were confirmed as Pt satellites by running the ^1H n.m.r. spectrum at both 80 and 200MHz. In each case a coupling ($^3J_{PtH}$) of 24.5Hz was observed. The ^1H n.m.r. spectrum of $[Pt(L^1)_2](BPh_4)_2$ (run in d^6 dmso and CD_3NO_2) showed an identical 1:4:1 pattern for the macrocyclic resonances. Additionally comparison of the macrocyclic and phenyl resonances confirmed the stoichiometry for the complex.

The ^1H n.m.r. spectrum of $[Pt(L^1)_2]^{2+}$ sharply contrasts with the spectrum for the analogous triaza macrocyclic complex $[Pt(L^4)_2]^{2+}$ for which a much broader unresolved signal is observed.[48] In this system the broadness of the signal was ascribed to a fluxionality in the complex cation.

Figure 2.2.I Electronic Spectrum of $[Pt(L^1)_2](PF_6)_2$ in a) $H_2O/\sim10^{-4}$M; b) $CH_3CN/\sim10^{-2}$M

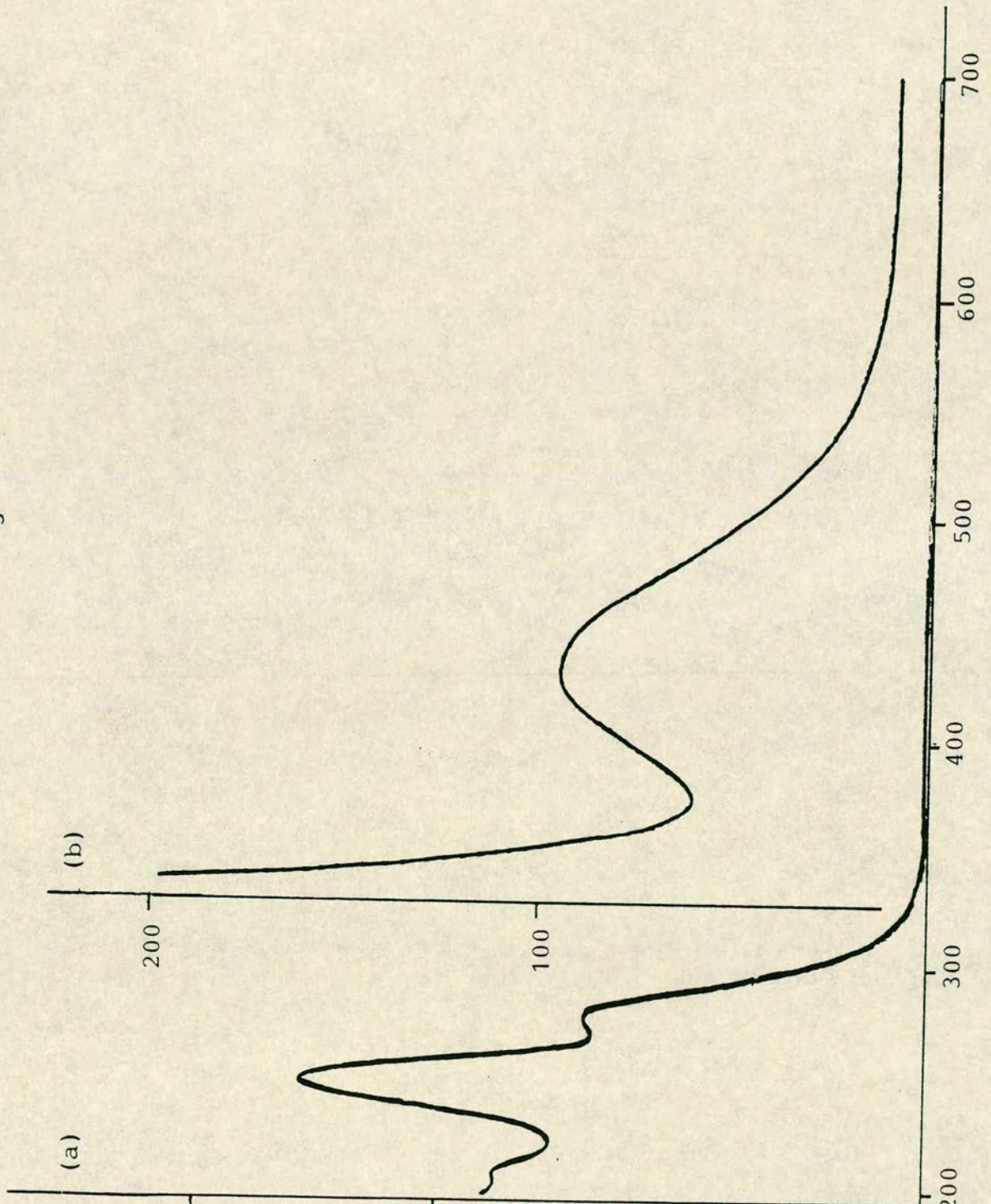

Figure 2.2.II ^{1}H n.m.r. of $[Pt(L^{1})_{2}](PF_{6})_{2}$ in $CD_{3}CN$

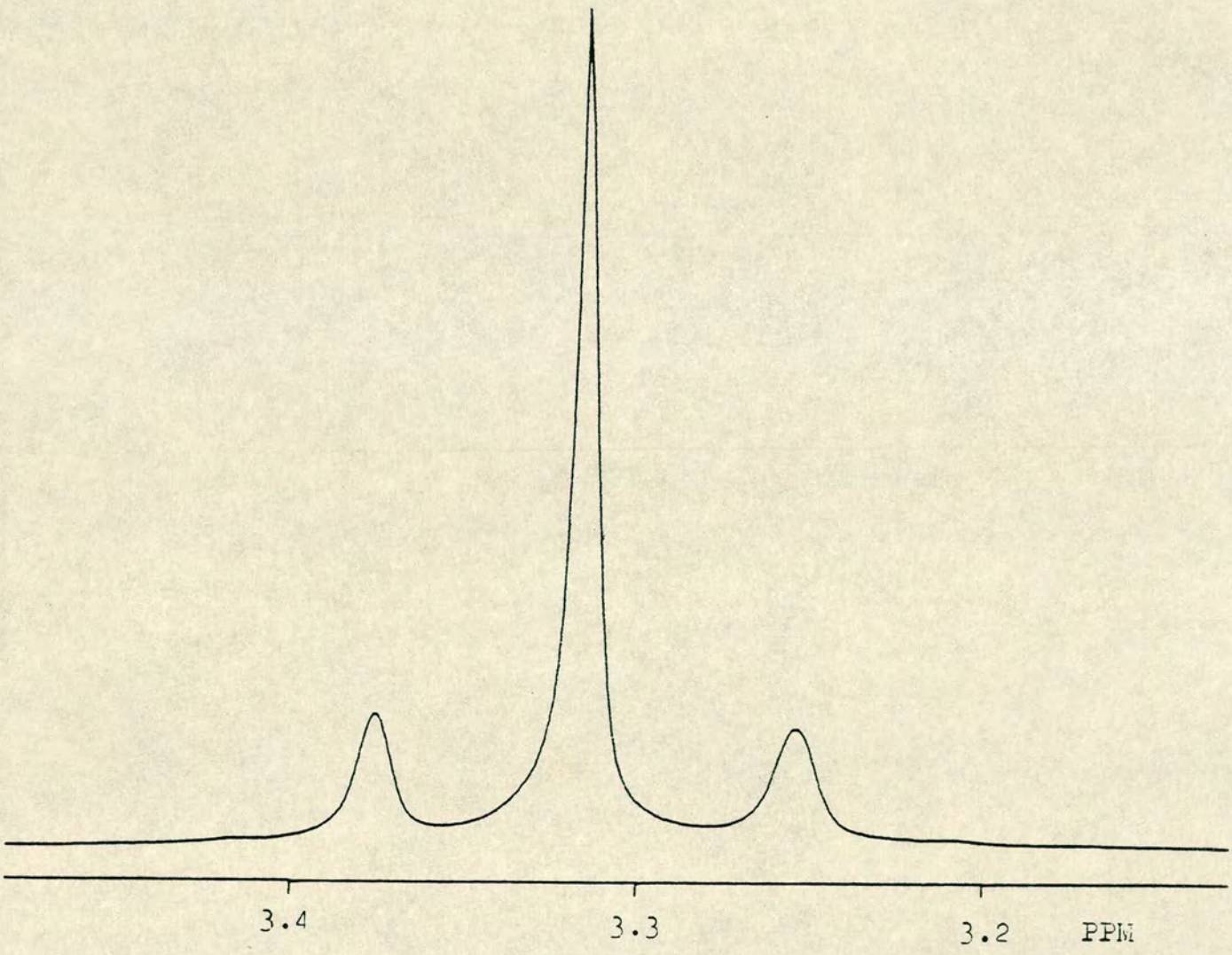

For the $[Pt(L^1)_2]^{2+}$ cation, in which a sharp singlet is observed for the central resonance a degree of fluxionality is also proposed. Such a fluxionality in which ligand scrambling is rapid on the n.m.r. time scale would lead to the observation of a time averaged signal for the interchangeable macrocyclic protons.

The origin of a possible fluxionality in the $[Pd(L^1)_2]^{2+}$ cation probably occurs via apical interaction of a thia donor to the PtS_4 square plane, so facilitating a bond-making/bond-breaking process. It should be noted however reducing the temperature of the n.m.r. sample to -35°C (freezing point of CD_3CN = -40°C) did not cause the observed spectrum to change.

It was clearly of importance to determine the degree of extra apical interaction of the ligand donor set to the Pt(II) centre in $[Pt(L^1)_2]^{2+}$. Additionally since little structural work had been carried out upon platinum metal thio ether complexes a single crystal X-ray diffraction study was undertaken on $[Pt(L^1)_2](PF_6)_2$.

2.3 The single crystal X-ray structure of $[Pt(L^1)_2](PF_6)_2$

Crystal data: $C_{12}H_{24}PtS_6.^{2+}\ 2PF_6^-$ M = 854.7 monoclinic space group $P2_1$, a = 11.848(4) b = 17.817(6) c = 11.750(11)Å β = 98.06(4)° U = 2456Å^3 D_c = 1.77 gcm^{-3} Z = 4. At

convergence R, R_w = 0.044, 0.048 respectively for 2721 data.

A summary of selected bond lengths and angles are given in Table 2.3.I. The resulting structure (Figures 2.3.II, and 2.3.III) showed two independent cations and four PF_6^- anions per asymmetric unit of the monoclinic cell. In both cations the Pt atoms are co-ordinated by four sulphur atoms in a square plane, with Pt-S distances in the range 2.25-2.30Å. However an elongated square pyramidal geometry is achieved in each case by the third atom in one of the two macrocycles co-ordinating apically (Pt-S(1B), Pt-S(1D) = 2.885(7), 2.925(11)Å). The angle of the axial Pt-S bond to the S_4 plane is near octahedral ($<S_{eq}PtS_{ax}$ = 84.0°, 97.2°). In both cations the remaining sulphur atom is unco-ordinated (Pt S = 4.04, 4.18Å).

The '4+1' co-ordination geometry observed in $[Pt(L^1)_2]^{2+}$ differs substantially from the geometry observed in the $[Pt(L^4)_2]^{2+}$ complex cation. This structure appears to be retained in solution, with the visible absorption at λ_{max} = 432 nm for the complex likely to be a d-d transition in the modified ligand field (2) for the complex.

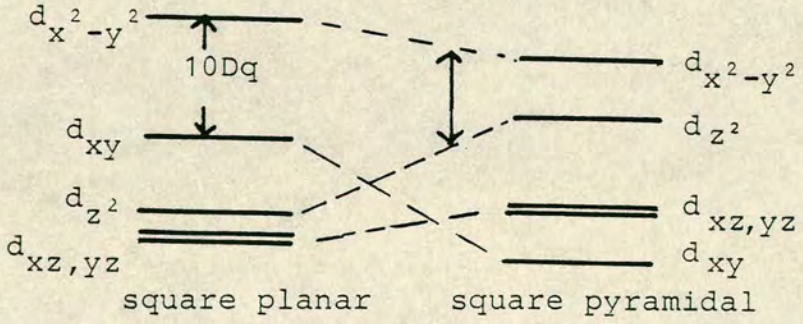

(2)

Table 2.3.I Important bond lengths and angles (with esd's) for the two independent $[Pt(L^1)_2]^{2+}$ cations

Bond lengths (Å)

Pt-S(4A)	2.261(7)	Pt-S(1B)	2.885(7)
Pt-S(7A)	2.246(8)		
Pt-S(4B)	2.293(8)		
Pt-S(7B)	2.305(8)		
Pt-S(4C)	2.259(7)	Pt-S(1D)	2.905(11)
Pt-S(7C)	2.259(8)		
Pt-S(4D)	2.287(8)		
Pt-S(7D)	2.308(8)		

Bond angles (degrees)

S(4A)-Pt-S(7A)	89.5(3)	S(1B)-Pt-S(4B)	84.65(24)
S(4B)-Pt-S(7B)	89.1(3)	S(1B)-Pt-S(7B)	85.54(24)
S(4C)-Pt-S(7C)	89.8(3)	S(1D)-Pt-S(4D)	85.5(3)
S(4D)-Pt-S(7C)	88.8(3)	S(1D)-Pt-S(7D)	81.0(3)

Figure 2.3.II View of the single crystal X-ray structure of $[Pt(L^1)_2]^{2+}$ (1)

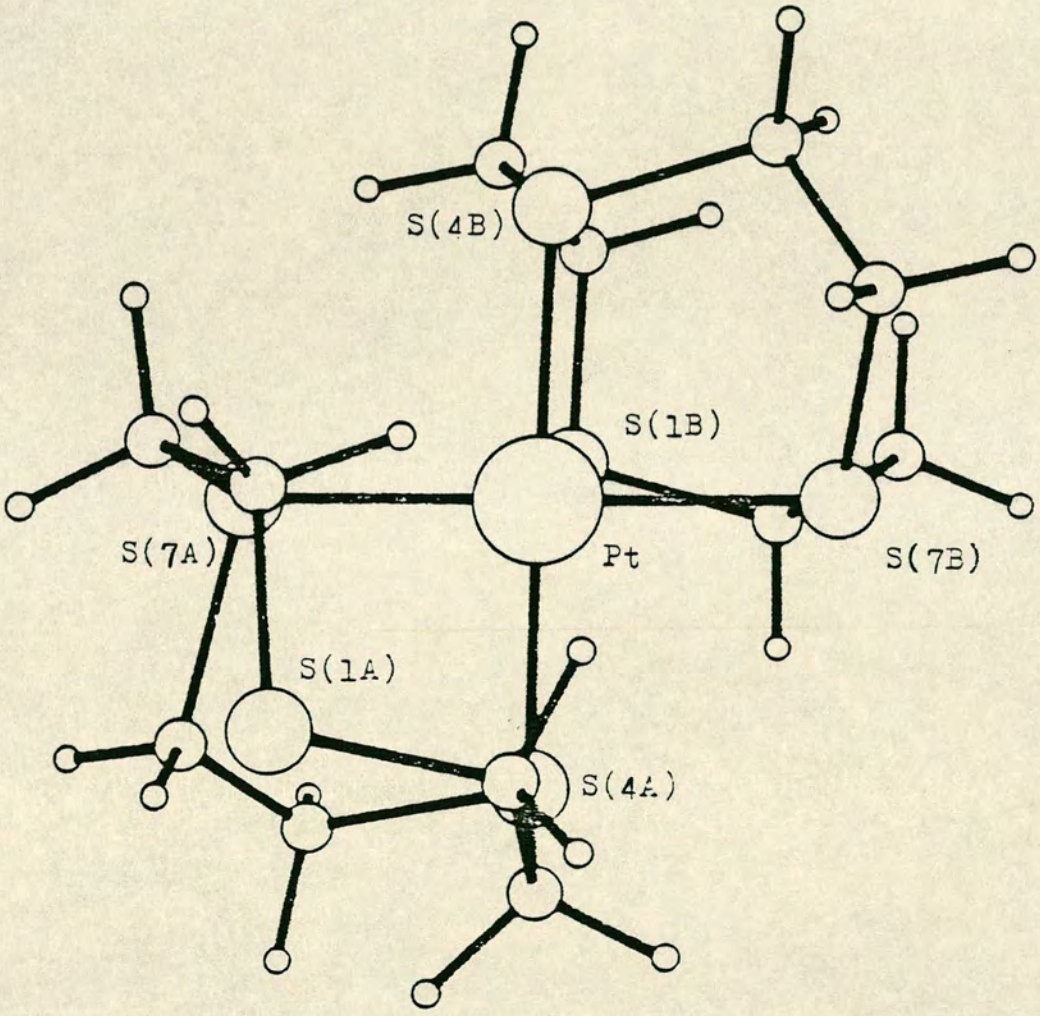

Figure 2.3.III View of the single crystal X-ray structure of $[Pt(L^1)_2]^{2+}$ (2)

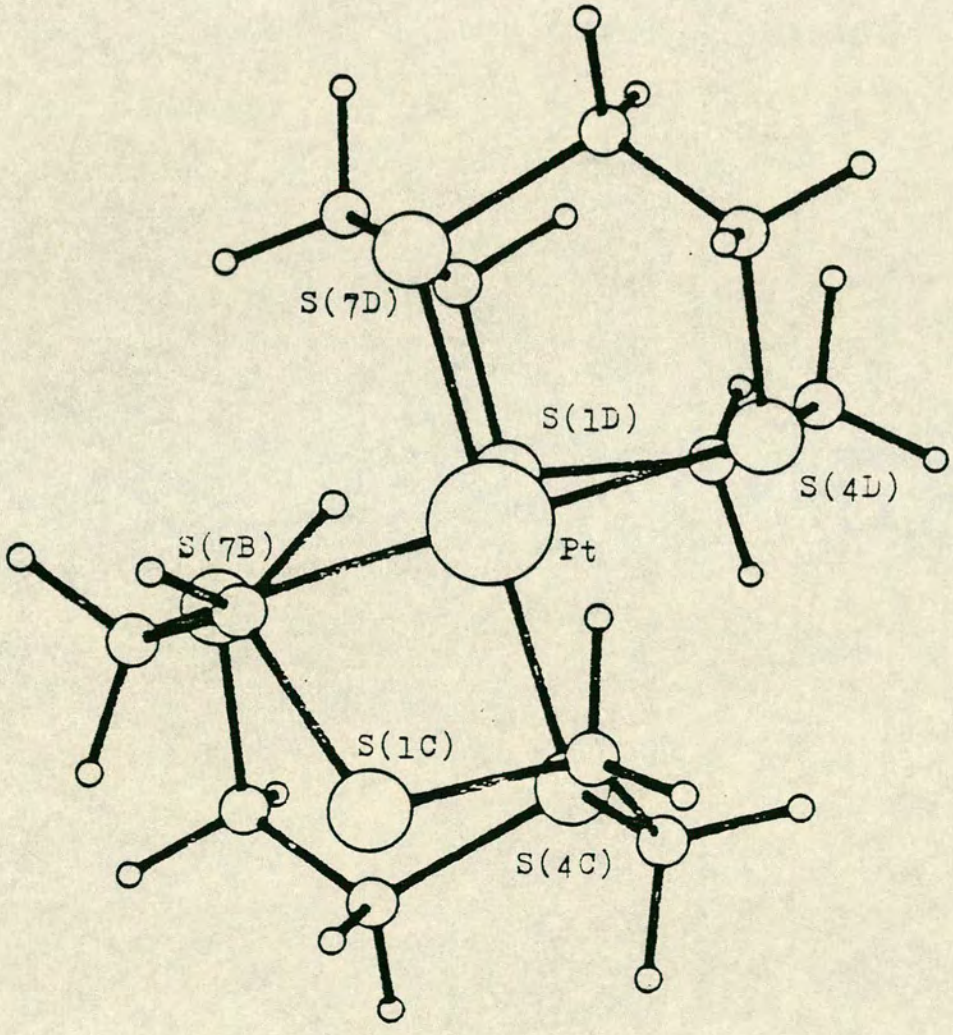

The presence of an additional thia interaction to the PtS_4 plane in $[Pt(L^1)_2]^{2+}$ would support a fluxional nature for the cation in solution. Were the cation to retain the solid state structure in solution a complex series of resonances would be expected for the macrocycle protons in the ^1H n.m.r. spectrum. Although chemical equivalence cannot be ruled out, the simplified ^1H n.m.r. spectrum observed does point to a fluxional system. Significantly in the n.m.r. spectra of rigid $[M(L)_2]$ and $[M(L)X_n]$ species[41,48] the L^1 resonances are complex. The presence of the weakly co-ordinating axial thia donor is likely to provide the 'handle' for a facile ligand scrambling process in which concomitant bond formation/weakening occurs with little energetic change.

Clearly, however, to prove the fluxionality or otherwise of the $[Pt(L^1)_2]^{2+}$ cation in solution low temperature n.m.r. studies are required to observe a slowing of the scrambling mechanism. Preliminary results, however, in CD_3CN at -35°C shows no observable change in the ^1H n.m.r. spectrum from the room temperature signal.

Although the dominant stereochemistry of Pt(II) is square planar, a number of pentaco-ordinate species have been reported. Pentaco-ordination is thought to be facilitated by use of π bonding ligands[118,119] as a consequence of increased d orbital participation. Experimental evidence supports this reasoning, all pentaco-ordinate species having been characterised for π acceptor ligands. $[Pt(SnCl_3)_5]^{3-}$ has been structurally characterised in the solid state[120] while n.m.r. data indicates that divinylphosphine

or 2,4-dimethylphosphole platinum(II) halide complexes $[PtL_2X_2]$ are in equilibrium with pentaco-ordinate $[PtL_3X_2]$ species in the presence of excess ligand (3).[121]

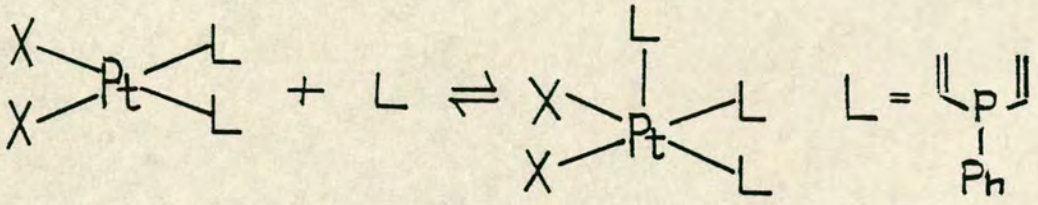

(3)

Dithiacarbamate and dithiaphosphate adducts of Pt(II) phosphines also show a tendency to pentaco-ordination in solution.[122]

It seems likely that it is the π bonding ability of the trithia macrocycle L^1 that is responsible for the observed 4+1 stereochemistry in the $[Pt(L^1)_2]^{2+}$ complex cation.

2.4 Redox chemistry of $[Pt(L^1)_2]^{2+}$

Cyclic voltammetry of $[Pt(L^1)_2](PF_6)_2$ in acetonitrile (Figure 2.4.I) shows an oxidation wave, with Epa = +0.46V and a return wave at Epc = +0.315V (all quoted potentials vs $Fc/Fc^+ = 0$). Although chemically reversible (Ipa/Ipc = 1.0), the large peak separation of 145 mV indicates a significant structural rearrangement on oxidation. Since oxidation of the free ligand L^1 occurs at +1.0V,[31] it seemedreasonable to conclude that oxidation of $[Pt(L^1)_2]^{2+}$ is metal based. Controlled potential electrolysis of $[Pt(L^1)_2]^{2+}$ at +0.5V under N_2 in acetonitrile

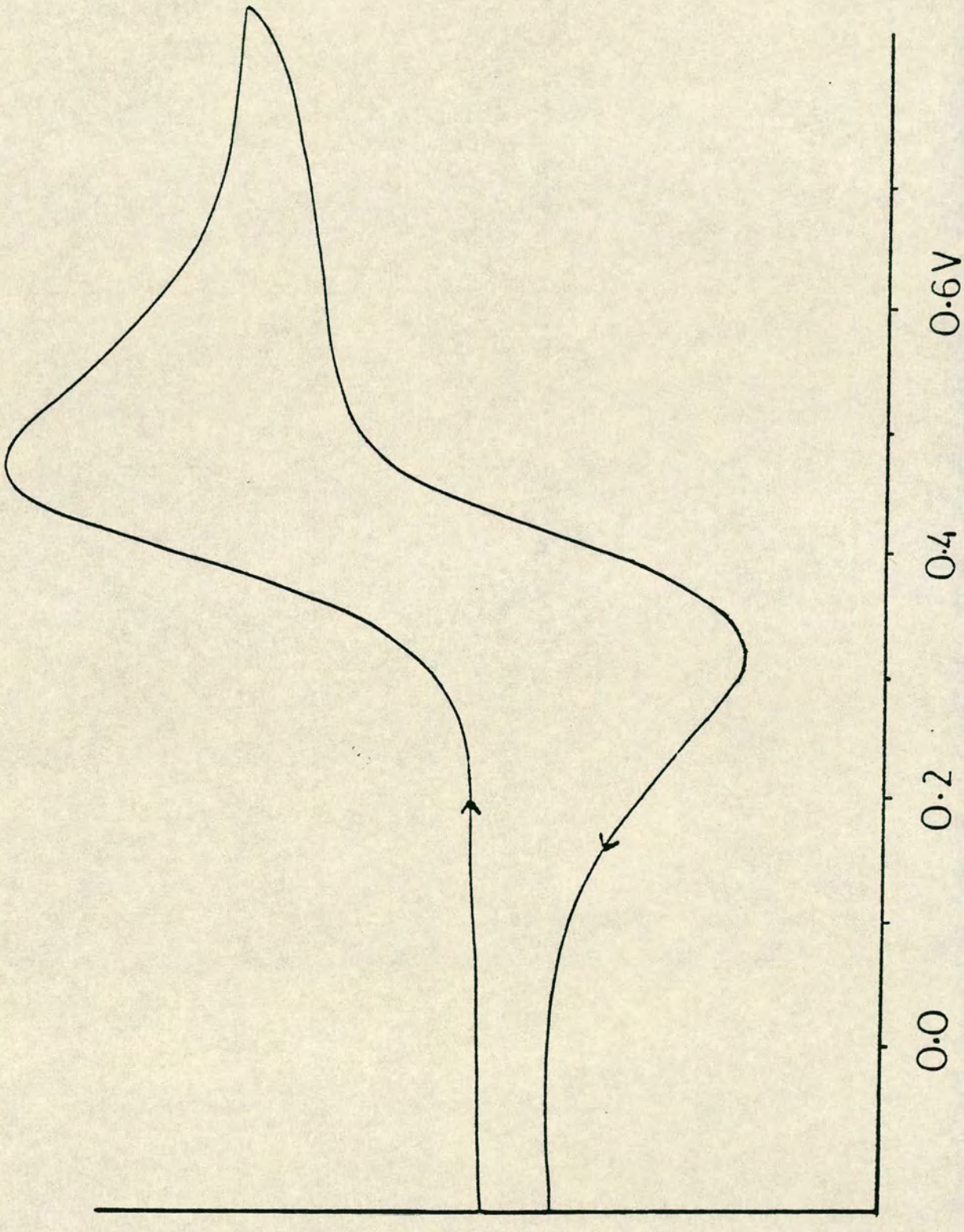

Figure 2.4.I Cyclic voltammogram of $[Pt(L^1)_2](PF_6)_2$ in CH_3CN/0.1M $TBAPF_6$

afforded a stable oxidised product (λ_{max} = 401 nm (ε = 3030 $M^{-1}cm^{-1}$) 271 ($\sim$13000)) in an isosbestic manner (λ_{iso} = 253 nm). The solution was observed to show a very strong esr signal (CH_3CN 77K) indicating the formation of a d^7 Pt(III) species. The anisotropic signal (Figure 2.4.II) shows $g_{\perp}$ = 2.044 $g_{\parallel}$ = 1.987 with hyperfine coupling to ^{195}Pt (I = ½ 33.8%) with $A_{\perp}$ $\sim$30G, $A_{\parallel}$ $\sim$85G. The anisotropic broadened signal is characteristic for unpaired electron density primarily residing on the metal centre.[123] Additionally, the observation $g_{\perp} > g_{\parallel} \sim 2$, is predicted[124] for a d^7 low spin tetragonally elongated octahedran, consistent for a genuine Pt(III) centre.

The electrogenerated $[Pt(L^1)_2]^{3+}$ cation shows a high stability in solution, decomposing slowly only over a number of days at room temperature. This stability enabled a quantitative measurement of the number of electrons transferred in the oxidation of $[Pt(L^1)_2]^{2+}$ to be made. Measurement of the intensity of the charge transfer band at λ_{max} = 401 nm (due to the oxidised species) as a function of the electrogeneration potential gave a value for n, the number of electrons transferred, close to unity. These measurements were performed using an optically transparant thin layer electrode (OTTLE) by T.I. Hyde.

The origin of the charge transfer band in $[Pt(L^1)_2]^{3+}$ is likely to be a ligand (n) $\rightarrow$ metal (eg^*) transition in which the thia macrocycle is behaving as a π donor.

Addition of diethyl ether to acetonitrile solutions of $[Pt(L^1)_2]^{3+}$ followed by washing with dichloromethane gave

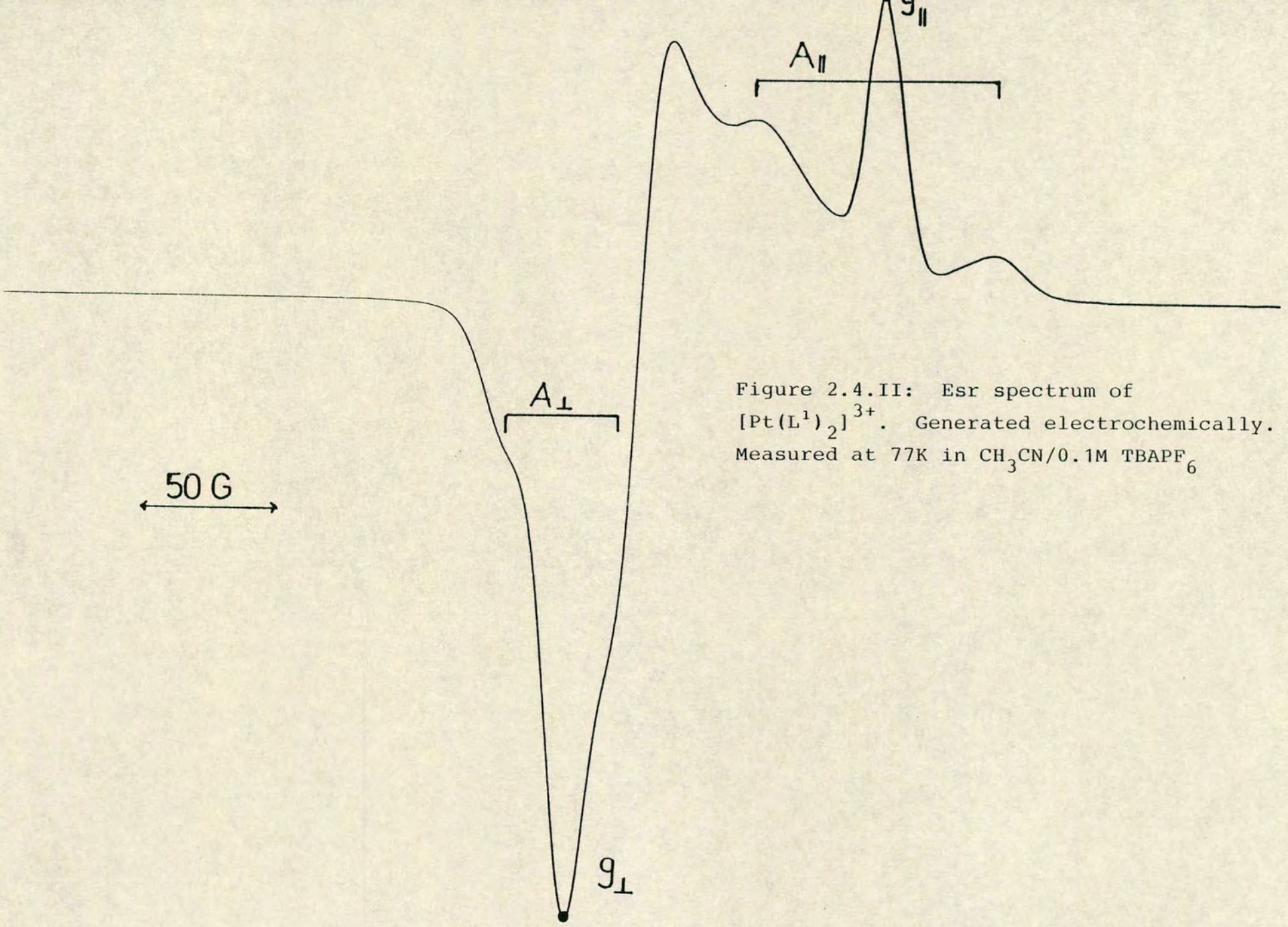

Figure 2.4.II: Esr spectrum of $[Pt(L^1)_2]^{3+}$. Generated electrochemically. Measured at 77K in CH_3CN/0.1M $TBAPF_6$

a green-yellow air and moisture sensitive solid, presumably $[Pt(L^1)_2](PF_6)_3$.

Using 50% or 70% aqueous $HClO_4$ as a chemical oxidant, the $[Pt(L^1)_2]^{2+}$ cation (λ_{max} = 432 nm (ε = 95 M^{-1} cm^{-1}), 277 (6935), 245 (12500)) is converted (Figure 2.4.III) in an isosbestic manner (λ_{iso} = 256 nm) into the intensely yellow green $[Pt(L^1)_2]^{3+}$ cation (λ_{max} = 401 nm (ε = 4390 $M^{-1}cm^{-1}$), 271 (13,650)) as observed in the electrogeneration experiment. The frozen glass esr spectrum of the $[Pt(L^1)_2]^{3+}$ cation in 70% aqueous $HClO_4$ (Figure 2.4.IV) is essentially the same as the esr spectrum of the electrogenerated $[Pt(L^1)_2]^{3+}$ cation in acetonitrile, with $g_\perp$ = 2.039 $g_\parallel$ = 1.987. The resolution however of the hyperfine coupling to ^{195}Pt (I = ½ 33.8%) is improved ($A_\perp$ = 45G $A_\parallel$ = 90G), and a second hyperfine coupling of 5G is now also observable; this is likely to be a longer range proton interaction.

In contrast to the electrogenerated $[Pt(L^1)_2]^{3+}$ cation, the chemically generated $[Pt(L^1)_2]^{3+}$ cation in 70% $HClO_4$ slowly underwent a further oxidation, again in an isosbestic manner (λ_{iso} = 352, 273, and 230 nm), to give the colourless esr silent $[Pt(L^1)_2]^{4+}$ cation, (λ_{max} = 289 nm (ε = 17,800 $M^{-1}cm^{-1}$)) (Figure 2.4.V).

The formulation of this final oxidised product, which could be obtained as a white microcrystalline solid from more concentrated solutions in $HClO_4$, was made upon observation that attempts to recrystallise the air and moisture sensitive solid in a non-oxidising environment, led to the re-formation of the $[Pt(L^1)_2]^{2+}$ cation, as characterised by

Figure 2.4.III

Electronic Spectrum showing oxidation of $[Pt(L^1)_2]^{2+}$ to $[Pt(L^1)_2]^{3+}$ in 50% aqueous $HClO_4$ solution

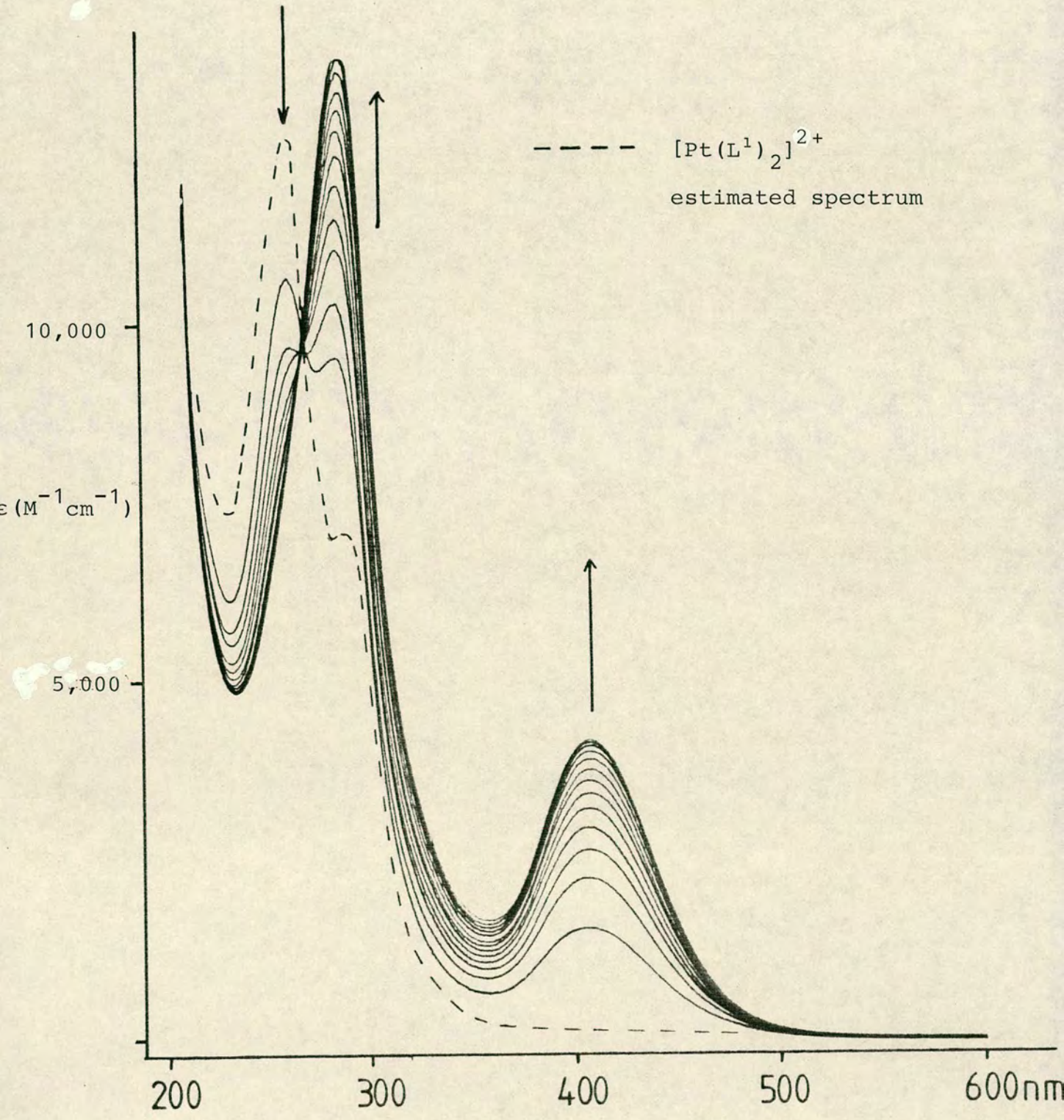

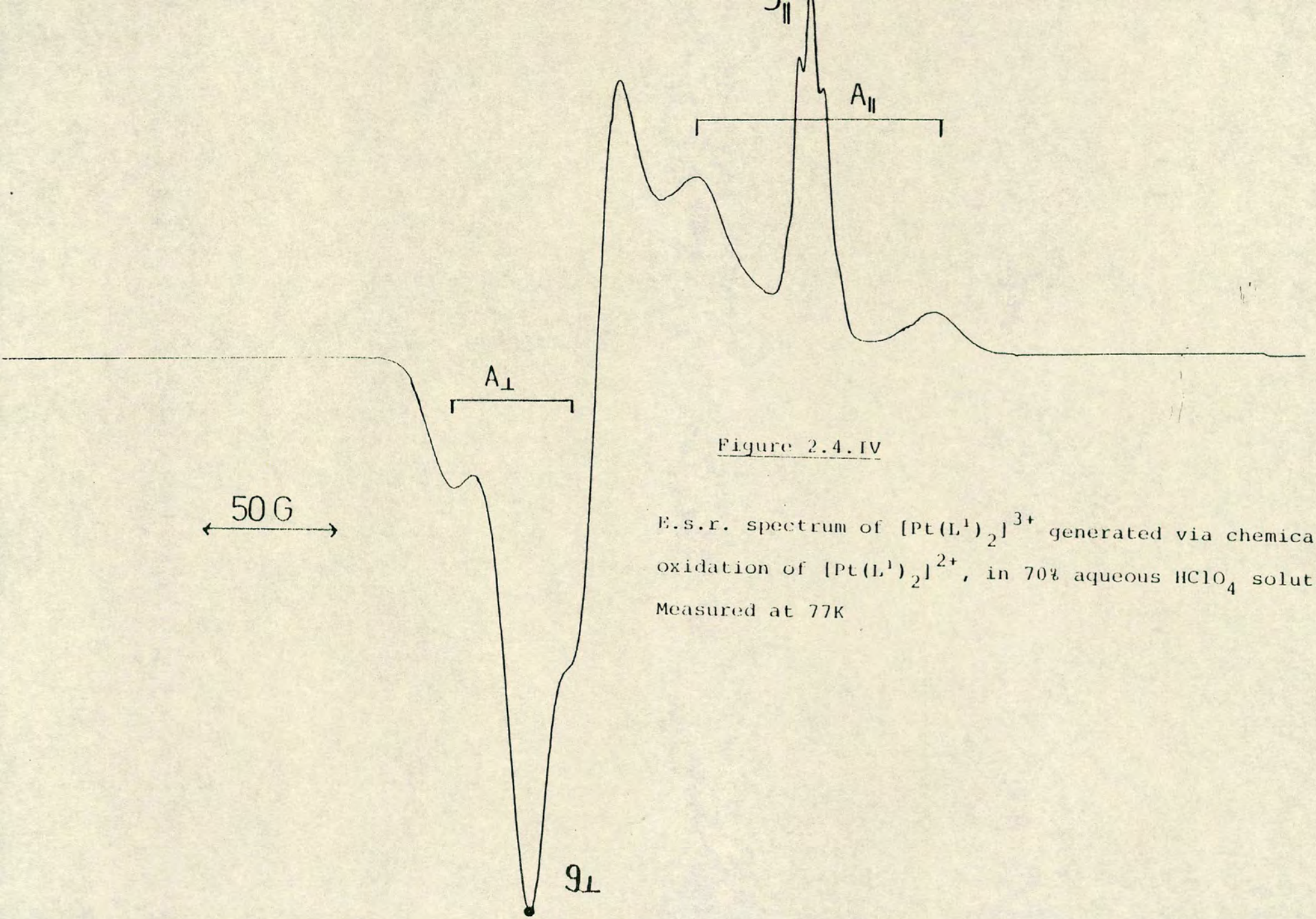

Figure 2.4.IV

E.s.r. spectrum of $[Pt(L^1)_2]^{3+}$ generated via chemical oxidation of $[Pt(L^1)_2]^{2+}$, in 70% aqueous $HClO_4$ solution. Measured at 77K

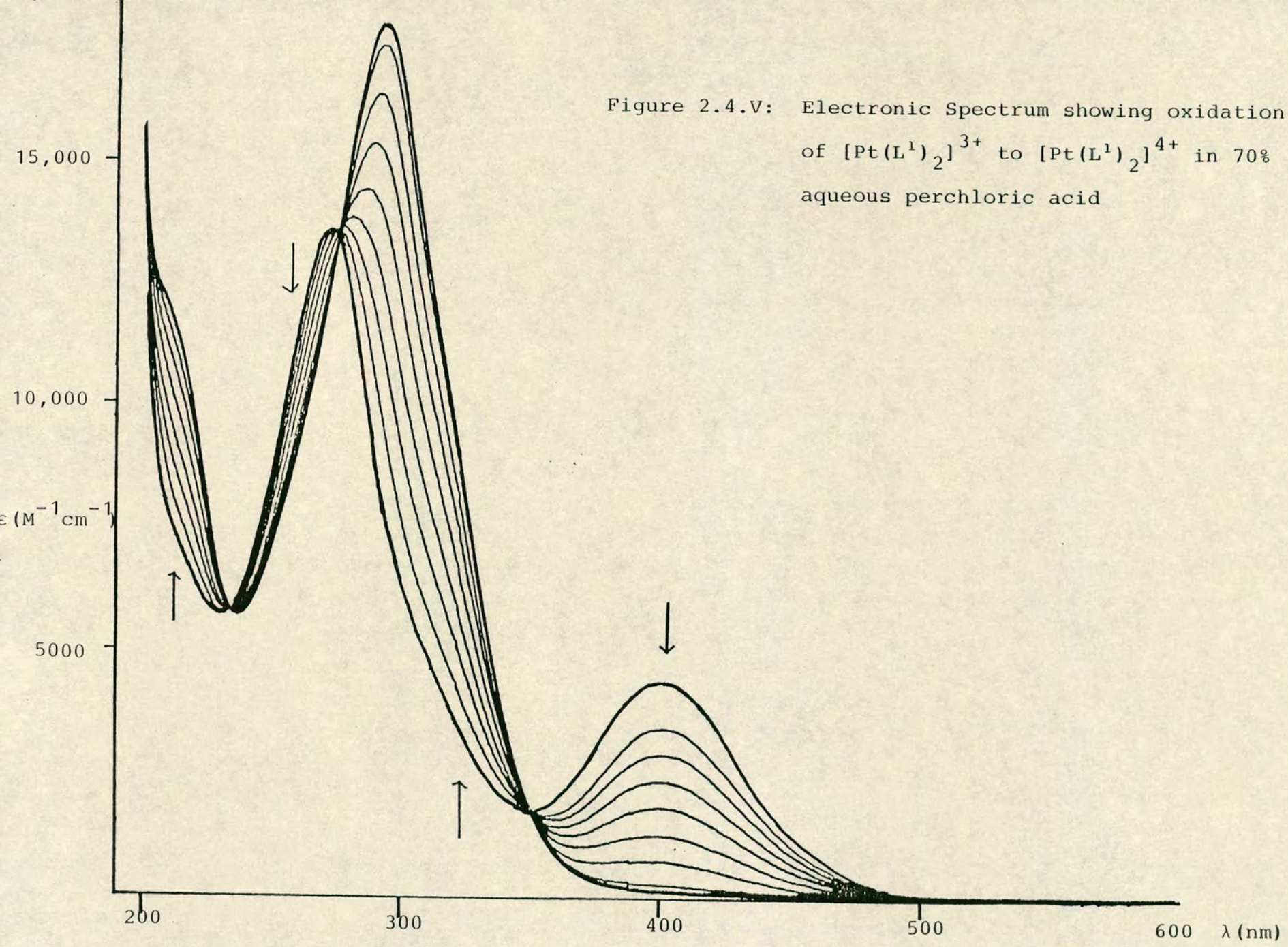

Figure 2.4.V: Electronic Spectrum showing oxidation of $[Pt(L^1)_2]^{3+}$ to $[Pt(L^1)_2]^{4+}$ in 70% aqueous perchloric acid

infra-red and electronic spectroscopy. This would seem to discount the possibility of ligand oxidation to give a sulphoxide species as recently observed in the chemical oxidation of $[Fe(L^1)_2]^{2+}$. [125] Clearly it is hoped to obtain structural characterisation of the $[Pt(L^1)_2]^{4+}$ cation via a single crystal X-ray diffraction study.

Relative to the oxidation of $[Pt(L^1)_2]^{2+}$ to $[Pt(L^1)_2]^{3+}$ the subsequent oxidation of $[Pt(L^1)_2]^{3+}$ to $[Pt(L^1)_2]^{4+}$ is markedly slower. For 2 x 10^{-2}M solutions the time required for the initial oxidation is *ca.*90 minutes at room temperature, whereas the second oxidation occurs only over *ca.*10 hours. The sluggishness of the second oxidation may explain the absence of an observable (III)/(IV) couple in the cyclic voltammogram. In the electrogeneration experiments there was evidence of the $[Pt(L^1)_2]^{4+}$ cation being formed, but only after prolonged times, at potentials of *ca.* 0.5V (vs Fc/Fc^+).

Certainly relative to the triaza analogue, the $[Pt(L^1)_2]^{4+}$ species is significantly destabilised, however this may be a primary reason for the extra-ordinary stability of the $[Pt(L^1)_2]^{3+}$ cation, since disproportionation will be disfavoured. Cyclic voltammetry indicates a substantial rearrangement upon oxidation of $[Pt(L^1)_2]^{2+}$, and this is consistent for the transformation of the pentaco-ordinated $[Pt(L^1)_2]^{2+}$, to a distorted octahedral geometry for $[Pt(L^1)_2]^{3+}$. Few genuine monomeric Pt(III) complexes have been reported in the literature. A number of dithiolene[126] and closely related Pd(II) systems[127] (4) can be readily oxidised to yield paramagnetic species. In these systems

however the unpaired electron density has been shown to largely reside on the delocalised ligand based orbitals, and so may be more accurately regarded as Pt(II)/ligand radical systems.

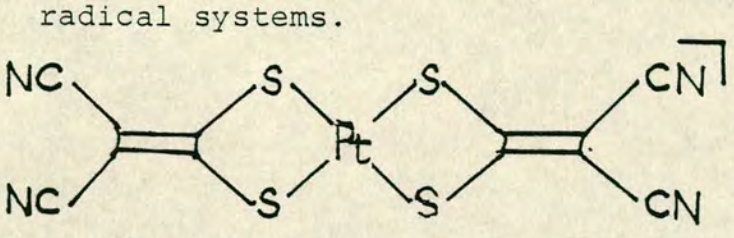

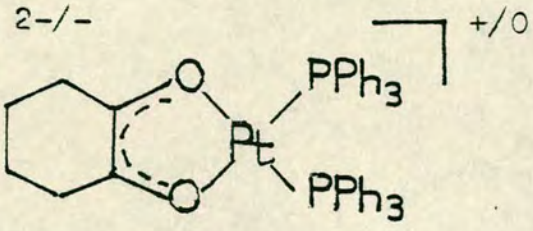

(4)

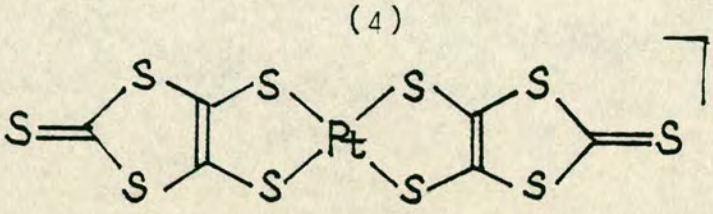

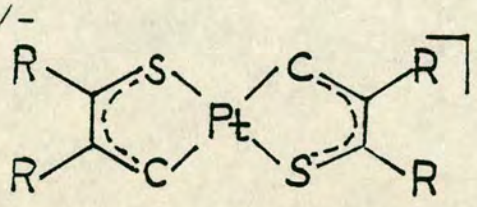

The complex $[Pt(NH_3)_2(SCN)_2I]$,[128] initially formulated as a monomeric Pt(III) species is now believed to have a chain polymeric structure.[129] Similarly a crystal structure of $[Pt(DMG)_2](ClO_4)$[130] also indicates a degree of association between Pt(III) centres. Genuine metal based mononuclear d^7 species can be generated as transients via pulse radiolysis of Pt(II) or Pt(IV) host lattices.[131,132] A recent example is the macrobicyclic complex $[Pt(diamsar)]^{3+}$ (5) generated via its d^6 precursor.[133] The resulting species in a host lattice of $[Pt(diamsar)]^{4+}$ at low temperatures shows an e.s.r. spectrum which very closely

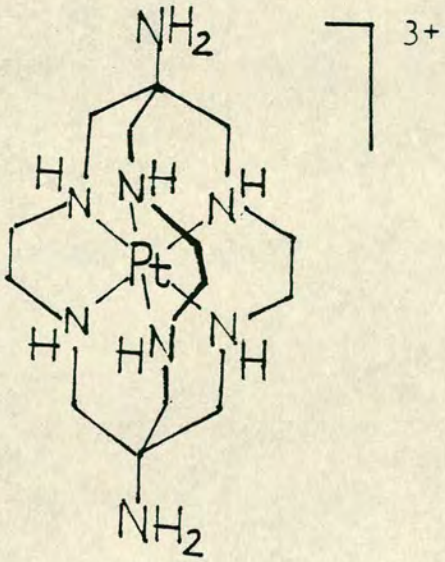

(5)

resembles that obtained in our system, with g = 2.01 $A_{\perp}$ = 60G. Recently the d^7 $[Pt(C_6Cl_5)_4]^-$ ion (6) [134] was obtained via chemical oxidation of the square planar d^8 $[Pt(C_6Cl_5)_4]^{2-}$ species. Magnetic measurements upon the air and moisture stable oxidised product indicated an orbital contribution to the magnetic moment suggesting the unpaired electron density to reside primarily at the metal centre. However no esr evidence is presented, so the location of the unpaired electron remains in some doubt. A crystal structure determination of this deep blue complex reveals it to be essentially isostructural to the d^8 precursor.

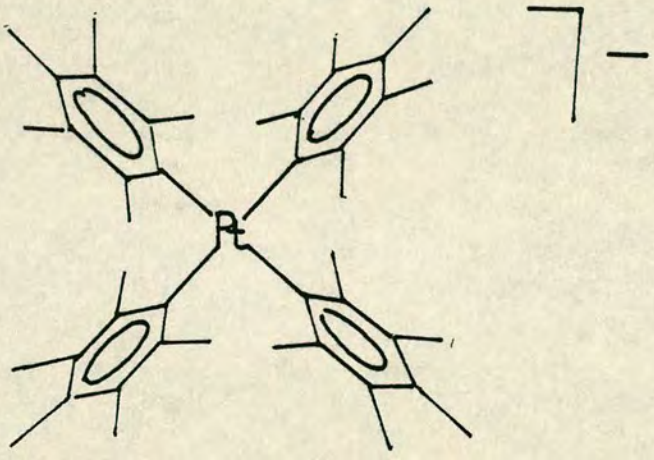

(6)

The high degree of stability associated with the $[Pt(L^1)_2]^{3+}$ cation is primarily due to the kinetic stability of the macrocyclic system and perhaps just as importantly the adaptability of the ligand to adjust to the stereochemical demands of the d^7 Pt(III) centre. The importance of this factor can be demonstrated via the electrochemistry of the related macrocyclic thio ether systems $[Pt(L^2)]^{2+}$ and $[Pt(L^3)]^{2+}$ (L^2 = 1,4,8,11-tetrathiacyclotetradecane, L^3 = 1,4,7,10,13,16-hexathiacyclooctadecane).

Before leaving the $[Pt(L^1)_2]^{2+}$ system, it is observed that although a rich oxidation chemistry is observed there is no significant reductive electrochemistry. There is only tentative evidence for an irreversible reduction of $[Pt(L^1)_2]^{2+}$ in acetonitrile at -40°C at *ca.*-1.2V vs Fc/Fc^+. This may appear somewhat disappointing in view of the 'soft' nature of the ligand, and the previous ready observation of Pt(I) in the literature, albeit primarily for metal-metal bonded complexes with π acceptor ligands.[135,136]

2.5 Studies upon related thia macrocyclic complexes of platinum

2.5.1 Synthesis, characterisation and electrochemistry of $[Pt(L^2)]^{2+}$

The $[Pt(L^2)]^{2+}$ cation was synthesised by reaction of $PtCl_2$ or K_2PtCl_4 with L^2. Refluxing K_2PtCl_4 with a slight excess of L^2 in a water-methanol mixture led to formation of the colourless $[Pt(L^2)]^{2+}$ cation. Addition of NH_4PF_6 precipitated the PF_6^- salt which could be recrystallised from water to give colourless crystals of $[Pt(L^2)](PF_6)_2$. Unlike the Ni analogue[65] the $[Pt(L^2)]^{2+}$ cation is stable to hydrolysis, even in hot water, thus reflecting the inertness of the heavier transition elements relative to the first row metals. The ^1H n.m.r. spectrum of $[Pt(L^2)](PF_6)_2$ in CD_3CN differs substantially from that observed for $[Pt(L^1)_2]^{2+}$, with a series of complex resonances being observed for the macrocyclic protons between

δ_H = 2.8-3.8 ppm. The $[Pt(L^2)]^{2+}$ cation shows peaks at M^+ = 609, 464 corresponding to $[Pt(L^2)](PF_6)^+$ and $[Pt(L^2)]^+$ in the f.a.b. mass spectrum in a glycerol dmf matrix. Electrochemistry of $[Pt(L^2)](PF_6)_2$ in acetonitrile shows the absence of any redox behaviour and presumably the $[Pt(L^2)]^{3+}$ cation is unable to be stabilised by the square planar co-ordination of the macrocycle.

2.5.2 Synthesis, characterisation and electrochemistry of $[Pt(L^3)]^{2+}$

The single crystal X-ray structure of $[Pt(L^3)]^{2+}$ has already been reported.[137] The cation (7) shows an essentially square planar co-ordination about the metal centre, with the

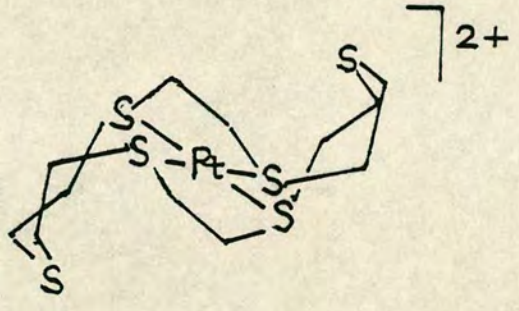

(7)

remaining thia donors at a distance of 3.38Å from the metal centre. The weakness of the secondary interaction may be as a consequence of either steric or electronic factors. If the latter is responsible then the $[Pt(L^3)]^{3+}$ cation should be stabilised as the hexathia macrocyclic ligand can re-adjust to the specific stereochemical demands of the metal centre. If however the macrocyclic ligand is too small to co-ordinate octahedrally about the third row transition metal then $[Pt(L^3)]^{3+}$ would not be

stabilised, and no electrochemical activity for $[Pt(L^3)]^{2+}$ would be expected in the oxidation range. In order to investigate the electrochemistry of the $[Pt(L^3)]^{2+}$ cation the PF_6^- salt rather than the previously characterised BPh_4^- salt was synthesised. Reaction of K_2PtCl_4 with a slight excess of L^3 in a refluxing water/methanol mixture led to the formation of the pale yellow $[Pt(L^3)]^{2+}$ cation. Addition of $NH_4PF_6^-$ precipitated the PF_6^- salt which was recrystallised from water. The ^1H n.m.r. spectrum of $[Pt(L^3)](PF_6)_2$ in CD_3CN showed a complex unsymmetrical series of resonances so that a high degree of fluxionality, as suspected for $[Pt(L^1)_2](PF_6)_2$ seems to be ruled out. Cyclic voltammetry upon the $[Pt(L^3)]^{2+}$ cation in acetonitrile showed total inactivity over the solvent range, and so suggests a conformational barrier to stabilisation of $[Pt(L^3)]^{3+}$.

2.6 Mononuclear Pt(II) complexes incorporating one L^1 ligand

Wieghardt *et al.*[48] have reported the monomeric complexes (8), (9) and (10) by reaction of 1,4,7-triazacyclononane (L^4) with K_2PtCl_4 in a 1:1 molar ratio at 80°C in aqueous

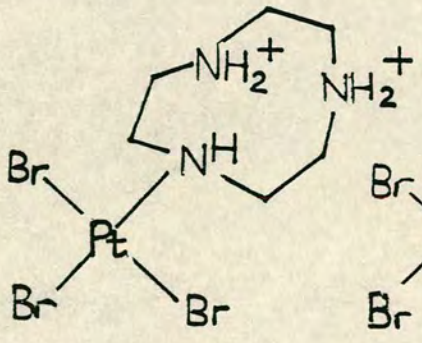

(8)

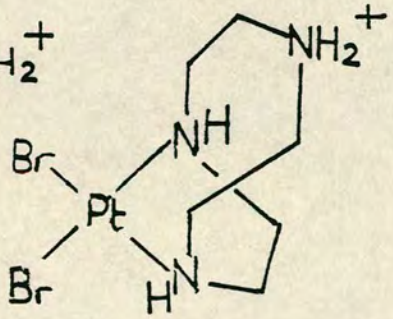

(9)

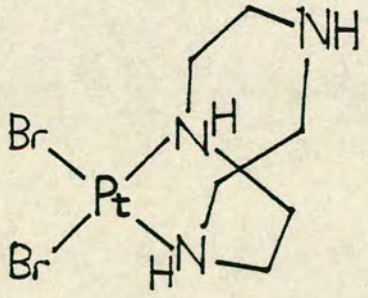

(10)

solution in the presence of Br^- ion at progressively higher pH values.

Reaction of L^1 with K_2PtCl_4 in refluxing acetonitrile/dichloromethane (v.v = 3:1) led to the formation of *cis*-$[Pt(L^1)Cl_2]$. Orange crystals of the pure product were obtained via recrystallisation from nitromethane. The complex was characterised by elemental analysis, ^1H n.m.r. and infra-red spectroscopy, the latter confirming the *cis* co-ordination in the complex (11) in which the ligand is essentially bidentate.

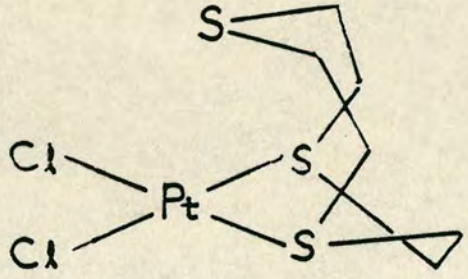

(11)

The degree of interaction of the remaining thia donor with the metal centre is not known, but by analogy with $[Pd(L^1)Cl_2]$ which has been crystallographically characterised (Chapter 3) a weak interaction may occur. If *cis*-$[Pt(L^1)Cl_2]$ is allowed to react with an excess of triphenyl phosphine in refluxing acetonitrile dichloromethane, the orange $[Pt(L^1)(PPh_3)_2]^{2+}$ cation is obtained. This could be trapped out as its PF_6^- salt and recrystallised from water to give crystalline $[Pt(L^1)(PPh_3)_2](PF_6)_2$. The ^1H n.m.r. spectrum of the salt in CD_3CN shows a complex but symmetrical series of resonances for the L^1 protons, and a rigid *cis* conformation in which the macrocycle is bidentate appears likely (12).

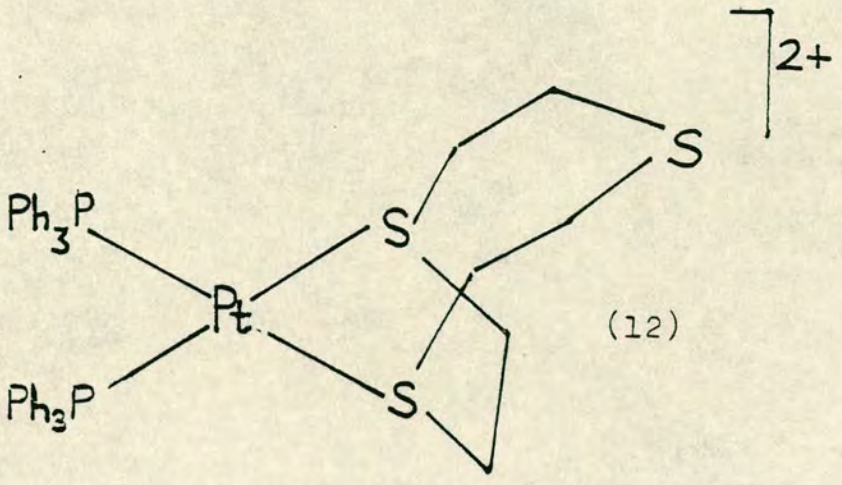

(12)

2.7 Summary

The structural and redox properties of the $[Pt(L^1)_2]^{2+}$ cation illustrates the relevance of the study of second and third row transition metal complexes with L^1 (1,4,7-trithiacyclanonone). Both the single crystal X-ray structure, and solution behaviour of the $[Pt(L^1)_2]^{2+}$ cation indicate the presence of a significant additional thia interaction to the 'PtS_4' square plane, probably as a consequence of the limited π bonding nature of the trithia ligand. Even more interesting is the remarkable stabilisation of the d^7 Pt(III), $[Pt(L^1)_2]^{3+}$ complex cation obtained either chemically or via electrogeneration. The long life time of the $[Pt(L^1)_2]^{3+}$ cation may enable future success in isolating and structurally characterising this cation via a single crystal X-ray diffraction study. The isolation of the d^6 $[Pt(L^1)_2]^{4+}$ cation further demonstrates the utility of L^1 to stabilise a range of metal oxidation states, and full characterisation of this complex cation, particularly via ^1H n.m.r. and diffraction studies, are clearly areas for future active research.

2.8 Experimental

Infra-red spectra (4000-250 cm^{-1}) were recorded on a Perkin-Elmer 548 spectrometer using the KBr disc method. ^1H n.m.r. spectra were obtained on Bruker WP80 and Bruker WP200 instruments operating at 80.13Hz and 200.13MHz respectively, and unless otherwise stated were run at room temperature. Electron impact mass spectroscopy was carried out using a Kratos MS902 spectrometer. Fast atom bombardment (f.a.b.) mass spectra were obtained in glycerol/dmf matrices on a Kratos MS50TC spectrometer. Electronic spectra were recorded using a Pye-Unicam SP8-400 spectrophotometer. Esr spectra were recorded on frozen glasses at 77K, using a Bruker ER200D X band spectrometer. Electrochemical measurements were performed on a Bruker E310 Universal Polarograph. All readings were taken using a three electrode potentiostatic system in acetonitrile containing 0.1M $TBAPF_6$ as supporting electrolyte. Cyclic voltammetric measurements were carried out using a double platinum electrode, and an Ag/Ag^+ reference electrode. All potentials are quoted vs ferrocene/ferrocenium ion (Fc/Fc^+) = 0V. Microanalysis were performed by the Chemistry Department, University of Edinburgh. All reactions were carried out using solvents of analar grade. Except where stated an inert atmosphere was not required.

Starting materials

Platinum(II) dichloride, $PtCl_2$ and potassium tetrachloroplatinate(II) K_2PtCl_4 were provided as generous loans from

Johnson-Matthey PLC.

Synthesis of 1,4,7-trithiacyclononane (L^1).

L^1 was prepared, using a modified procedure to that described by Sellmann and Zapf.[67] Instead of $(Me_4N^+)_2(^-S(CH_2)_2S(CH_2)_2S^-)$ the disodium salt $(Na^+)_2(^-S(CH_2)_2S(CH_2)_2S^-)$ was used. This salt was prepared by reaction of the parent dithiol $HS(CH_2)_2S(CH_2)_2SH$, with two molar equivalents of sodium ethoxide in ethanol. At no stage of the reaction prior to the formation of the air stable $[Mo(L^1)(CO)_3]$ were any of the air sensitive products isolated, the initial complex $[Mo(CO)_3(CH_3CN)_3]$ being reacted *in situ* with the disodium salt of the thiol, under strictly inert conditions. $[Mo(L^1)(CO)_3]$ was worked up, as according to the literature, to give L^1, which upon recrystallisation gave 5.4 g pure L^1. Overall yield 53%. Elemental analysis: Found C=40.1; H=6.84; calculated for $C_6H_{12}S_3$, C=40.1; H=6.71%. Infra-red, mass spectra and ^1H n.m.r. spectra (80MHz) all corresponded to the literature values.[64,67]

1,4,8,11-Tetrathiacyclotetradecane (L^2) was purchased from Aldrich and used without further purification. 1,4,7,10,13,16-Hexathiacyclooctadecane (L^3) was prepared via literature methods[138] or purchased from Aldrich.

Synthesis of complexes

$[Pt(L^1)_2](PF_6)_2$

K_2PtCl_4 (0.150 g 3.6×10^{-4}mol) was reacted with L^1

(0.140 g 7.8 x 10^{-4}mol) in water/methanol (v:v = 1:1 30 ml) under reflux for 1 hr to yield an orange solution of the complex cation $[Pt(L^1)_2]^{2+}$. Addition of excess NH_4PF_6 followed by cooling of the solution gave an orange-yellow solid which could be recrystallised from water (*ca.* 10 ml) to give orange crystals of $[Pt(L^1)_2](PF_6)_2$ in 70% yield.

Elemental analysis: Found C=16.9; H=2.81; S=23.58, 23.24% (Butterworth Co); Calculated for $[Pt(L^1)_2](PF_6)_2$ C=17.04; H=2.86; S=22.75%. Infra-red spectrum (L^1 bands) 2990, 2946, 1442, 1410, 1307, 1289, 1184, 1157, and 1129 cm^{-1}. Mass spectrum (f.a.b.) M^+ = 555, $[Pt(L^1)_2]^+$ (^{195}Pt). Electronic spectrum: λ_{max} = 432 nm (ε = 95 M^{-1} cm^{-1}) 278 (6935) 245 (12850) CH_3CN and H_2O (Figure 2.2.I). ^1H n.m.r. (CD_3CN 80,200MHz) δ_H = 3.31 (24H s $CH_2(L^1)$); ^{195}Pt satellites, $^3J_{PtH}$(av) = 24.5Hz at both 80 and 200MHz (Figure 2.2.II).

$[Pt(L^1)_2](BF_4)_2$ could be prepared as orange crystals using a similar procedure but via addition of $NaBF_4$ to the $[Pt(L^1)_2]^{2+}$ cation. Elemental analysis: Found C=19.4, 19.5; H=3.26, 3.30%; Calculated for $[Pt(L^1)_2](BF_4)_2$ C=19.76; H=3.32%. The BPh_4^- salt of $[Pt(L^1)_2]^{2+}$ was prepared via addition of $NaBPh_4$. Recrystallisation from a nitromethane/toluene or nitromethane/ether solution gave crystals of $[Pt(L^1)_2](BPh_4)_2.2CH_3NO_2$. These large red-pink crystals slowly effloresced on standing to give the yellow $[Pt(L^1)_2](BPh_4)_2$ species. Elemental analysis: Found C=60.0; H=5.36%: Calculated for $[Pt(L^1)_2](BPh_4)_2$

C=60.34; H=5.40%. ^{1}H n.m.r. (CD_3NO_2 80MHz) δ_H = 3.34 (24H s $CH_2(L^1)$); ^{195}Pt satellites, $^{3}J_{PtH}$ = 24Hz. δ_H = 6.9-7.5 (40H m $CH(BPh_4^-)$).

Generation of $[Pt(L^1)_2]^{3+}$

a) Controlled potential electrolysis

Electrogeneration of $[Pt(L^1)_2]^{3+}$ was performed via controlled pontential electrolysis of $[Pt(L^1)_2](PF_6)_2$ (50 mg) in acetonitrile at a potential of +0.5V under a nitrogen atmosphere. The yellow green $[Pt(L^1)_2]^{3+}$ cation, λ_{max} = 401 nm (ε = 3030 $M^{-1}cm^{-1}$) 271 (*ca.*∿13,000), is stable in dry acetonitrile for a number of hours. Esr spectrum (CH_3CN 77K) $g_\perp$ = 2.044 $g_\parallel$ = 1.987 $A_\perp$∿30G $A_\parallel$ = 85G (Gain = 3.2 x 10^2) (Figure 2.4.II).

b) Chemical oxidation

Treatment of $[Pt(L^1)_2](PF_6)_2$ (20 mg) with 70% aqueous $HClO_4$ (5 ml), led to formation of $[Pt(L^1)_2]^{3+}$ after *ca.*90 minutes at room temperature: Electronic spectrum: λ_{max} = 401 nm (ε = 4390 $M^{-1}cm^{-1}$) 271 (13,650). Esr spectrum (70% $HClO_4$ 77K) $g_\perp$ = 2.039 $g_\parallel$ = 1.987 $A_\perp$ = 44G $A_\parallel$ = 90G (^{195}Pt I = ½ 33.8%) A_H ∿5G (Gain = 4 x 10^2) (Figures 2.4.III, IV).

$[Pt(L^1)_2]^{4+}$

A white microcrystalline solid, believed to contain the $[Pt(L^1)_2]^{4+}$ cation, was obtained upon prolonged oxidation of $[Pt(L^1)_2]^{2+}$ in 70% aqueous $HClO_4$. The dry

solid was both air and moisture sensitive with reduction to $[Pt(L^1)_2]^{2+}$ occurring on heating in water.

Electronic spectrum for $[Pt(L^1)_2]^{4+}$, λ_{max} = 289 nm (17,800 $M^{-1}cm^{-1}$) (Figure 2.4.V/70% aqueous $HClO_4$). Esr spectrum: silent.

cis-$[Pt(L^1)Cl_2]$

$PtCl_2$ (0.120 g, 4.5×10^{-4}) and L^1 (0.082 g, 4.5×10^{-4}mol) were reacted in acetonitrile/dichloromethane (v:v = 3:1 60 ml) under reflux for 24 hours in a nitrogen atmosphere. The yellow solution was filtered hot and allowed to cool. Addition of diethyl ether afforded the product as a yellow solid. Recrystallisation from nitromethane yielded orange crystals which were dried *in vacuo:* Yield = 60%. Elemental analysis: Found C=16.0; H=2.7%. Calculated for *cis*-$[Pt(L^1)Cl_2]$ C=16.1; H=2.7%. Infra-red spectrum 2960, 2930, 1438, 1404, 1305, 1281, 1266, 1248, 1182, 1144, 932, 886, 806, 318 and 304 cm^{-1}. ^1H n.m.r. spectrum (d^6 DMSO 80MHz) δ_H = 3.28 (12H br s $CH_2(L^1)$).

$[Pt(L^1)(PPh_3)_2](PF_6)_2$

$[Pt(L^1)Cl_2]$ (0.080 g, 1.79×10^{-4}mol) and PPh_3 (0.094 g, 3.6×10^{-4}mol) were refluxed in acetonitrile (20 ml) for 30 minutes to yield an orange solution of $[Pt(L^1)(PPh_3)_2]^{2+}$. The solution was filtered, evaporated to dryness and redissolved in a minimum quantity of methanol. Addition of NH_4PF_6 afforded yellow crystals of $[Pt(L^1)(PPh_3)_2](PE_6)_2$ in 70% yield. Elemental analysis: Found C=42.1 H=3.5%;

Calculated for $[Pt(L^1)(PPh_3)_2](PF_6)_2$ C=42.4; H=3.6%. Infra-red spectrum, 3080, 1480, 1435, 1410, 1095, 995, 840, 753, 745, 597, 554, 539, 522, 510 and 493 cm^{-1}. ^1H n.m.r. spectrum (CD_3CN 80MHz) δ_H = 2.2-2.8 (12H m CH_2 (L^1)), 7.4-7.5 (40H m $CH(BPh_4^-)$).

$[Pt(L^2)](PF_6)_2$ (L^2 = 1,4,8,11-tetrathiacyclotetradecane)

Reaction of K_2PtCl_4 (0.120 g, 2.9 x 10^{-4}mol) with L^2 (0.085 g, 3.2 x 10^{-4}mol) in refluxing acetonitrile/dichloromethane (v:v = 3:1 20 ml) for 4 hours resulted in the formation of the off-white $[Pd(L^2)]Cl_2$, which was washed with water, methanol and dichloromethane. The salt was dissolved in a minumum of hot water (20 ml) and NH_4PF_6 added to precipitate the PF_6^- salt. Colourless crystals of pure $[Pt(L^2)](PF_6)_2$ were obtained on recrystallisation from water. Later syntheses used water/methanol as the initial reaction solvent (as for the $[Pt(L^1)_2]^{2+}$ complexes) which led to the product being obtained more efficiently. Yield = 60%. Elemental analysis: Found C=15.9; H=2.68%; Calculated for $[Pt(L^2)](PF_6)_2$ C=15.94; H=2.68%. Infra-red spectrum: (L^2 bands). 3000, 2939, 2910, 2885, 2815, 1423, 1409, 1287, 1208 and 1138 cm^{-1}. Mass spectrum (f.a.b.) M^+ = 609 $[Pt(L^2)](PF_6)^+$, 464 $[Pt(L^2)]^+$. ^1H n.m.r. spectrum (CD_3CN 80MHz) δ_H = 2.8-3.7 (20H CH_2 (L^2)).

$[Pt(L^3)](PF_6)_2$ (L^3 = 1,4,7,10,13,16-hexathiacyclooctadecane)

Reaction of K_2PtCl_4 (0.100 g, 2.4 x 10^{-4}mol) with L^3 (0.067 g, 2.5 x 10^{-4}mol) led to the formation of $[Pt(L^3)]^{2+}$

after *ca.* 2 hrs in refluxing water/methanol (v:v = 1:1 30 ml). Addition of a large excess of NH_4PF_6 selectively precipitated the PF_6^- salt which could be recrystallised from water/acetonitrile (v:v = 1:1 30 ml) to give a pale yellow solid. Yield 40%. Elemental analysis: Found C=16.8; H=2.83%. Calculated for $[Pt(L^3)](PF_6)_2$ C=17.04; H=2.83%. Infra-red spectrum (L^3 bands). 2995, 2948, 1422, 1287, 1260, 1176, 1132 and 1120 cm^{-1}. ^1H n.m.r. spectrum (CD_3CN 80MHz) δ_H = 2.8-3.7 ppm (24H br m $CH_2(L^3)$).

CHAPTER 3

1,4,7-Trithiacyclononane Complexes of Palladium

3 1,4,7-Trithiacyclononane Complexes of Palladium

3.1 Introduction

The results obtained in the previous chapter clearly indicated that a study of palladium complexes of 1,4,7-trithiacyclononane - in particular the $[Pd(L^1)_2]^{2+}$ cation, should be undertaken.

For $[Pt(L^1)_2]^{2+}$ a one electron oxidation to $[Pt(L^1)_2]^{3+}$ is observable both chemically and electrochemically, with a second oxidation to $[Pt(L^1)_2]^{4+}$ also observable in concentrated perchloric acid. In the Pd system both the (II)/(III) and (III)/(IV) couples would be expected to be less readily attainable. However, this may lead to increased stabilisation of the $[Pd(L^1)_2]^{3+}$ cation, since further oxidation for the hexathia complex to $[Pd(L^1)_2]^{4+}$ may be highly disfavoured. Additionally, a comparable study of the reductive electrochemistry of $[Pd(L^1)_2]^{2+}$ and $[Pt(L^1)_2]^{2+}$ may show that the $[Pd(L^1)_2]^{+}$ cation may be significantly more stable than the highly transient reduction product for the third row transition metal.

The chemistry of palladium is even more dominated by the +2 oxidation state than for platinum. Pd(0) is only observed for phosphine complexes[139] whilst Pd(IV) is generally only observed in complexes of the most electronegative elements[140] eg $PdCl_6^{2-}$. Generally the complexes of Pd(IV) are of marginal stability and are readily reduced eg $[Pd(py)_2Cl_4]$ which readily loses halogen in moist air.[141] As for Pt, the (I) and (III) oxidation states are very poorly

defined for monomeric complexes.[142]

Pd(II) complexes, as with their Pt analogues, show predominantly square planar co-ordination about the metal centre. Additional co-ordination to the Pd(II) centre however does occur in some complexes, often involving a degree of π bonding. The macrocyclic (1),[86] (2)[143] or tripod (3)[144] complexes shown below represent just three of a steadily increasing number of pentaco-ordinate Pd(II) systems.[143-146]

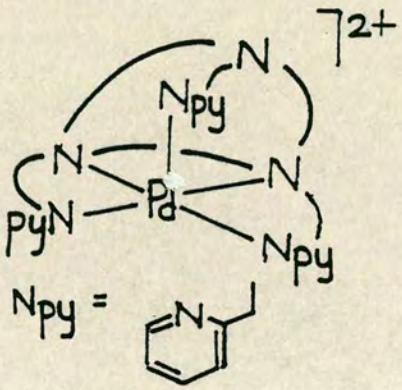

(1)

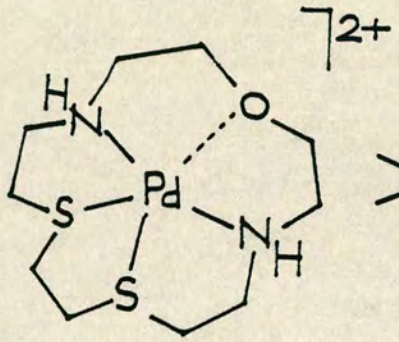

(2)

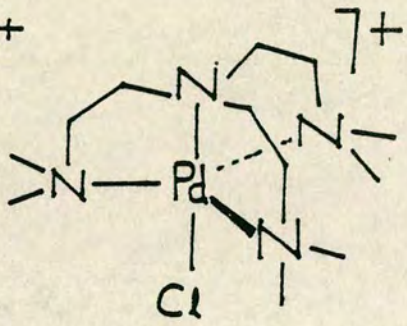

(3)

The observation of additional thia co-ordination in $[Pt(L^1)_2]^{2+}$ leading to a distorted square pyrimidal structure, led us to the expectation of a novel co-ordination geometry also around $[Pd(L^1)_2]^{2+}$.

Results and Discussion

3.2 Synthesis and characterisation of $[Pd(L^1)_2]^{2+}$

Reaction of K_2PdCl_4 with two molar equivalents of 1,4,7-trithiacyclononane (L^1) in refluxing water/methanol (v:v = 1:1) for 30 minutes leads to the formation of a blue solution from which the complex cation $[Pd(L^1)_2]^{2+}$

could be isolated as its PF_6^- or BF_4^- salt. Recrystallisation from water led to the formation of well formed crystals of $[Pd(L^1)_2](PF_6)_2$ or $[Pd(L^1)_2](BF_4)_2$. In addition to infra-red and microanalytical data the identity of the $[Pd(L^1)_2]^{2+}$ cation was confirmed by f.a.b. mass spectroscopy which showed peaks at $M^+ = 610$, 465 for $[Pd(L^1)_2](PF_6^-)^+$ and $[Pd(L^1)_2]^+$ respectively. A variable concentration conductivity study of $[Pt(L^1)_2](PF_6)_2$ in nitromethane gave a value of $\Lambda_o - \Lambda_e$ vs $C_e^{\frac{1}{2}}$ of 485 $\Lambda_o = 96.3$, consistent for a 2:1 electrolyte.[147]

As in $[Pt(L^1)_2]^{2+}$ additional thia co-ordination to the 'MS_4' square plane is suggested by the electronic spectrum, and possibly ^1H n.m.r. data. $[Pd(L^1)_2](PF_6)_2$ dissolves readily in acetonitrile or nitromethane to give blue solutions (λ_{max} = 615 nm (ε = 54 $M^{-1}cm^{-1}$), 296 (15,100), CH_3CN / H_2O: Figure 3.2.I) indicating a substantial modification to the relative d-orbital energy levels occurring in this system. The ^1H n.m.r. spectrum of $[Pd(L^1)_2]^{2+}$ in CD_3CN (Figure 3.2.II(a)) both at room temperature and -35°C shows only a sharp singlet ($\delta_H = 3.30$) - probably as a result of a high degree of fluxionality in the system in which the chemical and magnetic inequivalence of the protons is lost on the n.m.r. timescale. An alternative explanation for the ^1H n.m.r. spectrum is that the inequivalent protons have an identical chemical shift. Low temperature ^1H n.m.r. studies are thus required to conclusively explain the dynamics of the system. Indeed in d^6-acetone (Figure 3.2.II(b)) a complex second order signal is observed for

Figure 3.2.I Electronic spectrum of $[Pd(L^1)_2]^{2+}$ in a) H_2O/ $\sim 10^{-4}$M; b) CH_3CN/ $\sim 10^{-2}$M

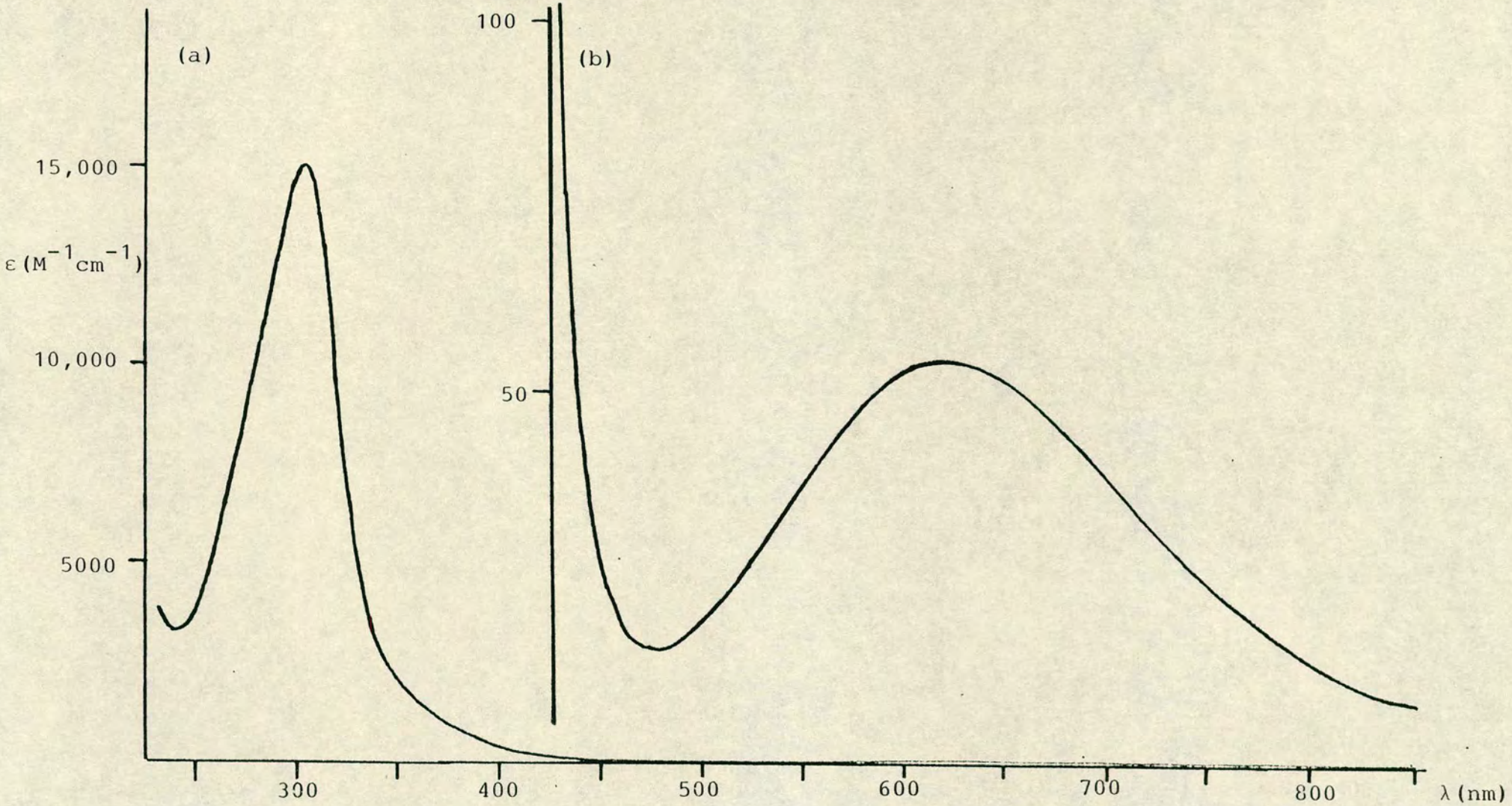

Figure 3.2.II ^1H n.m.r. of $[Pd(L^1)_2](PF_6)_2$ in a) CD_3CN; b) d^6-acetone

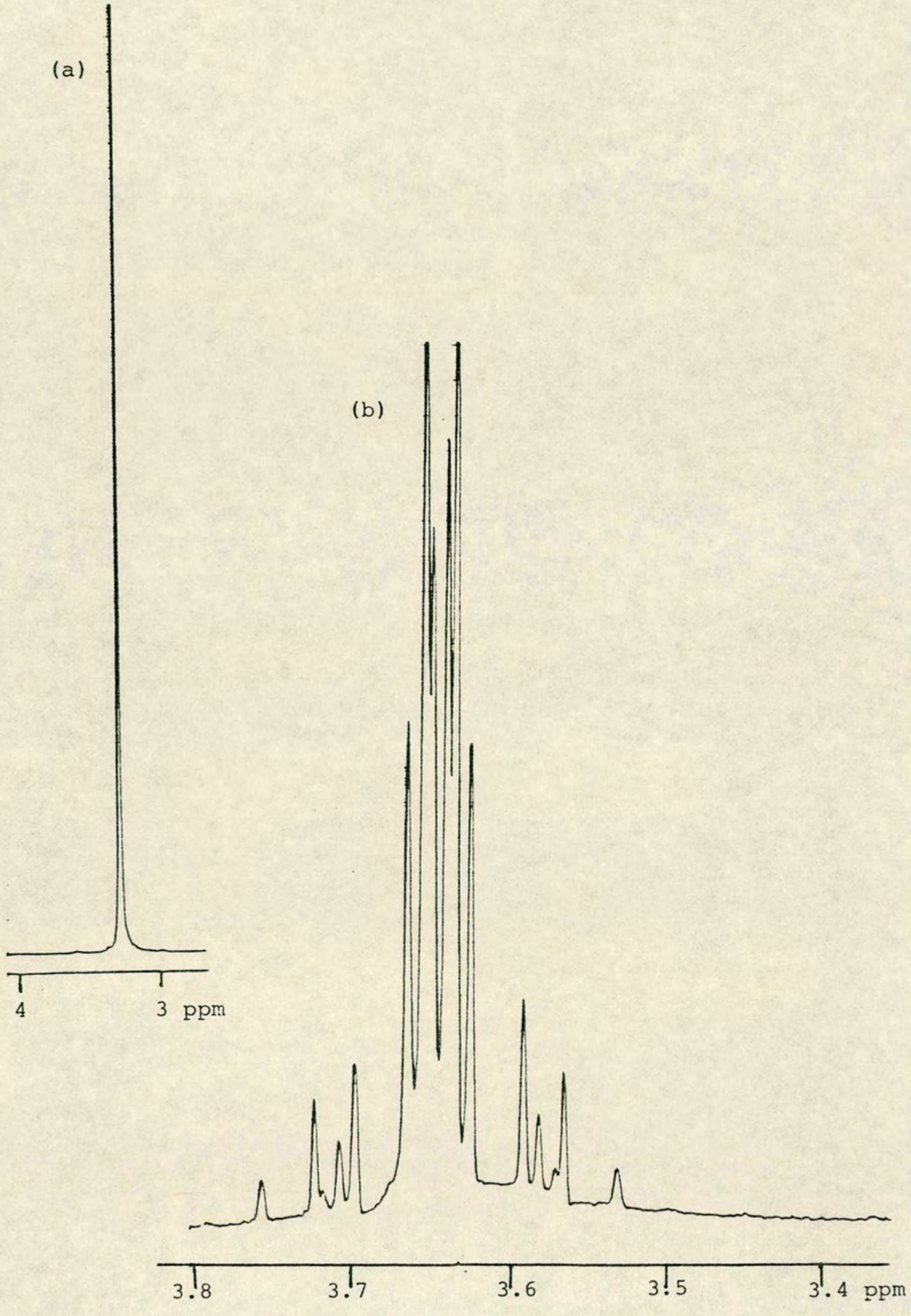

the ligand protons, possibly as a result of solvent interaction with the complex cation. In view of the novel electronic spectra, and the observation of an unusual geometry about $[Pt(L^1)_2]^{2+}$ a single crystal X-ray diffraction study was undertaken upon $[Pd(L^1)_2](PF_6)_2$.

3.3 The single crystal X-ray structure of $[Pd(L^1)_2](PF_6)_2$

Crystal data: $C_{12}H_{24}PdS_6^{2+}.2PF_6^-$. M = 756.9 monoclinic. Space group C2/c, a = 17.879(8), b = 15.627(13), c = 11.476(8) Å, β = 125.92(4)°, U = 2597 Å^3, D_c = 1.936 g cm^3, D_e = 1.96 g cm^{-3}, Z = 4. At convergence R,R_w = 0.0565, 0.0654 for 1153 data.

A summary of selected bond lengths and angles are given in Table 3.3.I. A view of the $[Pd(L^1)_2]^{2+}$ cation is shown in Figure 3.3.II. The Pd(II) ion occupies an inversion centre, and is co-ordinated by an approximate square plane of four thia donors from the two centrasymmetrically related molecules of L^1 (Pd-S_{eq} = 2.332(3), 2.311(3) Å < $S_{eq}PdS_{eq}$ = 88.63(11)°). The remaining similarly related sulphur atoms participate in significant apical interactions to give overall a tetragonally distorted octahedral stereochemistry about Pd(II) (Pd.S_{ax} = 2.952(4) Å < $S_{ax}PdS_{eq}$ = 83.13(10), 83.24(11)°. To our knowledge this structure represents the closest approach to octahedral geometry for any Pd(II) complex.

The complex $[Pd(2\text{-}(2'\text{-thienyl})pyridine)_2Br_2]$ (4)[148] shows a weak Pd..S interaction at 3.05 Å while in the highly

Table 3.3.I Important bond lengths and angles (with esd's) for $[Pd(L^1)_2]^{2+}$

Bond lengths (Å)

Pd -S(1)	2.952(4)	C(3)-S(4)	1.854(14)
Pd -S(4)	2.332(3)	S(4)-C(5)	1.812(13)
Pd -S(7)	2.311(3)	C(5)-C(6)	1.491(19)
S(1)-C(2)	1.799(14)	C(6)-S(7)	1.837(15)
S(1)-C(9)	1.809(15)	S(7)-C(8)	1.795(14)
S(2)-C(3)	1.467(19)	C(8)-C(9)	1.515(20)

Bond angles (degrees)

S(1)-Pd-S(4)	83.13(10)	Pd-S(4)-C(3)	108.2(4)
S(1)-Pd-S(7)	83.24(11)	Pd-S(4)-C(5)	99.5(4)
S(4)-Pd-S(7)	88.63(11)	Pd-S(7)-C(6)	104.5(5)
Pd-S(1)-C(2)	90.3(5)	Pd-S(7)-C(8)	104.5(5)
Pd-S(1)-C(9)	94.6(5)		

Figure 3.3.II View of the single crystal X-ray structure of $[Pd(L^1)_2]^{2+}$

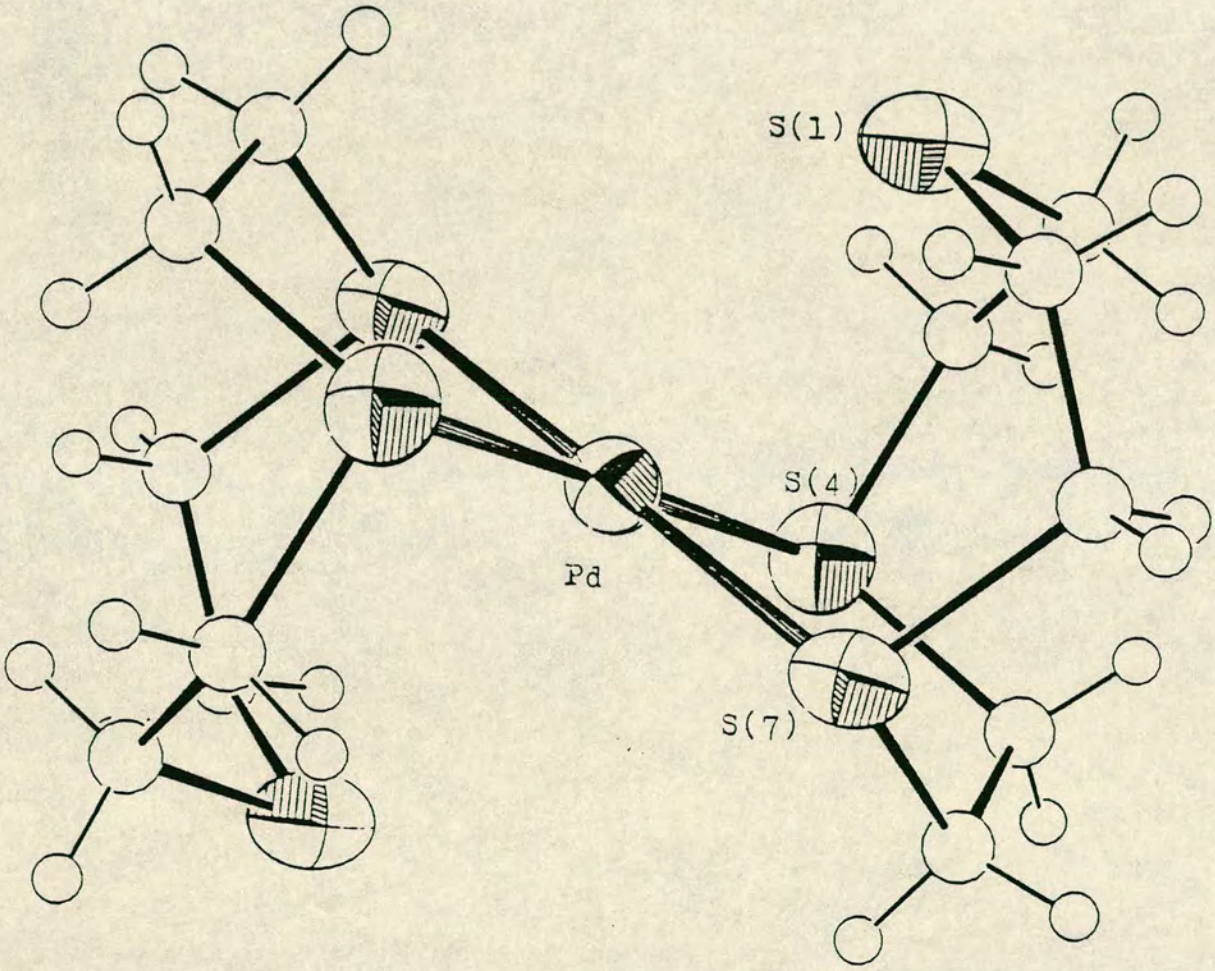

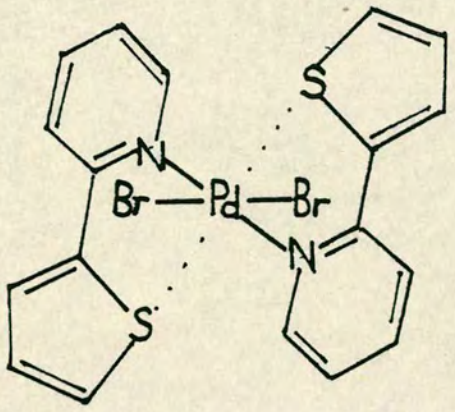

(4)

distorted octahedral complex $[Pd(L^3)](BPh_4)_2$ [137]

$Pd\cdot\cdot S_{ax}$ = 3.273 Å - essentially non bonding.

The structure of $[Pd(L^1)_2]^{2+}$, best described as showing '4+2' co-ordination, differs substantially from the $[Pt(L^1)_2]^{2+}$ species, which shows '4+1' co-ordination around the metal centre. A direct comparison of the apical thia interactions of the two cations suggests that in $[Pt(L^1)_2]^{2+}$ one of the apical interactions [Pt-S_{ax} = 2.885(7)) is somewhat stronger than the interaction in the Pd system (Pd-S_{ax} = 2.952(4) Å), but at the expense of the other, for which no interaction with the metal centre is evident (Pt···S = 4.04 Å). The geometry about the Pd(II) centre in $[Pd(L^1)_2]^{2+}$ is consistent with the observed electronic spectrum for the complex. The position and intensity of visible absorption (λ_{max} = 615 nm (ε = 54 M^{-1} cm^{-1}) is expected for a d-d transition in the modified ligand field (5) caused by the apical thia interaction.

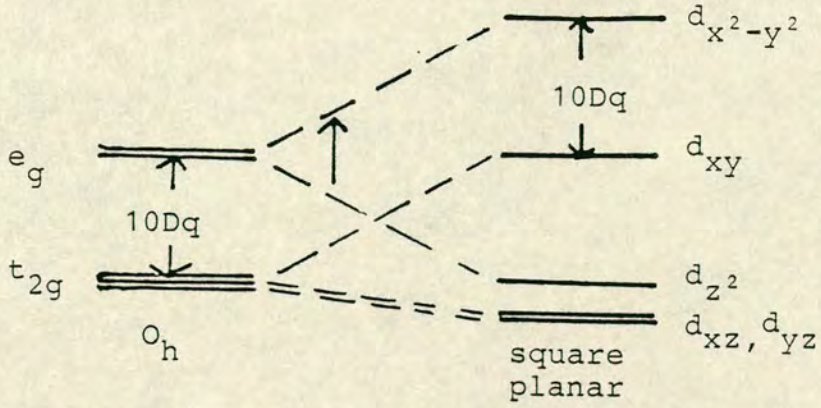

(5)

Independent studies by Wieghardt *et al.*[149] upon the reflectance spectra of solid $[Pd(L^1)_2](PF_6)_2$ shows a shift in the visible absorption maximum to λ_{max} = 575 nm suggesting that a slight modification to the structure (and the possibility of fluxionality) may arise in solution.

3.4 Redox chemistry of $[Pd(L^1)_2]^{2+}$

In view of the rich redox chemistry observed for the $[Pt(L^1)_2]^{2+}$ cation, it was clearly important to monitor the redox chemistry of the $[Pd(L^1)_2]^{2+}$ cation. Cyclic voltammetry of $[Pd(L^1)_2](PF_6)_2$ in acetonitrile shows a chemically reversible oxidation (Figure 3.4.I - all potentials quoted relative to Fc/Fc^+ = 0) with Epa = +0.65V, Epc = +0.56V ΔE = 84 mV $E_{\frac{1}{2}}$ = +0.605V. A second ill-defined oxidation wave was observed at +1.2V and was essentially irreversible. An irreversible reduction wave is also seen which became chemically reversible only at -40°C at high scan rates (Figure 3.4.II), with $E_{\frac{1}{2}}$ = -0.85V ΔE = 85 mV.

The reversible Pd(II)/(III) couple (as confirmed by quantitative measurements), $E_{\frac{1}{2}}$ = +0.605V, can be compared with the analogous processes for the nickel and platinum analogues which occur at +0.97 [31] and +0.385V respectively.

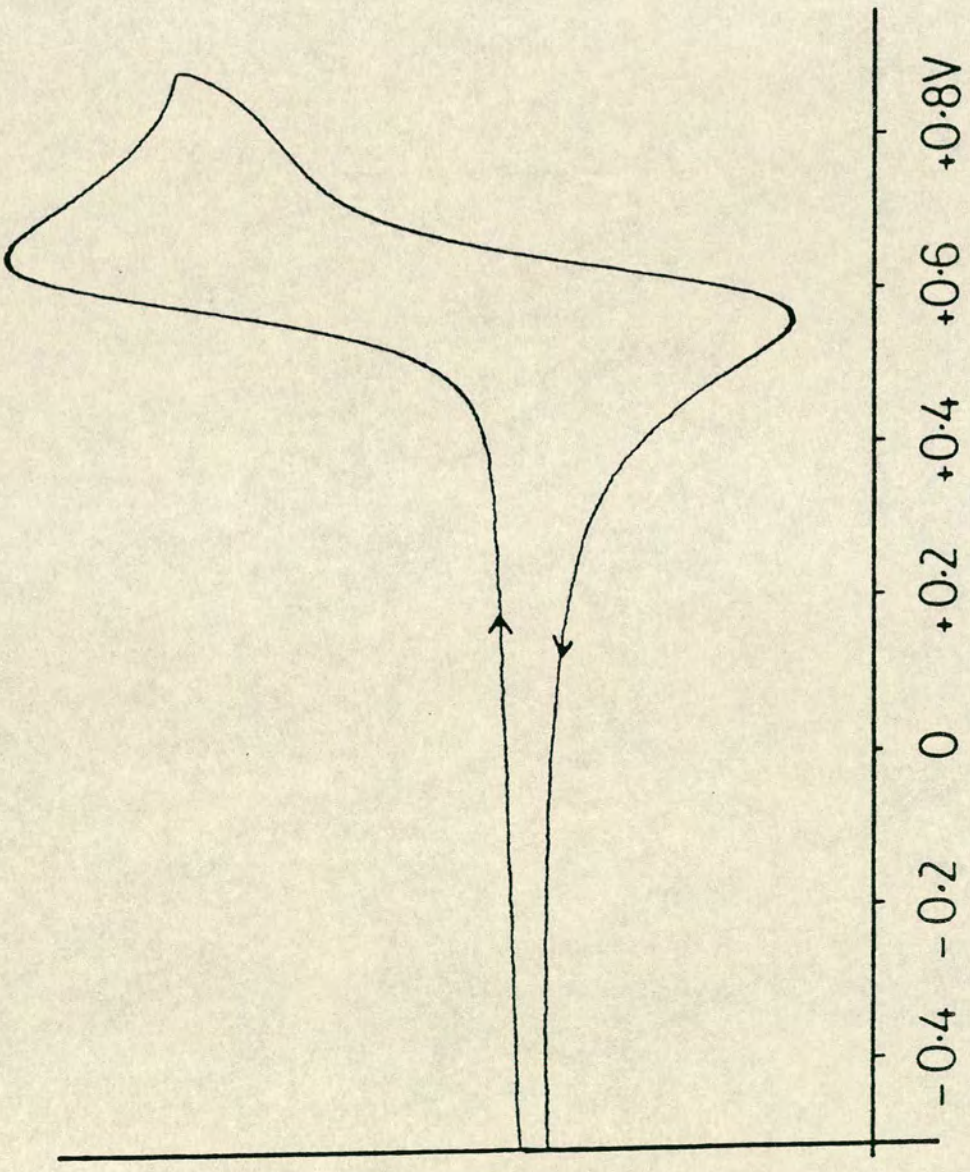

Figure 3.4.I Oxidative cyclic voltammogram of $[Pd(L^1)_2]^{2+}$ in $CH_3CN/0.1M\ TBAPF_6$

Figure 3.4.II Reductive cyclic voltammogram of $[Pd(L^1)_2]^{2+}$ in CH_3CN/0.1M $TBAPF_6$ at 233K

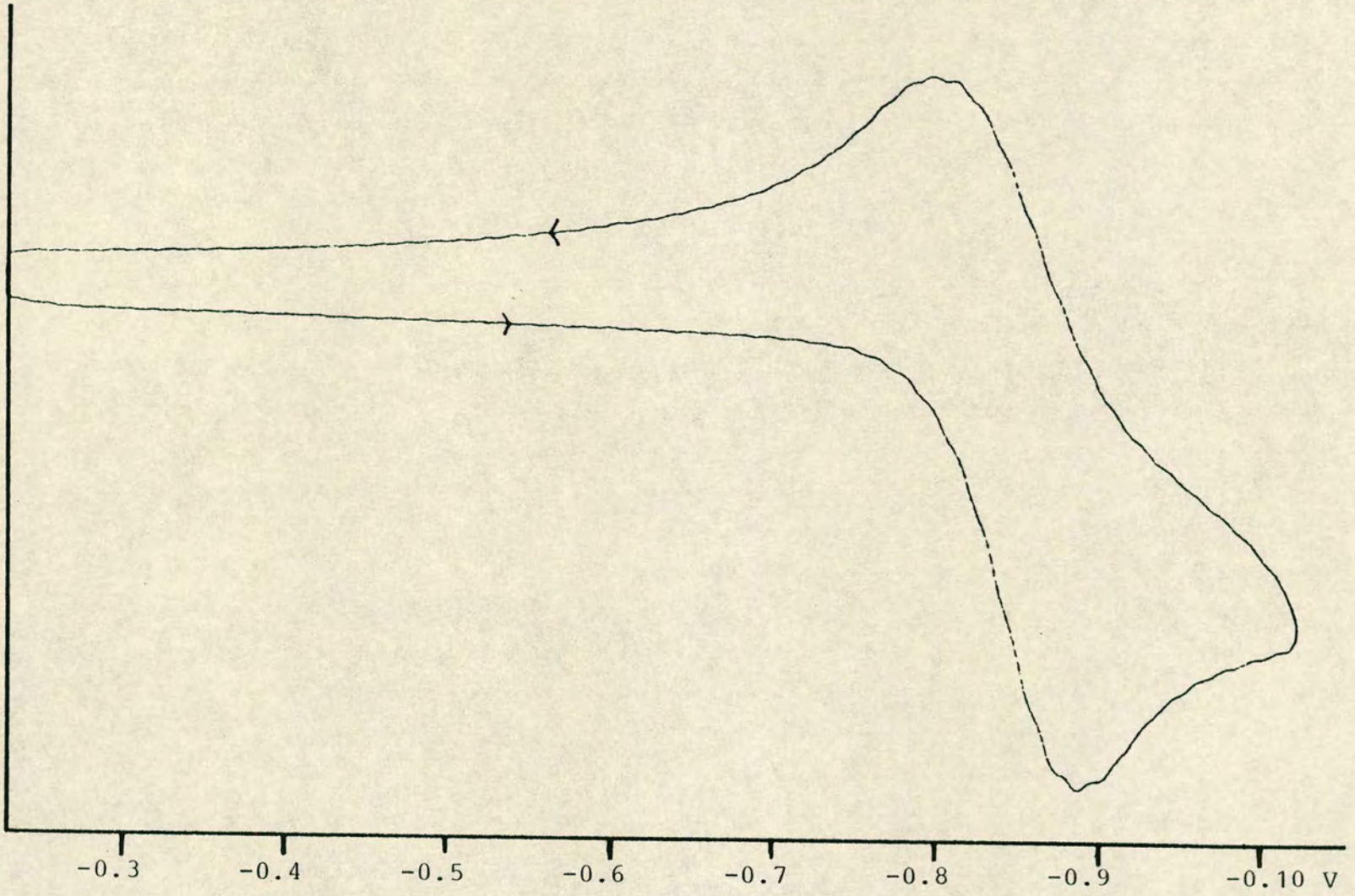

Although oxidation for $[Pd(L^1)_2]^{2+}$ occurs at a higher potential than for $[Pt(L^1)_2]^{2+}$ the process is still essentially metal based. A ligand based oxidation seems unlikely, on the basis that oxidation of the free ligand only occurs at +0.99V [31], and that for the recently characterised $[Ru(L^1)_2]^{2+}$ cation[150] redox stability is shown up to +1.4V.

Controlled potential electrolysis of a solution of $[Pd(L^1)_2]^{2+}$ in acetonitrile at +0.7V generated an intensely orange-red esr active solution (λ_{max} = 477 nm (ε = 5340 M^{-1} cm^{-1}), 341 (16100), 230 ($\sim$10,000)) in an isosbestic manner (λ_{iso} = 610, 315, 260, 214 nm). This electrogenerated solution was highly stable, and could be cleanly reconverted back to the $[Pd(L^1)_2]^{2+}$ cation, in an isosbestic manner. As with the $[Pt(L^1)_2]^{2+/3+}$ system the stability of the oxidised form enabled quantitative measurements of the concentration of oxidised and reduced forms to be measured at varying electrogeneration potentials, and this confirmed the oxidation to be a one electron process.

The intense charge transfer band in $[Pd(L^1)_2]^{3+}$, centred at 477 nm is probably a ligand (n) $\rightarrow$ metal (eg^*) transition, as observed in the related Pt system.

Acetonitrile solutions of the $[Pd(L^1)_2]^{3+}$ cation were observed to slowly decompose on standing to the $[Pd(L^1)_2]^{2+}$ cation in an isosbestic manner. Chemical oxidants such as Ce^{4+}, NO^+ or $S_2O_8^{2-}$ readily generated the $[Pd(L^1)_2]^{3+}$ cation, but the most effective means was by use of 60-70% $HClO_4$ in which the $[Pd(L^1)_2]^{3+}$ cation generated was stabilised indefinitely. In 60% $HClO_4$ the oxidation of

Figure 3.4.III Electronic spectrum showing oxidation of $[Pd(L^1)_2]^{2+}$ to $[Pd(L^1)_2]^{3+}$ in 60% aqueous $HClO_4$ solution

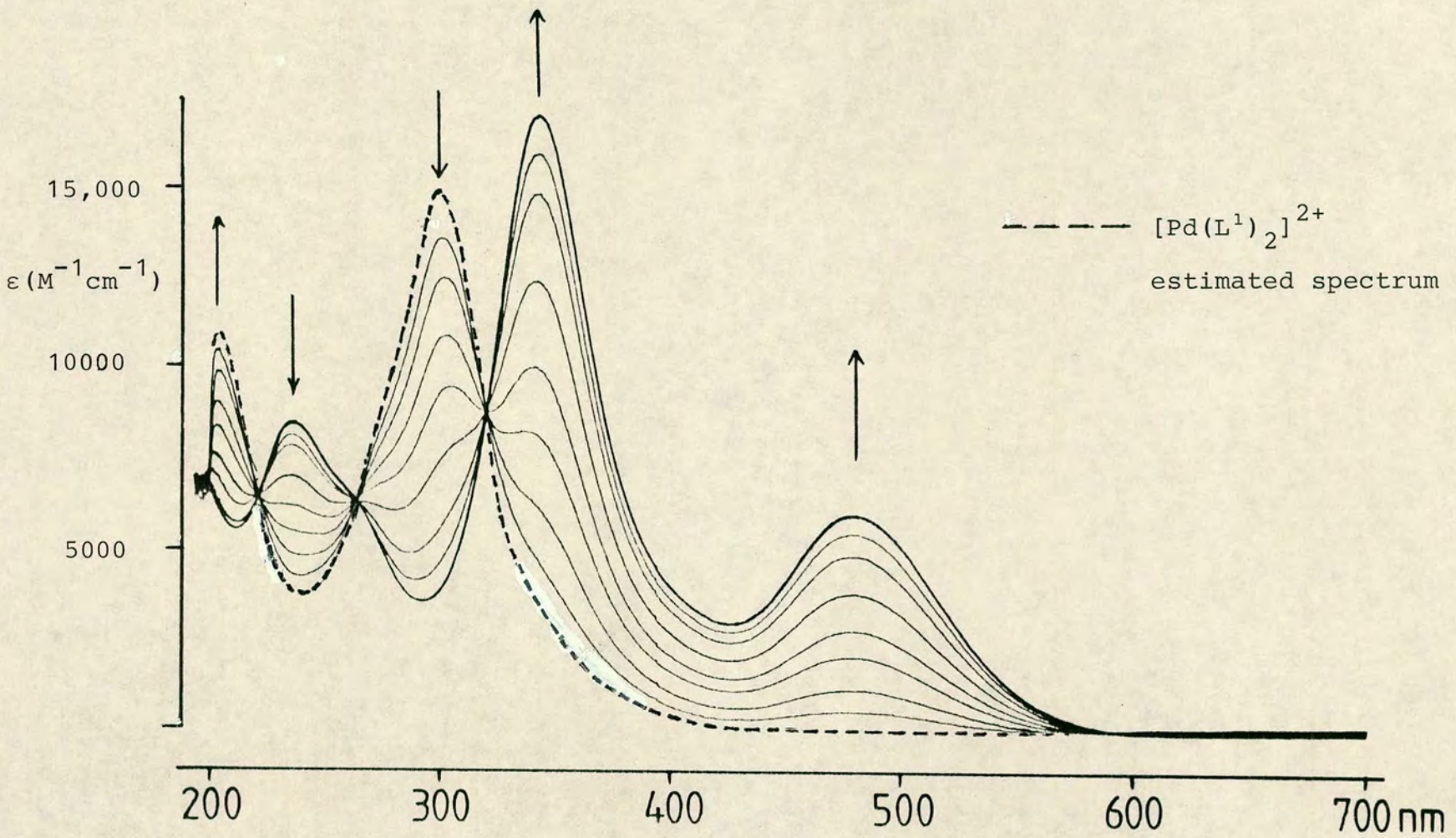

$[Pd(L^1)_2]^{2+}$ to $[Pd(L^1)_2]^{3+}$ (λ_{max} = 477 nm (ε = 5,800 M^{-1} cm^{-1}) 340 (16,130) 230 (7650)) could be monitored by observation of the electronic spectrum with time (Figure 3.4.II). The isosbestic conversion (λ_{iso} = 587, 315, 257 and 215 nm) occurred over *ca.* 30 minutes using a concentration of $\sim 10^{-4}$M $[Pd(L^1)_2](PF_6)_2$ in the oxidising medium. The electronic spectrum of the oxidised product was essentially identical to that for the electrogenerated $[Pd(L^1)_2]^{3+}$ cation in acetonitrile.

3.5 E.s.r. studies of $[Pd(L^1)_2]^{3+}$

Both electrogenerated acetonitrile solutions of $[Pd(L^1)_2]^{3+}$ and 70% aqueous perchloric acid solutions of the same species showed intense frozen glass esr spectra. A frozen acetonitrile solution of freshly electrogenerated $[Pd(L^1)_2]^{3+}$ showed a strong anisotropic broadened signal (Figure 3.5.I) with $g_{\perp}$ = 2.048 $g_{\parallel}$ = 2.008 g_{av} = 2.032, characteristic of a paramagnetic species in which the unpaired electron density primarily resides on the metal centre.[123]

Allowing complete oxidation of 10^{-2}M solutions of $[Pd(L^1)_2]^{2+}$ in 70% aqueous perchloric acid at 50°C for four hours, led to complete conversion to the $[Pd(L^1)_2]^{3+}$ cation. A frozen glass esr spectrum (Figure 3.5.II) of this shows a substantially improved resolution relative to the electrogenerated species. The $g_{\perp}$ and $g_{\parallel}$ components of the signal are now much more distinct, with $g_{\perp}$ = 2.049 $g_{\parallel}$ = 2.009.

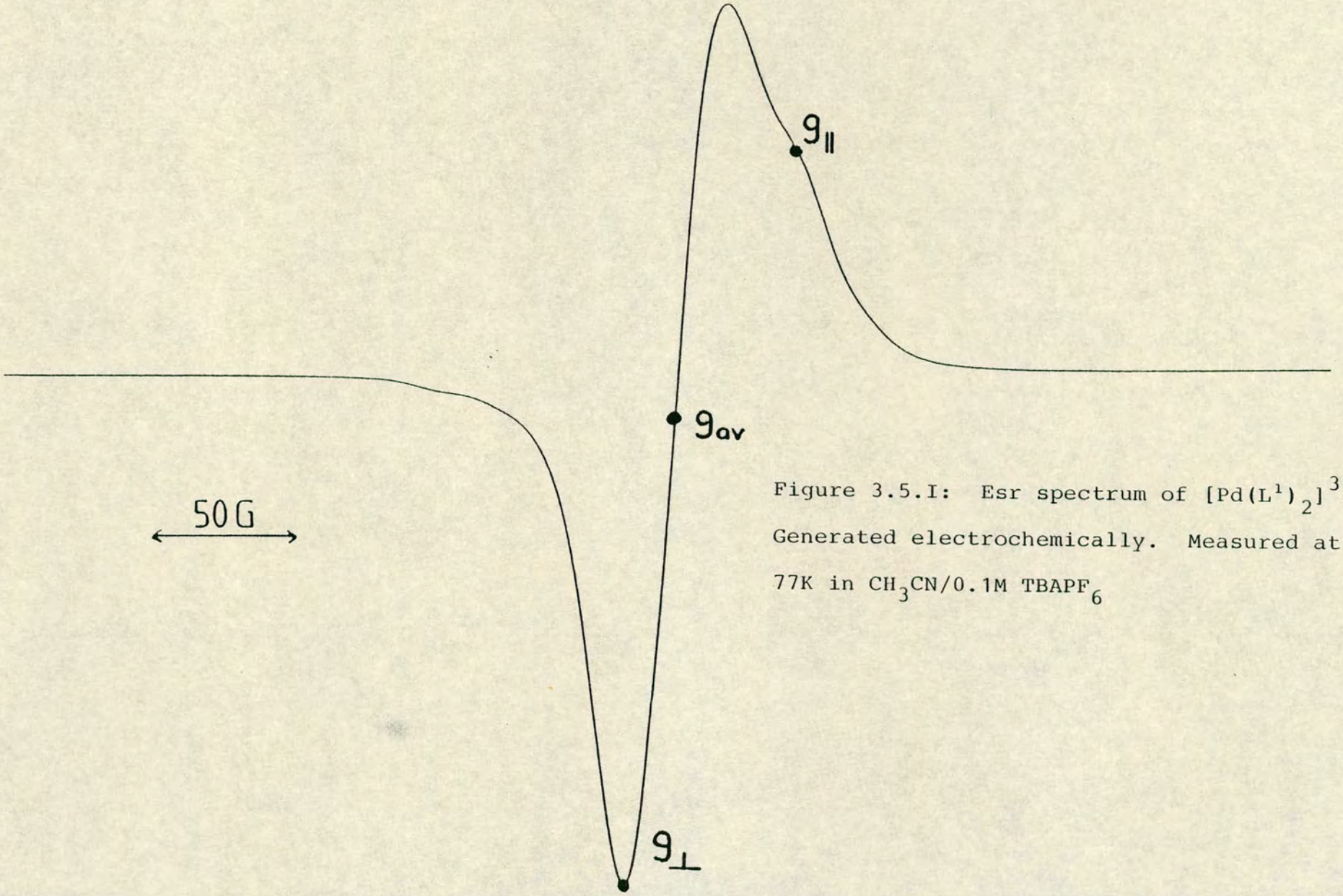

Figure 3.5.I: Esr spectrum of $[Pd(L^1)_2]^{3+}$ Generated electrochemically. Measured at 77K in CH_3CN/0.1M $TBAPF_6$

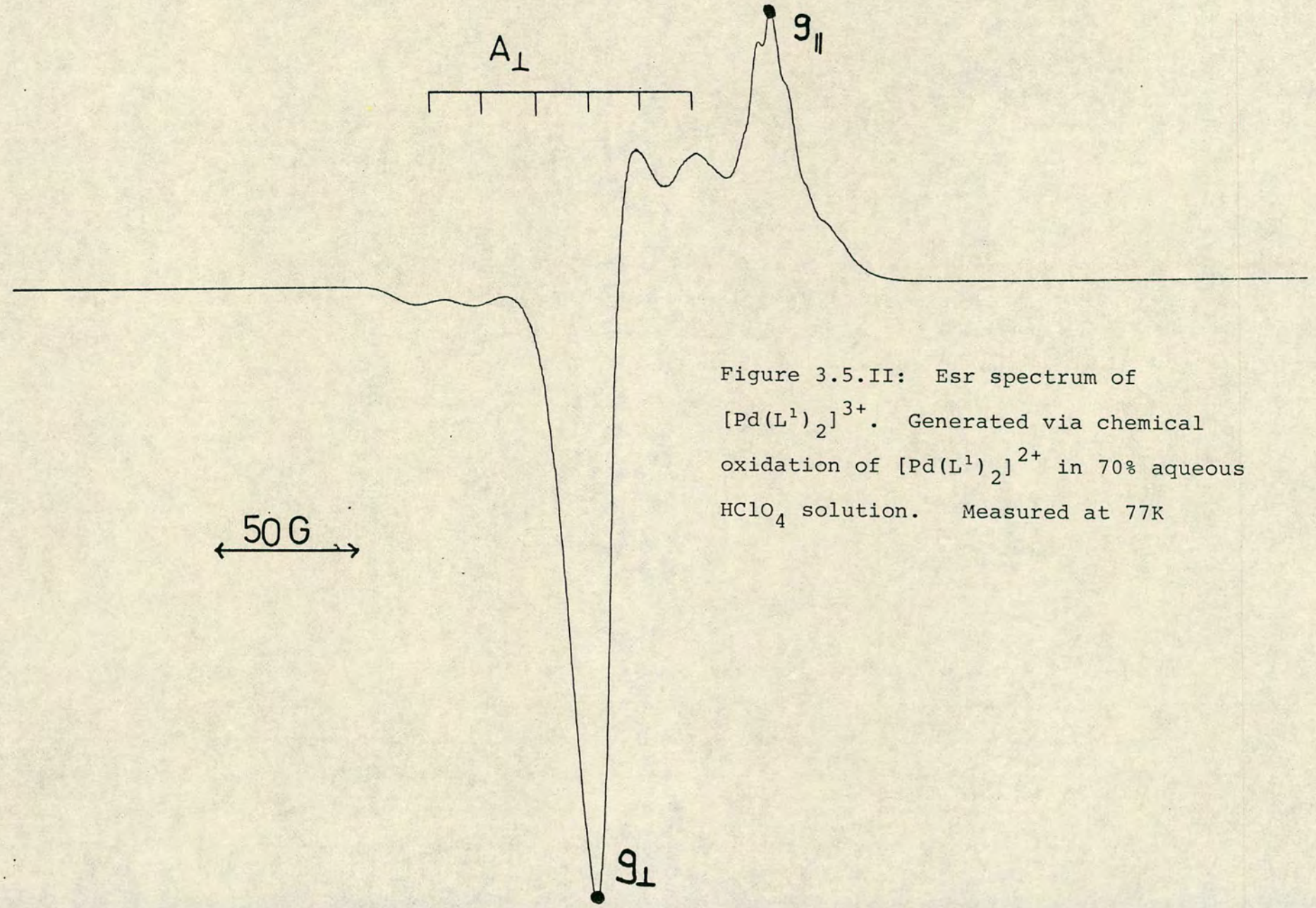

Figure 3.5.II: Esr spectrum of $[Pd(L^1)_2]^{3+}$. Generated via chemical oxidation of $[Pd(L^1)_2]^{2+}$ in 70% aqueous $HClO_4$ solution. Measured at 77K

Hyperfine coupling to ^{105}Pd (I = 5/2, 22.2%) is now clearly observable in the $g_{\perp}$ region, of magnitude 20G. This hyperfine coupling in the strongly anisotropic signal provides further evidence for a metal based paramagnetic species, and as for the $[Pt(L^1)_2]^{3+}$ cation, the observation $g_{\perp} > g_{\parallel} \sim 2$ is also consistent for a tetragonally elongated octahedral d^7 species being formed.[124] A second hyperfine coupling of ~5G is observable in the $g_{\parallel}$ region, which is tentatively assigned to a long range proton interaction. The improved resolution of this spectrum in frozen 70% aqueous $HClO_4$ may be due, in part, to the absence of base electrolyte.[151]

3.6 The single crystal X-ray structure of $[Pd(L^1)_2]^{3+}$ $(H_3O)^+(ClO_4)_4 \cdot 3H_2O$

Allowing solutions of the $[Pd(L^1)_2]^{3+}$ cation in 70% aqueous $HClO_4$ cool to room temperature led to the formation of well formed orange-red crystals. These were shown to be paramagnetic on running an esr spectrum of a frozen aqueous solution. An infra-red spectrum of the highly air and moisture sensitive crystals indicated the presence of L^1 and perchlorate ion. During the preparation of the disc, reduction clearly occurred, as indicated by its green colour. Aqueous solutions of the orange-red crystals were rapidly reduced to give the $[Pd(L^1)_2]^{2+}$ cation, as shown by spectroscopic studies. Since the crystals were almost certain to contain the $[Pd(L^1)_2]^{3+}$ cation, a crystal structure determination would be highly desirable. Although the crystals were indefinitely stable in perchloric acid,

removal from this medium led to instant fracturing. To prevent this the crystal had to be sealed in a Lindemann tube in the presence of some mother liquor. This and further protective measures ensured that no decomposition occurred, and led to the collection of a good quality data set.

Crystal data: $C_{12}H_{24}PdS_6^{3+}.H_3O^+.4ClO_4^-.3H_2O$. M = 938.0 monoclinic. Space group C2/c, a = 20.664(4); b = 9.2335(17); c = 20.218(4) Å β = 124.514(13)° U = 3179 Å^3 D_c = 1.959 g cm^{-3} Z = 4. At convergence R,R_w = 0.0311, 0.0390 respectively for 1809 data.

A summary of selected bond lengths and angles are given in Table 3.6.I. A view of the $[Pd(L^1)_2]^{3+}$ cation is shown in Figure 3.6.II. The Pd(III) ion lies on an inversion centre, with Pd-S(1) = 2.5448(15), Pd-S(4) = 2.3558(14), Pd-S(7) = 2.3692 Å, to give overall a tetragonally elongated octahedral geometry (<SPdS = 87.17-88.88°) entirely consistent for a low spin Pd(III) d^7 system undergoing a Jahn-Teller distortion.

Relative to $[Pd(L^1)_2]^{2+}$ the axial thia donors S(1), S(1)', are brought in towards the more positive 3+ metal centre and this is linked to a slight elongation of the equatorial Pd-S bond lengths.

Associated with the $[Pd(L^1)_2]^{3+}$ cation in the structure are four perchlorate ions, an oxonium ion (H_3O^+) and three water molecules. The identification of the H_3O^+ cation in the crystal was made on the basis of the electron difference map around the O atom. Additionally, the complex cation can be

Table 3.6.I Important bond lengths and angles (with esd's) for $[Pd(L^1)_2]^{3+}$

Bond lengths (Å)

Pd-S(1)	2.5448(15)	C(3)-S(4)	1.817(6)
Pd-S(4)	2.3558(14)	S(4)-C(5)	1.824(6)
Pd-S(7)	2.3692(15)	C(5)-C(6)	1.509(9)
S(1)-C(2)	1.827(6)	C(6)-S(7)	1.823(6)
S(1)-C(9)	1.826(6)	S(7)-C(8)	1.837(6)
C(2)-C(3)	1.513(9)	C(8)-C(9)	1.505(9)

Bond angles (degrees)

S(1)-Pd-S(4)	87.33(5)	Pd-S(1)-C(2)	101.02(20)
S(1)-Pd-S(7)	87.17(5)	Pd-S(1)-C(9)	97.07(21)
S(4)-Pd-S(7)	88.88(5)	Pd-S(4)-C(3)	101.22(20)
		Pd-S(4)-C(5)	103.27(20)

Figure 3.6.II View of the single crystal X-ray structure of $[Pd(L^1)_2]^{3+}$

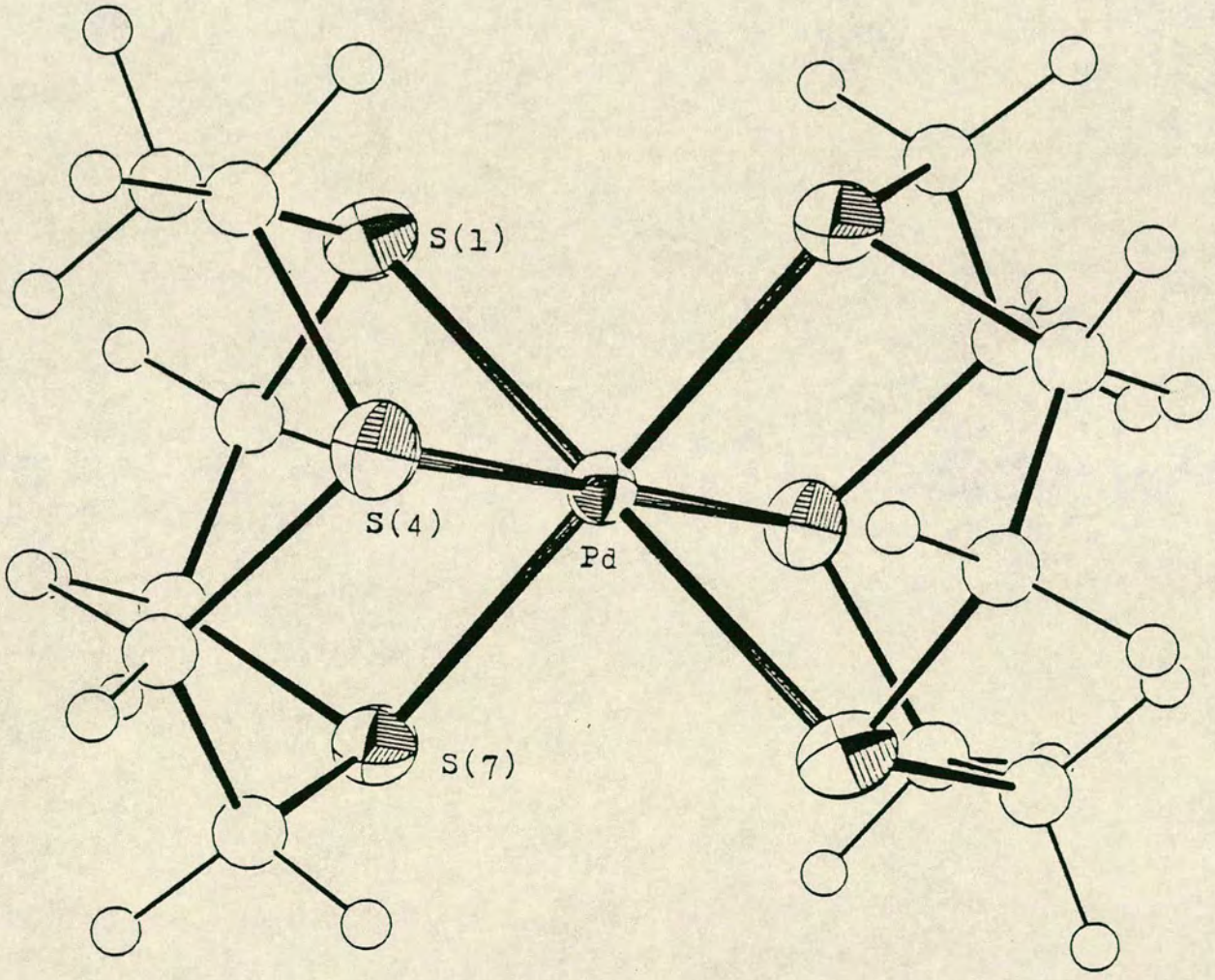

identified as $[Pd(L^1)_2]^{3+}$ since a hypothetical d^6 $[Pd(L^1)_2]^{4+}$ cation, as well as not showing esr activity, would be expected to be perfectly octahedral. In all d^6 low spin $[M(L)_2]^{n+}$ systems so far crystallographically characterised (M = Fe(II) L=L^4,[31] M = Fe(II),[41] Ru(II),[150] Co(III),[41] Rh(III) L=L^1) none of the M-S distances varies by more than 0.018Å whereas in $[Pd(L^1)_2]^{3+}$ the mean difference between the axial and equatorial Pd-S bond lengths is 0.182Å. For the d^7 $[Co(L^1)_2]^{2+}$ cation[64] a Jahn-Teller distortion is also present but instead a tetragonal compression is observed. In $[Ni(L^4)_2]^{3+}$, also a low spin d^7 species, the mean difference between axial and equatorial bond lengths is 0.138Å for the tetragonally elongated octahedral structure.[43]

Literature reports of monomeric Pd(III) complexes are very scarce. In contrast to Pt[152] not even dimeric diamagnetic Pd(III) dimers have been characterised. The only previous report of a metal based monomeric Pd(III) species is the gray hygroscopic solid $NaPdF_4$, synthesised under high pressure from NaF and Pd_2F_6.[153] The solid state esr of this material shows $g_\perp > g_\parallel \sim 2$, as observed in our system. Palladium in a formal oxidation state of +3 has been characterised in a variety of dithiolene complexes but these are more accurately regarded as Pd(II) - ligand radical systems.[126]

3.7 Studies upon related thia and aza macrocyclic complexes of palladium

3.7.1 Synthesis, characterisation, structure and electrochemistry of $[Pd(L^2)]^{2+}$

The importance of stereochemical and electronic control upon the redox chemistry of palladium(II) was investigated through the preparation of $[Pd(L^2)]^{2+}$ (L^2 = 1,4,8,11-tetrathiacyclotetradecane), $[Pd(L^3)]^{2+}$ (L^3 = 1,4,7,10,13,16-hexathiacyclooctadecane) and $[Pd(L^4)_2]^{2+}$ (L^4 = 1,4,7-triazacyclononane).

The $[Pd(L^2)]^{2+}$ cation was synthesised by reaction of K_2PdCl_4 with a slight excess of L^2 in refluxing water/methanol (v:v = 1:1) for *ca.* 30 minutes. Addition of NH_4PF_6 gave the PF_6^- salt as a yellow solid, which was recrystallised from water to give yellow crystals of $[Pd(L^2)](PF_6)_2$. Like the Pt analogue this complex was stable to hydrolysis even in hot aqueous solution - in sharp contrast to $[Ni(L^2)]^{2+}$.[65] F.a.b. mass spectra of the complex showed peaks at M^+ = 519, 374, corresponding to $[Pd(L^2)](PF_6)^+$ and $[Pd(L^2)]^+$ respectively. Although the complex was a yellow colour this is not due to absorption maxima in the visible region, but rather the tail of an intense higher energy charge transfer band. The ^1H n.m.r. spectrum for $[Pd(L^2)](PF_6)_2$ showed, as expected, a complex series of resonances for the bound L^2 macrocycle (δ_H = 2.8-3.8 ppm).

Due to the general paucity of structurally characterised platinum metal thioether complexes and more importantly to

elucidate the conformation adopted by the macrocyclic ligand, a single crystal X-ray structure determination was undertaken on the complex.

Crystal data: $C_{10}H_{20}PdS_4^{2+}\ 2PF_6^-$ M = 664.85, orthorhombic. Space Group $P_{na}2$, a = 13.947, b = 13.878, c = 11.1865Å U = 2165Å^3 D_c = 2.039 g cm^{-3} Z = 4. At convergence R, R_w = 0.0483, 0.0643 for 1486 data. A summary of selected bond lengths and angles are given in Table 3.7.1.I. Two views of the $[Pd(L^2)]^{2+}$ cation are shown in Figures 3.7.1.II and 3.7.1.III. The Pd(II) centre is co-ordinated by an approximate square plane of the four thia donors from the tetradentate macrocycle. The Pd-S bond distances vary from 2.25-2.31Å and the SPdS' band angles vary from 87.8-95.1°. The macrocycle adopts an *endo* conformation which contrasts with the *exo* structure observed for the free ligand, in which the lone pairs point outwards from the macrocycle cavity.[115] The second edge-on view of the cation clearly shows the conformation adopted by the methylene chains of the macrocyclic ligand. These are all directed to one face of the PdS_4 plane with the Pd atom lying slightly above the equatorial plane of the four sulphur atoms by 0.0381Å. The structural conformation adopted by the macrocycle is similar to that observed in the isoelectronic $[Rh(L^2)]^+$ cation, which shows a weak interaction with a second $[Rh(L^2)]^+$ cation to give overall a loosely dimeric structure.[116] In the $[Pd(L^2)]^{2+}$ cation however there is no analogous interaction, perhaps as a consequence of the increased charge on the metal centre.

Table 3.7.1.I Important bond lengths and angles (with esd's) for $[Pd(L^2)]^{2+}$

Bond lengths (Å)

Pd-S(1)	2.292(10)
Pd-S(4)	2.242(9)
Pd-S(7)	2.308(8)
Pd-S(11)	2.278(10)

Bond angles (degrees)

S(1)-Pd-S(4)	87.8(3)
S(1)-Pd-S(8)	176.9(3)
S(1)-Pd-S(11)	88.1(3)
S(4)-Pd-S(8)	95.1(3)
S(4)-Pd-S(11)	175.0(3)
S(8)-Pd-S(11)	88.9(3)

Figure 3.7.1.II View of the single crystal X-ray structure of $[Pd(L^2)]^{2+}$

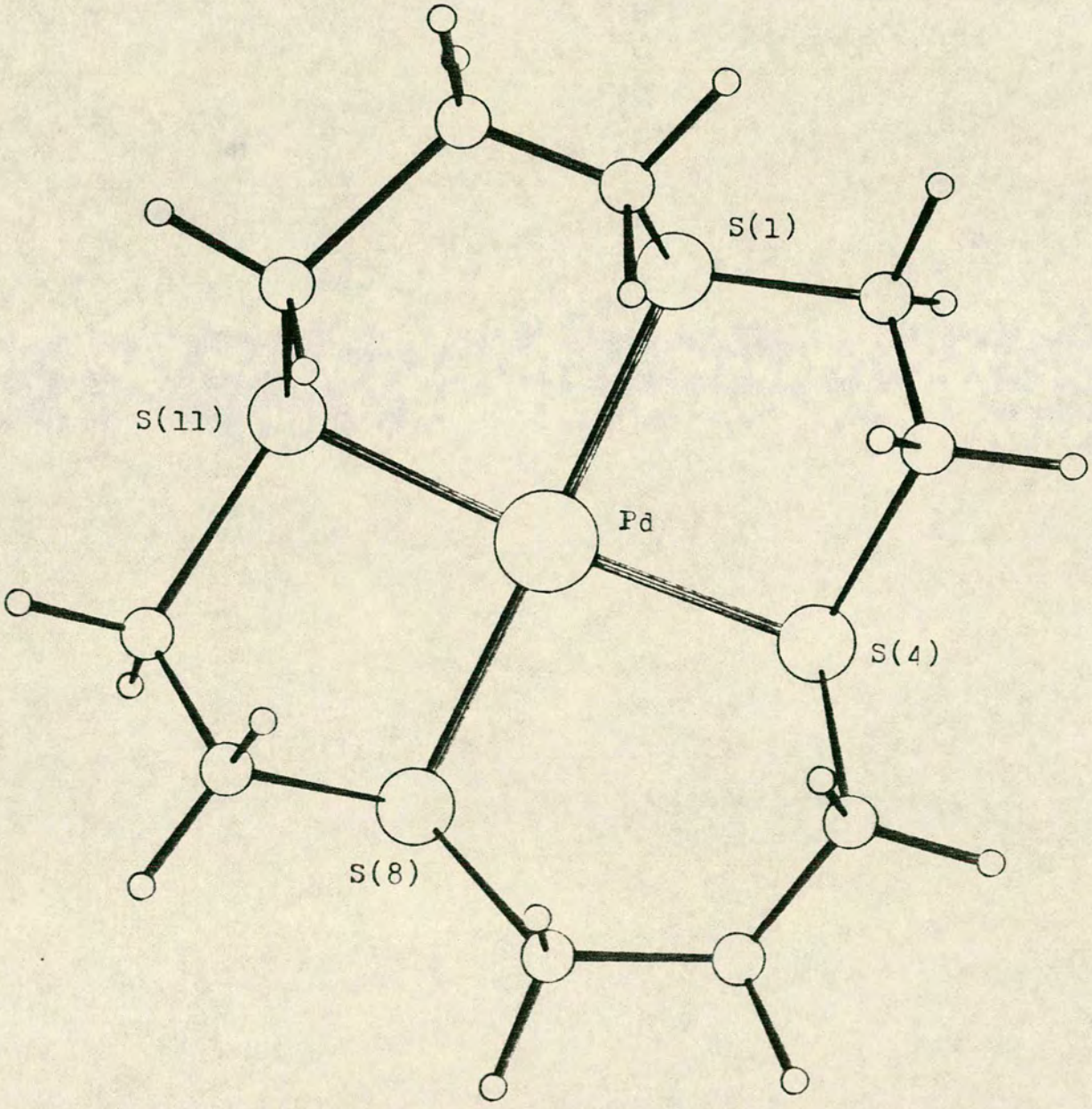

Figure 3.7.1.III View of the single crystal X-ray structure of $[Pd(L^2)]^{2+}$

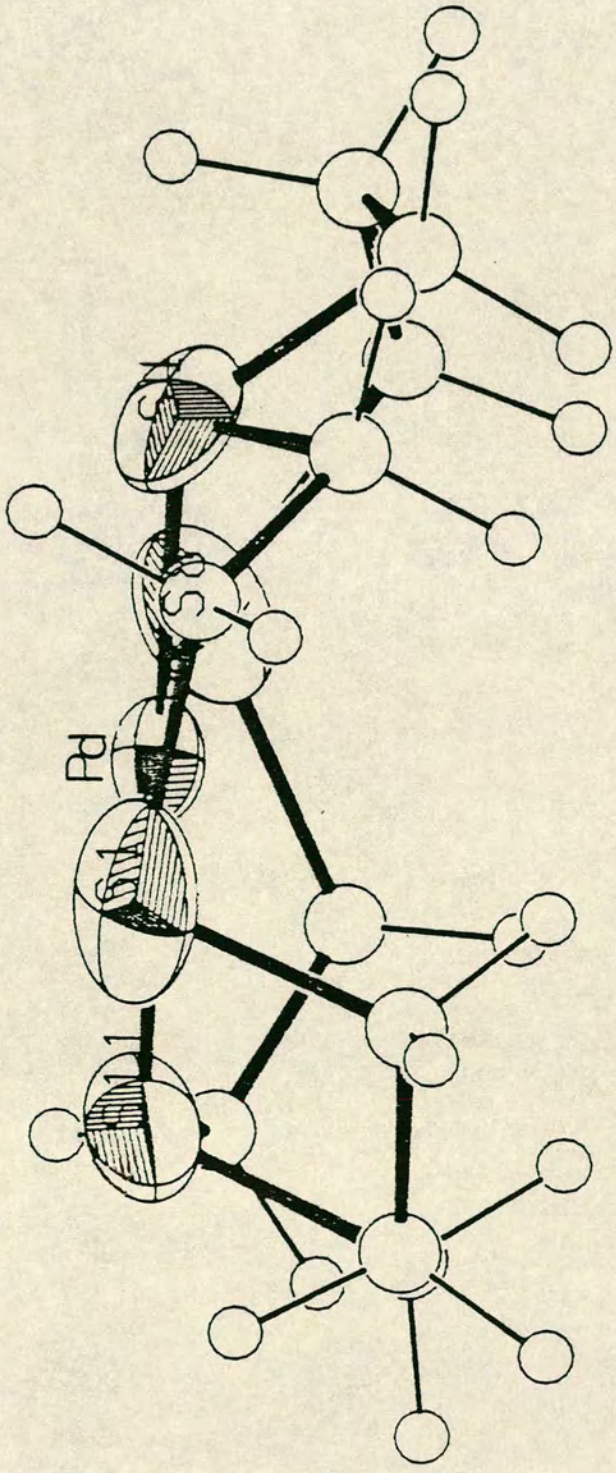

An electrochemical study upon the $[Pd(L^2)]^{2+}$ cation in acetonitrile showed total inactivity in the oxidation range underlining, as for the $[Pt(L^2)]^{2+}$ cation, the importance of stereochemical factors in observation of the d^7 or d^6 oxidation states which require an octahedral or tetragonally distorted octahedral geometry for optimum stabilisation.

Reduction of $[Pd(L^2)]^{2+}$ to $[Pd(L^2)]^{+}$ occurs irreversibly at room temperature but at -40°C and high scan rates a chemically reversible wave at $E_{\frac{1}{2}}$ = -0.875V ΔE = 65 mV was observed (Figure 3.7.1.IV). The short lifetime of the $[Pd(L^2)]^{+}$ cation can be contrasted with $[Pd(tmc)]^{+}$ [155] or $[Pd(tbc)]^{+}$ [156] (tmc = tetramethylcyclam (5), tbc = tetrabenzyl cyclam (6)) which have a long lifetime in solution, despite being obtained at more cathodic potentials.

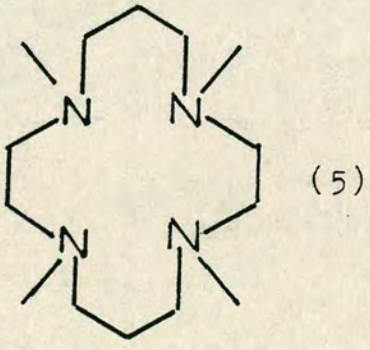

(5)

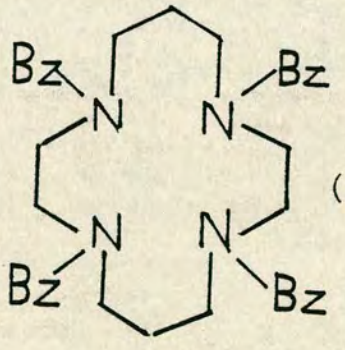

(6)

An explanation for the instability of $[Pd(L^2)]^{+}$ may be as a result of dimerisation leading to the formation of a Pd-Pd bond. Assuming ligand rearrangement does not occur on reduction there would be little steric hindrance to dimerisation due to the adopted conformation of the macrocycle in the complex. Presumably only at low temperature

Figure 3.7.1.IV Cyclic voltammogram of $[Pd(L^2)]^{2+}$ in CH_3CN/0.1M $TBAPF_6$ at 233K

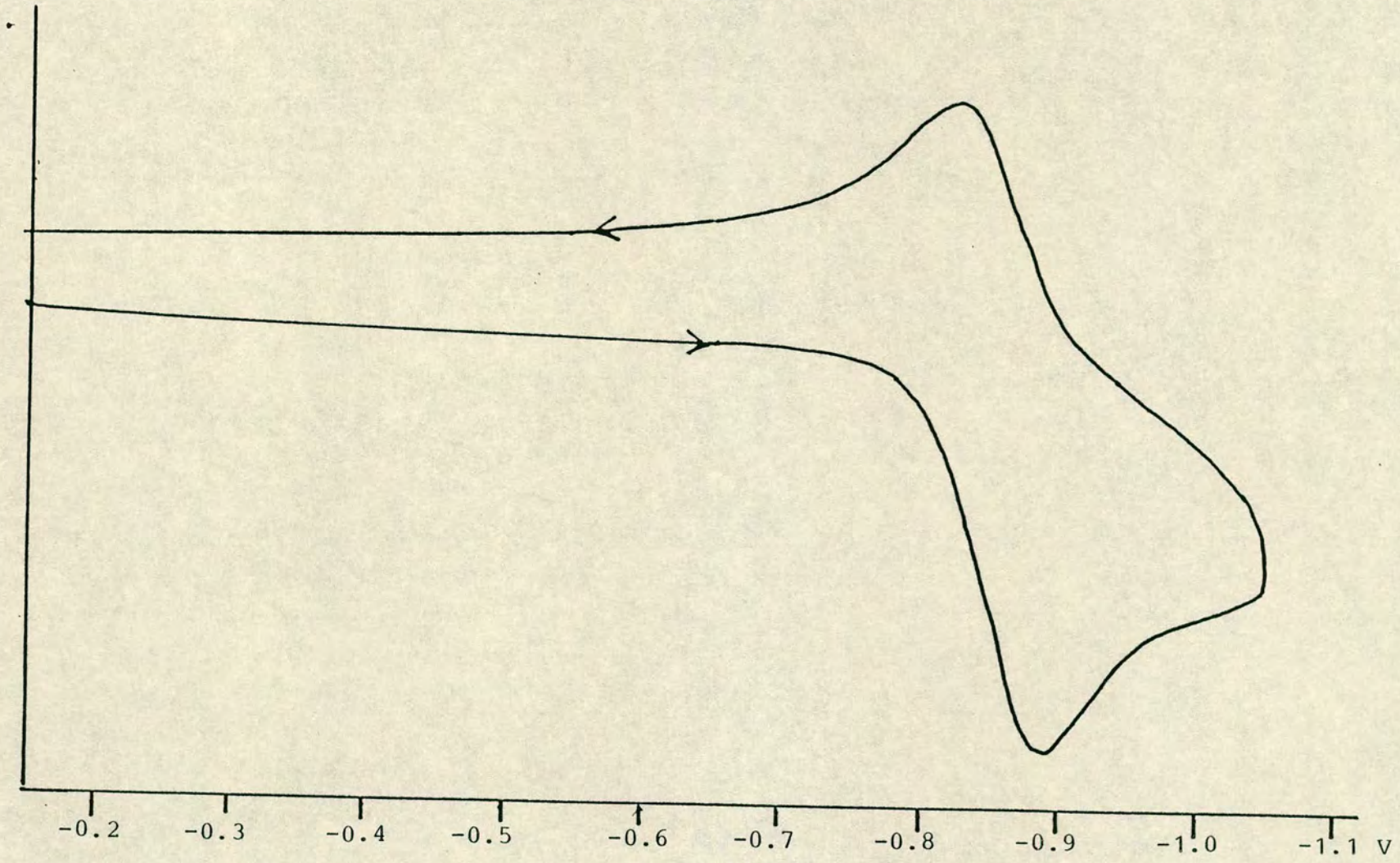

and high scan rates would dimerisation be slow enough to observe the reversible couple. Both $[Pd(tmc)]^+$ and $[Pd(tbc)]^+$ by contrast would not be expected to dimerise, as the resultant cofacial interactions would be very severe. To determine whether a $[Pd_2(L^2)_2]^{2+}$ dimer cation is obtained, either a variable concentration electrochemical study, or an attempt to isolate and characterise the reduced species could be made. Significantly Pd(I) chemistry is dominated by dimeric Pd-Pd bonded complexes eg $[Pd_2(CNCH_3)_6]^{2+}$ [157] and $[Pd(dppm)_2Cl_2]$.[158]

3.7.2 Synthesis, characterisation and electrochemistry of $[Pd(L^3)]^{2+}$

The $Pd(L^3)]^{2+}$ cation, which has been structurally characterised as its BPh_4^- salt[137] (L^3 = 1,4,7,10,13,16-hexathiacyclooctadecane) was synthesised as the PF_6^- salt from K_2PdCl_4 and L^3 in refluxing water/methanol (v:v = 1:1) for 1 hr. Addition of NH_4PF_6 gave the product which was recrystallised from an acetonitrile/water mixture. The f.a.b. mass spectrum shows a peak at M^+ = 466 characteristic of the $[Pd(L^3)]^{2+}$ ion. The ^1H n.m.r. spectrum shows a singlet at δ_H = 3.25 ppm possibly as a consequence of fluxionality, or of chemical equivalence in the solvent used (CD_3CN). Like the $[Pt(L^3)]^{2+}$ cation, to which the Pd analogue is isostructural, no redox activity is shown either in the oxidation or reduction range in acetonitrile. The absence of a Pd(II)/(I) couple appears surprising as the electronic and steric environment for the metal centre differs little in $[Pd(L^2)]^{2+}$ and $[Pd(L^3)]^{2+}$.

3.7.3 Synthesis, characterisation and electrochemistry of $[Pd(L^4)_2]^{2+}$

In view of the interesting electrochemistry for $[Pd(L^1)_2]^{2+}$ an investigation of the related $[Pd(L^4)_2]^{2+}$ cation was made (L^4 = 1,4,7-triazacyclononane). An improved synthetic procedure for the formation of $[Pd(L^4)_2]^{2+}$ involved the reaction of K_2PdCl_4 with the neutral L^4 ligand in a 2:5 molar ratio in water at *ca.* 90°C for 30 minutes. Addition of NH_4PF_6 precipitated $[Pd(L^4)_2](PF_6)_2$ which upon recrystallisation from water gave the pure salt as light yellow crystals. During the course of this work McAuley reported the structure of the $[Pd(L^4)_2]^{2+}$ cation which is isostructural to the Pt analogue.[159]

The ^1H n.m.r. spectrum of $[Pd(L^4)_2]^{2+}$ in acetonitrile shows in addition to the amine protons (as a broad singlet δ_H = 4.12 ppm) a complex multiplet for the methylene protons at 80MHz. On increasing the field strength to 360MHz the methylene signal is split into two multiplet sets centred at δ_H = 3.03 ppm (Figure 3.7.3.I) with a separation of 0.3 ppm. The ^{13}C n.m.r. spectrum of $[Pd(L^4)_2]^{2+}$ also in CD_3CN shows only a singlet at δ_C = 51.95 ppm which appears inconsistent with the square planar geometry reported for the complex. A possible interpretation is that $[Pd(L^4)_2]^{2+}$ is fluxional in solution, but that internal couplings are retained for the magnetically inequivalent protons.

Voltammetry upon the $[Pd(L^4)_2]^{2+}$ cation reveals an oxidation wave at -0.03V vs Fc/Fc^+ in acetonitrile, a significantly lower potential than observed for the Pd(II)/(III)

Figure 3.7.3.I ^{1}H n.m.r. of $[Pd(L^{4})](PF_{6})_{2}$ in $CD_{3}CN$ showing the methylene resonances of L^{4} only, run at 360MHz

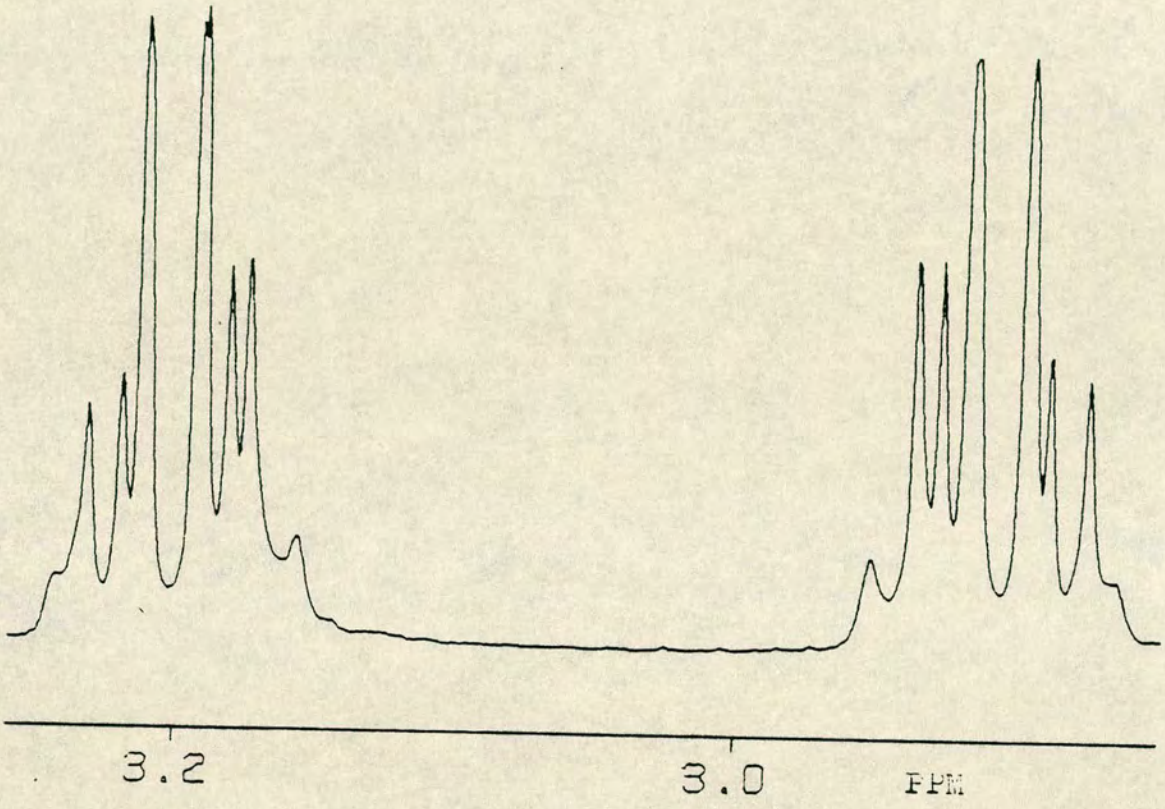

couple for $[Pd(L^1)_2]^{2+}$. Chemical oxidation of $[Pd(L^4)_2]^{2+}$ with peroxodisulphate ion at pH 2 in aqueous solution gave an esr active red solution. The frozen glass esr spectrum is consistent for a d^7 Pd(III) species, the anisotropic signal showing $g_\perp = 2.136$ $g_\parallel = 2.011$. Superhyperfine coupling to ^{14}N (I = 1 100%), $A_H = 25\,G$ is also evident in the $g_\parallel$ region, with a 1:2:3:2:1 intensity characteristic of an interaction with two of the axially co-ordinated ligand donors.[160] There is no evidence however for coupling to ^{105}Pd (I = ½ 22.2%). The chemically generated oxidised species only has a limited lifetime (*ca.* 2 hrs) in solution, but is clearly worth further investigation.

3.8 Mononuclear Pd(II) complexes incorporating one L^1 ligand

cis-$[Pd(L^1)Cl_2]$ was prepared by reaction of $PdCl_2$ with one equivalent of L^1 in nitromethane/dichloromethane (v:v = 3:1). Recrystallisation from nitromethane afforded red crystals of the product. A single crystal diffraction study (Figure 3.8.I) shows the Pd centre to occupy a somewhat distorted square planar environment with the two co-ordinated thia donors mutually *cis* (Pd-S = 2.2672(17), 2.2457(17)Å). The two remaining sites are occupied by chlorine, with Pd-Cl distances of 2.3316(21), 2.3326(21)Å. Compared with $[Pd(L^1)_2]^{2+}$ the $Pd-S_{eq}$ distances are shortened by an average of 0.065Å as a consequence of the *trans* influence of chlorine. The remaining sulphur atom of L^1 lies at a distance of 3.1400(21)Å, and so is (in contrast to

$[Pd(L^1)_2]^{2+}$) essentially non-bonding. The angle to the PdS_4 plane is also further from octahedral than for $[Pd(L^1)_2]^{2+}$, with $<S_{ax}PdS_{eq}$ = 78.42(5), 81.14(5)°. The crystals (prepared by Y. Roberts) refined well to give a final R factor of 0.0181 for 798 reflections. Very recently Wieghardt *et al.* have published the crystal structure of the bromo analogue *cis*-$[Pd(L^1)Br_2]$ which is essentially isostructural to our complex.[149]

Treatment of either $[Pd(L^1)_2]^{2+}$ or *cis*-$[Pd(L^1)Br_2]$ with excess triphenyl phosphine led to the formation of the *cis*-$[Pd(L^1)(PPh_3)_2]^{2+}$ cation. Addition of PF_6^- and recrystallisation from nitromethane/methanol gave orange crystals of $[Pd(L^1)(PPh_3)_2](PF_6)_2$.

The ^1H n.m.r. spectrum of the complex in CD_3CN, as for the Pt analogue showed a complex symmetrical multiplet for the methylene protons of L^1 (δ_H = 2.7-3.8 ppm).

Figure 3.8.I View of the single crystal X-ray structure of *cis*-$[Pd(L^1)Cl_2]$

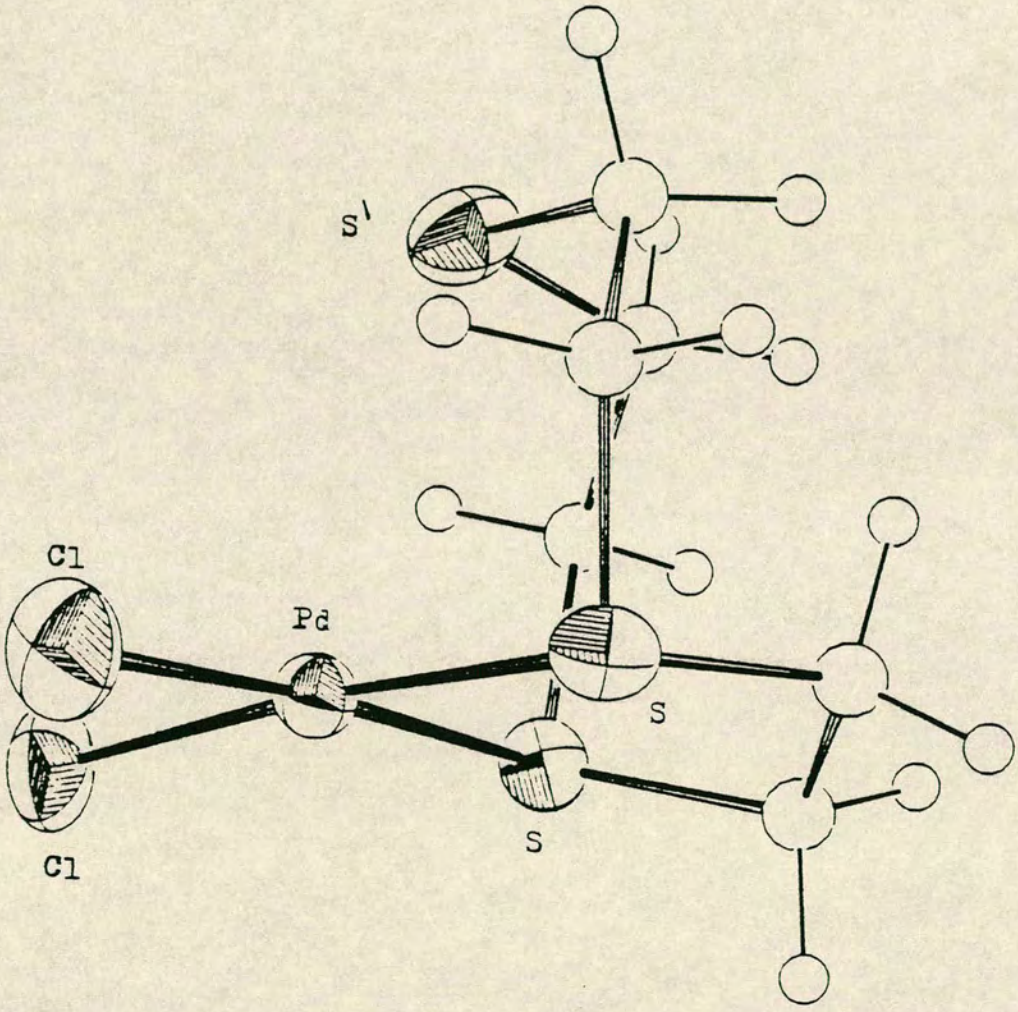

3.9 Summary

$[Pd(L^1)_2]^{2+}$ like $[Pt(L^1)_2]^{2+}$ shows a significant apical thia interaction to the square planar d^8 centre. This interaction in the distorted octahedral structure most clearly manifests itself in the electronic spectrum in which a low energy d-d transition is clearly observable.

The redox chemistry of $[Pd(L^1)_2]^{2+}$ shows both a one electron oxidation and reduction. The isolation of the d^7 $[Pd(L^1)_2]^{3+}$ cation beautifully demonstrates the value of the L^1 macrocycle in the stabilisation of unusual oxidation states. The tetragonally distorted geometry of $[Pd(L^1)_2]^{3+}$ is entirely consistent with theoretical expectations. Measurement of the magnetic moments of the Pd(III) and Pt(III) species are required. Although solid state measurements are probably precluded due to the aerial instability of the complexes an Evan's method solution measurement[42] in deuterated perchloric acid should be feasible. The $[M(L^1)_2]^{3+}$ cations should show a magnetic moment somewhat greater than a spin only value (1·73 BM) as a result of an orbital contribution to the magnetic moment.

In contrast to $[Pt(L^1)_2]^{2+}$ and $[Pt(L^2)]^{2+}$ the palladium analogues both show significant reduction chemistry to give the short-lived d^9 species.

Additionally preliminary studies upon $[Pd(L^4)_2]^{2+}$ show, as for the thia analogue, that the Pd(III) d^7 state may be stabilised.

Certainly both L^1 and L^4 are of significant potential use in future studies upon transition metal systems as a consequence of their remarkable redox behaviour.

3.10 Experimental

Conductivity measurements were made on a Portland Electronics 310 conductivity bridge in nitromethane at 298K. A 360MHz ^1H n.m.r. spectrum was run on a Bruker WH360 instrument. Other physical measurements were carried out as in Chapter 2.

Starting materials

Palladium(II) dichloride $PdCl_2$ and potassium tetrachloropalladate(II) K_2PdCl_4 were provided as generous loans from Johnson-Matthey plc.

Synthesis of 1,4,7-triazacyclononane

The trihydrochloride salt of 1,4,7-triazacyclononane $L^4.3HCl$ was synthesised according to a procedure developed by Pederson[161] (Scheme 3.10.1).

(i) $H_2N(CH_2)_2NH(CH_2)_2NH_2$ (51.5 g, 0.5 mol) and NaOH (60 g, 1.5 mol) were dissolved in water (400 ml) and transferred to a three-necked flask equipped with a stirrer, condenser and dropping funnel. P-toluenesulphonyl chloride (TsCl) (286.3 g, 1.5 mol) dissolved in diethyl ether (750 ml) was added dropwise. After two hours the tosylated product $TsNH(CH_2)_2NTs(CH_2)_2NHTs$ (1) was filtered and washed with water and diethyl ether. Yield 220 g (78%).

(ii) The sodium salt of the tritosylate dianion $(Na^+)_2$-$(^-TsN(CH_2)_2N(CH_2)_2Ts^-)$ (2) was obtained by addition of (1) (220 g, 0.39 mol) to a hot solution of NaOEt in ethanol (17.9 g, Na 0.78 mol, 400 ml). The white deliquescent salt

Scheme 3.10.1 Preparation of 1,4,7-triazacyclononane trihydrochloride $L^4.3HCl$

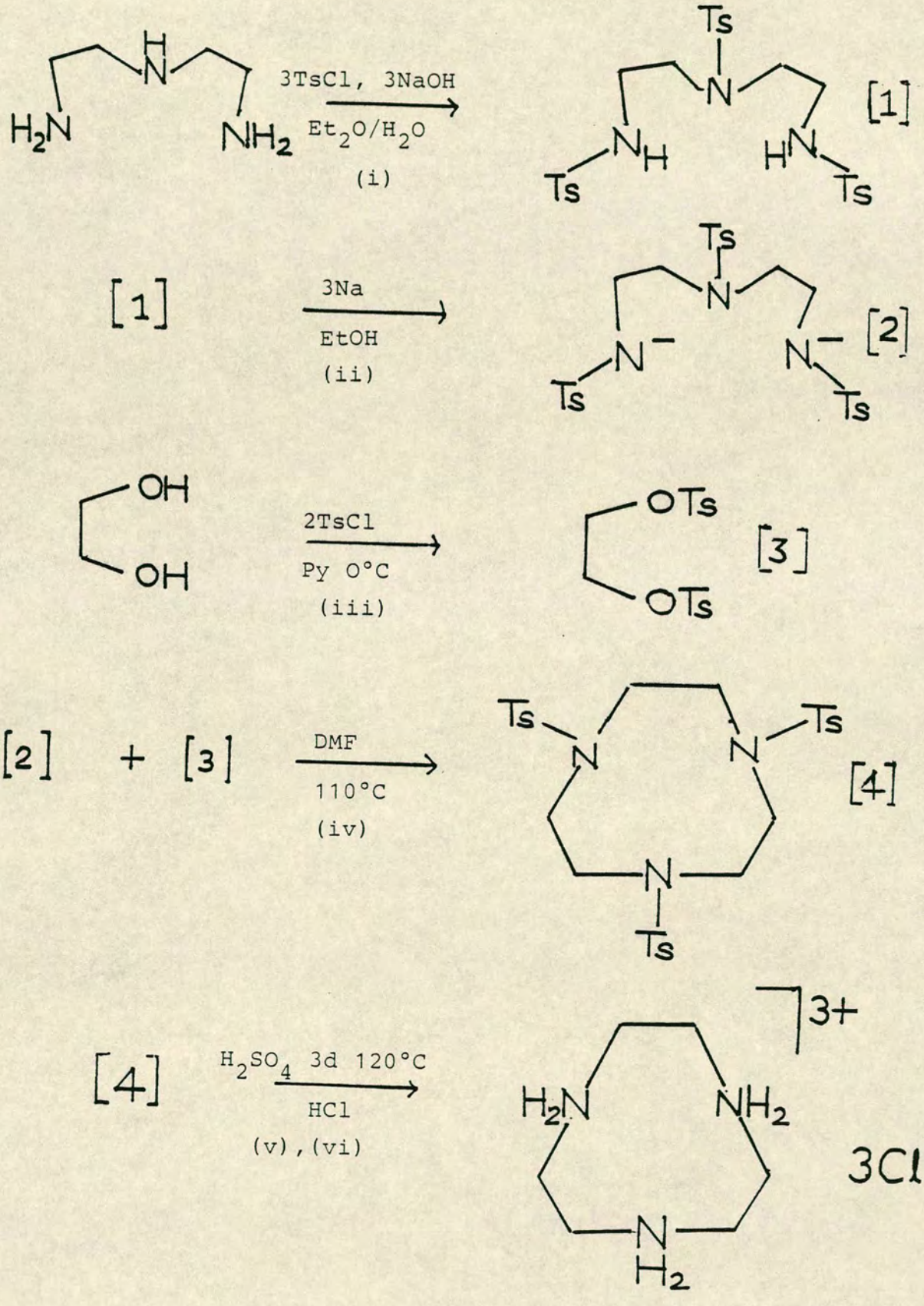

was obtained via rotary evaporation of the solution. Yield 230 g (98%).

(iii) To a solution of ethylene glycol (31 g, 0.5 mol) in pyridine (320 ml) at 0°C p-toluenesulphonylchloride (190.5 g, 1 mol) was added, maintaining the temperature at 5°C. The resulting porridge formed was poured two days later into ice cold water (2 litres) to remove pyH^+Cl^-. The product $TsO(CH_2)_2OTs$ was collected and washed with water. Yield 110 g (60%).

(iv) The disodium salt of the tritosylated amine (2) was dissolved in hot DMF (2 litres) and a DMF solution of the tosylated ester (3) (110 g, 0.297 mol; 1 litre) was added dropwise under a nitrogen atmosphere, maintaining the temperature at 110°C. After four hours the reaction mixture was poured into a 10 litre beaker, and water (*ca.* 6 litres) slowly added. The following day, the precipitated crude cyclic tritosylated amine (4) was collected and dried. This was dissolved in hot benzene (800 ml) and the insoluble impurities removed, most of the benzene was then removed by rotary evaporation and to the remaining solution, an equal volume (250 ml) of methanol was added. The pure product precipitated out of solution and was collected and dried. Yield 80 g (40%).

(v) The cyclic tritosylated amine (4) (80 g, 0.135 mol) was dissolved in 98% H_2SO_4 (50 ml) and heated to 120°C for three days. On cooling the resulting dark brown syrup was treated with diethyl ether (250 ml) and the mixture stirred to yield the semicrystalline sulphate salt $(L^4)_2(H_2SO_4)_3$

(vi) The sulphate salt of L^4 was converted to the trihydrochloride salt $L^4.3HCl$ on stirring with concentrated hydrochloric acid (12M 100 ml). The crude salt was filtered and purified by recrystallisation from a 6M HCl/methanol mixture (200 ml v:v = 1:1). The final stage of purification was undertaken by dissolving the solid in a minimum quantity of hot water, filtering impurities and adding 12M HCl/methanol to the clear filtrate to give the pure white trihydrochloride salt which was filtered and washed with diethyl ether. Yield = 15 g (12% based on overall reaction). Elemental analysis: Found C=29.57; H=7.58; N=17.61%. Calculated for $L^4.3HCl$ C=30.21; H=7.61; N=17.60%. Mass spectrum (electron impact) M^+ = 129 ($C_6H_{15}N_3^+$). ^1H n.m.r. spectrum (D_2O. 80MHz) δ_H = 3.61 (12H s CH_2 (L^1)).

(vii) The free ligand L^4, could be generated *in situ* by neutralisation with three molar equivalents of NaOH in water.

The remaining macrocyclic ligands were obtained as in Chapter 2. Additionally L^1 was purchased from Aldrich Co.

Synthesis of complexes

$[Pd(L^1)_2](PF_6)_2$

K_2PdCl_4 (0.150 g, 4.6×10^{-4}mol) was reacted with L^1 (0.170 g, 9.4×10^{-4}mol) in water/methanol (v:v = 1:1, 30 ml) under reflux for 30 minutes to yield a blue solution of the complex cation $[Pd(L^1)_2]^{2+}$. Addition of excess NH_4PF_6

followed by cooling of the solution yielded a green solid which was recrystallised from water (*ca.* 10 ml) to give green crystals of $[Pd(L^1)_2](PF_6)_2$ in 70% yield. Elemental analysis: Found C=18.9; H=3.14; Calculated for $[Pd(L^1)_2](PF_6)_2$: C=19.0; H=3.20. Infra-red spectrum 2982, 2960, 1441, 1413, 1407, 1303, 1289, 1193, 1152, 1129 and 840 cm^{-1}. Mass spectrum (f.a.b.) M^+ = 610 $[Pd(L^1)_2](PF_6)^+$ 465 $[Pd(L^1)_2]^+$. Electronic spectrum: λ_{max} = 615 nm (ε = 54 $M^{-1}cm^{-1}$) 298 (15,085) (CH_3CN and H_2O) (Figure 3.2.I). ^1H n.m.r. spectrum (CD_3CN 80MHz) δ_H = 3.30 (24H s CH_2 (L^1)). (Figure 3.2.II). ^1H n.m.r. spectrum (d^6 acetone 80MHz) δ_H = 3.63 (24H m CH_2 (L^1)). Conductivity (CH_3NO_2), plot of $\Lambda_e - \Lambda_o$ vs $c_e^{\frac{1}{2}}$ gives a slope of 485. Λ_o = 96.3.

$[Pd(L^1)_2](BF_4)_2$ could be prepared as dark green crystals using a similar procedure, but via addition of $NaBF_4$ to the $[Pd(L^1)_2]^{2+}$ cation. Elemental analysis: Found C=22.1; H=3.73%: Calculated for $[Pd(L^1)_2](BF_4)_2$ C=22.5; H=3.77%.

Recrystallisation of $[Pd(L^1)_2](PF_6)_2$ from nitromethane gave blue green crystals of $[Pd(L^1)_2](PF_6)_2.2CH_3NO_2$: Elemental analysis: Found C=18.7; H=3.37; N=3.29%: Calculated for $[Pd(L^1)_2](PF_6)_2.2CH_3NO_2$ C=19.1; H=3.44; N=3.19%.

Generation of $[Pd(L^1)_2]^{3+}$

a) Controlled potential electrolysis

Electrogeneration of $[Pd(L^1)_2]^{3+}$ was performed via

controlled potential electrolysis of $[Pd(L^1)_2](PF_6)_2$ (40 mg) in acetonitrile at a potential of +0.7V under a nitrogen atmosphere. The intensely orange-red $[Pd(L^1)_2]^{3+}$ cation, λ_{max} = 477 nm (ε = 5344), 341 (16100), 230 (9876) was stable for a number of hours in dry acetonitrile, decaying eventually to $[Pd(L^1)_2]^{2+}$. Esr spectrum (CH_3CN 77K) $g_\perp$ = 2.048 $g_\parallel$ = 2.008 (Gain = 6.3 x 10^2).

b) Chemical oxidation

$[Pd(L^1)_2](PF_6)$ (20 mg) was dissolved in 70% aqueous perchloric acid (*ca.* 5 ml) and heated to 50°C for four hours, this led to formation of the $[Pd(L^1)_2]^{3+}$ cation, which on cooling to room temperature gave crystals of $[Pd(L^1)_2](H_3O)(ClO_4)_4.3H_2O$. Solutions of $[Pd(L^1)_2]^{3+}$ obtained chemically show essentially identical electronic spectra to those observed electrochemically, λ_{max} = 477 nm (ε = 5,800 M^{-1} cm^{-1}), 340 (16,130), 230 (7,650). Esr spectrum (70% $HClO_4$ 77K) $g_\perp$ = 2.049 $g_\parallel$ = 2.009 $A_\parallel$ = 20G A_H = 5G (Gain = 1.25 x 10^2).

cis-$[Pd(L^1)_2Cl_2]$

$PdCl_2$ (0.080 g, 4.5 x 10^{-4}mol) and L^1 (0.082 g, 4.5 x 10^{-4}mol) were reacted in refluxing nitromethane/dichloromethane (v:v = 3:1, 60 ml) for 24 hours under nitrogen to give an orange-brown precipitate. The product was collected and dissolved in a minimum amount of hot nitromethane (30 ml). The solution was allowed to cool and reduced in volume to afford red crystals of *cis*-$[Pd(L^1)Cl_2]$

which were dried *in vacuo*. Yield = 60%. Elemental analysis: Found C=19.7; H=3.2%; Calculated for $[Pd(L^1)Cl_2]$ C=20.1; H=3.4%. Infra-red spectrum: 2958, 2930, 1437, 1403, 1308, 1300, 1282, 1263, 1247, 1180, 1144, 935, 887, 805, 332 and 312 cm^{-1}. ^1H n.m.r. spectrum (d^6 dmso 80MHz) δ_H = 3.3 (12H br s CH_2 (L^1)).

$[Pd(L^1)(PPh_3)_2](PF_6)_2$

a) $[Pd(L^1)Cl_2]$ (0.085 g, 1.82×10^{-4}mol) was treated with an excess of PPh_3 (0.10 g, 3.82×10^{-4}mol) in refluxing nitromethane (15 ml) for 30 minutes. Addition of NH_4PF_6 and diethyl ether (40 ml) gave the required complex as an orange precipitate. The pure crystalline salt was obtained by recrystallisation from nitromethane/methanol (v:v = 1:1 20 ml). Yield = 80%.

b) $[Pd(L^1)_2](PF_6)_2$ (0.040 g, 5.3×10^{-5}mol) was treated with an excess of PPh_3 (0.050 g, 1.91×10^{-4}mol) in acetonitrile (15 ml). Addition of diethyl ether to the solution gave the product which was recrystallised from nitromethane/methanol as above. Yield 80%. Elemental analysis: Found C=45.1; H=4.10%: Calculated for $[Pd(L^1)(PPh_3)_2](PF_6)_2$ C=45,8; H=3.84%. Infra-red spectrum: 1480, 1435, 1412, 1305, 1185, 1092, 998, 840, 750, 739, 704, 692, 529 and 514 cm^{-1}. Electronic spectrum λ_{max} = 478 nm. ^1H n.m.r. spectrum (CD_3NO_2 80MHz) δ_H = 2.74 (12H m CH_2 (L^1)) 7.3-7.7 (30H m CH (PPh_3)).

$[Pd(L^2)](PF_6)_2$: L^2 = 1,4,8,11-tetrathiocyclotetradecane

Reaction of K_2PdCl_4 (0.10 g, 3.1 x 10^{-4}mol) with L^2 (0.090 g, 3.4 x 10^{-4}mol) in refluxing acetonitrile/dichloromethane (v:v = 3:1 20 ml) for four hours resulted in the formation of a yellow precipitate of $[Pd(L^2)]Cl_2$. This was collected, washed with cold water, methanol and finally dichloromethane. The complex was dissolved in hot water and NH_4PF_6 added to precipitate $[Pd(L^2)](PF_6)_2$. Yellow crystals of the pure product were obtained upon recrystallisation from water. Yield = 75%. Later preparations of the same complex via reaction of K_2PdCl_4 and L^2 in refluxing water/methanol (v:v = 1:1) proved equally effective. Elemental analysis: Found C=17.9; H=3.0%. Calculated for $[Pd(L^2)](PF_6)_2$ C=18.1; H=3.0%. Infra-red spectrum (L^2 bands) 2998, 2938, 2910, 2886, 1428, 1410, 1307, 1284, 1253, 1208, 1170, 1136, 1028 and 840 cm^{-1}. Mass spectrum (f.a.b.) M^+ = 519 $[Pd(L^2)](PF_6)^+$ 374 $[Pd(L^2)]^+$. ^1H n.m.r. spectrum (CD_3CN 80MHz) δ_H = 2.8-3.8 (20H m CH_2 (L^2)).

$[Pd(L^3)](PF_6)_2$: L^3 = 1,4,7,10,13,16-hexathiacyclooctadecane

Reaction of K_2PdCl_4 (0.100 g, 3.1 x 10^{-4}mol) with L^3 (0.120 g, 3.3 x 10^{-4}mol) in refluxing water/methanol (v:v = 1:1 25 ml) for 30 minutes gave a brown solution of $[Pd(L^3)]^{2+}$. Addition of NH_4PF_6 gave a yellow-green solid which could be recrystallised from acetonitrile/water (v:v = 4:1 60 ml) to give the pure product. Yield = 60%. Elemental analysis: Found C=18.7; H=3.31%: Calculated for

$[Pd(L^3)](PF_6)_2$ C=19.0; H=3.31%. Infra-red spectrum (L^3 bands), 2990, 2942, 1423, 1290, 1247, 1180, 1149, 1110 and 1008 cm^{-1}. ^1H n.m.r. spectrum (CD_3CN 80MHz) δ_H = 3.25 (24H s CH_2 (L^3)). Mass spectrum (f.a.b.) M^+ = 466 $[Pd(L^3)]^+$.

$[Pd(L^4)_2](PF_6)_2$: L^4 = 1,4,7-triazacyclanonane

Reaction of K_2PdCl_4 (0.15 g, 4.6×10^{-4}mol) with $L^4$3HCl (0.26 g, 1.1×10^{-3}mol) neutralised with three equivalents of NaOH, in refluxing aqueous solution (15 ml) led to the formation of the yellow $[Pd(L^4)_2]^{2+}$ cation after 30 minutes. Addition of NH_4PF_6 precipitated the product, which was recrystallised from water to give pale yellow crystals of $[Pd(L^4)_2](PF_6)_2$ in 80% yield. Elemental analysis: Found C=21.7; H=4.63; N=12.8%. Calculated for $[Pd(L^4)_2](PF_6)_2$ C=22.0; H=4.62; N=12.8%. Infra-red spectrum (L^4 bands) 3285, 3103, 2925, 2885, 1455, 1431, 1358, 1132, 1038, 1007, 974 and 471 cm^{-1}. ^1H n.m.r. spectrum δ_H (CD_3CN 360MHz) δ_H = 3.20 (12H m CH_2 (L^4)) 2.92 (12H m CH_2 (L^4)) (CD_3CN, 80MHz) δ_H = 4.13 (4H br s NH (L^4)). ^{13}C n.m.r. (CD_3CN 50.32MHz) δ_C = 51.95 (12C s (L^4)).

Generation of $[Pd(L^4)_2]^{3+}$

Chemical oxidation of $[Pd(L^4)_2](PF_6)_2$ by $Na_2S_2O_8$ in acidic (pH 2) aqueous solution led to the formation of the red $[Pd(L^4)_2]^{3+}$ cation. This showed a moderate stability with a lifetime of *ca.* 2 hrs in solution. Esr spectrum

(H_2O 77K) $g_{\perp}$ = 2.136 $g_{\parallel}$ = 2.011 A_N (^{14}N I = 1,100%) = 25G (Gain = 3.2×10^4).

CHAPTER 4

1,4,7-Trithiacyclononane Complexes of Rhodium

4. 1,4,7-Trithiacyclononane complexes of rhodium

4.1 Introduction

The observation of a significant redox chemistry for $[Pd(L^1)_2]^{2+}$ and $[Pt(L^1)_2]^{2+}$ indicated that a similar study for $[Rh(L^1)_2]^{3+}$ and $[Ir(L^1)_2]^{3+}$ should be made. As with Pd, and Pt, Rh and Ir chemistry is dominated by the d^6 and d^8 oxidation states with the intermediate d^7 state only very poorly characterised for monomeric systems.[165] In contrast to Pd and Pt it is the d^6 state which is predominant for rhodium in which the Rh(III) centre shows octahedral co-ordination. The d^8 Rh(I) state is only observed for complexes in which π acceptor ligands (eg phosphine, olefin or carbonyl) are present.[166] A recent example however of stabilisation of Rh(I) by a ligand set of only limited π acceptor ability is of $[Rh(L^2)]^+$ [116] (L^2 = 1,4,8,11-tetrathiacyclotetradecane). The Rh(I) d^8 state as in the isolectronic Pd,Pt(II) states is usually characterised by square planar geometry about the metal centre.[166]

In this work the primary aim was the synthesis and electrochemistry of $[Rh(L^1)_2]^{3+}$. On the basis of the characterisation of $[Rh(L^2)]^+$ (above), and of the observed stabilisation of the d^7 Pd,Pt(III) systems in the previous chapters, stabilisation of both $[Rh(L^1)_2]^{2+}$ and $[Rh(L^1)_2]^+$ might be expected.

Results and Discussion

4.2 Synthesis and characterisation of $[Rh(L^1)_2]^{3+}$

The preparation of $[Rh(L^1)_2]^{3+}$ was less straight forward than for $[Pd(L^1)_2]^{2+}$ or $[Pt(L^1)_2]^{2+}$. $RhCl_3.xH_2O$ gave only $[Rh(L^1)Cl_3]$ under a variety of conditions, so a more labile starting material was saught.

If $RhCl_3.xH_2O$ was dissolved in water and refluxed in the presence of three equivalents of $AgNO_3$, AgCl precipitated and a yellow solution of "$Rh(H_2O)_6^{3+}$" remained. Refluxing an aliquot of this solution with two molar equivalents of L^1 in a water/methanol mixture (v:v = 1:1 25 ml) for 90 minutes led to the formation of $[Rh(L^1)_2]^{3+}$, which could be precipitated as its PF_6^- salt by addition of an excess of NH_4PF_6. This crude salt contained an orange impurity which was removed by washing with hot methanol. The cream coloured $[Rh(L^1)_2](PF_6)_3$ salt gave slightly off-white efflorescent crystals of $[Rh(L^1)_2](PF_6)_3.xH_2O$ upon recrystallisation from water. The electronic spectrum of $[Rh(L^1)_2]^{3+}$ showed an intense charge transfer band at λ_{max} = 270 nm (ε = 30,600 $M^{-1}cm^{-1}$), assigned as a ligand→metal transition. The ^1H n.m.r. spectrum for $[Rh(L^1)_2]^{3+}$ in CD_3NO_2 (Figure 4.2.I) showed a complex series of resonances for the macrocycle methylene protons (centred at δ_H = 3.77 ppm) which could be interpreted as an AA'BB' pattern for a rigidly held stereochemical ligand conformation for the octahedral complex.[167] The observed signal closely resembles that for the isoelectronic $[Co(L^1)_2]^{3+}$ [41,48] and

Figure 4.2.I ^{1}H n.m.r. of $[Rh(L^{1})_{2}]^{3+}$ in CD_3NO_2

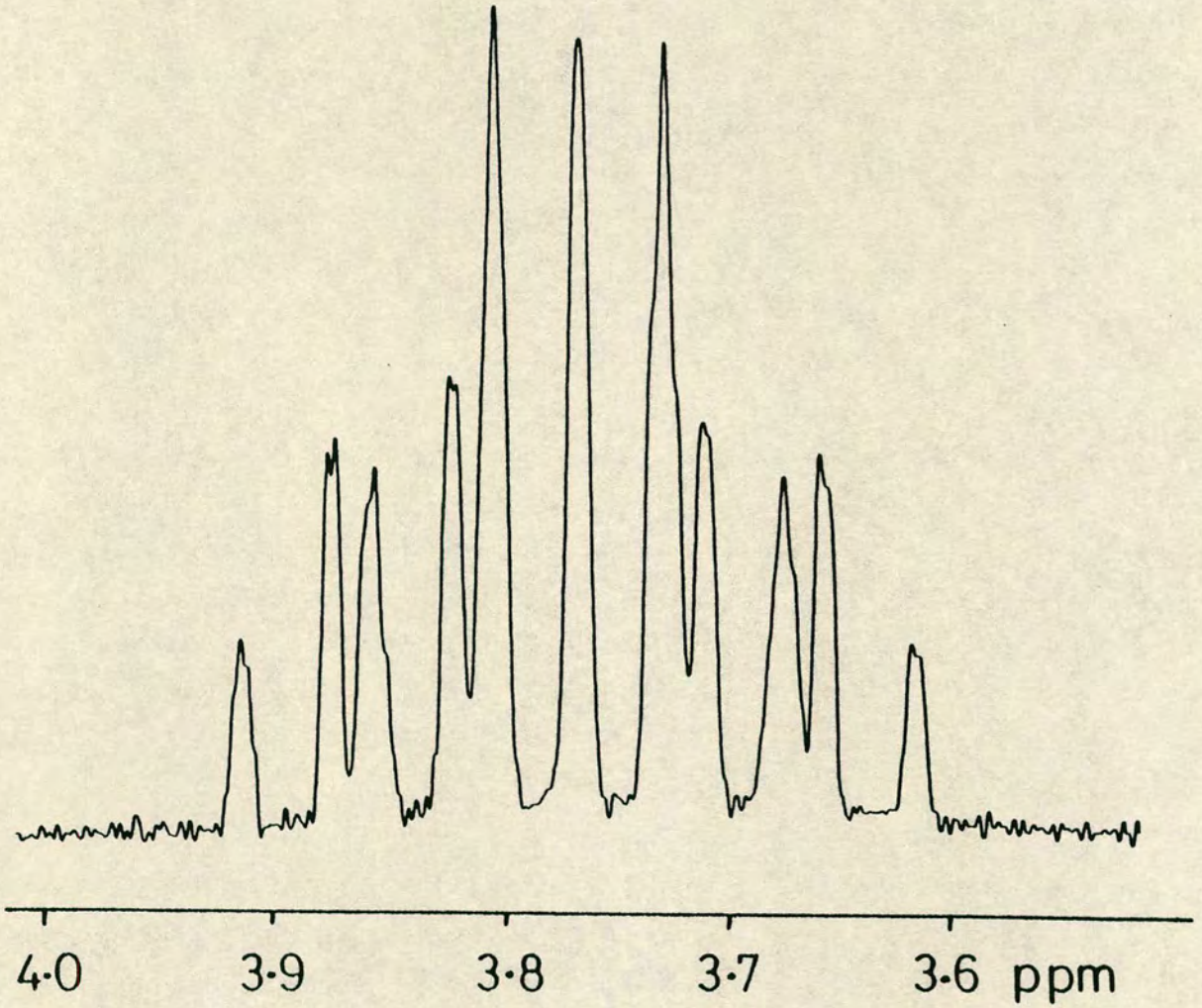

$[Pt(L^4)_2]^{4+}$ [48] complexes (L^4 = 1,4,7-triazacyclononane) It should be noted however that this ^1H n.m.r. data does not confirm octahedral geometry for $[Rh(L^1)_2]^{3+}$ as both the non octahedral $[Pd(L^1)_2]^{2+}$ (in d^6 acetone) and $[Pd(L^4)_2]^{2+}$ cations show similar spectra. To confirm whether the $[Rh(L^1)_2]^{3+}$ cation was octahedral a single crystal X-ray structural determination was undertaken.

4.3 The single crystal X-ray structure of $[Rh(L^1)_2](PF_6)_3$

Crystal data: $C_{12}H_{24}RhS_6^{3+}.3PF_6^-$ M = 898.3 monoclinic. Space Group I2/m a = 11.329(3), b = 9.692(3), c = 14,909(4)Å β = 101.77(2)° U = 1603Å^3 D_c = 1.861 g cm^3 Z = 2, R, R_w = 0.042, 0.072 respectively for 1007 data.

Important bond lengths and angles are given in Table 4.3.I. A view of the $[Rh(L^1)_2]^{3+}$ cation (Figure 4.3.II) shows almost perfect octahedral co-ordination with Rh-S = 2.3316(14), 2.3335(12)Å <SRhS = 88.78(5), 88.84(4)°. The Rh centre is also an inversion centre and two of the sulphur atoms S(4) and S(7) are related by symmetry. Water molecules were also present in the structure but were not well located.

The observed structure for $[Rh(L^1)_2]^{3+}$ is very similar to the isoelectronic $[Ru(L^1)_2]^{2+}$ cation[150] which was structurally characterised during the course of this work. The latter complex shows very similar M-S bond lengths (2.327-2.336Å) and angles to the $[Rh(L^1)_2]^{3+}$ complex cation. Additionally, however, the $[Ru(L^1)_2]^{2+}$ cation shows an interesting secondary interaction between the solvent molecules (dmso) and the bound macrocyclic ligand; this was not observed in our system.

Table 4.3.I Selected bond lengths and angles (with esd's) for $[Rh(L^1)_2](PF_6)_3$

Bond lengths (Å)

Rh-S(1)	2.3316(14)	S(4)-C(5)	1.813(13)
Rh-S(4)	2.3335(12)	C(5)-C(6)	1.532(18)
Rh-S(7)	2.3335(12)	C(6)-S(7)	1.856(13)
S(1)-C(2)	1.788(12)	S(7)-C(8)	1.796(12)
C(2)-C(3)	1.527(18)	C(8)-C(9)	1.503(18)
C(3)-S(4)	1.859(14)	C(9)-S(1)	1.870(14)

Bond angles (degrees)

S(1)-Rh-S(4)	88.78(5)	Rh-S(4)-C(5)	102.5(4)
S(1)-Rh-S(7)	88.78(5)	Rh-S(4)-C(3)	103.9(4)
S(4)-Rh-S(7)	88.84(4)	Rh-S(7)-C(8)	102.8(4)
Rh-S(1)-C(2)	102.9(4)	Rh-S(7)-C(6)	104.4(4)
Rh-S(1)-C(9)	103.0(4)		

Figure 4.3.II View of the single crystal X-ray structure of $[Rh(L^1)_2]^{3+}$

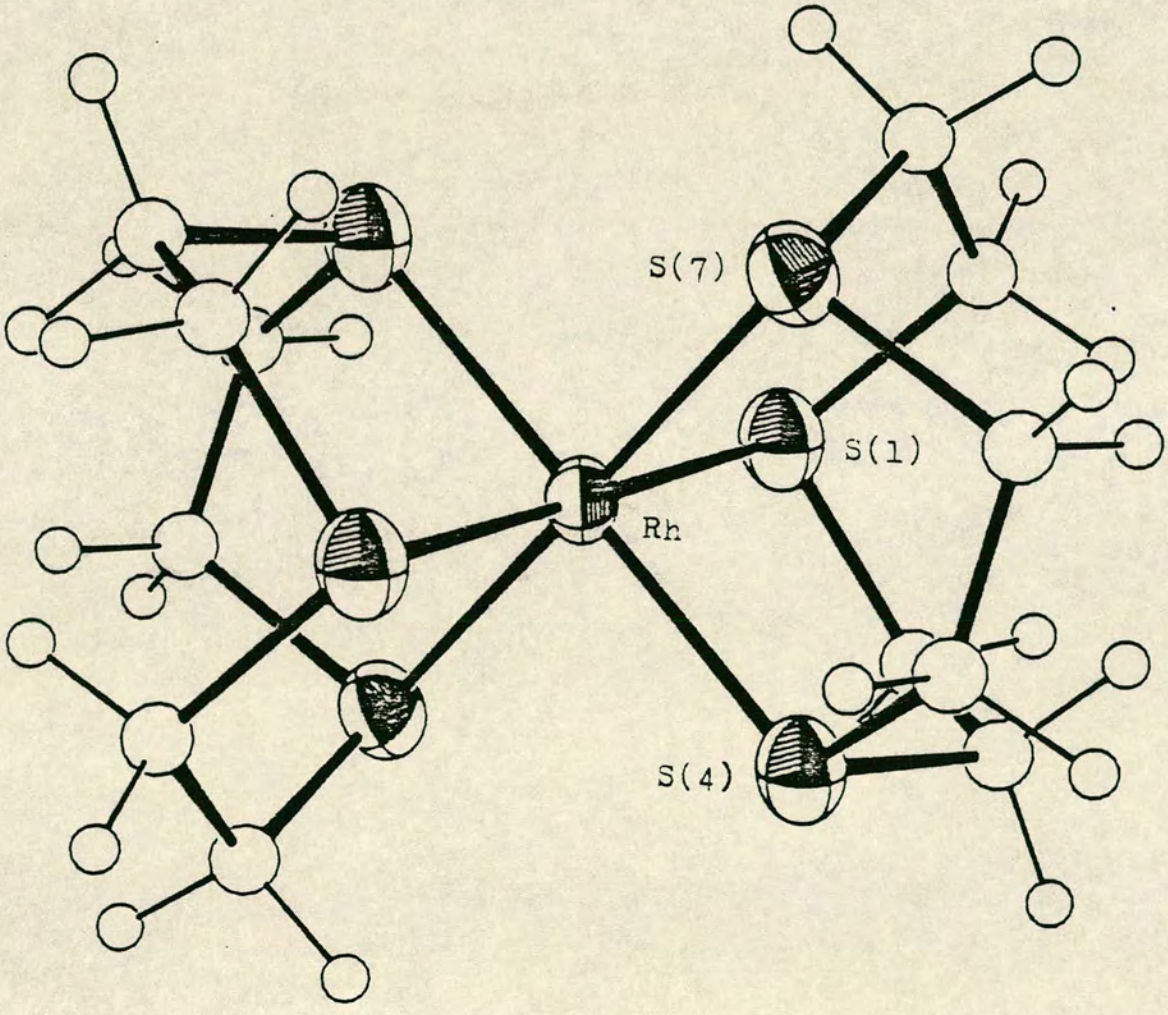

4.4 Electrochemistry of $[Rh(L^1)_2]^{3+}$

Cyclic voltammetry of $[Rh(L^1)_2](PF_6)_3$ in acetonitrile (100 mV s^{-1}) shows (Figure 4.4.I) two chemically reversible reductions at $^1E_{\frac{1}{2}}$ = -0.71V (Epc = -0.745V, Epa = -0.675V ΔEp = 71 mV) and $^2E_{\frac{1}{2}}$ = -1.08V (Epc = -1.145V, Epa = -1.015V, ΔEp = 127 mV) vs Fc/Fc^+. By direct comparison with the electrochemistry of the corresponding $[Co(L^1)_2]^{3+}$ system[31,68] ($^1E_{\frac{1}{2}}$ = -0.013V, $^2E_{\frac{1}{2}}$ = -0.086V) the two reductions are assigned as $[Rh(L^1)_2]^{3+/2+}$ and $[Rh(L^1)_2]^{2+/+}$ couples respectively. The ΔEp values are in accord with this interpretation, the relatively small structural change expected for the first reduction leading to a much more reversible value (71 mV) than for the second reduction (127 mV) in which a much more significant structural rearrangement is expected.

To obtain proof however of the formation of $[Rh(L^1)_2]^{2+}$ and $[Rh(L^1)_2]^{+}$ electrogeneration of these species was undertaken.

Controlled potential electrolysis of $[Rh(L^1)_2]^{3+}$ at -0.8V generated a pale brown solution, the frozen glass esr spectrum of which showed a broad slightly anisotropic signal with g_{av} = 2.06 (Figure 4.4.II). On electrogenerating for a further period of time, but at -0.85V the esr spectrum ran under the same conditions showed a much more anisotropic signal (Figure 4.4.III) with $g_{\perp}$ = 2.088, $g_{\parallel}$ = 2.007 . These spectra both indicated the formation of paramagnetic species indicative of formation, at least initially, of $[Rh(L^1)_2]^{2+}$. A tentative explanation for the observed

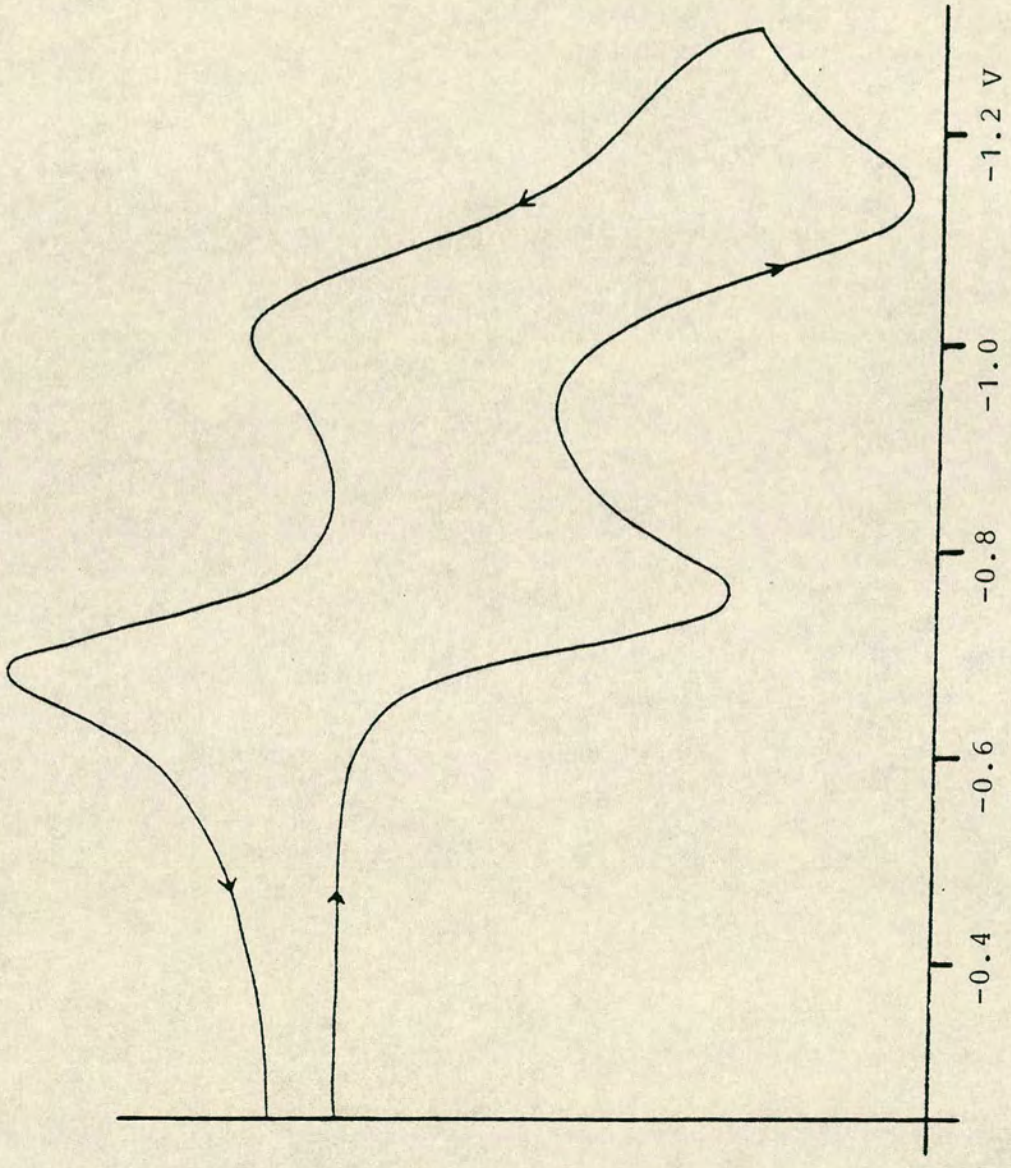

Figure 4.4.I Cyclic voltammogram of $[Rh(L^1)_2](PF_6)_3$ in CH_3CN/0.1M $TBAPF_6$

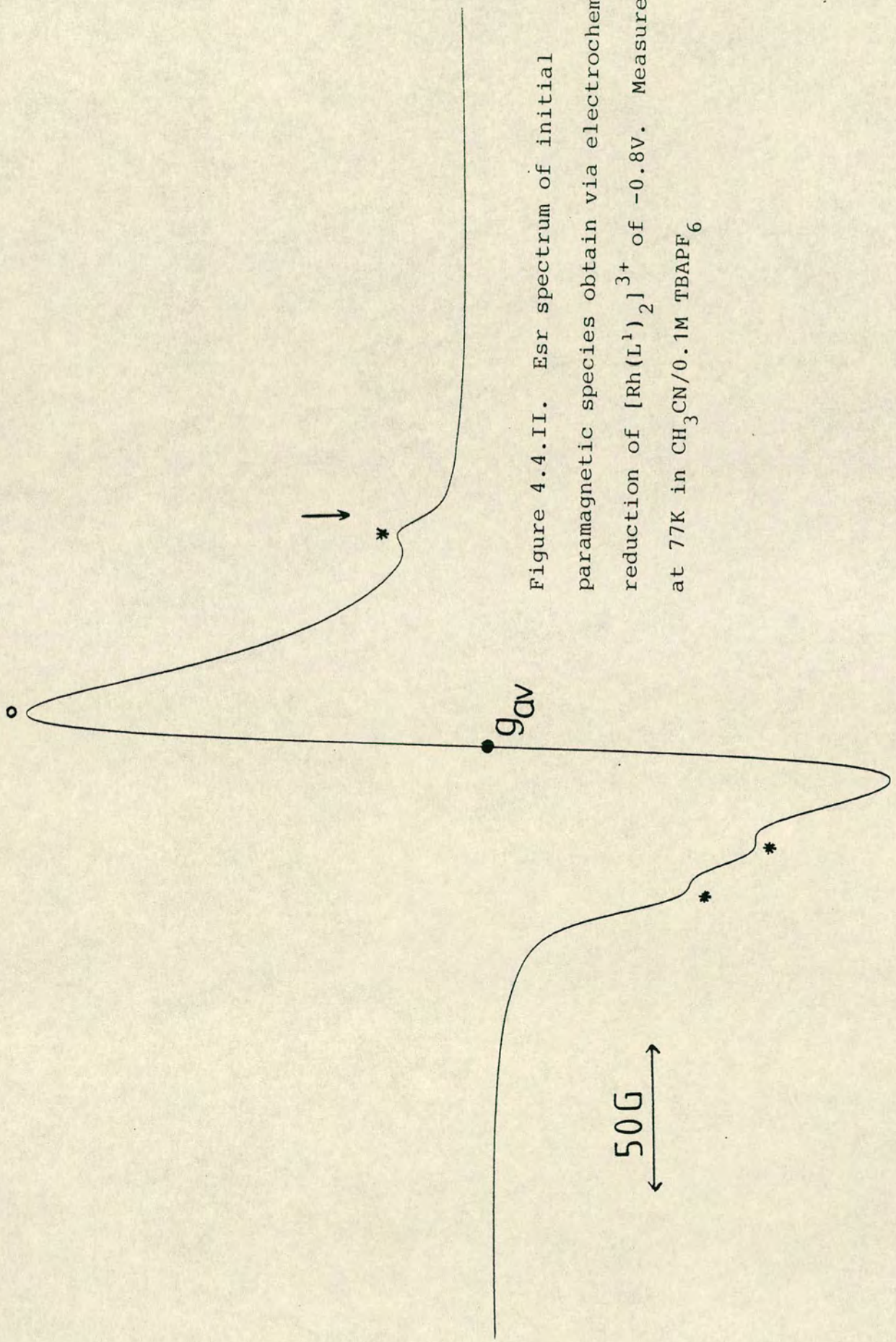

Figure 4.4.II. Esr spectrum of initial paramagnetic species obtain via electrochemical reduction of $[Rh(L^1)_2]^{3+}$ of -0.8V. Measured at 77K in CH_3CN/0.1M $TBAPF_6$

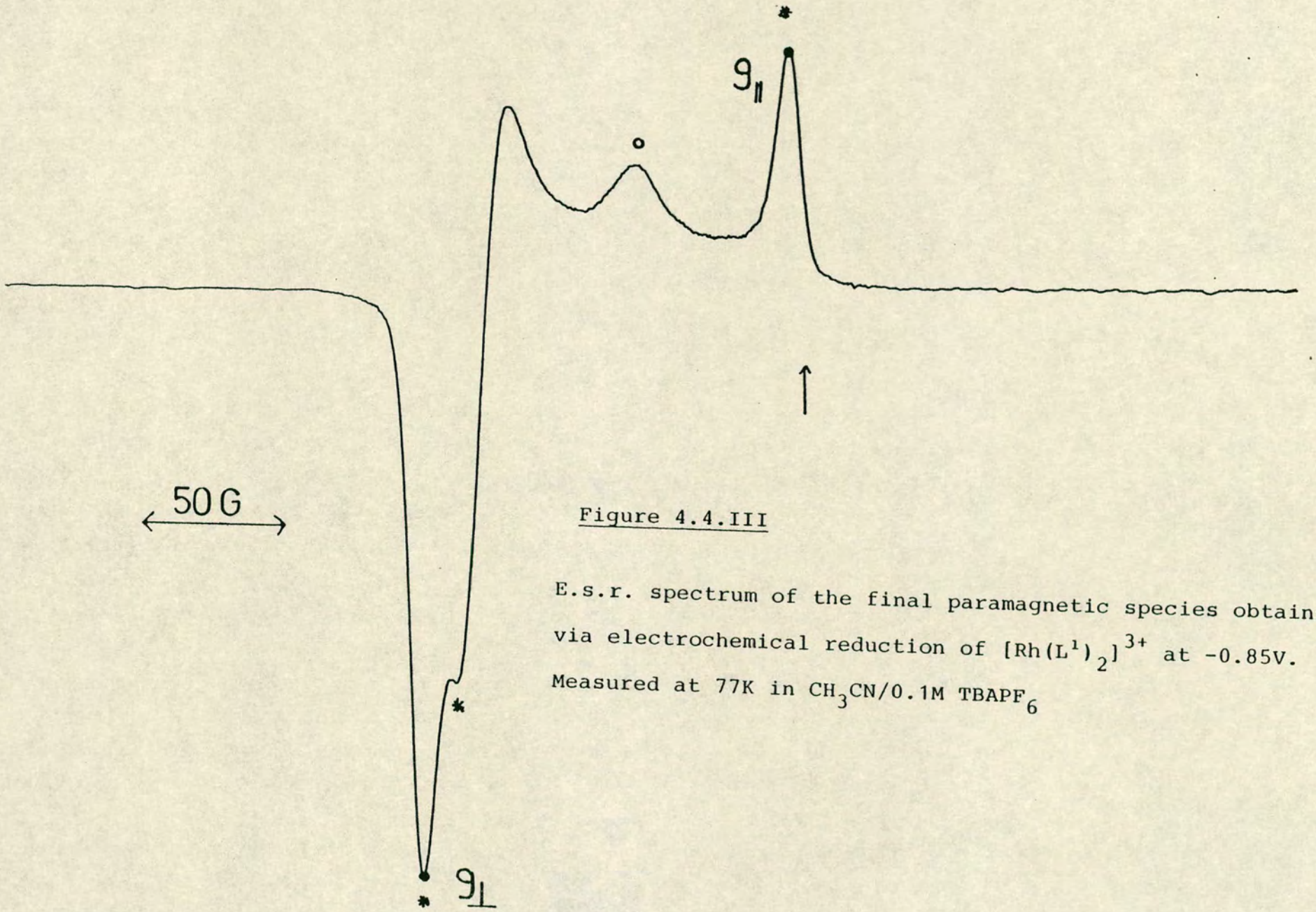

Figure 4.4.III

E.s.r. spectrum of the final paramagnetic species obtained via electrochemical reduction of $[Rh(L^1)_2]^{3+}$ at -0.85V. Measured at 77K in CH_3CN/0.1M $TBAPF_6$

data may be that the first signal (Figure 4.4.I) is averaged and represents a mixture of $[Rh(L^1)_2]^{3+}$ and $[Rh(L^1)_2]^{2+}$ in which intermolecular electron transfer occurs, and that the second signal (Figure 4.4.II) is of $[Rh(L^1)_2]^{2+}$ alone. If this is correct then the observation $g_\perp > g_\parallel \sim 2$ in this signal, as for the d^7 $[Pd(L^1)_2]^{3+}$ and $[Pt(L^1)_2]^{3+}$ cations, is consistent for the Jahn-Teller tetragonally elongated octahedral geometry expected for $[Rh(L^1)_2]^{2+}$ [124]. An alternative explanation of the observed experimental data is that the initially formed $[Rh(L^1)_2]^{2+}$ species may be highly reactive and that the second esr spectrum may be of a rearranged species.

Controlled potential electrolysis of $[Rh(L^1)_2]^{3+}$ at -1.2V gave an orange solution which showed a silent esr spectrum - possibly due to $[Rh(L^1)_2]^{+}$.

Clearly further extensive work has to be carried out to fully determine the nature of these reduced species. Specifically low temperature electrogeneration studies in conjunction with electronic spectroscopy using an optically transparant thin layer electrode (OTTLE), are envisaged.

Our studies indicate that the $[Rh(L^1)_2]^{2+}$ cation appears to be less stable than the isoelectronic $[Pd(L^1)_2]^{3+}$ or $[Pt(L^1)_2]^{3+}$ cations, possibly arising from an accessibility of both the d^8 and d^6 oxidation states via disproportionation, the d^8 state being stabilised by the π acceptor nature of L^1.

Although Rh(II) is well established in dimeric metal-metal bonded complexes[100] monomeric Rh(II) species are much

more poorly characterised. Examples of genuine Rh(II) d^7 complexes include $[RhCl_2(PCy_3)_2]$ [168] and $[RhCl_2[P(o\text{-}tol)_3]_2]$ [169] Like Pd and Pt a number of d^7 systems have been characterised with dithiolene ligands eg $[Rh(S_2C_2(CN)_2)_2]^{2-}$ [170] but these are likely to be more accurately regarded as Rh(III)-ligand radical systems.

4.5 Attempted synthesis of $[Rh(L^1)_2]^+$

The full characterisation of $[Rh(L^2)]^+$ [116] (L^2 = 1,4,8,11-tetrathiacyclotetradecane) and the evidence for $[Rh(L^1)_2]^+$ via electrochemical studies led to the hope that this cation could be synthesised directly via chemical means. The two Rh(I) starting materials selected for study were $[Rh_2(CO)_4Cl_2]$ (1) and $[Rh_2(C_2H_4)_4Cl_2]$ (2).

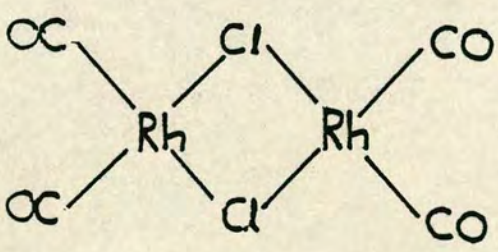

(1)

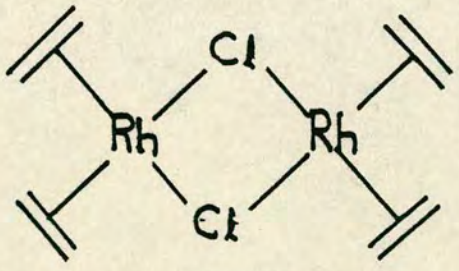

(2)

Reaction of $[Rh_2(CO)_4Cl_2]$ with four molar equivalents of L^1 in methanol resulted in the formation of a yellow solution from which an air stable yellow solid could be isolated upon addition of NH_4PF_6. An infra red spectrum of the solid indicated the presence of bridging carbonyl [171] (ν(CO) = 1793, 1745 cm^{-1}) and of bound L^1. However no Rh-Cl stretches were observed in the far infra red (down to 250 cm^{-1}). The probable formulation of the compound is thus $[Rh_2(CO)_2(L^1)_2](PF_6)_2$ (3).

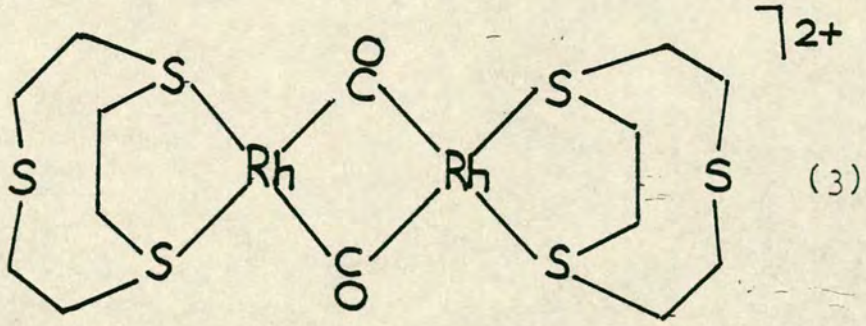

(3)

Carrying out the same reaction but in acetonitrile or dichloromethane led to the very rapid formation of an intensely blue product. This highly air sensitive material showed a very weak esr spectrum as a frozen glass in dichloromethane. This signal (g_1 = 2.033, g_2 = 2.023 g_3 = 2.011) closely resembled that for [Rh(OEP)(O_2)],[104] and may be as a consequence of partial oxidation of the sample.

Acetonitrile solutions of the air sensitive blue material showed two semi-reversible waves at $^1E_{\frac{1}{2}} \sim -0.7V$ ($\Delta Ep \sim 250$ mV) and $^2E_{\frac{1}{2}} \sim -1.1V$ ($\Delta Ep \sim 125$ mV) - possibly two oxidation processes for an $[Rh(L^1)_2]^+$ cation. Clearly however this interpretation is highly speculative, and future work is required to conclusively identify this deep blue air sensitive material.

In dichloromethane, but using $[Rh_2(C_2H_4)_4Cl_2]$ instead of $[Rh_2(CO)_4Cl_2]$, led to yet a different species being formed. Reaction of $[Rh_2(C_2H_4)_4Cl_2]$ with four molar equivalents of L^1 over four hours at 10°C led to the formation of an orange solution which, upon cooling, deposited well formed orange crystals. A structural determination of these however proved impossible due to their rapid efflorescence and their air and moisture sensitivity.

Infra-red data indicated that loss of ethylene had occurred, and L^1 had co-ordinated to the metal centre. A band at 292 cm^{-1} possibly indicative of an Rh-Cl stretch was present, suggesting a possible formulation $[Rh_2(L^1)_2Cl_2]$ (4) although elemental analysis of the crystalline solid was much closer for a formulation $[Rh(L^1)_2]Cl.(CH_2Cl_2)$ (5).

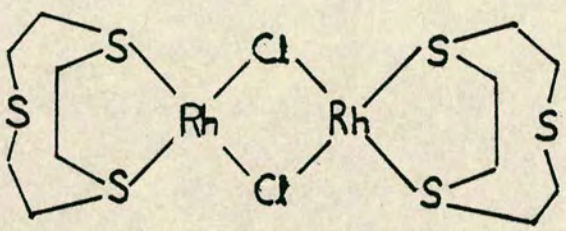

(4)

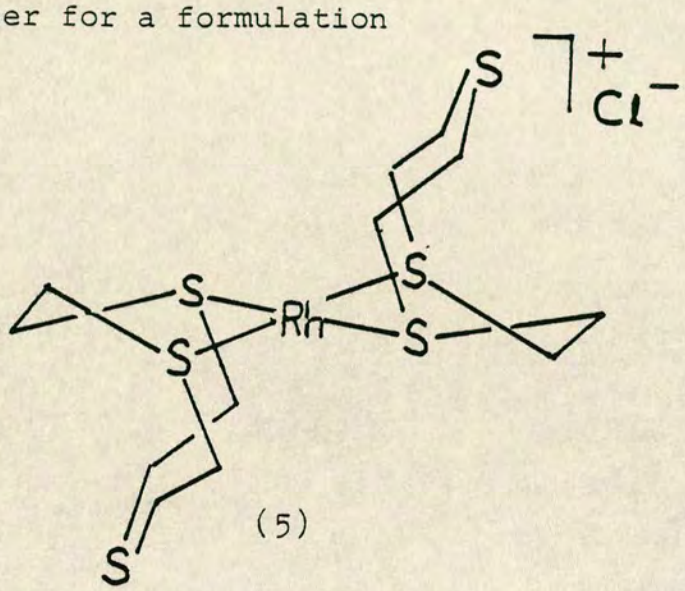

(5)

Clearly it would be highly desirable to obtain structural information for the d^8 $[Rh(L^1)_2]^+$ cation to see if, as for $[Pd(L^1)_2]^{2+}$ and $[Pt(L^1)_2]^{2+}$ a significant secondary interaction to the square plane is observed.

$[Rh(L^1)_2]^+$ would be expected to be highly reactive by analogy with $[Rh(L^2)]^+$.[116] Although the former may be stabilised to oxidative addition by protecting formally unbound thia donors, the stability of the system might by relatively reduced, compared with $[Rh(L^2)]^+$ since a macrocyclic stabilisation is now essentially absent.

4.6 Attempted preparation of $[M(L^1)_2]^{n+}$ systems (M = Ir, Ru and Os)

Unlike $Rh(H_2O)_6^{3+}$, $Ir(H_2O)_6^{3+}$ can be synthesised only with extreme difficulty.[172] Use of $IrCl_3.xH_2O$ as a starting material gave only $[Ir(L^1)Cl_3]$ as a pale green solid in dmso at 140°C. Attempts to obtain $[Ir(L^1)_2]^{3+}$ from this eg via heating in dmso in the presence of excess ligand, or via use of $TlPF_6$ to try and remove bound chloride proved unsuccessful. Very recently however $[Ir(L^1)_2]^{3+}$ has been synthesised via reaction of $IrCl_3$ with excess L^1 in ethylene glycol.[173]

$[Ru(L^1)_2]^{2+}$ was synthesised by reaction of $RuCl_3.xH_2O$ with an excess of L^1 in dmso, and from an aqueous solution of the cation the PF_6^- salt could be isolated on addition of NH_4PF_6. Independent work however showed[150] that both this cation and $[Os(L^1)_2]^{2+}$ could be more easily prepared via $[MCl_2(\eta^6\text{-arene})]_2$ complexes (M = Os,Ru) in the presence of excess L^1. Attempts to generate $[Os(L^1)_2]^{n+}$ species via Na_2OsCl_6 and L^1 however proved unsuccessful.

4.7 Summary

The observation of the d^6 Rh(III), d^7 Rh(II) and d^8 Rh(I) states in the $[Rh(L^1)_2]^{n+}$ system further underlines the ability of the L^1 ligand to stabilise a variety of metal oxidation states.

Clearly it was a disappointment to fail to identify conclusively the $[Rh(L^1)_2]^{2+}$ species. In contrast to $[Pd(L^1)_2]^{3+}$ or $[Pt(L^1)_2]^{3+}$ there is no evidence for the

growth of an intense visible charge transfer band upon formation of the d^7 species. It may be that the $[Rh(L^1)_2]^{2+}$ cation is reasonably stable and future work should be able to unambiguously identify it. Similarly the $[Rh(L^1)_2]^{+}$ cation might be expected to be isolated. Although it could not be conclusively identified in this project, the variety of products observed in its attempted synthesis has opened yet a further area of study, notably the nature and behaviour of the highly air sensitive blue species obtained by reaction of $[Rh_2(CO)_4Cl_2]$ and L^1.

In comparing the single crystal X-ray structures of $[Ru(L^1)_2]^{2+}$ [150] $[Rh(L^1)_2]^{3+}$ (d^6), $[Pd(L^1)_2]^{3+}$ (d^7) and $[Pd(L^1)_2]^{2+}$, $[Pt(L^1)_2]^{2+}$ we have a beautiful demonstration of the stereochemical control of platinum metals as a function of their d^n configuration. The almost perfect octahedral co-ordination of the d^6 species can be contrasted with the clear Jahn-Teller distortion for the d^7 species and the modified square planar co-ordination of the d^8 species.

With the successful preparation of $[Ir(L^1)_2]^{3+}$ [173] a direct electrochemical comparison with $[Rh(L^1)_2]^{3+}$ is clearly a priority, so as to complete a study of the $d^6/d^7/d^8$ manifold for the platinum metals (Rh,Ir,Pd,Pt) for which these states are accessible.

4.8 Experimental

All physical measurements were carried out as in Chapter 2.

Starting materials

$RuCl_3.xH_2O$, $RhCl_3.xH_2O$, $IrCl_3.xH_2O$ and OsO_4 were all provided as generous loans from Johnson-Matthey.
L^1 (1,4,7-trithiacyclononane) was prepared according to literature methods.[67] $[Rh_2(CO)_4Cl_2]$[175] and $[Rh_2(C_2H_4)_4Cl_2]$[176] were synthesised according to established literature procedures. All reactions involving Rh(I) were performed under nitrogen using Schlenk line techniques using solvents purified according to standard procedures.[174]

Synthesis of complexes

$[Rh(L^1)_2](PF_6)_3.xH_2O$

$RhCl_3.3H_2O$ (0.5 g, 1.90×10^{-3}mol) was refluxed in water (50 ml) with three molar equivalents of $AgNO_3$ (0.97 g, 5.70×10^{-3}mol) for four hours to give a yellow solution of "$Rh(H_2O)_6^{3+}$" and AgCl which was removed by filtration.

An aliquot of the "$Rh(H_2O)_6^{3+}$" solution (15 ml, 5.7×10^{-4}mol) was added to a methanolic solution (15 ml) of L^1 (0.215 g, 1.2×10^{-3}mol) and refluxed for ninety minutes. Addition of an excess of NH_4PF_6 to the resultant yellow-orange solution gave impure $[Rh(L^1)_2](PF_6)_3$ as a yellow-orange solid. An orange impurity was removed on heating the solid in methanol, and the cream coloured pure salt collected by filtration. Crystals of $[Rh(L^1)_2](PF_6)_3$

were obtained upon recrystallisation from water. Yield 0.200 g (40%). Since the crystals rapidly lost solvent on removal from water the single crystal X-ray structural determination was performed sealing a crystal in a Lindemann tube in the presence of mother liquor.

Elemental analysis (after drying *in vacuo*): Found C=16.2; H=2.7%. Calculated for [$Rh(L^1)_2(PF_6)_3$: C=16.0; H=2.7%. Infra-red spectrum (L^1 bands) 2985, 2948, 1444, 1411, 1300, 1289, 1270, 1248, 1178, 1134, and 840 cm^{-1}. ^1H n.m.r. spectrum (CD_3NO_2 80 and 200MHz) δ_H = 3.77 (24 H AA'BB' CH_2 (L^1)) (Figure 4.2.I). Electronic spectrum (T.I.Hyde), λ_{max} =270 nm (ε = 30,600 $M^{-1}cm^{-1}$). CH_3CN. Mass spectrum (f.a.b.). M^+ = 752 ($[Rh(L^1)_2](PF_6)_2^+$ = 753), M^+ = 607 ($[Rh(L^1)_2](PF_6)^+$ = 608), M^+ = 461 ($[Rh(L^1)_2]^+$ = 463).

$[Rh(L^1)_2]^{2+}$ and $[Rh(L^1)_2]^+$ were prepared *in situ* by controlled potential electrolysis of $[Rh(L^1)_2]^{3+}$ in acetonitrile (40 mg/5 ml) at -0.7V and -1.1V respectively (vs Ag/Ag^+) at a platinum gauze electrode.

$[Rh(L^1)_2]^{2+}$: Esr spectrum (I) (CH_3CN 77K) g_{av} = 2.06 (Gain = 2.5 x 10^2) (Figure 4.4.I). Esr spectrum (II) (CH_3CN 77K) $g_\perp$ = 2.088, $g_\parallel$ = 2.008 (Gain = 2.5 x 10^2) (Figure 4.4.II).

Reactions of Rh(I) with 1,4,7-trithiacyclononane (L^1)

$[Rh_2(CO)_4Cl_2]/L^1$

a) Dichloromethane. Addition of L^1 (0.095 g, 5.3 x 10^{-4}mol) to a dichloromethane solution (25 ml) of $[Rh_2(CO)_4Cl_2]$ (0.050 g, 1.3 x 10^{-4}mol) at 0°C led to the

rapid formation of a deep blue highly air sensitive product which precipitated out of solution. Esr spectrum (CH_2Cl_2 77K) $g_1 = 2.033$ $g_2 = 2.023$ $g_3 = 2.011$ (Grain = 1.6×10^5).

b) Acetonitrile. Under the same conditions a similar product was again obtained but showed a higher degree of solubility. Decomposition of the product was observed over a few hours even under a flow of nitrogen.

c) Methanol. Refluxing a solution of L^1 (0.10 g, 5.6×10^{-4}mol) and $[Rh_2(CO)_4Cl_2]$ (0.050 g, 1.3×10^{-4}mol) in methanol (20 ml) for 15 minutes gave a yellow solution. Addition of NH_4PF_6 to the cooled solution gave a yellow air stable product which was filtered and washed with methanol, dichloromethane and diethyl ether. Infra-red spectrum (carbonyl) 1794 (s), 1745 (vs). (L^1 bands) 1442, 1403, 1282, 1173 and 1125 cm^{-1}. Solutions of the product were air sensitive and attempted recrystallation led to slow decomposition of the product.

$[Rh_2(ethylene)_4Cl_2]/L^1$

L^1 (0.10 g, 5.6×10^{-4}mol) was added to a cold degassed solution of $[Rh_2(C_2H_4)_4Cl_2]$ (0.050 g, 1.3×10^{-4}mol) in dichloromethane (20 ml). Reaction proceeded steadily over a period of four hours taking care to maintain the temperature of *ca.* 10°C. On cooling the orange solution overnight in the fridge orange crystals of the reaction

product formed in the Schlenk tube. On removal from the solvent these crystals rapidly deteriorated.

Elemental analysis: Found C=26.3, 26.7%; H=4.42, 4.57%. Calculated for $[Rh(L^1)_2]Cl.CH_2Cl_2$. C=26.7; H=4.49%.

Infra-red spectrum: 3024, 2958, 2946, 2918, 2902, 1447, 1420, 1401, 1393, 1299, 1149, 1135, 1119, 1110, 927, 897, 827, 819, 814, 682, 485, 445 and 292 cm^{-1}.

CHAPTER 5

1,4,7-Trithiacyclononane Complexes of Nickel and Copper

5 1,4,7-Trithiacyclononane complexes of nickel and copper

5.1 Introduction

Wieghardt *et al.* have previously investigated the electrochemistry of the $[Ni(L^1)_2]^{2+}$ complex cation [31] (L^1 = 1,4,7-trithiacyclononane) and reported a one electron oxidation at +0.97V (vs Fc/Fc^+ = 0). At the time doubt was expressed as to whether this oxidation was ligand or metal based since oxidation of the free ligand L^1 occurs at a similar potential.[31]

To complete an electrochemical study upon the $[M(L^1)_2]^{2+}$ complexes of the nickel tried (Ni, Pd, Pt) a reinvestigation of this system was attempted. Esr spectroscopy was hoped to lead to a more definite understanding of the redox processes occurring in this system.

The characterisation of trivalent nickel is also relevant in a biological context, since several nickel containing enzymes[177] and oligopeptide complexes show nickel in this oxidation state.[178]

The second area of work in this chapter concerns co-ordination of L^1 to Cu(I). The discovery of thia co-ordination to copper in the blue copper proteins plastocyanin and azurin[179-181] has led to substantial interest in the study of model copper thia systems which may mimic the behaviour of the active biological systems. In the natural systems a primary 'S_2N_2' co-ordination is believed to occur about the metal centre. Metal ligation through thioethers has been considered not only to contribute to the anomalously

high redox potentials for these blue copper proteins but also their facility to participate in exceptionally rapid electron transfer processes.[182]

Recently stable thioether copper complexes have been prepared with the hexathia macrocycle L^3 (1,4,7,10,13,16-hexathiacyclooctadecane). Both $[Cu(L^3)]^+$ and $[Cu(L^3)]^{2+}$ have been structurally characterised.[70] In $[Cu(L^3)]^+$ the copper atom lies in a distorted tetrahedral environment with two short, and two long Cu-S bond distances being observed.

In the d^9 $[Cu(L^3)]^{2+}$ cation all the sulphur atoms are bound to the metal centre to give overall a tetragonally distorted octahedral geometry. Surprisingly despite the gross structural differences between $[Cu(L^3)]^+$ and $[Cu(L^3)]^{2+}$ a reversible one electron couple was observed via cyclic voltammetry. Also notable was the highly anodic potential (+0.72V vs SCE) at which this couple occurred.

Reaction of two molar equivalents of $[Cu(CH_3CN)_4]^+$ with L^3 leads to the formation of the binuclear $[Cu_2(L^3)_2(CH_3CN)_2]^{2+}$ species (1).[183]

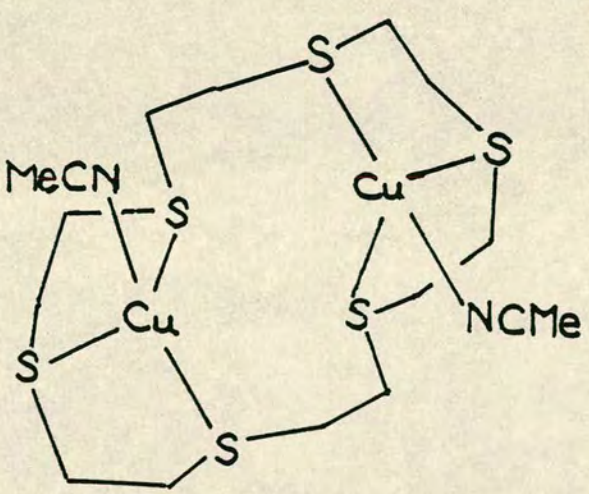

(1)

In this complex each Cu(I) centre has distorted tetrahedral 'S_3N' co-ordination, similar to the active site for the blue copper proteins. The complex in either acetonitrile or nitromethane solution was stable to oxidation, however addition of $HClO_4$ did lead to oxidation. This was suggested to occur via protonation of co-ordinated acetonitrile and may be of relevance to the acid mediated oxidation and dissociation of nitrogen donor ligands from Cu(I) at the active site of plastocyanin.[184] Other homoleptic thioethers of four or five co-ordinate copper have been studied by Rorabacher *et al.*[185,186]

In this work the synthesis of the $[Cu(L^1)]^+$ moiety is attempted with a view to investigate its interaction with a variety of nitrogen donors and π acceptor ligands (CO, olefins, phosphines). Such $[Cu(L^1)X]^+$ complexes might show novel electronic and redox properties.

Cooper *et al.*[70] have reported the electrochemistry of $[Cu(L^1)_2]^{2+}$ in nitromethane indicating a facile one electron quasi-reversible reduction at +0.61V (vs SCE) for the system.

Results and discussion

5.2 Electrochemical and esr studies upon $[Ni(L^1)_2]^{2+}$

$[Ni(L^1)_2](BF_4)_2$ and $[Ni(L^1)_2](PF_6)_2$ were synthesised according to literature procedures[31,64] and purified by recrystallisation from acetonitrile/diethyl ether. Enriched ^{61}Ni samples of $[Ni(L^1)_2](PF_6)_2$ were also prepared to aid in the interpretation of esr spectra. Cyclic voltammetry of $[Ni(L^1)_2]^{2+}$ in acetonitrile showed a chemically reversible oxidation (Figure 5.2.I(a)) close to the reported literature value[31] with $E_{\frac{1}{2}}$ = +0.96V ΔEp = 82 mV (vs Fc/Fc^+). However a previously unreported reduction was also observed for this system which became fully reversible at -25°C, with $E_{\frac{1}{2}}$ = -1.11V ΔEp = 90 mV (Figure 5.2.I(b)).

The identity of the oxidised species as $[Ni(L^1)_2]^{3+}$ was confirmed by electrogeneration of the yellow-orange cation in acetonitrile at +1.05V (vs Ag/Ag^+). This oxidised species as a frozen glass showed an anisotropic esr spectrum (Figure 5.2.II(a)) with $g_\perp$ = 2.084 $g_\parallel$ = 2.020, in full accord for a genuine metal based d^7 Ni(III) radical.[124,187] Enriched ^{61}Ni (I = 3/2 40%) samples of $[Ni(L^1)_2]^{3+}$ showed additional hyperfine coupling to ^{61}Ni, which became more distinct for a solution of $[Ni(L^1)_2]^{3+}$ obtained via chemical oxidation in 70% aqueous $HClO_4$. The frozen glass esr spectrum of this sample, for which $g_\perp$ = 2.092 $g_\parallel$ = 2.022 (Figure 5.2.II(b)) clearly shows the outer two ^{61}Ni coupled resonances in the expected 4 line signal in the $g_\perp$ region of the spectrum. The centre two

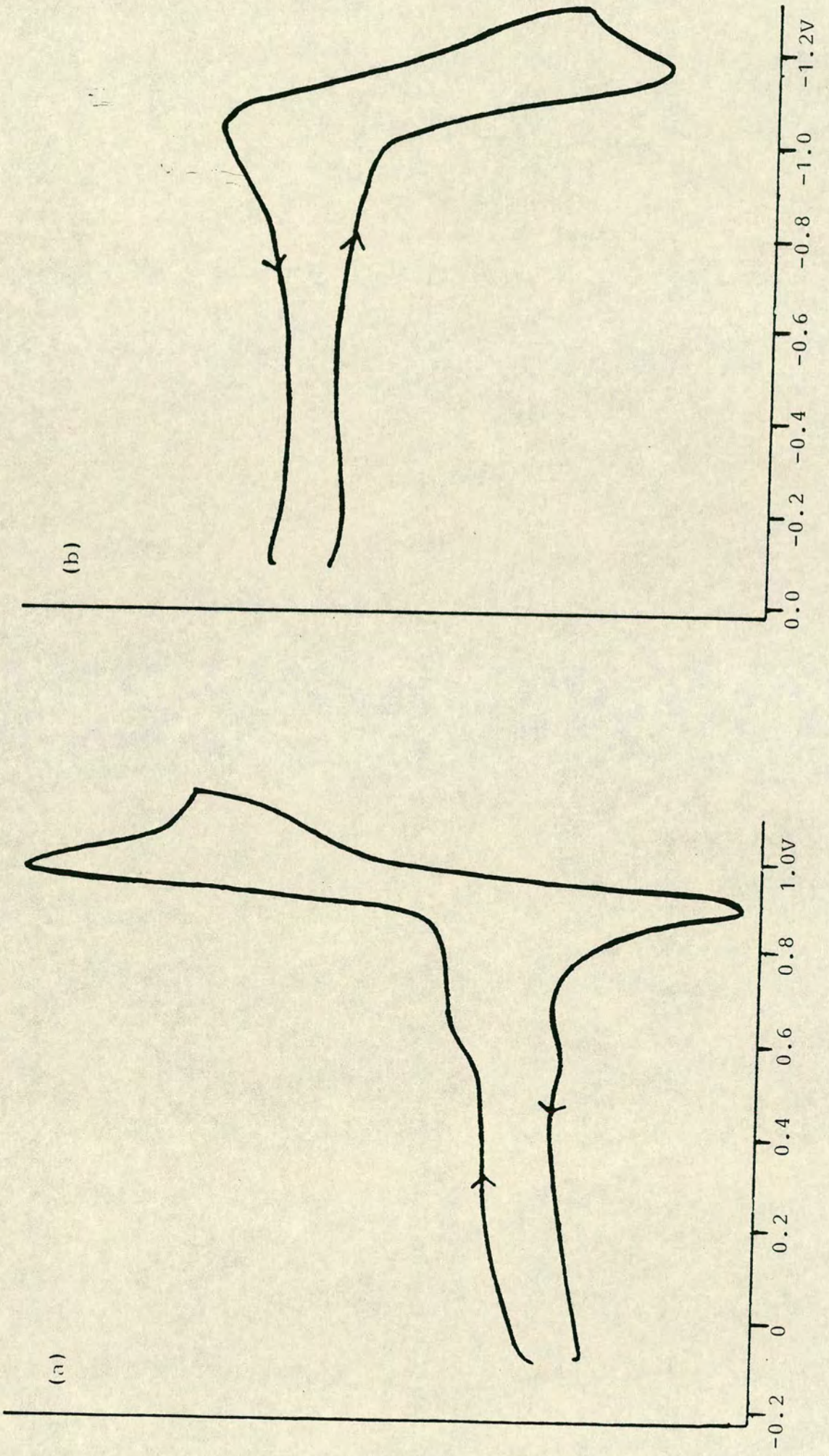

Figure 5.2.I: Cyclic voltammogram of $[Ni(L^1)_2]^{2+}$ in $CH_3CN/0.1M$ $TBAPF_6$

(a) oxidation range (b) reduction range

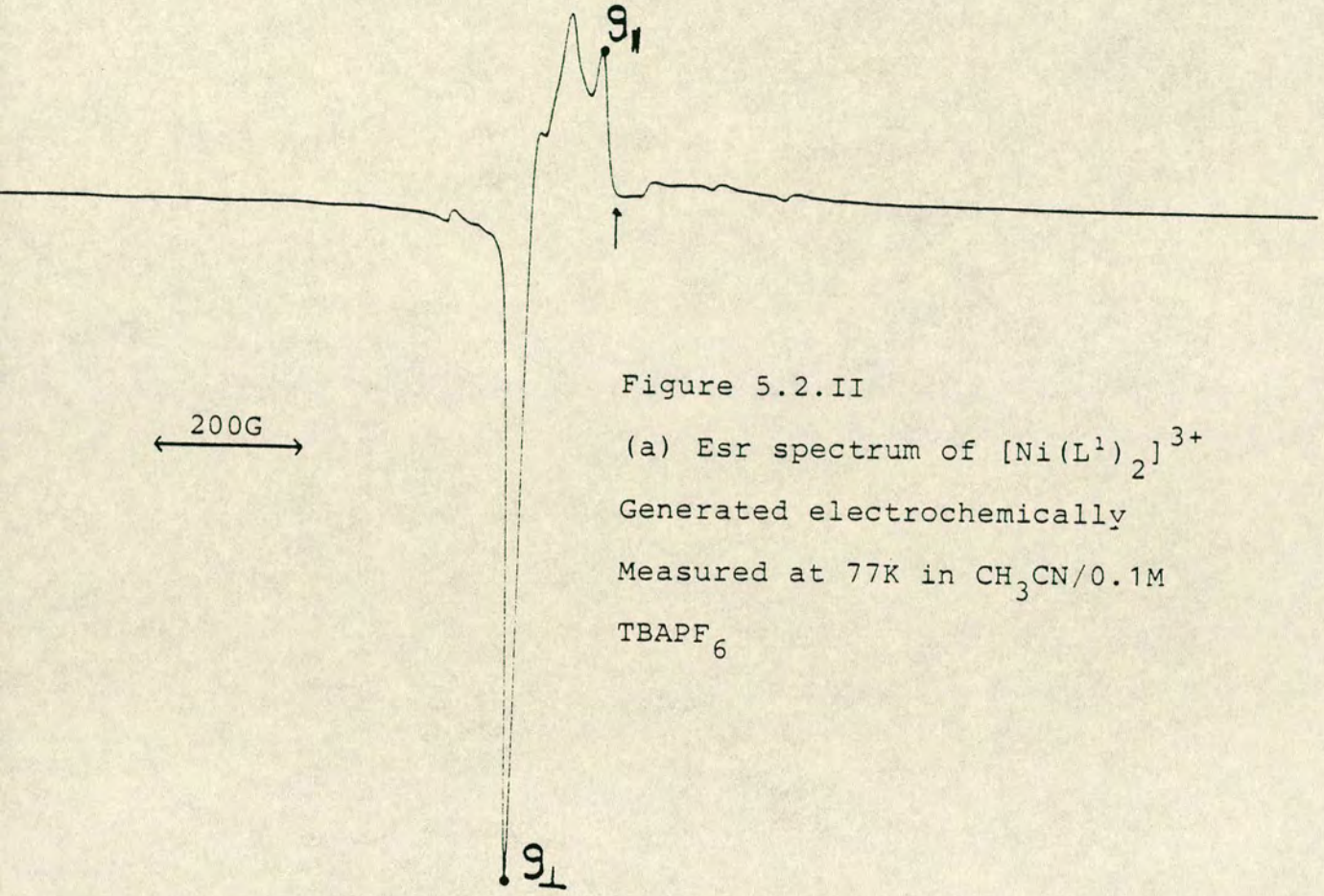

Figure 5.2.II

(a) Esr spectrum of $[Ni(L^1)_2]^{3+}$
Generated electrochemically
Measured at 77K in CH_3CN/0.1M
$TBAPF_6$

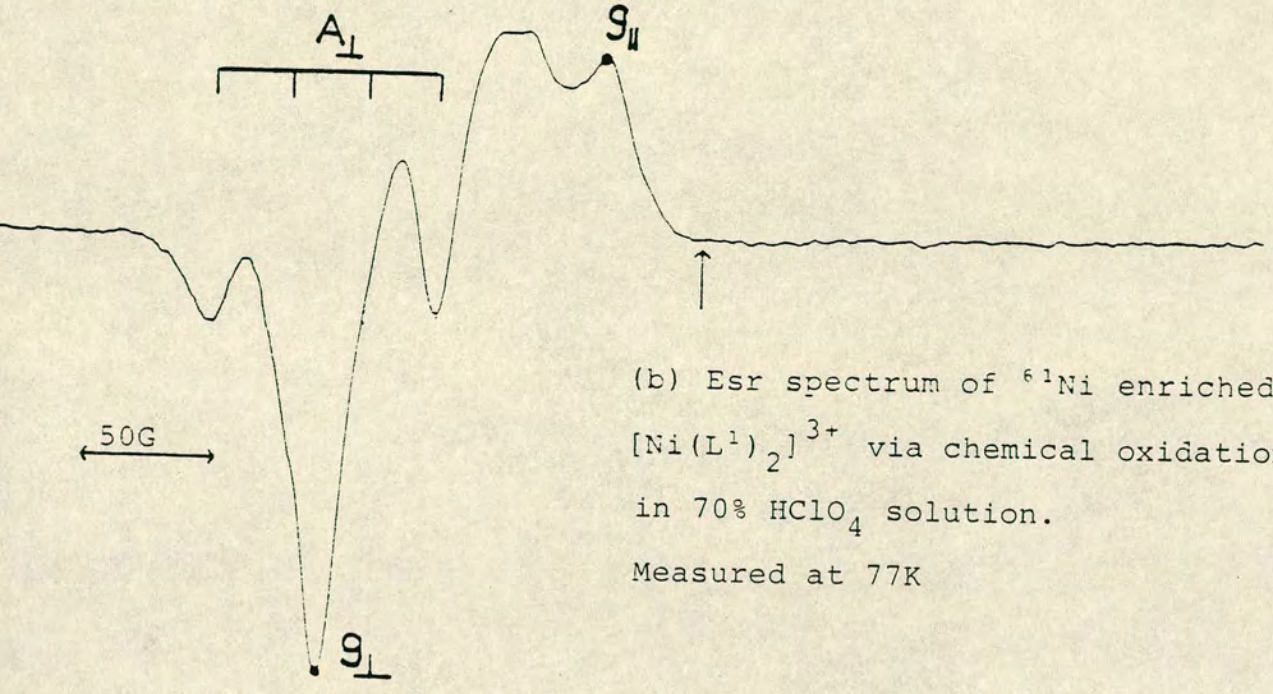

(b) Esr spectrum of ^{61}Ni enriched $[Ni(L^1)_2]^{3+}$ via chemical oxidation in 70% $HClO_4$ solution.
Measured at 77K

lines however are not evident as they remain masked by the more intense uncoupled $g_{\perp}$ signal. A value of $A_{\perp}$ of 30G is estimated for the hyperfine coupling to ^{61}Ni in this spectrum.

The initial formulation by Wieghardt *et al.*[31] of the oxidised species upon removal of an electron from $[Ni(L^1)_2]^{2+}$ as a ligand based radical was primarily based upon the similarity of the oxidation potential of L^1 and of $[Ni(L^1)_2]^{2+}$. Recent studies[150] have however shown that upon binding to a metal centre, ligand redox processes seem to be suppressed, so that for $[Ru(L^1)_2]^{2+}$ [150] redox inactivity is shown between -2.2 and +1.4V (vs $Fc/Fc^+ = 0$) in acetonitrile.

In this work, both the observed hyperfine coupling and the anisotropy in the esr spectrum for $[Ni(L^1)_2]^{3+}$ suggests a metal rather than a ligand based radical.

Ni(III) has been observed in a large number of complexes,[187,188] with structurally characterised examples including $[Ni(bipy)_3]^{3+}$ [189] $[Ni(L^4)_2]^{2+}$ [43] (L^4 = 1,4,7-triazacyclononane) $[Ni(cyclam)Cl_2]^+$ [190] and $[Ni(L^4.3CH_2CO_2)]$.[75] All of these show the sequence $g_{\perp} > g_{\parallel} \sim 2$ as observed in our systems, eg for $[Ni(L^4)]^{3+}$ $g_{\perp} = 2.12$ $g_{\parallel} = 2.03$ [43] $[Ni(L^1)_2]^{3+}$ is however the first hexathia complex in which the d^7 state is stabilised for nickel, doubtless as a consequence of kinetic stability and co-ordinative flexibility of L^1 as discussed previously.

The observation of a reduction wave for $[Ni(L^1)_2]^{2+}$ obviously led to an attempt to electrogenerate the reduced species. In some experiments this was successful, with

controlled potential electrolysis at -1.1V (vs Ag/Ag^+) in acetonitrile resulting in the formation of the green $[Ni(L^1)_2]^+$ cation. An esr spectrum of this as a frozen glass showed a highly anisotropic signal with $g_{\parallel} = 2.173$ and $g_{\perp} = 2.055$, indicative of a metal based d^9 species (Figure 5.2.III).[187,124] Ni(I) species have been characterised in a variety of macrocyclic systems[187] eg $[Ni(cyclam)]^+$ which shows $g_{\parallel} = 2.261$ $g_{\perp}$ 2.060.[192]

Unfortunately only a preliminary study of $[Ni(L^1)_2]^{3+}$ and $[Ni(L^1)_2]^+$ could be made. Future studies would probably centre upon low temperature electrogeneration studies in conjunction with esr and electronic spectroscopy.

Even for the brief study made upon this system it is clearly evident that the $[Ni(L^1)_2]^{2+}$ cation, as for $[Pd(L^1)_2]^{2+}$ and $[Pt(L^1)_2]^{2+}$ shows a significant and interesting redox behaviour.

The $[Ni(L^1)_2]^+$ cation in particular may be of potential use in the activation and rearrangement of small molecule substrates and so may act as a viable homogeneous catalytic reagent.[191,193]

5.3 Preparation and reactions of $[Cu(L^1)(CH_3CN)]^+$

Refluxing $[Cu(CH_3CN)_4](ClO_4)$ and L^1 in an equimolar ratio for four hours led to the formation of the $[Cu(L^1)(CH_3CN)]^+$ complex cation (2) which was isolated as the perchlorate salt upon addition of diethyl ether.

Figure 5.2.III Esr spectrum of $[Ni(L^1)_2]^+$ generated electrochemically.

Measured at 77K in CH_3CN/0. M $TBAPF_6$

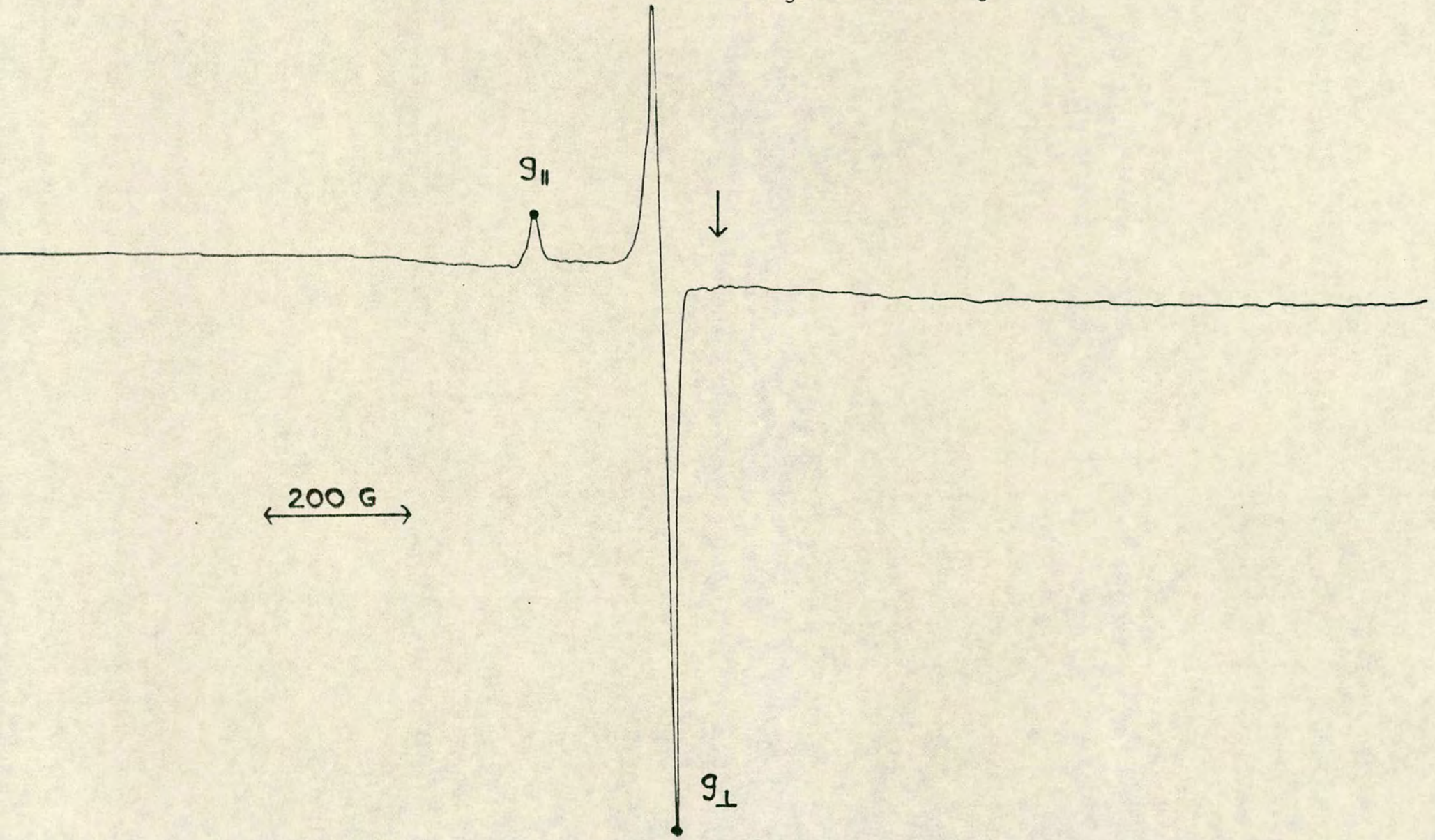

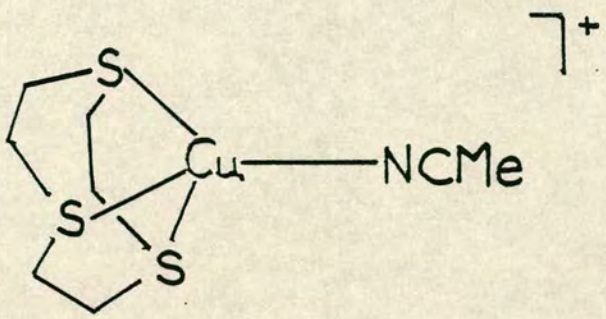

(2)

The cation appears to be air stable in the solid state, but solutions upon standing slowly turned yellow. A ^1H n.m.r. spectrum of the cation (in CD_3NO_2) confirmed the presence of L^1 and acetonitrile in a 1:1 ratio. In preliminary studies the cation appeared not to react with CO and gave only ill defined air sensitive products with pyridine or PEt_3. However reaction of warm acetonitrile solutions of $[Cu(L^1)(CH_3CN)]$ with PPh_3 or $AsPh_3$ gave air stable crystalline adducts $[Cu(L^1)(PPh_3)](ClO_4)$ and $[Cu(L^1)(AsPh_3)](ClO_4)$ as confirmed by elemental analysis and by ^1H n.m.r. spectroscopy. Comparison of the ^1H n.m.r. spectra for the phosphine adduct (run in CD_3NO_2) and the arsine adduct (run in CD_3CN) (Figures 5.3.I and 5.3.II) indicate a higher degree of complexity for the resonances of the phosphine adduct.

This difference may simply be a result of the different solvent used in each case.

Cyclic voltammetry of $[Cu(L^1)(AsPh_3](ClO_4)$ in acetonitrile showed complex behaviour. Continual sweeping

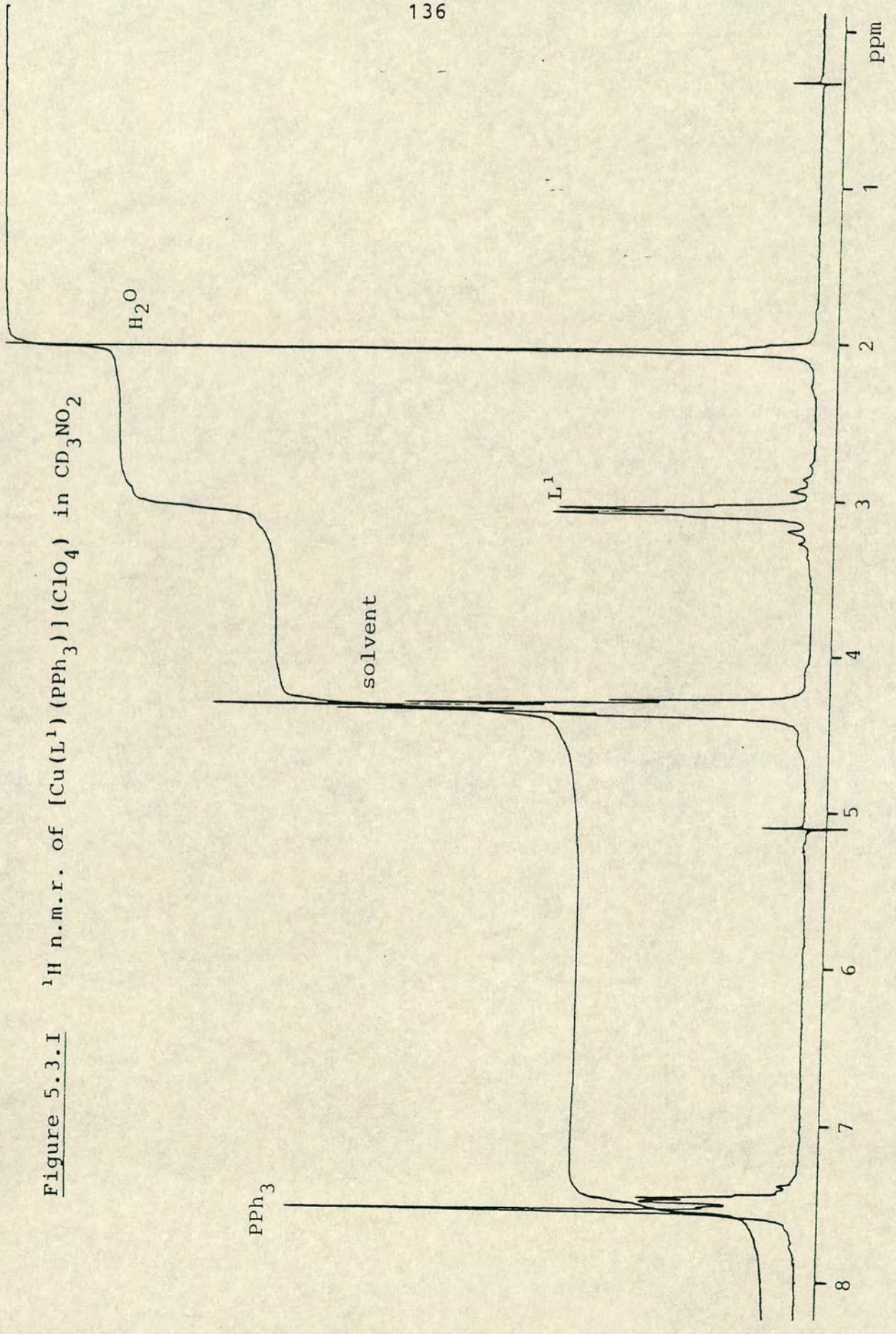

Figure 5.3.I ^1H n.m.r. of $[Cu(L^1)(PPh_3)](ClO_4)$ in CD_3NO_2

Figure 5.3.II ^1H n.m.r. of $[Cu(L^1)(AsPh_3)]^+$ in CD_3CN

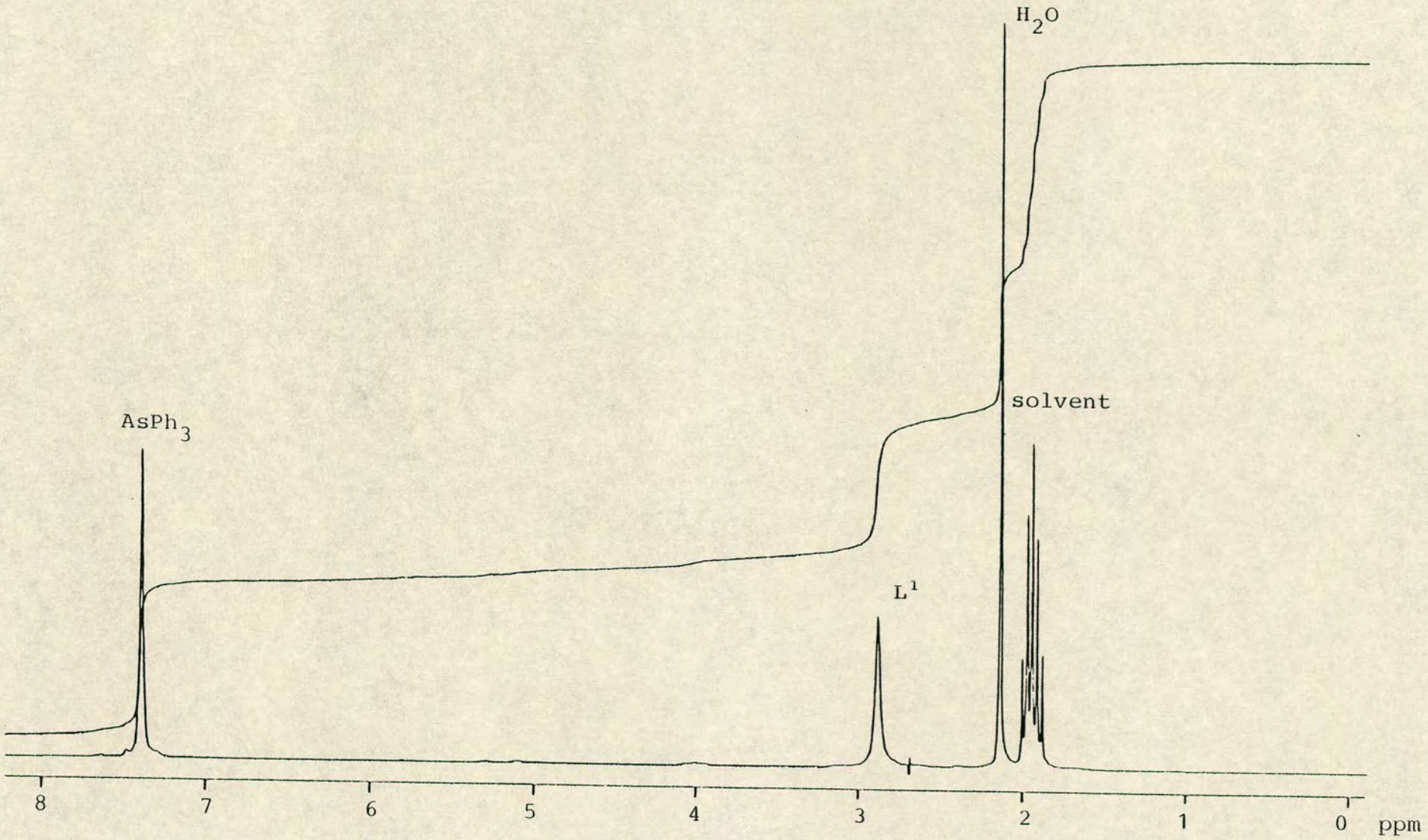

between -0.2V and +1.2V (vs Fc/Fc^+) generated two essentially chemically reversible couples. These were clearly due to transient species generated in solution as indicated by the loss of this response after a time lapse of 10 seconds between sweeps.

Oxidation of Cu(I) to Cu(II) is generally associated with an increase in co-ordination number and the transient species generated at the electrodes may well be 5 or 6 co-ordinate solvated species e.g. $[Cu(L^1)(AsPh_3)(CH_3CN)_{1 \text{ or } 2}]^{+/2+}$.

5.4 The single crystal X-ray structure of $[Cu(L^1)(AsPh_3)](ClO_4)$

A noticeable feature for the 'blue' copper proteins is the distorted tetrahedral geometry around the metal centre, and so a primary reason for the determination of the single-crystal X-ray structure of $[Cu(L^1)(AsPh_3)]^+$ was to observe the co-ordination at the Cu(I) centre.

Crystal data. $C_{24}H_{27}AsCuS_3^+ClO_4^-$ M = 649.6 rhombohedral. Space Group $R\bar{3}$ a = 11.127(6) c = 37.255(12)Å U = 4612Å^3 Z = 6, D_c = 1.403 g cm^{-3}. At the present state of refinement R = 0.059 for 492 data. A partial disorder present in the bound macrocycle is still being modelled.

Important bond lengths and angles are given in Table 5.4.I. A view of the complex cation is shown in Figure 5.4.II.

The cation is located on a crystallographic 3-fold

Table 5.4.I Selected bond lengths and angles (with esd's) for $[Cu(L^1)(AsPh_3)]^+$

Bond lengths (Å)

Cu-As	2.297(4)
Cu-S	2.315(6)
As-C	1.926(14)

Bond angles (degrees)

As-Cu-S	122.5(4)
S-Cu-S	94.0(5)
C-As-Cu	115.7(4)
C-As-C	102.4(6)

Torsion angle

C-As-Cu-S = 23.7(5)° (and ±120°)

Figure 5.4.II View of the single crystal X-ray structure of $[Cu(L^1)(AsPh_3)]^+$

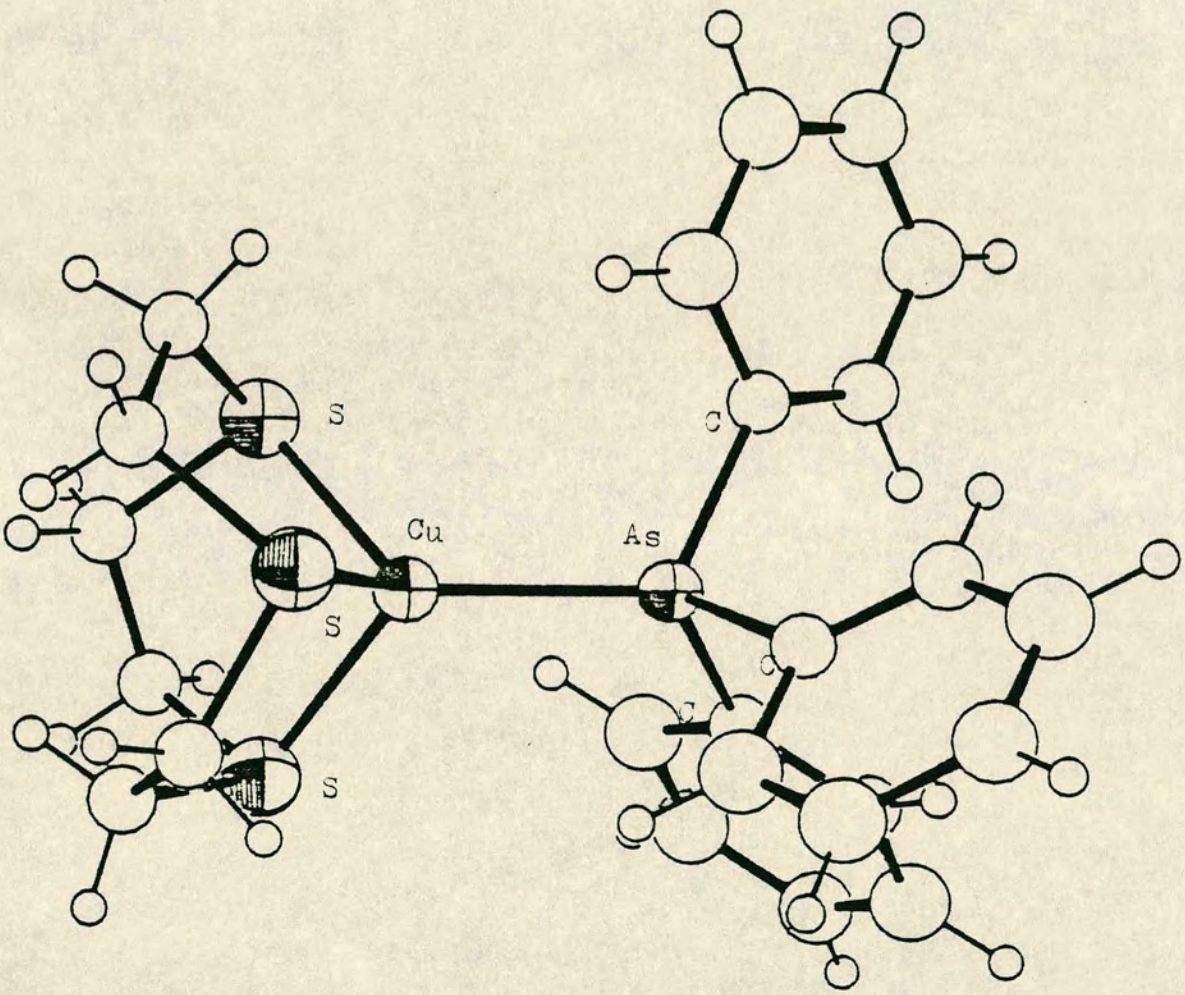

axis, and so has imposed C_3 symmetry. Distorted tetrahedral co-ordination occurs about the Cu(I) centre. The small 'bite' of the L^1 ligand gives <SCuS bond angles of 94.0(5)° - substantially reduced from tetrahedral.

The bound ligand L^1 and the phenyl groups of the bound arsine do not sterically interact and the observed <SCu-AsC torsion angle of 23.7(5)° is almost certainly due to crystallographic packing forces.

5.5 Future work upon copper 'S_3N' systems

It is the catalytic and redox behaviour of 'S_3N' systems based upon the $[Cu(L^1)]^+$ moiety and nitrogen donor ligands that is perhaps of most interest. To such an end it is the preparation and behaviour of adducts such as $[Cu(L^1)(pyridine)]^+$ or $[Cu(L^1)(NEt_3)]^+$ that requires most study. Certainly initial results indicate a heightened reactivity of the $[Cu(L^1)(py)]^+$ derivative and so is of possible significance in understanding the role of the blue copper proteins.

5.6 Experimental

All physical measurements were carried out as in Chapter 2. $[Cu(NCMe)_4](ClO_4)$ was synthesised by A. Lavery. L^1 (1,4,7-trithiacyclononane was purchased from Aldrich Co.

Preparation of $[Ni(L^1)_2](PF_6)_2$ and $[Ni(L^1)_2](BF_4)_2$

$[Ni(L^1)_2](BF_4)_2$ was synthesised according to the

literature procedure[64] but recrystallised from acetonitrile/diethyl ether instead of ethanol. The PF_6^- salt was made by reaction of L^1 (0.14 g, 7.8 x 10^{-4}mol) with $Ni(NO_3)_2.6H_2O$ (0.10 g, 3.8 x 10^{-4}mol) in ethanol (25 ml) under reflux for 2 hrs to yield $[Ni(L^1)_2]^{2+}$. Addition of an excess of NH_4PF_6 precipitated the product which was washed with ethanol, dichloromethane and diethyl ether. Recrystallisation from acetonitrile/diethyl ether gave pure crystalline $[Ni(L^1)_2](PF_6)_2$. Yield 190 mg (70%). An enriched ^{61}Ni sample of $[Ni(L^1)_2](PF_6)_2$ was prepared by a similar procedure but on one fifth the previous scale.

^{61}Ni metal was provided as a generous gift from B.P. Chemicals. Enriched ^{61}Ni, $Ni(NO_3)_2.6H_2O$ was prepared from this by reaction with nitric acid (T.I. Hyde).

Elemental analysis and infra-red data were in accord with literature values for these salts.[31,64]

Preparation of $[Ni(L^1)_2]^{3+}$

(a) Controlled potential electrolysis

Controlled potential electrolysis of a solution of $[Ni(L^1)_2](PF_6)_2$ (40 mg) in acetonitrile (5 ml) at +1.1V (vs Ag/Ag^+) generated the yellow orange $[Ni(L^1)_2]^{3+}$ cation. Esr spectrum: (CH_3CN 77K) $g_\perp = 2.084$ $g_\parallel = 2.020$ (Gain = 1.25 x 10^4) (Figure 5.3.II(a)).

(b) Chemical oxidation

Chemical oxidation of a solution of $[Ni(L^1)_2](PF_6)_2$ (20, 2^* mg) in 70% aqueous $HClO_4$ (5, 2^* ml) (* enriched ^{61}Ni)

at 40°C for two hours give yellow-orange solutions of $[Ni(L^1)_2]^{3+}$. Esr spectrum: (70% $HClO_4$ 77K) $g_\perp = 2.092$ $g_{||} = 2.022$ $A_\perp^* = 30G$ (Gain = 1.6×10^4). (Figure 5.2.II(b)).

Preparation of $[Ni(L^1)_2]^+$

Controlled potential electrolysis of a solution of $[Ni(L^1)_2](PF_6)_2$ (40 mg) in acetonitrile (5 ml) at -1.1V (vs Ag/Ag^+) generated the green $[Ni(L^1)_2]^+$ cation. Esr spectrum (CH_3CN 77K) $g_\perp = 2.055$ $g_{||} = 2.173$ (Gain = 8×10^4). (Figure 5.2.III).

Preparation of $[Cu(L^1)(CH_3CN)](ClO_4)$

$[Cu(CH_3CN)_4](ClO_4)$ (0.23 g, 7.03×10^{-4}mol) and L^1 (0.130 g, 7.22×10^{-4}mol) react in refluxing acetonitrile (30 ml) under a nitrogen atmosphere to give initially a dark yellow species. Continued refluxing however leads to the formation of a colourless solution of the product. Addition of diethyl ether (50 ml) to the cooled solution gave the white crystalline air stable salt $[Cu(L^1)(CH_3CN)]^+(ClO_4)$ in high yield. ^1H n.m.r. spectrum (CD_3NO_2 80MHz) $\delta_H = 2.08$ (3H br s CH_3CN) 3.10 (12H br s CH_2 (L^1)).

Synthesis of complexes

$[Cu(L^1)(PPh_3)](ClO_4)$

$[Cu(L^1)(CH_3CN)](ClO_4)$ (0.100 g, 2.6×10^{-4}mol) was dissolved in warm acetonitrile and a solution of PPh_3

(0.070 g, 2.7 x 10^{-4}mol) in acetonitrile added. On cooling the product crystallised out of solution. Recrystallisation from nitromethane (5 ml) gave the pure crystalline salt. Yield = 125 mg (70%). Elemental analysis: Found C=46.8;, 46.9; H=4.38, 4.42%. Calculated for $[Cu(L^1)(PPh_3)](ClO_4)$ C=47.6; H=4.49%. Infra-red spectrum: (L^1 bands) 1437, 1404, 1328, 1303 and 1279 cm^{-1} (PPh_3 bands) 3040, 1478, 815, 748, 709, 695, 620, 529, 502 and 440 cm^{-1}. ^1H n.m.r. spectrum (CD_3NO_2 80MHz) δ_H = 3.06 (12H m CH_2 (L^1)) 7.5 (15H m CH (PPh_3)) (Figure 5.3.I).

$[Cu(L^1)(AsPh_3)](ClO_4)$

This was prepared in a similar manner to the above complex. Elemental analysis: Found C=44.0, 44.1; H=4.11, 4.16%. Calculated for $[Cu(L^1)(AsPh_3)](ClO_4)$ C=44.4; H=4.19%. Infra-red spectrum: (L^1 bands) 1437, 1404, 1333, 1302, 1278 cm^{-1}, ($AsPh_3$ bands) 3044, 1480, 813, 740, 694, 620, 473, 346 and 322 cm^{-1}. ^1H n.m.r. spectrum (CD_3CN 80MHz) δ_H = 2.87 (12H br s CH_2 (L^1)) 7.40 (15H br s CH ($AsPh_3$)) (Figure 5.3.II).

CHAPTER 6

Reaction of tri- and tetradentate macrocyclic ligands with dirhodium carboxylates $[Rh_2(O_2CR)_4]$

6. Reaction of tri- and tetradentate macrocyclic ligands with dirhodium carboxylates $[Rh_2(O_2CR)_4]$

6.1 Introduction

Dirhodium carboxylate complexes, first characterised in 1962,[194,195] show a characteristic 'lantern' structure (1) analogous to the formally metal metal non bonding copper(II) systems[196] and the multiply metal-metal based rhenium, technetium, tungsten, molybdenum, chromium, ruthenium and osmium systems.[96]

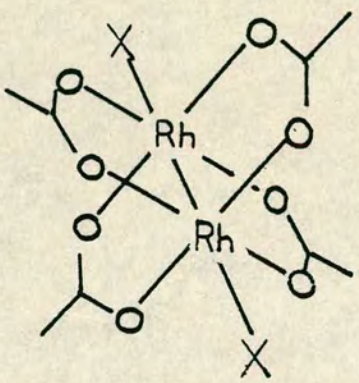

(1)

In the dirhodium systems there is a formal metal bond order of unity resulting from a $\sigma^2\pi^4\delta^2\delta^{*2}\pi^{*4}$ electronic configuration. In contrast to the '$M_2(O_2CR)_4$' species of other metals $[Rh_2(O_2CR)_4]$ shows a pronounced tendency to form axial adducts with donor ligands X under ambient conditions to give $[Rh_2(O_2CR)_4X_2]$ species,[100,195] and a large number of structurally characterised complexes of this type have been reported.[100]

The high degree of stability of the $[Rh_2(O_2CR)_4]$ unit coupled with the ease with which it forms axial adducts make this unit an ideal reagent in the preparation of

exodentate macrocyclic complexes.

The availability of just the one labile site at each metal centre should restrict the co-ordination of the macrocyclic ligand so that only exo co-ordination can result. Were the macrocyclic ligand to bind to more than one metal centre a polymeric structure would be obtained.

In addition to axial adducts of type $[Rh_2(O_2CR)_4X_2]$ where X is a monodentate ligand ($C^{197-199}$ $N^{200-215,165,100}$ $O^{165,216}$ $P^{217-220}$ $S^{165,221}$ or As^{222} donor), with bi or polyfunctional ligands, complexes of 1:1 stoichiometry $[Rh_2(O_2CR)_4X]$ result. Such 1:1 complexes have been characterised for bidentate amines such as hydrazine,[223] ethylene diamine,[165] o-phenylene diamine,[165] durene diamine (DDA)[224] (2) and phenazine (PHZ)[224] (3).

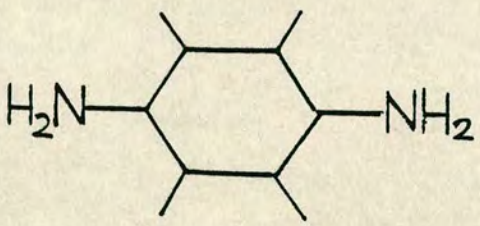

(2)

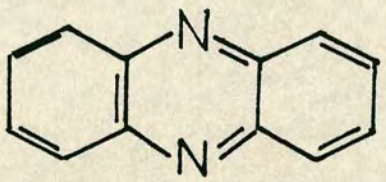

(3)

The complexes of the latter two ligands have been structurally characterised[224] (R=Et) and show a chain polymeric structure, in each case (4).

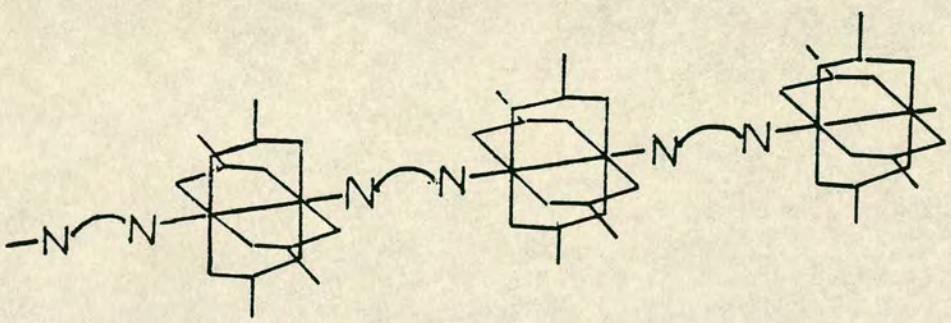

(4)

For the $[Rh_2(O_2CR)_4]$ unit to be retained only one of the donor atoms of the bi- or polydentate ligand may bind to each metal centre. For tri- and tetradentate macrocyclic ligands such co-ordination will lead to an exodentate conformation being adopted by the macrocycle. For the tridentate macrocycles L^1, L^4 and L^5, co-ordination with up to three metal centres is possible. Co-ordination to more than one metal centre, however, has not yet been observed for any of those macrocycles. Similarly for the tetradentate macrocycles L^2, cyclam and tmc in which co-ordination to four separate metal centres may occur, only L^2 has been characterised so far in an exodentate binding mode.[111-113]

Although the dominant chemical behaviour of $[Rh_2(O_2CR)_4]$ systems is axial attachment more forcing reaction conditions can lead to equatorial substitution. In this way carboxylate ligands may be replaced by a variety of usually bidentate bridging ligands such as acetamidate,[225] sulphate,[226] CO_3^{2-},[227] hydrogen phosphate[228] and hydroxypyridine.[229] In some cases equatorial replacement leads to the formation of an unsupported metal-metal bond notably with the macrocycle H_2L (5), which co-ordinates as a dianion to give

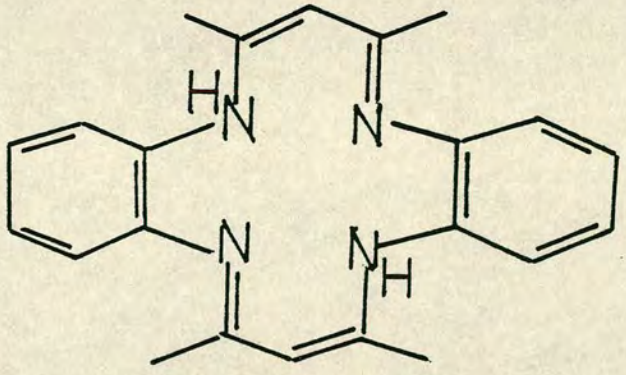

(5)

the binuclear $[Rh_2L_2]$ species.[109,110] Similar systems $[Rh_2P_2]$ (P = OEP^{2-} TPP^{2-})[104,108] and $[Rh_2(dmg)_4(PPh_3)_2]$[230] (dmg^- = dimethylglyoximate) also containing an unsupported Rh-Rh bond have also been prepared, but via monomeric reagents.

The isolation of a complex $[Rh_2(cyclam)_2]^{4+}$ would be of interest not only in terms of structural and redox properties, but also as a precursor of a highly reactive d^7 $[Rh(cyclam)]^{2+}$ radical which may undergo a number of binding and insertion reactions with a variety of small molecule substrates. Such reactivity has been well characterised for related Rh_2 and Ir_2 porphyrin systems.[107,108]

Although the investigation of equatorial insertion reactions into $[Rh_2(O_2CR)_4]$ by use of macrocyclic ligands was not the primary aim of this section of this work, it serves as a link into the chemistry investigated in the final chapter in which multiply metal-metal bonded systems are reacted with macrocyclic ligands (cyclam, H_2L) for which equatorial substitution is the expected mode of reaction.

Results and Discussion

6.2 Synthesis and characterisation of exodentate macrocyclic complexes

6.2.1 Cyclam

Reaction of dirhodium carboxylates $[Rh_2(O_2CR)_4]$ R = Me (acetate) Et (propionate), ^nPt (n-butyrate) CMe_3 (pivalate) or $C_6H_4CMe_3$ (t-butylbenzoate) as either slurries (R = Me, $C_6H_4CMe_3$) or solutions (R = Et ^nPr, CMe_3) with cyclam in methanol at room temperature led to the formation of pink precipitates in each case. Elemental analyses indicated a stoichiometry $[(Rh_2(O_2CR)_4)(cyclam)]_n$ for all these adducts. The nature of the products obtained remained unaltered even if a large excess of the macrocycle was used. The speed of reaction depended upon the solubility of the dirhodium carboxylate starting material so that the acetate and t-butylbenzoate required *ca.* 48 hrs for complete reaction to occur whereas the more soluble reagents reacted virtually instantly.

The pink colour of the adducts observed was highly indicative of axial co-ordination by a nitrogen donor ligand to the $[Rh_2(O_2CR)_4]$ unit.[100,195] Bands due to co-ordinated cyclam were clearly evident in the infra-red spectrum (Table 6.5.I), most notably two sharp N-H stretches at *ca.* 3300 and 3200 cm^{-1}. A very intense band at *ca.* 1600 cm^{-1} (ν_{CO_2}(asym)) in each of the adducts was diagnostic of retention of the $[Rh_2(O_2CR)_4]$ unit. Reaction of these 1:1 adducts with pyridine led in each case to the formation of

the well characterised $[Rh_2(O_2CR)_4(py)_2]$ complexes[195] so providing confirmatory evidence for the presence of the $[Rh_2(O_2CR)_4]$ unit in the 1:1 cyclam adducts.

The observed stoichiometry for the dirhodium carboxylate cyclam adducts strongly suggested a chain polymeric structure to be present as observed in $[Rh_2(O_2CEt)_4(DDA)]$ and $[Rh_2(O_2CEt)_4(PHZ)]$.[224] This would imply that only two of the four available donors of the macrocyclic ligand are participating in binding to (separate) metal centres. A preliminary crystal structure for the free macrocycle cyclam[231] indicates that two of the donor atoms participate in transannular hydrogen bonding. If a similar conformation is adopted by the macrocycle in these adducts then only two of the nitrogen donors are readily available for bonding to metal centres (6), so leading to the observed stoichiometry.

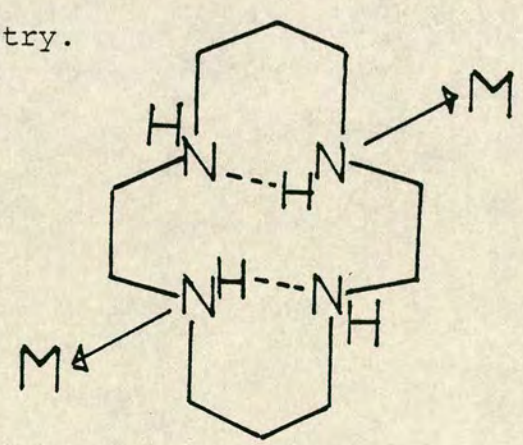

(6)

The infra-red spectrum of $[Rh_2(O_2CMe)_4(cyclam)]$ strongly supports this interpretation with the bands due to cyclam in the complex remaining essentially unchanged compared with the free ligand.

Ideally a crystal structure for one of these adducts would have been desirable but it proved impossible to

obtain single crystals suitable for an X-ray diffraction study.

A major problem was the general insolubility of all these polymeric products. Indeed in the pure state only $[Rh_2(O_2C^nPr)_4(cyclam)]_n$ could be dissolved (and only in hot benzene) to give a red-pink solution (λ_{max} = 535 nm). ^1H n.m.r. in d^6-benzene confirmed a 4:1 carboxylate:macrocycle ratio in the complex. Although insoluble by itself $[Rh_2(O_2C^nPr)_4(cyclam)]_n$ dissolved in chloroform in the presence of excess ligand. A likely explanation is that break-up of the polymeric structure occurs and that discrete species such as $[Rh_2(O_2C^nPr)_4(cyclam)_2]$ form in solution (λ_{max} = 536 nm). Evidence for this comes from that heating $[Rh_2(O_2C^nPr)_4(cyclam)]_n$ in chloroform alone led to adduct cleavage with the colour of the solution turning from pink → green. Subsequent addition of cyclam however to this green solution regenerated the red colour (λ_{max} = 536 nm).

Addition of CH_2Cl_2 to either of these solutions suspected to contain discrete $[Rh_2(O_2C^nPr)_4(cyclam)_2]$ species reprecipitated the polymeric 1:1 adduct $[Rh_2(O_2C^nPr)_4$-(cyclam)] only.

6.2.2 L² (1,4,8,11-tetrathiacyclotetradecane) and tmc (tetramethylcyclam)

Both these tetradentate macrocyclic ligands reacted with dirhodium carboxylates $[Rh_2(O_2CR)_4]$ (R = Me, Et or ^nPr) under ambient conditions in methanol to give pink

polymeric adducts, characteristic for either nitrogen or sulphur axial attachment to the $[Rh_2(O_2CR)_4]$ unit.[100] Infra-red spectra indicated retention of the $[Rh_2(O_2CR)_4]$ unit in the adducts with the observation of the diagnostic intense carboxyl stretch at *ca.* 1600 cm^{-1}. For the L^2 tetrathia macrocycle adducts of 2:1 stoichiometry $[(Rh_2(O_2CR)_4)_2(L^2)]_n$ were obtained. This formulation is consistent only for an extended structure in which all of the four donor atoms of the macrocyclic ligand are bound to separate metal centres, and in which all the Rh sites participate in an apical interaction. The resulting stoichiometry is illustrated schematically (below) (7).

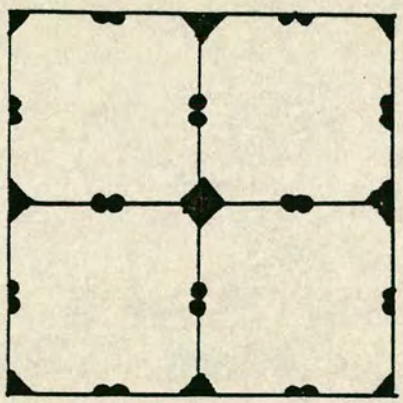

(7)

Presumably L^2 participates in complete exodentate co-ordination and so can be contrasted with cyclam for which only two of the donor atoms are involved in bonding to separate Rh centres.

In the tmc adducts of $[Rh_2(O_2CR)_4]$ 2:1 stoichiometry is also observed (R = Me, Et) however for the butyrate, the tmc adduct was non-stoichiometric this probably reflecting steric interactions between the methyl groups of the

macrocycle and the hydrocarbon chains of the n-butyrate ligands. Tmc, then like L^2 particpates in full co-ordination to the Rh centres. For L^2 this behaviour is perhaps not surprising noting the exodentate structure of the free ligand[115] and a number of its complexes.[111-113] For tmc, the solid state structure of which is unknown, the observation of exodentate co-ordinate is more interesting, not only since it is previously uncharacterised for the ligand, but since the presence of N-methyl groups appear not to seriously restrict this mode of co-ordination. Interestingly, tmc differs from cyclam in its bonding to $[Rh_2(O_2CR)_4]$ and so it appears even more likely that the transannular interactions in cyclam are responsible for its restricted exodentate co-ordination.

Both the L^2, and tmc propionate and butyrate adducts dissolved in chloroform in the presence of excess ligand, again probably attributable to the formation of discrete 1:2 adducts in solution.

6.2.3 L^1(1,4,7-trithiacyclononane), L^4(1,4,7-triazacyclononane), L^5(1,4,7-trimethyl-1,4,7-triazacyclononane)

Reaction of these tridentate macrocyclic ligands with $[Rh_2(O_2CR)_4]$ (R = Me, Et or ^nPr) at room temperature led once again to the formation of pink polymeric adducts. For L^1 and L^4 elemental analysis indicated the formation of 3:2 adducts $[(Rh_2(O_2CR)_4)_3(L)_2]_n$ in each case. For L^5 (8) a similar stoichiometry was observed except for the butyrate derivative, perhaps as a consequence of steric factors.

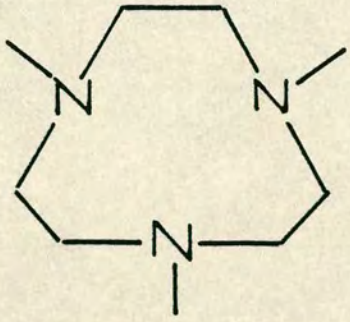

(8)

The observed 3:2 stoichiometry is only consistent for all three of the ligand donor atoms binding to separate Rh centres, in an extended structural array as schematically shown below (9).

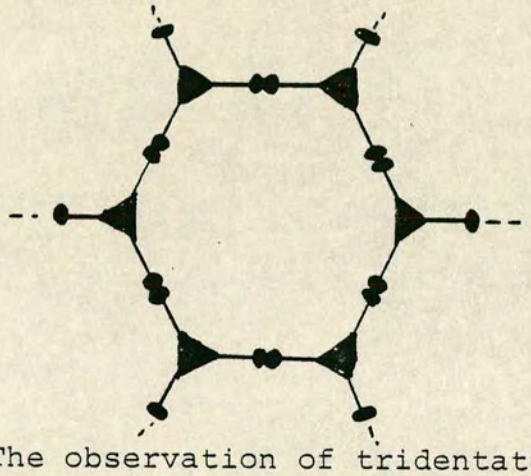

▼ = L^1, L^4 or L^5

● = $Rh_2(O_2CR)_4$

(9)

The observation of tridentate exodentate co-ordination is the first example of such a co-ordination mode for these normally endodentate systems. Rearrangement of these macrocycles thus must occur on complexation. In the L^4 adducts the infra-red spectra all show just one N-H stretch, further indicating equivalent bonding of all three of the donor atoms to separate metal centres.

All the characterised adducts of these tridentate macrocyclic ligands (R = Et, ^nPr) dissolve in chloroform in the presence of excess ligand possibly due to formation of $[Rh_2(O_2CR)_4L_2]$ species in solution (L = L^1, L^4 or L^5).

6.3 Equatorial substitution reactions of $[Rh_2(O_2CR)_4(cyclam)]_n$ adducts

Refluxing $[Rh_2(O_2CR)_4(cyclam)]_n$ adducts in benzene in the presence of excess cyclam under nitrogen led to the formation of highly air sensitive green solutions. For the acetate adduct (R = Me) this process occurred over *ca.* 4 hrs but for the propionate and butyrate adducts reaction was complete over 90 minutes and 30 minutes respectively. For the latter two adducts, red solutions were obtained prior to the formation of the green solutions. These air stable solutions were identical to the postulated $[Rh_2(O_2CR)_4(cyclam)_2]$ species described earlier, and may act as precursors to binuclear $[Rh_2(cyclam)_2]^{4+}$ species responsible for the green air sensitive solutions.

The air sensitive green solutions - shown to be diamagnetic by esr spectroscopy - decomposed on exposure to air to give a mixture of ill-defined products which showed no absorption maxima in the visible region.

The observation that $[Rh_2(O_2CMe)_4(PPh_3)_2]$ failed to react with cyclam under the same reaction conditions suggested axial co-ordination of cyclam to be a necessary requirement for further (possibly equatorial) reaction to occur.

The highly air sensitive nature of the green solutions described above precluded any positive identification of any of the species in the solution. Interestingly, these green solutions were not observable in any other solvents tested except possibly for THF.

Scheme 6.3.I Summary of reactions of $[Rh_2(O_2CR)_4(cyclam)]_n$

R = Me, Et, ^nPr

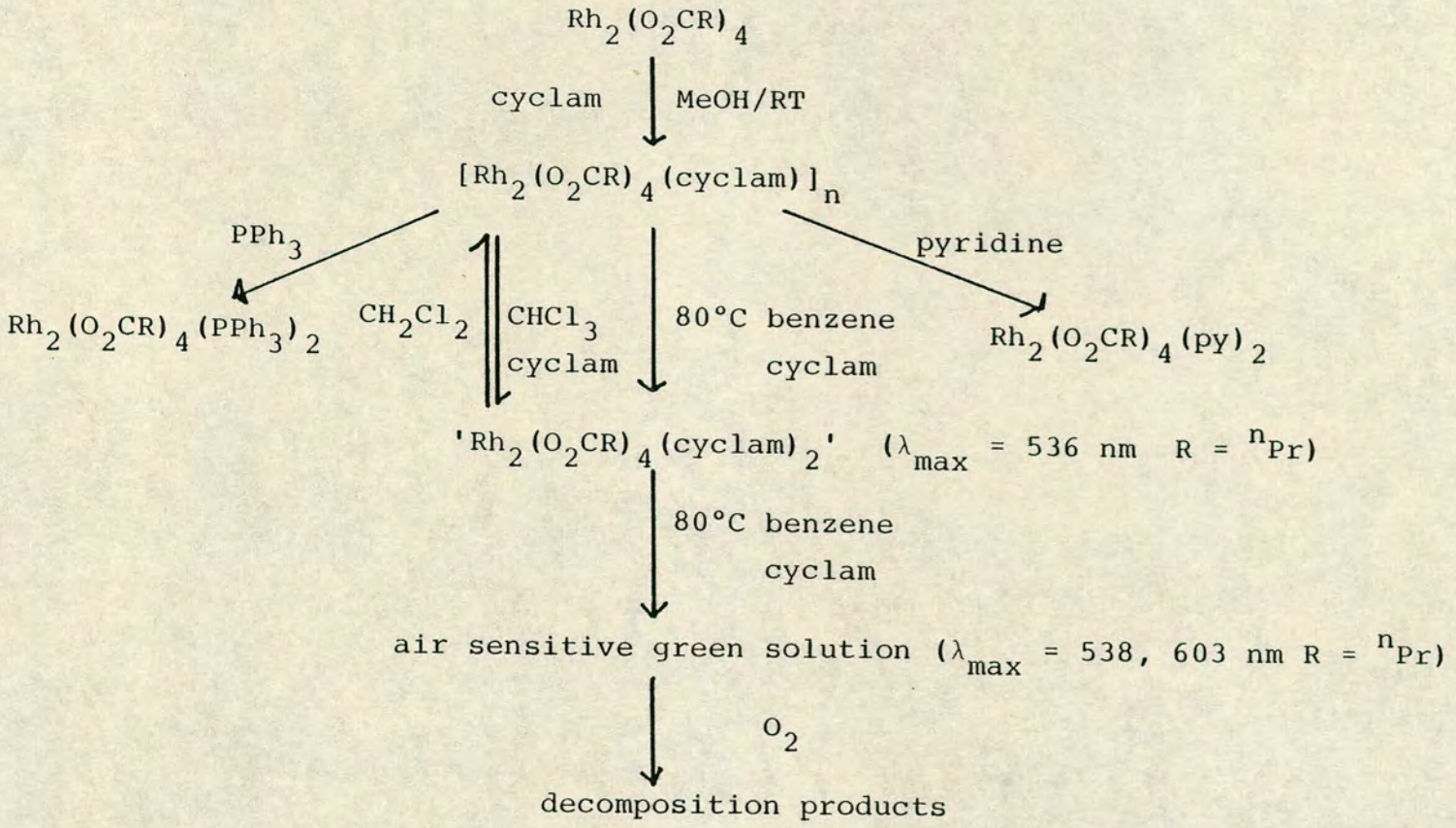

6.4 Summary

The observation of exodentate co-ordination of all the tri- and tetradentate thia and aza macrocycles to the $[Rh_2(O_2CR)_4]$ moiety strongly suggests that kinetic factors are primarily responsible for the lack of complexes showing this mode of co-ordination. The $[Rh_2(O_2CR)_4]$ moiety is ideally suited for the observation of fully exodentate co-ordination even for macrocycles which are endo in their free state such as L^1, L^4, L^5, cyclam and probably tmc. The anomalous behaviour of cyclam, which alone does not act as an n, unidentate system but only co-ordinates to separate metal centres through two of the four potential donor atoms strongly suggests the transannular hydrogen bonding interactions found in the free ligand are retained. The one major disappointment was the inability to obtain crystals suitable for X-ray diffraction for any of these adducts, yet the predictive power of simple elemental analysis, often considered as a routine check for purity, is underscored in this work.

Perhaps it is the behaviour of these exodentate adducts in the presence of excess ligand under more forcing reaction conditions, in particular the possible observation of equatorial exchange to give unsupported metal-metal bonded dimers that is of greatest interest in any future work upon these systems.

6.5 Experimental

Infra-red spectra were measured as nujol or HCB (hexachlorobutadiene) mulls using KBr or CsI plates; or as KBr discs. Microanalyses were performed by the University of St. Andrews Chemistry Department and by the University of Edinburgh Chemistry Department. All solvents were purified according to standard procedures.[174] All other physical measurements were carried out as in Chapter 2.

Starting materials

$RhCl_3.xH_2O$ was provided as generous loans from Johnson-Matthey. Cyclam and tmc were purchased from Strem Co., and Lancaster Synthesis; tmc was also prepared from cyclam according to the literature procedure.[233] All other ligands were obtained as discussed previously except for L^5 for which the synthesis is outlined below.

Synthesis of L^5 (1,4,7-trimethyl-1,4,7-triazacyclononane)

$L^4.3HCl$ (2 g, 8.4×10^{-3} mol) was dissolved in a formaldehyde/formic acid/water mixture (v:v = 10:10:1 25 ml) and refluxed for 48 hours. To the cooled solution an equal volume of water was added and NaOH slowly added to raise the pH to 12, keeping the temperature below 10°C. The trimethylated free amine L^5 was then extracted into chloroform (4 x 100 ml) and dried over anhydrous sodium sulphate. Subsequent removal of the chloroform left an oily residue, which was dissolved in water (10 ml), filtered,

and then acidified with 12M HCl (20 ml). Methanol (20 ml) was then added and the white precipitate of $L^5.3HCl$ collected by filtration. The trihydrochloride could be recrystallised from 6M HCl/methanol (v:v = 1:1, 20 ml) Yield = 1.2 g (50%) ^1H n.m.r. spectrum (D_2O 80MHz) δ_H = 3.81 (9H s CH_3), 3.11 (12H s CH_2).

Preparation of dirhodium carboxylates

$[Rh_2(O_2CMe)_4(MeOH)_2]$ was prepared according to the literature procedure.[234] The corresponding propionate, butyrate and pivalate complexes were prepared from the acetate by carboxylate exchange in a hot or refluxing solution of the neat carboxylic acid (*ca.* 0.40 g $[Rh_2(O_2CMe)_4](MeOH)_2$ in 15 ml acid) under a nitrogen atmosphere for 90 minutes. The excess acid was then removed either by use of a fast stream of nitrogen or via rotary evaporation to leave the product in quantitative yield. The exchanged carboxylates were recrystallised from acetone/water or acetone/methanol mixtures. The 4-t-butylbenzoate derivative was obtained by heating the acetate in a melt of 4-t-butylbenzoic acid for 4 hours (*ca.* 0.40 g $[Rh(O_2CMe)_4](MeOH_2)$ in 25 ml acid). The exchanged complex $[Rh_2(O_2C.C_6H_4.CMe_3)_4]$ was recovered by dissolving the cooled melt in ethanol and collecting the insoluble product by filtration. The purity of the acetate and t-butylbenzoate were checked by the preparation of their pyridine adducts. Elemental analysis (R = $C_6H_4CMe_3$) Found C=60.58; H=5.88; N=2.74%. Calculated for

$[Rh_2(O_2CR)_4(py)_2]$ C=60.45; H=5.82; N=2.61%.

Synthesis of Complexes

$[Rh_2(O_2CR)_4(cyclam)]_n$ (R=Me, Et, ^nPr, CMe_3 and $C_6H_4CMe_3$)

Reaction of dirhodium carboxylates $[Rh_2(O_2CR)_4]$ (R = Me, Et, ^nPr, CMe_3 or $C_6H_4CMe_3$) with a slight molar excess of cyclam in methanol at room temperature gave the 1:1 cyclam adducts $[Rh_2(O_2CR)_4(cyclam)]_n$ as pink solids in quantitative yield. The rate of adduct formation depended upon the solubility of the initial carboxylate so that for R = Et, ^nPr or CMe_3 the product formed almost instantaneously whereas for R = Me, $C_6H_4CMe_3$ a total reaction time of one, or preferably two, days was required. The products were collected by filtration, washed with methanol and diethyl ether and air dried. Elemental analysis and selected infra-red data are given in Table 6.5.I. Electronic spectra (R = ^nPr) λ_{max} = 535 nm (benzene). λ_{max} = 536 nm ($CHCl_3$/in presence of excess ligand)). ^1H n.m.r. spectrum (R = ^nPr, d^6-benzene 200MHz) δ_H = 0.86 (12H t $O_2CCH_2CH_2CH_3$) 1.63 (8H sextet $O_2CCH_2CH_2CH_3$), 2.27 (8H br $O_2CCH_2CH_2CH_3$) 3.52 (16H br αα' cyclam), β-cyclam (4H) and NH (4H) resonances were not clearly observed.

$[(Rh_2(O_2CR)_4)_2(L)]_n$ (L = L^2 or tmc, R = Me, Et or ^nPr)

Tmc adducts of dirhodium carboxylates were obtained by an analogous procedure to the preparation of the corresponding cyclam adducts. 2:1 adducts were obtained in each case except for R = ^nPr. L^2(1,4,8,11-tetrathiacyclotetradecane)

Table 6.5.I Elemental analyses* and selected infra-red data for dirhodium carboxylate cyclam adducts $[Rh_2(O_2CR)_4(cyclam)]_n$

R	%C	%H	%N	ν(N-H)/cm^{-1}	ν(CO_2 asym)/cm^{-1}
Me	33.05(33.66)	5.62(5.65)	8.52(8.72)	3300,3200	1596
Et	38.00(37.84)	6.42(6.35)	8.21(8.02)	3320,3215	1590
^nPr	41.29(41.39)	7.05(6.95)	7.59(7.42)	3318,3218	1596
CMe_3	44.66(44.45)	7.39(7.46)	6.65(6.91)	3320,3215	1590
$C_6H_4CMe_3$	57.91(58.17)	6.90(6.87)	4.76(5.03)	3312,3303,3203	1599

* Calculated values in parenthesis

adducts of dirhodium carboxylates were prepared in an analogous procedure except that a dichloromethane/methanol (v:v = 1:1) solution was used so as to dissolve L^2; again 2:1 adducts were obtained. Elemental analyses for both tmc, and L^2 adducts are given in Table 6.5.II. Electronic spectrum: $[(Rh_2(O_2CEt)_4)_2(tmc)]$ λ_{max} = 544 nm ($CHCl_3$ in presence of excess tmc).

$\underline{[(Rh_2(O_2CR)_4)_3(L)_2]_n}$ $\underline{(L = L^1, L^4 \text{ or } L^5, R = Me, Et \text{ or } {}^nPr)}$

L^1 adducts of dirhodium carboxylates were obtained by an analogous procedure to the preparation of the L^2 adducts (above). The L^4(1,4,7-triazacyclanonane) and L^5(1,4,7-trimethyl-1,4,7-triazacyclononane) adducts were obtained via addition of aqueous solutions (3×10^{-4}mol, 5 ml) of the neutralised hydrochloride salts of L^4 or L^5 to methanol or acetone solutions (20 ml) of the dirhodium carboxylate ($1{,}5 \times 10^{-4}$mol) at room temperature. The pink adducts were collected and washed with water, methanol and diethyl ether, and air dried. Yields were *ca.* 90%. All these products (except L = L^5 R = ${}^nPr$) analysed as 3:2 adducts (Table 6.5.II). Electronic spectra (R = ${}^nPr$) L = L^1 λ_{max} = 537 nm, L^4, λ_{max} = 545 nm, L^5, λ_{max} = 542 nm ($CHCl_3$ in presence of excess ligand). Infra-red spectra: ν(N-H) = 3300 cm^{-1} (L = L^4, R = Me); 3298 cm^{-1} (Et) 3296 cm^{-1} (${}^nPr$).

Table 6.5.II Elemental analyses* for dirhodium carboxylate macrocyclic ligand adducts $[(Rh_2(O_2CR)_4)_2(L)]_n$ (L = L^2,tmc) and $[(Rh_2(O_2CR)_4)_3(L)_2]_n$ (L = L^1,L^4,L^5)

		%C	%H	%N or S
L^2 :	R = Me	27.48(27.10)	3.82(3.85)	11.0(11.13)
	Et	31.97(32.29)	4.66(4.78)	9.83(10.14)
	^{n}Pr	36.60(36.64)	5.46(5.56)	9.28(9.31)
tmc:	R = Me	32.26(31.60)	5.15(4.95)	5.17(4.91)
	Et	36.41(36.43)	5.77(5.79)	4.55(4.47)
L^1 :	R = Me	26.20(25.64)	3.78(3.59)	-
	Et	30.82(31.08)	4.54(4.56)	-
	^{n}Pr	35.47(35.62)	5.41(5.38)	9.5(9.7)
L^4 :	R = Me	27.24(27.29)	4.44(4.20)	5.27(5.30)
	Et	32.75(32.90)	5.05(5.18)	4.76(4.80)
	^{n}Pr	38.12(37.51)	6.16(5.98)	4.25(4.37)
L^5 :	R = Me	29.26(30.23)	4.90(4.71)	4.98(5.03)
	Et	35.99(35.31)	5.91(5.55)	4.36(4.57)

* Expected values in parenthesis

Preparation of green air sensitive solutions

Reaction of $[Rh_2(O_2CR)_4(cyclam)]_n$ (R = Me, Et, ^nPr) (1×10^{-4}mol) with cyclam (1×10^{-3}mol) in benzene (30 ml) under reflux in a strictly inert atmosphere led to the formation of green air sensitive solutions. For R = CMe_3 or $C_6H_4CMe_3$ however no such solutions were formed even on extended reflux (>6 hrs). The green solutions (λ_{max} = 542, 602 nm (R = Et), λ_{max} = 538, 603 nm (R = ^nPr)) rapidly decomposed on exposure to air to give a mixture of products showing a nondescript electronic spectrum. Both the green solutions and decomposition products were esr silent.

In the cases R = Et, ^nPr the formation of the air sensitive green solutions were preceded by the 1:1 adduct dissolving to give pink-red solutions (λ_{max} = 536 nm).

CHAPTER 7

Reaction of Tetra-aza Macrocyclic Ligands with Multiply Metal-metal Bonded Binuclear Systems

7 Reaction of tetraaza macrocyclic ligands with multiply metal-metal bonded binuclear systems

7.1 Introduction

In the previous chapter the interaction of $[Rh_2(O_2CR)_4]$ systems with a variety of tri- and tetra-aza macrocyclic ligands was investigated. In virtually all these reactions axial attachment occurred to the $[Rh_2(O_2CR)_4]$ unit under ambient conditions to give polymeric products in which exo co-ordination of the macrocycles was observed. In this chapter the reaction of tetra-aza macrocycles with $[Mo_2Cl_8]^{4-}$, $[Mo_2(O_2CMe)_4]$, $[Ru_2(O_2CMe)_4Cl]$ and $[Os_2(O_2CR)_4Cl_2]$ (R = Me, Et. ^nPr) is investigated. These binuclear systems are closely related to $[Rh_2(O_2CMe)_4]$ but instead show a metal-metal bond order greater than unity.[96] At the outset of the project some of these systems had been characterised in cofacial dimeric macrocyclic systems, and in this work it was hoped to extend this series of complexes, with the tetra-aza macrocycles cyclam (1) and H_2L (2).

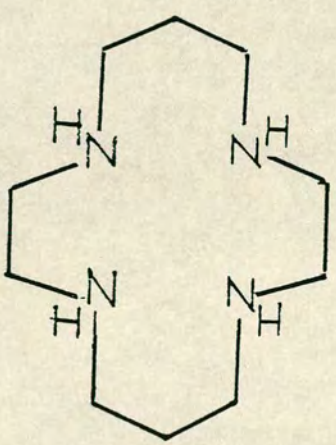

(1)

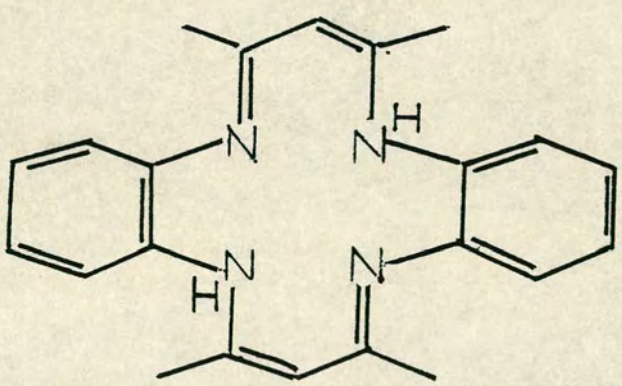

(2)

The multiply metal-metal bonded carboxylate, and chloride complexes (above) differ significantly from $[Rh_2(O_2CMe)_4]$ in their mode of reactivity, and react predominantly via equatorial exchange rather than formation of axial adducts, as a description of their chemistry shows (below).

In $[Mo_2(O_2CMe)_4]$ which shows a metal-metal bond order of 4, carboxylate exchange is the dominant reaction mode, for example, exchange with other carboxylate groups,[235] chloride,[236] or bromide.[237] The product via chloride exchange $[Mo_2Cl_8]^{4-}$ is more labile than the tetracarboxylate and is used to prepare a whole host of $[Mo_2(L\text{-}L)_4]^{n+}$, $[Mo_2(L\text{-}L)_2Cl_4]$ and $[Mo_2L_4Cl_4]$ species (L-L = $H_2N(CH_2)_2NH_2$,[238] $^-O_2CCH_2NH_3^+$,[239] SO_4^{2-} [240] dppm, dppe etc,[241] L = phosphine[242]). At the conclusion of this work $[Mo_2(TPP_2)]$[106] (TPP^{2-} = dianion of tetraphenylporphyrin) was reported and structurally characterised by a single crystal X-ray diffraction study. In this work it was hoped to characterise $[Mo_2L_2]$ (L = dianion of H_2L = tetramethyldibenzotetraaza-annulene (2)) and $[Mo_2(cyclam)_2]^{4+}$ via equatorial exchange of the macrocycles with $[Mo_2(O_2CMe)_4]$ or $[Mo_2Cl_8]^{4-}$. Cofacial dimeric systems of this type, by analogy with previously characterised systems[102-107] would be expected to show interesting structural, redox and catalytic behaviour.

For ruthenium, the best characterised multiply bonded systems are the mixed valence (II,III) carboxylates, occurring either as $[Ru_2(O_2CR)_4]^+$, $Ru_2(O_2CR)_4Cl$ or $[Ru_2(O_2CR)_4Cl_2]^-$ [99,101] $[Ru_2(O_2CMe)_4Cl]$ characterised by a quartet ground state can

react with H_2L to give the cofacial dimer $[Ru_2L_2]^+$ [109] which contains an unsupported Ru = Ru bond of length 2.267(3)Å (bond order = 2.5).[110] Significantly a doublet ground state is observed for the complex indicating the δ^* level to be below the π^* level in the metal-metal bond, in contrast to $Ru_2(O_2CMe)_4Cl$. Both chemical and electrochemical oxidation and reduction of $[Ru_2L_2]^+$ are observed to give $[Ru_2L_2]^{2+}$ and $[Ru_2L_2]$ respectively. By contrast $[Ru_2(O_2CMe)_4]^+$ shows a very limited electrochemistry, and the reduced species $[Ru_2(O_2CMe)_4]$ has only recently been obtained via chemical means.[243]

$[Ru_2L_2]^{2+}$ $(\sigma^2\pi^4\delta^2\delta^{*2}\pi^{*2})$ is diamagnetic, and would be expected to show a bond order of 3. The reduced species $[Ru_2L_2]$ shows a triplet ground state $(\sigma^2\pi^4\delta^2\delta^{*2}\pi^{*1}_{xz}\pi^{*1}_{yz})$ and a reduction of bond order to 2 is indicated by the longer Ru=Ru bond length (2.379(1)Å) relative to $[Ru_2L_2]^+$.[110] The small core size and framework flexibility of the ligand dianion L^{2-} allows it to complex to a metal centre forming out of plane complexes.[244]

This behaviour is observed in the systems described above, and also for the closely related $[Rh_2L_2]$ species, with the separation of the cofacial ligands remaining almost constant,[110] despite an M-M bond length variation of 2.267-2.625Å. In these systems the M-M bond length is essentially dependent only on the formal bond order since the cofacial steric interactions of the macrocycles can be disregarded. The structural characterisation of $[M_2L_2]$ complexes of bond order higher than 2.5 is thus clearly a

priority to see if such behaviour was maintained for even shorter metal-metal bond lengths.

As stated in the introduction porphyrin dimers of type $[Ru_2P_2]$ ($P = OEP^{2-}$, TPP^{2-}) have been fully investigated.[102,103] These systems show similar magnetic behaviour to the dibenzotetraaza-annulene systems but differ in that cofacial steric interactions are now more significant. Furthermore these systems have only been successfully synthesised via monomeric starting materials. In this work it was hoped to prepare $[Ru_2(cyclam)_2]^{n+}$ n = 4 or 5 and to compare it directly to the other cofacial dimeric macrocyclic systems.

Os_2^{n+} systems (n = 5 or 6) first characterised through $[Os_2(hp)_4Cl_2]$ [245] (hp = hydroxypyridine) and $[Os_2(O_2CR)_4Cl_2]$ [256] show a greater tendency toward bond cleavage than do the corresponding Mo, Ru or Rh systems to give usually monomeric Os(II) or Os(IV) products. Equatorial exchange reactions do however occur, e.g. with 2-hydroxypyridine, carboxylate, 2,2,2-trifluoroacetate[256] or chloride (under anhydrous conditions). $[Os_2Cl_8]^{2-}$ obtained via the latter reaction represented the first example of an unsupported Os≡Os bond.[246]

In this work it was hoped to characterise unsupported dimers of type $[Os_2L_2]^{2+}$ and $[Os_2(cyclam)_2]^{n+}$ to extend redox and magnetic studies upon the as yet poorly understood Os_2 multiple metal-metal bond system.

Results and Discussion

7.2 Reaction of multiply metal-metal bonded systems with cyclam

7.2.1 Molybdenum

Reaction of $[Mo_2(O_2CMe)_4]$ with two molar equivalents of cyclam in methanol at room temperature gave a pale green solution (λ_{max} = 590 nm) which became more intense on heating. However, even on prolonged reaction in the presence of excess cyclam, most of the $[Mo_2(O_2CMe)_4]$ remained unreacted. The green air sensitive solution failed to precipitate out of solution on addition of $NaBPh_4$ or NH_4PF_6 suggesting that a neutral species - possibly an axial cyclam adduct of $[Mo_2(O_2CMe)_4]$ was formed. Attention then turned to the more labile $[Mo_2Cl_8]^{4-}$ ion which might be expected to react more readily via equatorial exchange. Refluxing a suspension of $K_4[Mo_2Cl_8]$ with cyclam in a 1:2 molar ratio in dry methanol led to the formation of a deep blue air sensitive solution (λ_{max} = 598 nm) from which the blue ClO_4^-, PF_6^- or BPh_4^- salts could be obtained. The f.a.b. mass spectrum of the initial chloride salt showed peaks centred at M^+ = 669, and 633 which may correspond to $[Mo_2(cyclam)_2]Cl_2^+$ [M^+ = 666 (^{98}Mo)) and $[Mo_2(cyclam)_2]Cl^+$ (M^+ = 631) respectively.

Accurate elemental analysis were not obtainable for any of these species, as all attempts to recrystallise any of these species invariably led to decomposition. As a result definite characterisation was impossible although

infra-red data clearly suggested the co-ordination of cyclam had occurred. The formation of $[Mo_2(cyclam)_2]^{4+}$ would be consistent with the observed electronic spectrum. The fully allowed $\delta \rightarrow \delta^*$ transition expected for such a species may be expected to occur at the energy observed (16,700 cm^{-1}), somewhat lower than for $[Mo_2Cl_8]^{4-}$ (19,000 cm^{-1}), due to an expected lengthening and weakening of the Mo-Mo quadruple bond.[247]

Upon exposure to air the freshly generated blue cation was observed to decay in an isosbestic manner (λ_{iso} = 516 nm) to give an ill characterised brown species.

7.2.2 Ruthenium

Reaction of $[Ru_2(O_2CMe)_4Cl]$ and cyclam in a 1:2 molar ratio in a variety of solvents (but most efficiently in THF) under reflux for 2 hours led to the formation of an air sensitive yellow solid. Fresh solutions of this solid in methanol gave the PF_6^- and BPh_4^- salts as solids on addition of the appropriate counter ion. Left in solution however the complex cation (λ_{max} = 400 nm CH_2Cl_2) rapidly decomposed, initially in isosbestic manner (λ_{iso} = 365, 441 nm) to give an ill defined brown species. This instability in solution prevented recrystallisation of either the PF_6^- or BPh_4^- salts of the complex cation, and as a consequence of this accurate microanalytical data for either of these salts was not possible, even under strictly deoxygenated or anhydrous conditions.

The infra-red spectrum of the PF_6^- salt, indicated

cyclam and acetate both to be present but not chloride. On the basis of the microanalytical data a formulation $[Ru(cyclam)(O_2CMe)]_n(PF_6)_n$ (n = 1 or 2) is tentatively suggested.

7.2.3 Osmium

Reaction of $[Os_2(O_2CR)_4Cl_2]$ (R = Me, Et or ^nPr) with cyclam in a 1:2 molar ratio at room temperature led in each case to the formation of intensely purple air sensitive solutions after *ca.* 8 hrs. This may appear surprising since the acetate starting material is virtually insoluble in dichloromethane relative to the propionate or butyrate. The reaction product formed was stable in a variety of solvents, and displayed solvent dependent electronic spectra. Thus for the product (R = Me) in dichloromethane λ_{max} = 536 nm ($\varepsilon \sim 5000\ M^{-1}cm^{-1}$) but in water, λ_{max} = 506 nm. It appears likely that the product may display a significant interaction with the solvent.

Elemental analysis for the initial product (R = Me) indicated an empirical formula $[Os(cyclam)(O_2CMe)Cl]$. Infra-red spectra indicated bound cyclam and acetate but not chloride. An Evans method nmr measurement also indicated the product to be diamagnetic.[42] F.a.b. mass spectra showed molecular peaks corresponding to the $[Os(cyclam)(O_2CMe)]^+$ ion suggesting the initial product to be $[Os(cyclam)(O_2CMe)]^+Cl^-$. The ionic nature of the species was confirmed by the preparation of the BPh_4^- salt of the cation upon treatment of an aqueous, or methanol solution

with $NaBPh_4$. The resulting solid analysed approximately for $[Os(cyclam)(O_2CMe)](BPh_4)$ but its air sensitivity led to difficulties in its purification by recrystallisation, and also despite a great deal of effort crystals suitable for X-ray diffraction could not be obtained. Infra-red spectra however indicated retention of acetate, but not chloride in the BPh_4^- salt.

The solution behaviour of the formulated $[Os(cyclam)(O_2CMe)]^+$ ion was clearly intriguing. Such a cation, which may have a number of possible structures (3) could well be envisaged to participate in solvent interaction, so altering the visible chromophore.

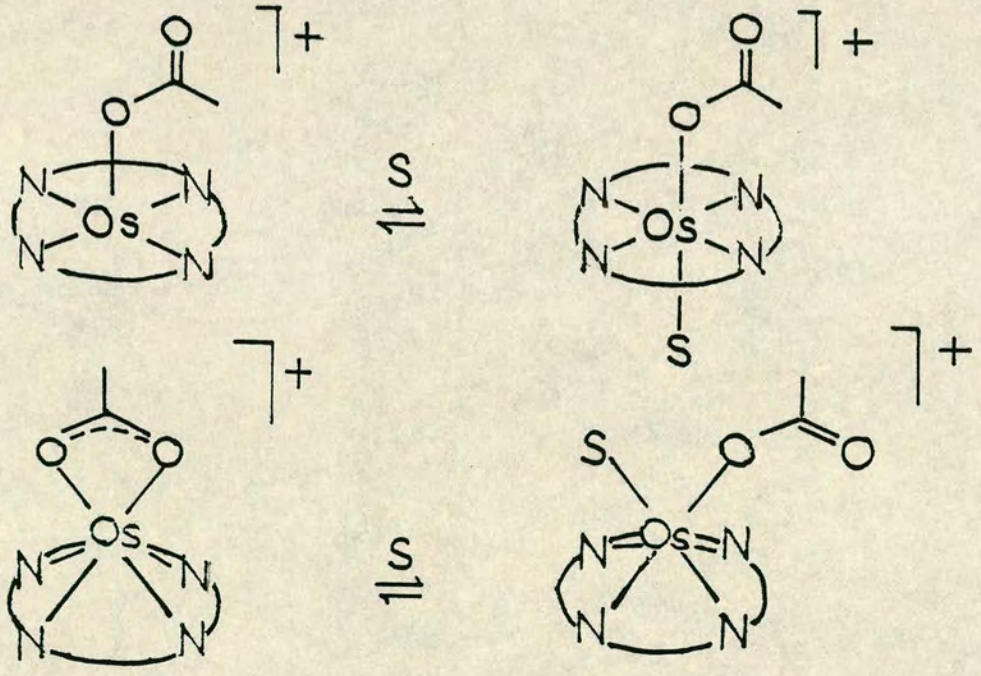

(3)

The intense visible absorption for the complex cation (λ_{max} = 506 nm ε = 5 x 10^3 $M^{-1}cm^{-1}$ in H_2O) is probably a metal (t_{2g}) → carboxylate (π^*) charge transfer transition.

On exposure to air the visible absorption decays in an isosbestic manner (λ_{iso} = 392, 332 nm). The butyrate complex (λ_{max} = 544 nm $CHCl_3$) decomposes in a similar manner (λ_{iso} = 460, 352 nm) upon exposure to air.

7.3 Reaction of multiply metal-metal bonded systems with H_2L (H_2L = tetramethyldibenzotetraaza-annulene)

Reaction of $[Os_2(O_2CMe)_4Cl_2]$ with H_2L in methanol under reflux led to the formation of a dark brown solution from which only a mixture of ill-defined air sensitive products could be isolated.

$K_4[Mo_2Cl_8]$ and H_2L reacted in refluxing methanol to give a red-purple solution. The purple solid isolated on addition of diethyl ether to the cooled solution gave purple crystals upon recrystallisation from dichloromethane/ chloroform. These showed an electronic spectrum with λ_{max} = 490 nm in water. On standing however this absorption decays completely after *ca.* 1 day. This behaviour suggests that formation of the 2,4-dimethyl diazapenium ion (4) has occurred in this reaction,[257] possibly as a consequence of some residual acidity in the $K_4[Mo_2Cl_8]$ starting material.

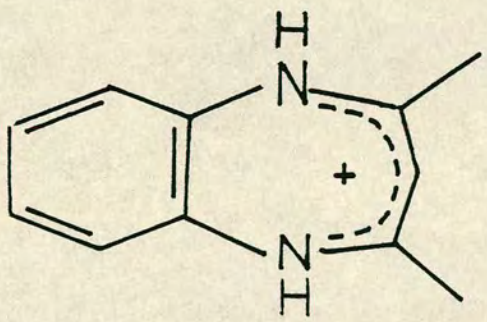

(4)

No reaction between $[Mo_2Cl_8]^{4-}$ and H_2L was observed in any other solvent, nor did $[Mo_2(O_2CMe)_4]$ and H_2L react even under vigorous reaction conditions.

The ready conversion of H_2L to a diazapenium ion even under only very slightly acidic conditions was clearly a severe problem, as the highly labile $[Mo_2Cl_8]^{4-}$ ion is difficult to obtain totally free of acid. Addition of alkali to the reaction mixture unfortunately led to instant decomposition of the reaction mixture although perhaps a non nucleophilic base such as DBU may prove more successful.

7.4 Preparation, structural characterisation and reactivity of $[Mo(CO)_4(H_2L')]$ H_2L' = 5,7,12,14-tetramethyldibenzo-[b,i]-1,4,8,11-tetraazacyclotetra-2,4,6,9,11,14-hexaene

The only reported reaction of H_2L with molybdenum is the formation of $[Mo(CO)_4(H_2L')]$ by reaction of $Mo(CO)_6$ with H_2L in a diglyme/petrol ether mixture (v:v = 10:1) at 105°C[248]. Bell and Dabrowiak assigned the product on the basis of mass spectra, ^1H n.m.r. and infra-red spectroscopy. A cis $Mo(CO)_4L$ co-ordination, suggesting bidentate co-ordination of the macrocycle, was assigned on the basis of the carbonyl stretching region. The ^1H n.m.r. spectrum indicated that migration of one of the amino protons to the methine C atom of the di-iminato ring had occurred, with the other amino proton retained, to convert the bound macrocyclic ligand to H_2L' (5).

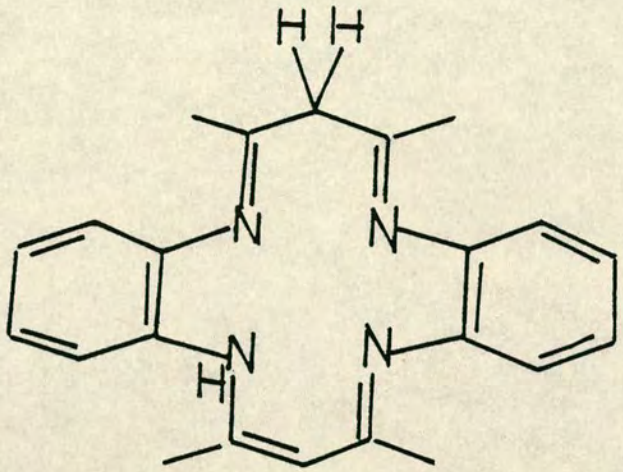

(5)

This complex was resynthesised according to the literature method and a single crystal X-ray diffraction study was undertaken with a view to investigating these structural predictions and assessing the conformation adopted by the macrocycle in the complex.

Crystal data $[Mo(CO)_4(C_{22}H_{24}N_4)]$ M = 552.4 triclinic Space group $P\bar{1}$ a = 8.909(6) b = 9.361(6) c = 16.544(6)Å α = 89.36(4) β = 78.03(5) ν = 67.77(5)° U = 1246Å^3 Z = 2 D_c = 1.473 g cm^{-3} R = 0.0502 for 2958 observed data. Selected bond lengths and angles are given in Table 7.4.I. Two views of the molecule are given in Figures 7.4.II and 7.4.III. A slightly distorted octahedral geometry is observed around Mo(O) with the macrocycle bound in a cis manner about the metal atom. The Mo-C distances trans to N are significantly shorter Mo-C(1*) = 1.956(6), Mo-C(2*) = 1.957(6)Å, than those cis to N, Mo-C(3*) = 2.027(6),

Table 7.4.I: Bond angles and lengths (with esd's) for $[Mo(CO)_4(H_2L')]$

Bond lengths (Å)

Mo-C(1*)	1.956(6)	N(11)-C(12)	1.278(7)
Mo-C(2*)	1.957(6)	C(2) -C(3)	1.394(8)
Mo-C(3*)	2.027(6)	C(2) -C(15)	1.372(8)
Mo-C(4*)	2.008(6)	C(3) -C(18)	1.388(8)
Mo-N(1)	2.271(4)	C(5) -C(5A)	1.485(9)
Mo-N(11)	2.278(4)	C(5) -C(6)	1.374(9)
N(1)-C(2)	1.439(7)	C(6) -C(7)	1.408(9)
N(1)-C(14)	1.281(7)	C(7) -C(7A)	1.511(10)
N(4)-H(4N)	0.82(7)	C(9) -C(10)	1.391(8)
N(4)-C(3)	1.398(7)	C(12)-C(12A)	1.484(8)
N(4)-C(5)	1.354(8)	C(12)-C(13)	1.510(8)
N(8)-C(7)	1.318(8)	C(13)-C(14)	1.510(8)
N(8)-C(9)	1.412(7)	C(14)-C(14)	1.492(8)
N(11)-C(10)	1.444(7)		

Bond angles (degrees)

C(1*)-Mo-C(2*)	89.3(3)	Mo -N(11)-C(10)	117.1(3)
C(1*)-Mo-C(3*)	82.3(3)	Mo -N(11)-C(12)	124.1(4)
C(1*)-Mo-C(4*)	84.0(3)	C(10)-N(11)-C(12)	118.2(5)
C(1*)-Mo-N(1)	96.54(22)	N(1)-C(2) -C(3)	119.7(5)
C(1*)-Mo-N(11)	174.87(22)	N(1)-C(2) -C(15)	119.3(5)
C(2*)-Mo-C(3*)	85.5(3)	N(4)-C(3) -C(2)	118.5(5)
C(2*)-Mo-C(4*)	86.3(3)	N(4)-C(3) -C(18)	123.8(5)
C(2*)-Mo-N(1)	174.16(22)	N(4)-C(5) -C(5A)	120.3(5)
C(2*)-Mo-N(11)	95.4(22)	N(4)-C(5) -C(6)	119.9(5)
C(3*)-Mo-C(4*)	164.1(3)	N(8)-C(7) -C(6)	120.5(5)
C(3*)-Mo-N(1)	95.05(21)	N(8)-C(7) -C(7A)	122.6(6)
C(3*)-Mo-N(11)	100.10(21)	C(6)-C(7) -C(7A)	116.9(6)
C(4*)-Mo-N(1)	94.44(21)	N(8)-C(9) -C(10)	118.5(5)
C(4*)-Mo-N(11)	94.25(21)	N(8)-C(9) -C(19)	122.9(5)
N(1) -Mo-N(11)	78.76(16)	N(11)-C(10)-C(9)	118.6(5)
Mo -N(1)-C(2)	116.6(3)	N(11)-C(10)-C(22)	120.8(5)
Mo -N(1)-C(14)	123.8(4)	N(11)-C(12)-C(12A)	125.7(5)
C(2)-N(1)-C(14)	119.4(5)	N(11)-C(12)-C(13)	117.3(5)
H(4N)-N(4)-C(3)	114. (5)	N(1)-C(14)-C(13)	117.8(5)
H(4N)-N(4)-C(5)	118 (5)	N(1)-C(14)-C(14A)	125.8(5)
C(3) -N(4)-C(5)	127.1(5)	C(13)-C(14)-C(14A)	116.4(5)
C(7) -N(8)-C(9)	125.1(5)		

Figure 7.4.II View of the single crystal X-ray structure of $[Mo(CO)_4(H_2L')]$

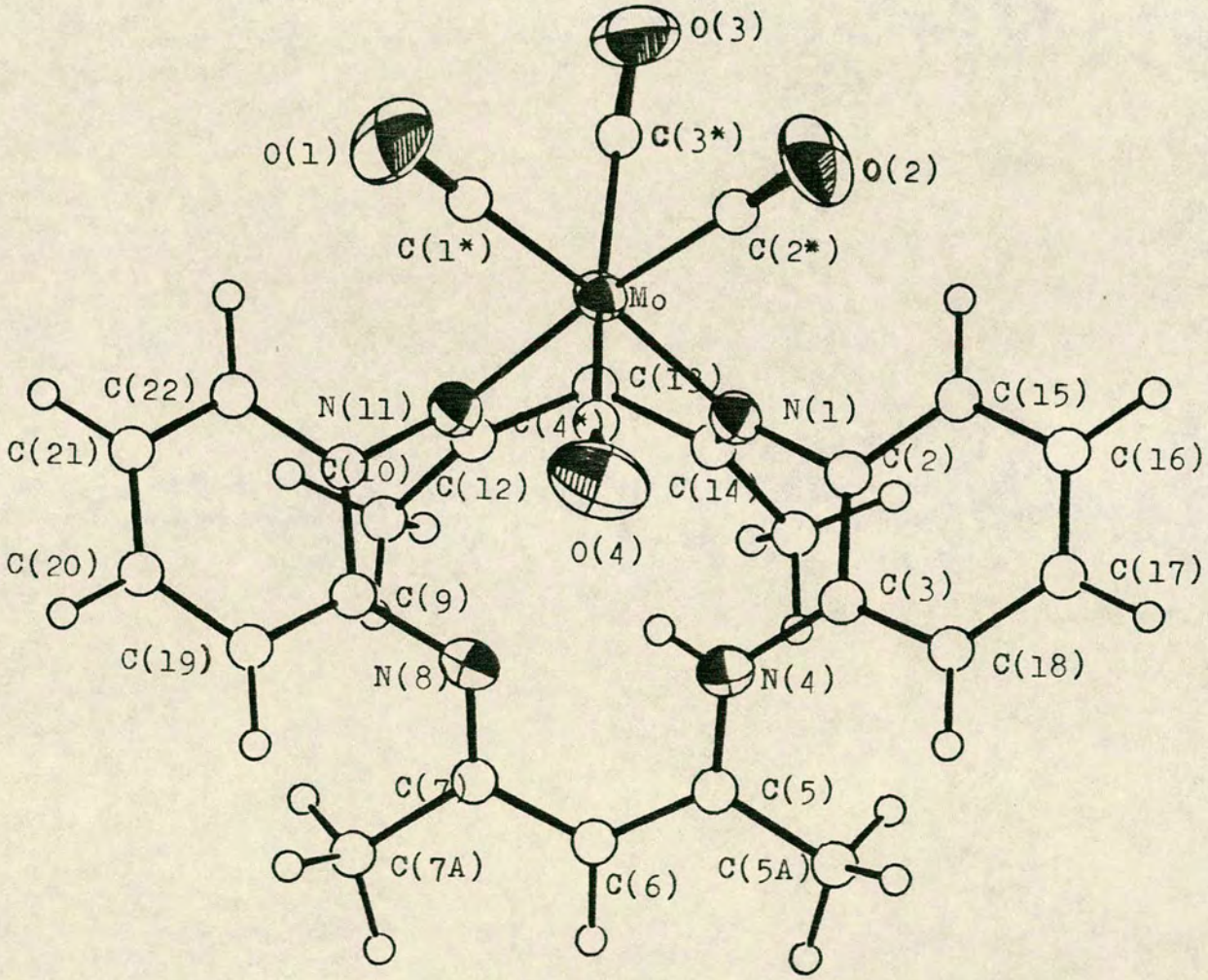

Figure 7.4.III View of the single crystal X-ray structure of $[Mo(CO)_4(H_2L')]$

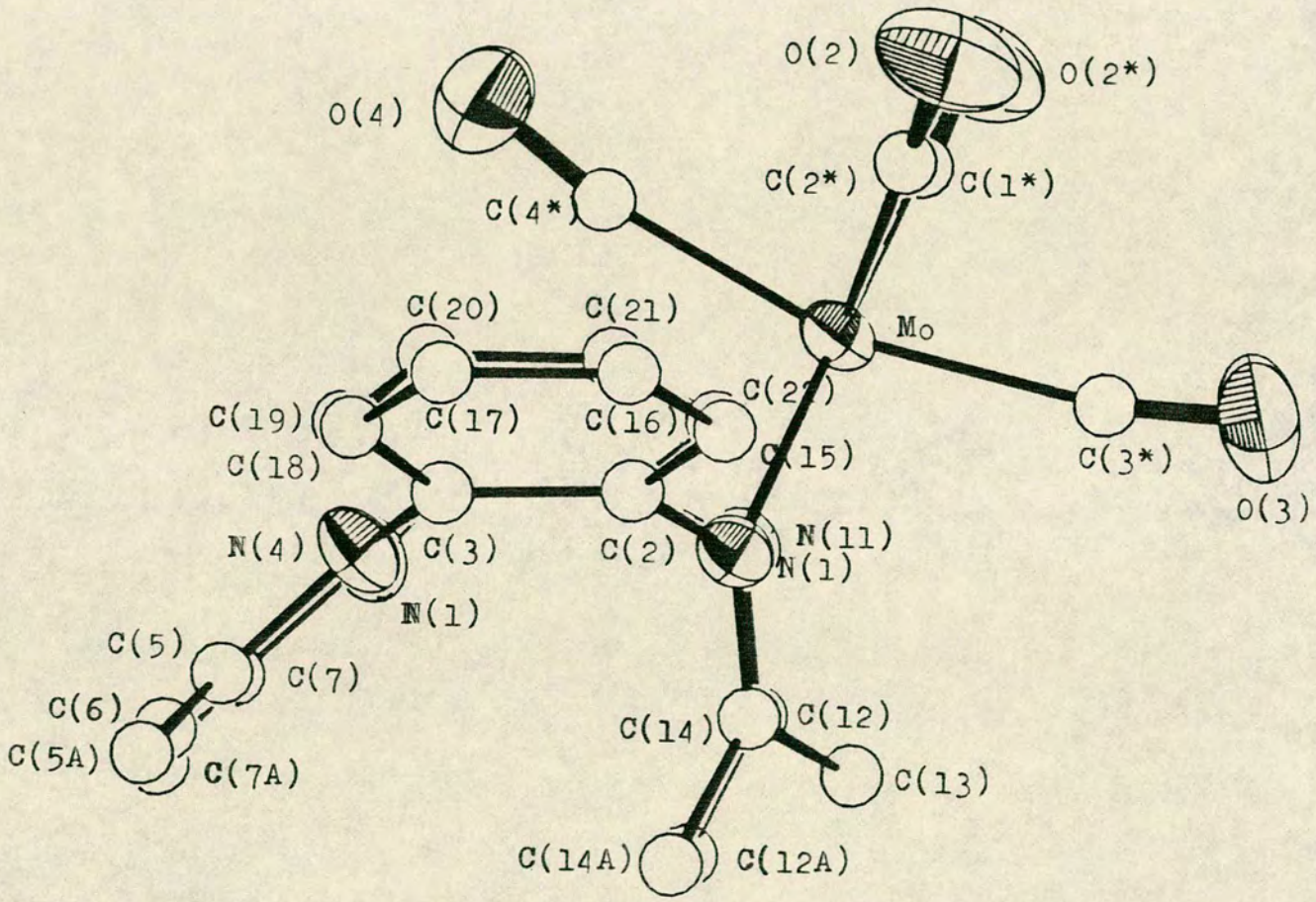

Mo-C(4*) = 2.008(6)Å. The macrocycle adopts a symmetrical conformation, with an approximate mirror plane of symmetry passing through Mo(1), C(3*), O(3), C(4*), O(4), C(6) and C(13). The crystal structure of the complex confirms protonation of the methine C(13) atom, with C(12)-N(11) = 1.278(7), C(14)-N(1) = 1.281(7) indicating C=N double bond character for these linkages (6). The <C(12)-C(13)-C(14)

(6)

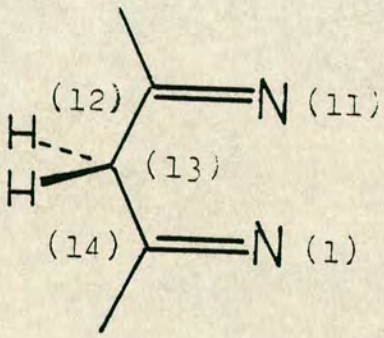

N(11)-C(12) = 1.278(7) Å
C(12)-C(13) = 1.510(8) Å
C(13)-C(14) = 1.510(8) Å
C(14)-N(1) = 1.281(7) Å

bond angle of 110.8° further indicates the Sp^3 nature of C(13). For the other (unchanged) diiminato ring (7) the dominant canonical form is indicated below. The amine hydrogen is on N(4), with a secondary contact to N(8).

(7)

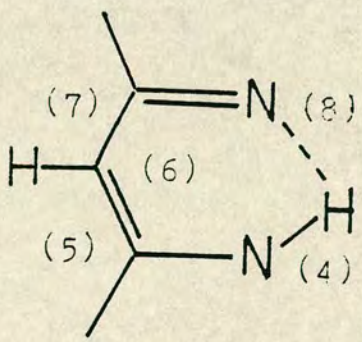

N(8)-C(7) = 1.318(8) Å
C(7)-C(6) = 1.408(9) Å
C(6)-C(5) = 1.374(9) Å
C(5)-N(4) = 1.354(8) Å

N(4)-H = 0.82(7) Å
N(8)-H = 2.00(7) Å
<N(8)-H-N(4) = 135(6) Å

In this complex the migration of the amino proton is thought to be facilitated by warping of the macrocycle upon co-ordination.

The overall structure of the molecule confirms the predictions made by spectroscopic techniques, and represents yet a further example of the co-ordinative flexibility of

H_2L. This ligand normally co-ordinates as a dianion to give 4,[249] 5[250] or 6 co-ordinate[251] complexes. In all its complexes the ligand adopts a characteristic saddle shape as a consequence of steric interactions of the di-iminato ring methyl groups with benzenoid rings. This is also clearly observable in the rearranged macrocycle H_2L' in this present complex. The saddle shape adopted also leads to a displacement of the metal from the N_4 plane. This characteristic enables the formation of cofacial metal-metal bonded dimers (discussed previously) in which cofacial steric interactions are reduced to a minimum, and thus a species $[Mo_2L_2]$ should also be able to be stabilised.

The ligand H_2L can show a further co-ordination mode in the complexes $[(Rh(CO)_2)L]$ and $[(Re(CO)_3)_2L]$ for which the macrocycle co-ordinates to two separate metal carbonyl fragments.[252]

Photolysis of $[Mo(CO)_4(H_2L')]$ was attempted to try and induce removal of carbonyl groups and lead to dimerisation of the complex. In pyridine, photolysis at 350 nm over a period of many days, led to a complete disappearance of carbonyl stretches in the infra-red spectrum. However, the two products isolated from the solution were free ligand H_2L and an ill defined solid containing pyridine but no indication of bound macrocyclic ligand; clearly dimerisation was not induced by photolysis under these conditions.

Interestingly, chloroform solutions of $[Mo(CO)_4(H_2L')]$ slowly decomposed on standing to give the 2,4-dimethyl-diazapenium ion, as identified by electronic spectroscopy, ^1H n.m.r., and solution behaviour.

7.5 Summary

This area of the project proved the most challenging and time consuming, and ultimately the least successful. In terms of the initial aim, to characterise a number of cofacial metal metal bonded macrocyclic systems only for the reaction between $[Mo_2Cl_8]^{4-}$ and cyclam, was there possible evidence for such a species ($[Mo_2(cyclam)_2]^{4+}$). The aerial instability of the products characterised in most of these reactions made recrystallisation and purification difficult. The only fully characterised system proved to be the air stable $[Mo(CO)_4(H_2L')]$ complex previously prepared by Bell and Dabrowiak,[248] and a single crystal X-ray structure confirmed a novel migration of an amino hydrogen of the bound macrocycle to the methine site of one of di-iminato rings.

7.6 Experimental

All reactions were performed under a nitrogen atmosphere using Schlenk line techniques unless otherwise stated. All solvents were purified according to standard procedures.[174] Infra-red spectra were recorded as nujol or HCB (hexachlorobutadiene) mulls using KBr or CsI plates. Fast atom bombardment mass spectra were recorded, courtesy of Imperial College, London. All other physical measurements were as carried out as in Chapter 2.

Starting materials

$Mo(CO)_6$ was purchased from Aldrich Co. Cyclam was purchased from Strem Co. $RuCl_3.xH_2O$, OsO_4 and Na_2OsCl_6 were provided as generous loans from Johnson-Matthey plc. $[Mo_2(O_2CMe)_4]$,[253] $[Ru_2(O_2CMe)_4Cl]$ [254] and $K_4[Mo_2Cl_8]$ [236] were all prepared via established literature methods, and their purity checked by elemental analysis and infra-red spectroscopy. H_2L (tetramethyldibenzotetraaza-annulene) was prepared via the method of Goedken *et al.*[255] and its purity checked by elemental analysis, ^1H n.m.r. infra-red and electronic spectroscopy.

$[Os_2(O_2CR)_4Cl_2]$ (R = Me, Et, ^nPr)

$[Os_2(O_2CMe)_4Cl_2]$ was prepared essentially via the literature method[256] by reaction of OsO_4 with hydrochloric acid in the presence of $FeCl_3$ to generate the $OsCl_6^{2-}$ anion. This was then refluxed in acetic acid/anhydride (v:v = 1:1) for 4 hours rather than the 10 hours suggested as this often led to substantial decomposition. The observed yields were comparable to those quoted in the literature.

In the preparation of $[Os_2(O_2CEt)_4Cl_2]$ and $[Os_2(O_2C^nPr)_4Cl_2]$ it was important to work up the product fairly quickly as overnight storing in the fridge led to decomposition.

Synthesis of complexes

$[Mo_2(O_2CMe)_4]$/cyclam

$[Mo_2(O_2CMe)_4]$ (0.050 g, 1.17×10^{-4} mol) and cyclam

(0.05 g, 2.5 x 10^{-4}mol) were stirred in methanol (30 ml). This led to the formation of a green colouration (λ_{max} = 590 nm) which intensified on heating. However a substantial quantity of unreacted $[Mo_2(O_2CMe)_4]$ remained even on prolonged heating or on addition of further cyclam (0.1 g). No solids could be obtained on addition of either NH_4PF_6 or $NaBPh_4$ to this air sensitive green solution.

$\underline{K_4[Mo_2Cl_8]/cyclam}$

$K_4[Mo_2Cl_8]$ (0.200 g, 3.15 x 10^{-4}mol) and cyclam (0.150 g, 7.5 x 10^{-4}mol) reacted in refluxing methanol (20 ml) for 1 hour to give an intense blue, highly air sensitive solution (λ_{max} = 598 nm). The KCl byproduct was removed by filtration and the product could be obtained by addition of diethyl ether. Addition of $NaBPh_4$ or NH_4PF_6 to fresh methanol solutions also gave blue solids. Recrystallisation of these proved impossible as decomposition always resulted. Infra-red spectrum: ν_{N-H} = 3200 cm^{-1}. Mass spectrum (f.a.b.) M^+ = 669, 633 ($[Mo_2(cyclam)_2]Cl_2^+$ = 666 (^{98}Mo) $[Mo_2(cyclam)_2]Cl^+$ = 631).

$\underline{[Ru_2(O_2CMe)_4Cl]/cyclam}$

$[Ru_2(O_2CMe)_4Cl]$ (0.200 g, 4.22 x 10^{-4}mol) and cyclam (0.180 g, 9.0 x 10^{-4}mol) were refluxed in THF (30 ml) for two hours to give a yellow air sensitive solid. Filtration of the supernatant and addition of methanol or dichloromethane to this solid resulted in the formation of a highly air sensitive yellow solution (λ_{max} = 400 nm CH_2Cl_2).

Since rapid decomposition of these solutions occurred even under Schlenk line conditions counter ions such as PF_6^-, BPh_4^- or ClO_4^- had to be added rapidly. The yellow salts obtained showed a higher degree of stability and could be stored indefinitely under nitrogen. Since all attempts to recrystallise these solids led to decomposition accurate microanalytical data were not obtainable. Infra-red spectrum (PF_6^- salt) ν_{N-H} = 3190 cm^{-1}, ν_{CO_2}(asym) = 1560 cm^{-1}, ν_{CO_2}(sym)? = 1440-1400 cm^{-1}.

[$Os_2(O_2CR)_4Cl_2$] (R = Me, Et, ^nPr)/cyclam

[$Os_2(O_2CMe)_4Cl_2$] (0.100 g, 1.4 x 10^{-4}mol) and cyclam (0.60 g, 3 x 10^{-4}mol) were reacted in dichloromethane (20 ml) for *ca.* 8 hrs at room temperature to give an intensely purple solution (λ_{max} = 536 nm, $\varepsilon \sim 5 \times 10^3$ $M^{-1}cm^{-1}$). Addition of diethyl ether precipitated the product which could be recrystallised from a dichloromethane/diethyl ether solution: Elemental analysis: Found C=30.4; H=5.98; N=11.67%. Calculated for [Os(cyclam)(O_2CMe)]Cl: C=29.7; H=5.61; N=11.55%. Infra-red spectrum: ν_{N-H} = 3250 cm^{-1}, ν_{CO_2}(asym) 1570 cm^{-1}, ν_{CO_2}(sym?) 1440 cm^{-1}. ^1H n.m.r. spectrum ($CDCl_3$ 200MHz) δ_H = 0.91 (3H s CH_3CO_2?) 1.88 (4H quintet β CH_2 (cyclam)) 2.97 (8H s α' CH_2 (cyclam)) 3.06 (8H t α CH_2 (cyclam)). Mass spectrum (f.a.b.), M^+ = 450, 448, [$^{192\ 190}$Os(cyclam)(O_2CMe)]$^+$ = 451, 449.

Aqueous solutions of this initial product (λ_{max} = 406 nm) gave purple solids analysing fairly well for [Os(cyclam)(O_2CMe)](BPh_4) on addition of $NaBPh_4$.

$[Os_2(O_2CEt)_4Cl_2]$ and $[Os_2(O_2C^nPr)_4]$ reacted with cyclam in dichloromethane under the same conditions. as $[Os_2(O_2CMe)_4Cl_2]$ to give similar but distinct purple air sensitive species.

<u>$[Mo(CO)_4(H_2L')]$ H_2L' = 5,7,12,14-tetramethyl dibenzo[b,i]-1,4,8,11-tetraazacyclotetra-2,4,6,9,11,14-hexaene</u>

This complex was synthesised via the literature procedure.[248] $Mo(CO)_6$ (1 g, 3.8×10^{-3}mol) and H_2L (1.4 g, 4.1×10^{-3}mol) were refluxed under nitrogen for four hours at 105°C in a diglyme/petrol ether (100-120°) mixture (v:v = 10:1, 120 ml). Cooling the solution gave yellow tabular crystals suitable for X-ray diffraction Yield 50%. Elemental analysis: Found C=56.3; H=4.34; N=10.07%. Calculated for $[Mo(CO)_4(C_{22}H_{24}N_4)]$ C=56.5; H=4.38; N=10.14%. Infra-red spectrum was in accord with literature values. ^{1}H n.m.r. spectrum (CD_3Cl 80MHz) δ_H = 1.91 (6H s CH_3), 2.03 (6H s CH_3), 3.87 (2H s CH_2), 4.78 (1H s CH), 7.15 (8H m CH), 12.74 (1H br s NH). The ^{1}H n.m.r. spectrum differs from the reported spectrum in the literature ($(CD_3)_2O$ 100MHz) in which the methylene signal is clearly an AB resonance δ_H = 4.19, 3.59, J = 13.5Hz.[248]

The analagous tungsten complex could be obtained in a similar manner to the molybdenum complex. Elemental analysis: Found C=49.08; H=3.80; N=8.70%. Calculated for $[W(CO)_4(C_{22}H_{24}N_4)]$ C=48.77; H=3.78; N=8.75%. Infra-red spectrum was in accord with literature values.[248]

^{1}H n.m.r. spectrum ($CDCl_3$ 80MHz) δ_H = 1.94 (6H s CH_3), 2.04 (6H s CH_3) 3.89 (2H AB (J_{HH} = 22Hz) CH_2) 4.79 (1H s CH), 7.15 (8H m CH), 12.74 (1H br s NH). On standing in chloroform both $[Mo(CO)_4(H_2L')]$ and $[W(CO)_4(H_2L')]$ decompose to give species containing the 2,4-dimethyl-diazapenium ion.

References

1. D.K. Cabbiness and D.W. Margerum, J.Am.Chem.Soc., 91, 6540 (1969).
2. J.F. Endicott and B. Durham in 'Co-ordination Chemistry of Macrocyclic Compounds' Ed. G.A. Melson, Plenum New York, 1979, pp.408-415, 442-5 and references within.
3. K.M. Smith, 'Porphyrins and Metalloporphyrins' Amsterdam, 1976.
4. J.M. Rifkind in 'Inorganic Biochemistry', Ed. G.L. Eichhorn, Elsevier, Amsterdam, Ch . 25, 'Hemoglobin and Myoglobin', pp.832-902.
5. H.A. Harbury and R.H.L. Marks in 'Inorganic Biochemistry', Chp.26, 'Cytochromes b and c', pp.902-955.
6. (a) H.A.O.Hill in 'Inorganic Biochemistry', Ch.30, 'Corrinoids', pp.1067-1136.
   (b) D.G. Brown 'The Chemistry of Vitamin B_{12} and related Inorganic Systems', Prog.Inorg.Chem., 18, 177 (1973).
7. J.J. Katz in 'Inorganic Biochemistry', Ch . 29, 'Chlorophyll', pp.1022-1066.
8. E. Breslow in 'Inorganic Biochemistry', Ch.7, 'Metal Protein Complexes', pp.227-252.
9. V.L. Goedken in 'Co-ordination Chemistry of Macrocyclic Compounds', Ed. G.A. Melson, Ch. 10, 'Natural Product Model Systems', pp.603-654 and references within.
10. J.F. Endicott and B. Durham in 'Co-ordination Chemistry of Macrocyclic Compounds', pp.405-408 and references within.

11. (a) J.F. Endicott and B. Durham in 'Co-ordination Chemistry of Macrocyclic Compounds', Ch.6, 'Chemical Reactivity in Constrained Systems', pp.405-460 and references within.
(b) C.-K. Poon, Co-ord.Chem.Rev., 10, 1 (1973).

12. L.J. Boucher in 'Co-ordination Chemistry of Macrocyclic Compounds', Ch.8, 'Co-ordination Chemistry of Porphyrins', pp.517-536.

13. L.J. Boucher in 'Co-ordination Chemistry of Macrocyclic Compounds', Ch.7, 'Metal Complexes of Phthalocyanines', pp.461-516.

14. (a) C.K. Poon, T.C. Lau, C.L. Wong and Y.P. Kan, J.Chem. Soc.,Chem.Commun., 1641 (1983) and references within.
(b) B. Bosnich, C.K. Poon and M.L. Tobe, Inorg.Chem., 4, 1102 (1965).

15. N.F. Curtis, J.Chem.Soc., 4409 (1060).

16. D.K. Cabbiness and D.W. Margerum, J.Am.Chem.Soc., 92, 2151 (1970).

17. T.E. Jones, L.L. Zimmer, L.L. Diaddario, D.B. Rorabacher and L.A. Ochrymowycz, J.Am.Chem.Soc., 97, 7163 (1985).

18. D.H. Busch, K. Farmery, V. Goedken, V. Katovic, A.C. Melnyk, C.R. Sperati and N. Tokel, Advan.Chem. Ser., 100, 44 (1971).

19. F.P. Hinz and D.W. Margerum, Inorg.Chem., 13, 2941 (1974).

20. J.D. Lamb, R.M. Izatt, J.J. Christiansen and D.J. Eatough, in 'Co-ordination Chemistry of Macrocyclic Compounds', pp.166-169 and references within.

21. C.F. Bell, 'Principles and Applications of Metal Chelation', Oxford University Press, 1977.

22. R.M. Clay, Personal communication.

23. Y. Hung, L.Y. Martin, S.C. Jackels, A.M. Tait and D.H. Busch, J.Am.Chem.Soc., 99, 4029 (1977).

24. B.B. Wayland and H.W. Bosch, J.Chem.Soc.,Chem.Commun., 900 (1986).

25. (a) D. Pletcher and D.J. Pearce, J.Electroanal.Chem., 197, 317 (1986).

(b) J.P. Sauvage, M. Beley, J.P. Collin and R. Ruppert, J.Chem.Soc.,Chem.Commun., 1315 (1984).

(c) J.P. Sauvage, M. Beley, J.P. Collin and R. Ruppert, J.Am.Chem.Soc., 108, 7461 (1986).

(d) D. Fischer and P. Eisenberg, J.Am.Chem.Soc., 102, 2361 (1980).

26. (a) J.P. Collmann and K. Kim, J.Am.Chem.Soc., 108, 7847 (1986) and references within.

(b) N. Herron, M.Y. Charan and D.H. Busch, J.Chem.Soc., Dalton Trans., 1491 (1984).

(c) J.P. Collmann, R.R. Gagne, T.R. Halbert, J.C. Marchon and C.A. Reed, J.Am.Chem.Soc., 95, 7868 (1973).

27. B.B. Wayland and B.A. Woods, J.Chem.Soc.,Chem.Commun., 700 (1981). Also see ref.24.

28. (a) R.R. Durrand, C.S. Bencosme, J.P. Collmann and F.C. Anson, J.Am.Chem.Soc., 105, 2710 (1983).

(b) J.P. Collmann, M. Marracco, P. Denisevich, C. Kovel and F.C. Anson , J.Electroanal.Chem., 101, 117 (1979).

29. J.S. Alper and L.J. Zompa, J.Inorg.Nucl.Chem., 42, 1693 (1980).

30. R.S. Glass, G.S. Wilson and W.N. Setzer, J.Am.Chem. Soc., 102, 5068 (1980).

31. K. Wieghardt, H.-J. Kuppers and J. Weiss, Inorg. Chem., 24, 3067 (1985).

32. P.M. Collmann, H.C. Freeman, J.M. Guss, M. Murata, V.A. Norris, J.A.M. Ramshaw and M.P. Venkatappa, Nature (London), 272, 319 (1978).

33. F.A. Cotton and R.A. Watton 'Multiple Bonds between Metal Atoms', Wiley Interscience, New York, 1982, p.91.

34. H. Koyama and T. Yoshino, Bull.Chem.Soc.Jpn., 45, 481 (1972).

35. R. Yang and T. Zompa, J.Inorg.Chem., 15, 1499 (1976).

36. L. Zompa, J.Inorg.Chem., 17, 2531 (1978).

37. L. Zompa and T.N. Margulis, Inorg.Chim.Acta, 28 L 157 (1978).

38. K. Wieghardt, W. Schmidt, W. Herrmann and H.J. Kuppers, Inorg.Chem., 22, 2953 (1983).

39. A.D. Beveridge, A.J. Lavery, M.D. Walkinshaw and M. Schroder, J.Chem.Soc.,Dalton Trans., 373 (1987).

40. J.C.A. Boeyens, A.G.S. Forbes, R.D. Hancock and K. Wieghardt, Inorg.Chem., 24, 2926 (1985).

41. H.J. Küppers, A. Neves, C. Pomp, D. Ventur, K. Wieghardt, B. Nuter and J. Weiss, Inorg.Chem., 25, 2400 (1986).

42. D.F. Evans, J.Chem.Soc., 2003 (1959).

43. K. Wieghardt, W. Walz, B. Nuber, J. Weiss, A. Ozarowski, H. Stratemeier and D. Reinen, Inorg.Chem., 25, 1650 (1986).

44. P. Chaudhuri, K. Oder, K. Wieghardt, J. Weiss, J. Reedyk, W. Hinricks, J. Wood, A. Ozerowski, H. Stratemeier and D. Reinen, Inorg.Chem., 25, 2951 (1986).

45. A. McAuley, P.R. Newman and O. Olubuyide, Inorg. Chem., 23, 1938 (1984).

46. K. Wieghardt, W. Schmidt, B. Nuber, E. Prikner and J. Weiss, Chem.Ber., 113, 36 (1980).

47. K. Wieghardt, W. Herrmann, M. Koppen, I. Jibril and G. Huttner, Z.Naturforsch B.39, 1335 (1984).

48. K. Wieghardt and M. Keppen, J.Chem.Soc.,Dalton Trans., 1869 (1983).

49. M. Nonoyama, Inorg.Chim.Acta, 20, 53 (1976).

50. M.S. Okamoto and E.K. Barefield, Inorg.Chim.Acta, 17, 91 (1976).

51. K. Wieghardt, M. Hahn, W. Swiridoff and J. Weiss, Inorg.Chem., 23, 94 (1984).

52. M.N. Bell and M. Schroder, Pure and Applied Chemistry, 1987, in press.

53. M. Nonoyama, J.Inorg.Nucl.Chem., 39, 550 (1977).

54. K. Wieghardt, M. Koppen, B. Nuber and J. Weiss, J.Chem.Soc.,Chem.Commun., 1530 (1986).

55. K. Wieghardt, L. Bossak, K. Volckmar, W. Swaridoff and J. Weiss, Inorg.Chem., 1984, 23 (1987).

56. K. Wieghardt, P. Chaudhuri, B. Nuber and J. Weiss, Inorg.Chem., 21, 3086 (1982).

57. K. Wieghardt, U. Bossek, L. Zsionyai, G. Huttner, G. Bloudin, J.-J. Girerd and F. Babonneau, J.Chem.Soc., Chem.Commun., 651 (1987).

58. K. Wieghardt, I. Tolksdorf and W. Herrmann, Inorg. Chem., 24, 1230 (1985).

59. K. Wieghardt, W. Schmidt, B. Nuber and J. Weiss, J.Chem.Ber., 112, 2220 (1979).

60. M. Hahn and K. Wieghardt, Inorg.Chem., 23, 3977 (1984).

61. P. Chaudhuri, M. Guttmann, D. Ventur, K. Wieghardt, B. Nuber and J. Weiss, J.Chem.Soc.,Chem.Commun., 1618 (1985).

62. P. Chaudhuri, K. Wieghardt, B. Nuber and J. Weiss, J.Chem.Soc.,Chem.Commun., 265 (1985).

63. S.E. Murray and F.R. Hartley, Chem.Rev., 81, 365 (1981).

64. W.N. Setzer, C.A. Ogle, G.S. Wilson and R.S. Glass, Inorg.Chem., 22, 266 (1983).

65. W. Rosen and D.H. Busch, J.Am.Chem.Soc., 91, 4694 (1969).

66. W. Rosen and D.H. Busch, Inorg.Chem., 9, 263 (1970).

67. D. Sellmann and L. Zapf, Angew.Chem., 96, 789 (1984); Angew.Chem.Int.Ed.Engl., 23, 807 (1984).

68. G.S. Wilson, D.D. Swanson and R.S. Glass, Inorg.Chem., 25, 3827 (1986).

69. J.-A.R. Hartmann, E.J. Hintsa and S.R. Cooper, J.Am. Chem.Soc., 108, 1208 (1986).

70. J.-A.R.Hartmann and S.R. Cooper, J.Am.Chem.Soc., 108, 1202 (1986).

71. K. Wieghardt, U. Bossek, J. Bonvoisin, P. Beauvillain, J.J. Girerd, B. Nuber, J. Weiss and J. Heinze, Angew. Chem., 98, 1026 (1986); Angew.Chem.Int.Ed.Engl., 25, 1030 (1986).

72. T. Arishima, K. Hamada and S. Takomoto, Nippon Kogaku Khaishi, 1119 (1973).

73. M. Takahashi and S. Takamoto, Bull.Chem.Soc.Jpn., 50, 3413 (1977).

74. M.J. van der Merwe, J.C.A. Boeyens and R.D. Hancock, Inorg.Chem., 24, 1208 (1985).

75. M.J. van der Merwe, J.C.A. Boeyens and R.D. Hancock, Inorg.Chem., 22, 3489 (1983).

76. K. Wieghardt, U. Bossek, P. Chaudhuri, W. Herrmann, B.C. Menke and J. Weiss, J.Inorg.Chem., 21, 3408 (1982).

77. K. Wieghardt, U. Bossek, M. Guttmann and J. Weiss, Z. Naturforsch B, Anorg.Chem.Org.Chem., 38B, 81 (1983).

78. B.A. Sayer, J.P. Michael and R.D. Hancock, Inorg.Chim. Acta, 77, L63 (1983).

79. L.R. Gahan, G.A. Lawrence and A.M. Sargeson, Aust.J. Chem., 35, 1119 (1982).

80. A. Hammershoi and A.M. Sargeson, Inorg.Chem., 22, 3554 (1983).

81. M.I. Kabachnik, T.Ya.Medred, Yu.M. Polikarpov, B.K. Shcherbakov, F.I. Bel'skii, E.I. Matrosov and M. Pasechnik, Izv.Akad.Nauk.SSSF Ser.Khim., 835 (1984).

82. M.Yu. Polikarpov, B.K. Shcherbakov, F.I. Bel'skii, T. Ya. Medred and M.I. Kabachnik, Izv.Nauk.SSSR Ser. Khim., 1669 (1982).

83. M.A. Konstantinovskaya, E. Sinyavskyaa, K.B. Shcherbakov, M. Yu Polikarpov, T. Ya Medred and M.I. Kabachnik, Zh.Neorg.Khim., 30, 2571 (1985).

84. K.B. Yatsimirskii, M.I. Kabachnik, E.I. Sinyavskaya, T. Ya Medred, M. Yu Polikarpov and B.K. Shcherbakov, Zh.Neorg.Khim., 29, 884 (1984).

85. K.B. Yatsimirshii, E.I. Sinyavskaya, L.V. Tsimbal, T. Ya Medred, B.K. Shcherbakov, Ya M. Polikarpov and M.I. Katachnik, Zh.Neorg.Khim., 29, 888 (1984).

86. K. Wieghardt, E. Schoffmann, B. Nuber and J. Weiss, Inorg.Chem., 25, 4877 (1986).

87. K. Wieghardt, M.K. Boymann, B. Nuber and J. Weiss, Inorg.Chem., 25, 1654 (1986).

88. M.N. Bell, unpublished work.

89. L.J. Zompa, Inorg.Chem., 17, 2531 (1978).

90. L. Fabbrizzi and D.M. Prosperpio, Abstract A44 XI International Symposium on Macrocyclic Chemistry, Florence 1986.

91. G.A. Melson and D.H. Busch, J.Am.Chem.Soc., 87, 1706 (1965).

92. L.T. Taylor and D.H. Busch, Inorg.Chem., 8, 1366 (1969).

93. S.C. Cummings and D.H. Busch, J.Am.Chem.Soc., 92, 1924 (1970).

94. F.A. Cotton and C.B. Harris, Inorg.Chem., 4, 330 (1965).

95. D. Lawton and R. Mason, J.Am.Chem.Soc., 87, 921 (1965).

96. F.A. Cotton and R.A. Walton 'Multiple Bonds between Metal Atoms', Wiley Interscience, New York, 1982.

97. F.A. Cotton, N.F. Curtis, C.B. Harris, B.F.G. Johnson, S.J. Lippard, J.T. Maque, W.R. Robinson and J.S. Wood, Science, 145, 1305 (1964).

98. F.A. Cotton and R.A. Walton, 'Multiple Bonds between Metal Atoms', Wiley Interscience, New York, 1982, pp.17-22.

99. A. Bino, F.A. Cotton and T.R. Felthouse, Inorg.Chem., 18, 9 (1979).

100. T.R. Felthouse, Prog.Inorg.Chem., 29, 73 (1982).

101. T.A. Stephenson and G. Wilkinson, J.Inorg.Nucl.Chem., 28, 2285 (1966).

102. J.P. Collmann, C.E. Barnes, T.J. Collins and P.J. Brothers, J.Am.Chem.Soc., 103, 7030 (1981).

103. J.P. Collmann, C.E. Barnes, P.N. Swepston and J.A. Ibers, J.Am.Chem.Soc., 106, 3500 (1984).

104. B.B. Wayland and A.R. Newman, Inorg.Chem., 20, 3093 (1981).

105. J.P. Collmann, P.J. Brothers, L. McElwee-White, E. Rose and L.J. Wright, J.Am.Chem.Soc., 107, 4570 (1985).

106. C.H. Yang, S.J. Dzugin and V.L. Gœdken, J.Chem.Soc., Chem.Commun., 1313 (1986).

107. K.J. Del Rossi and B.B. Wayland, J.Chem.Soc.,Chem. Commun., 1653 (1986).

108. J.E. Anderson, C.L. Yao and K.M. Kadish, Inorg.Chem., 25, 718 (1986).

109. L.F. Warren and V.L. Goedken, J.Chem.Soc.,Chem.Commun., 909 (1978).

110. G.C. Gordon, L.F. Warren, D.W. Detlaven and V.L. Goedken, Private communication.

111. N.W. Alcock, N. Herron and P. Moore, J.Chem.Soc.,Chem. Commun., 886 (1986).

112. R.E. De Simone and M.D. Glick, J.Am.Chem.Soc., 97, 942 (1975).

113. M. Bell, unpublished work.

114. M.N. Bell, A.J. Blake, M. Schroder and T.A. Stephenson, J.Chem.Soc.,Chem.Commun., 471 (1986).

115. R.E. De Simone and M.D. Glick, J.Am.Chem.Soc., 98, 762 (1976).

116. T. Yoshida, T. Ueda, T. Adachi, K. Yamamoto and T. Huguchi, J.Chem.Soc.,Chem.Commun., 1137 (1985).

117. F.R. Hartley, 'The Chemistry of Palladium and Platinum', Applied Science, 1973.

118. A.D. Westland, J.Chem.Soc., 3030 (1965).

119. (a) J.S. Wood, Prog.Inorg.Chem., 16, 227 (1972);
(b) J.K. Burdett, Inorg.Chem., 16, 3013 (1977);
(c) R. Hoffmann, Inorg.Chem., 14, 365 (1975).

120. R.D. Cramer, E.L. Jenner, R.V. Linsey and U.G. Stalberg, J.Am.Chem.Soc., 85, 1691 (1963).

121. M.S. Holt, J.H. Nelson and N.W. Alcock, Inorg.Chem., 25, 2288 (1986).

122. J.P. Fackler, J.A. Fetchin and W.C. Seidel, J.Am.Chem. Soc., 91, 2707 (1969).

123. B.A. Goodman and J.B. Raynor, 'Electron Spin Resonance of Transition Metal Complexes', Adv.Inorg. and Radiochem., 13, 135 (1970).

124. A.H. Maki, N. Edelstein, A. Davison and R.H. Holm, J.Am.Chem.Soc., 86, 4580 (1964).

125. K. Wieghardt, private communication.

126. (a) J.A. McCleverty, Prog.Inorg.Chem., 10, 49 (1968);
(b) R. Kirmse and W. Dietzsch, J.Inorg.Nucl.Chem., 39, 1157 (1977);
(c) R. Kirmse, J. Stack, W. Dietzsch, G. Steinecke and F. Hoyer, Inorg.Chem., 19, 2679 (1980).

127. (a) A. Davison, N. Edelstein, R.H. Holm and A.H. Maki, Inorg.Chem., 2, 1227 (1963).
(b) G.A. Bowmaker, P.D.W. Boyd and G.K. Campbell, Inorg.Chem., 22, 1208 (1983).

(c) A.Y. Girgis, Y.S. Sohn and A.L. Balch, Inorg. Chem., 14, 2327 (1975).

128. G.S. Muraveiskaya, M. Lavin and V.F. Sorokina, Zh.Neorg.Khim., 13, 1466 (1968).

129. R.J.H. Clark and M. Murata, J.Chem.Soc.,Dalton Trans., 524 (1982).

130. H. Endres, H.J. Keller, H. van der Sand and V. Doug, Z.Naturforsch, 33b, 843 (1978).

131. W.L. Walz, J. Lilie, R.T. Walters and R.J. Woods, Inorg.Chem., 19, 3284 (1980).

132. H.M. Kahn, W.L. Walz, J. Lilie and R.J. Woods, Inorg. Chem., 21, 1489 (1982).

133. H.A. Boucher, G.A. Lawrence, P.A. Lay, A.M. Sargeson, A.M. Bond, D.F. Sangster and J.C. Sullivan, J.Am.Chem. Soc., 105, 4652 (1983).

134. R. Uscn, J. Fornies, M. Tomas, B. Menjou, K. Sunkel and R. Bau, J.Chem.Soc.,Chem.Commun., 751 (1984).

135. M. Green, J.A.K. Howard, A. Laguna, L.E. Smart, J.L. Spencer and F.G.A. Stone, J.Chem.Soc.,Dalton Trans., 278 (1977).

136. A. Modinos and B. Woodward, J.Chem.Soc.,Dalton Trans., 1516 (1975).

137. A.J. Blake, R.O. Gould and A.J. Lavery, Angew.Chem., 98, 282 (1986); Angew.Chem.Int.Ed.Engl., 25, 274 (1986).

138. J.-A.R. Hartmann, R.E. Wolf, Jnr., B.M. Foxman and S.R. Cooper, J.Am.Chem.Soc., 105, 131 (1983).

139. S.E. Livingstone in 'Comprehensive Inorganic Chemistry', Vol.3, Pergamon, 1973, pp.1335-8.

140. S.E. Livingstone in 'Comprehensive Inorganic Chemistry', Vol.3, p.1329.

141. S.E. Livingstone, J.Proc.Roy.Soc.NS Wales, 85, 51 (1951); 86, 32 (1952).

142. (a) K. Broadley, G.A. Lane, N.G. Connelly and W.E. Gieger, J.Am.Chem.Soc., 105, 2486 (1983); (b) F.A. Cotton and G. Wilkinson 'Advanced Inorganic Chemistry', 4th Ed., p.950.

143. L.R. Louis, D. Pellisard and R. Weiss, Acta Crystallogr., B 30, 1889 (1974).

144. C. Senoff, Inorg.Chem., 17, 2320 (1978).

145. Z. Taira and S. Yamazaki, Bull.Chem.Soc.Jpn., 59, 649 (1986).

146. J.W. Collier, F.G. Mann, D.G. Watson and H.R. Watson, J.Chem.Soc., 1803 (1964).

147. R.D. Feltham and R.G. Hayter, J.Chem.Soc., 4587 (1964).

148. T.J. Giordano, W.M. Butler and P.J. Rasmusson, Inorg.Chem., 17, 1917 (1978).

149. K. Wieghardt, H.J. Kuppers, E. Raabe and C. Kruger, Angew.Chem., 98, 1136 (1986); Angew.Chem.Int.Ed. Engl., 25, 12 (1986).

150. M.N. Bell, A.J. Blake, H.J. Kuppers, M. Schroder and K. Wieghardt, Angew.Chem., 99, 253 (1987); Angew. Chem.Int.Ed.Engl., 26, 250 (1987).

151. S. Cockle, H.A.O. Hill, S. Ridsdale and R.J.P. Williams, J.Chem.Soc.,Dalton Trans., 2 (1972).

152. (a) J.D. Woolins and P.F. Kelly 'The Preparation and Properties of Compounds Containing Pt(III)', Co-ord. Chem.Rev., 115 (1985), pp.118-129.

(b) T.V. O'Halloran and S.J. Lippard, 'The Chemistry of Platinum in the +3 Oxidation State', Isr.J.Chem., 25 (1985), pp.132-137.

153. A. Tressaud, S. Khairoun, J.-M.Dance, J. Grannec, G. Demazeau and P. Hagenmuller, C.R.Acad.Sci.,Paris, Serie II, 295, 183 (1982).

154. R. Kirmse and W. Dietzsch, J.Inorg.Nucl.Chem., 38, 255 (1976).

155. A.J. Blake, T.I. Hyde and M. Schroder, J.Chem.Soc., Chem.Commun., 431 (1987).

156. T.I. Hyde, unpublished work.

157. (a) J.R. Boehm and A.L. Balch, Inorg.Chem., 16, 778 (1977);

(b) D.J. Doonan, A.L. Balch, S.Z. Goldberg, R. Eisenberg and J.S. Miller, J.Am.Chem.Soc., 97, 1961 (1975).

158. R.G. Holloway, B.R. Penfold, R. Cotton and M.McCormick, J.Chem.Soc.,Chem.Commun., 485 (1976).

159. A. McAuley, unpublished work.

160. R.I. Haines and A. McAuley, Inorg.Chem., 19, 719 (1980).

161. C.J. Pedersen, Private communication.

162. R.E. Stenkamp, L.C. Sieker, L.H. Jensen and J.ders-Loehr, Nature (London), 291, 514 (1983).

163. P. Reichard and A. Ehrenberg, Science, 221, 514 (1983).

164. G.C. Dismukes and Y. Siderer, Proc.Natl.Acad.Sci.USA, 78, 274 (1981).

165. T.R. Felthouse, 'The Chemistry Structure and Metal-bonding in Compounds of Rhodium(II), Prog.Inorg.Chem., 29 (1982), pp.76-77.

166. S.E. Livingstone in 'Comprehensive Inorganic Chemistry' Vol.3, pp.1237-1244.

167. D.W.H.Rankin, Private communication.

168. F.G. Meers, J.A.M. de Jong and P.M.H. Beaumond, J.Inorg.Nucl.Chem., 35, 1915 (1973).

169. M.A. Bennett and P.A. Longstaff, J.Am.Chem.Soc., 91, 6266 (1969).

170. E. Billig, S.I. Shupack, J.H. Waters, R. Williams and H.B. Gray, J.Am.Chem.Soc., 86, 926 (1964).

171. P.S. Braterman, Struct.Bonding, 26, 1 (1976).

172. H. Gamsjäger and P. Beutler, J.Chem.Soc.,Dalton Trans., 1415 (1979).

173. G. Reid, unpublished work.

174. D.D. Perrin, D.R. Perrin and W.F.Arma, 'Purification of Laboratory Chemicals', 2nd Ed. Pergamon.

175. J.A. McCleverty and G. Wilkinson, Inorg.Synth., 8, 211 (1966).

176. R. Cramer, Inorg.Synth., 15, 14 (1974).

177. (a) J.R. Lancaster, Science, 216, 1324 (1982); (b) R. Cammack, D. Patil, R. Aguirre and E.Hatchikian, FEBS Lett., 142, 289 (1982).

178. S.A. Jacobs and D.W. Margerum, Inorg.Chem., 23, 1195 (1984) and literature within.

179. H.C. Freeman in 'Co-ordination Chemistry', Vol.21, Ed. J.P. Laurent, Pergamon, Oxford, 1981, p.29.

180. L. Rydel and J.O. Lundgren, Nature (London), 261, 344 (1976).

181. E.T. Adman, R.E. Stenkamp, L.C. Sieker and J.H. Jensen, J.Mol.Biol., 123, 35 (1978).

182. Copper co-ordination Chemistry 'Biochemical and Inorganic Perspectives', K.D. Karlin and J. Zubieta, Adenine Press, New York, 1983.

183. R.O. Gould, A.J. Lavery and M. Schroder, J.Chem.Soc., Chem.Commun., 1492 (1985).

184. J.D. Sinclair-Day, M.J. Sisley, A.G. Sykes, G.C. King and P.E. Wright, J.Chem.Soc.,Chem.Commun., 505 (1985).

185. T.E. Jones, L.A. Ochrymowycz, D.B. Rorabacher, J.Am.Chem.Soc., 97, 7485 (1975).

186. V.B. Pett, L.L. Diaddario, Jnr., E.R. Dockal, P.W. Corfield, C. Ceccarelli, M.D. Glick, L.A. Ochrymowycz and D.B. Rorabacher, Inorg.Chem., 22, 3661 (1983).

187. 'Monovalent, Trivalent and Tetravalent Nickel' A. Chakravarty and K. Nag, Co-ord.Chem.Rev., 33, (1980), pp.114-121 and references within.

188. 'Synthesis and Reactions of Nickel(III) Complexes', R.I. Haines and A. McAuley, Co-ord.Chem.Rev., 39 (1981) pp.77-119.

189. D.J. Szalda, D.H. Macartney and N. Sutin, Inorg.Chem., 23, 3473 (1984).

190. T. Ito, M. Sugimato, K. Tonumi and H. Ito, Chem. Lett., 1477 (1981).

191. T.I. Hyde 'Studies on Transition Metal Tetraaza Macrocyclic Compounds', Ph.D.Thesis, University of Edinburgh, 1987, pp.134-140.

192. P.V. Lovecchio, E.S. Gore and D.H. Busch, J.Am.Chem. Soc., 96, 3109 (1974).

193. (a) J. Lewis and M. Schroder, J.Chem.Soc.,Dalton Trans., 1085 (1982);
(b) R.R. Gagne, D.M. Ingle and G.C. Lisensky, Inorg. Chem., 20, 1991 (1981).

194. I.I. Chernyaev, E.V. Shenderetskaya and A.A. Koryagina, Zh.Neorg.Khim., 5, 1163 (1960); Russ.J.Inorg.Chem., 5, 559 (1960).

195. S.A. Johnson, H.R. Hunt and H.M. Neumann, Inorg.Chem., 2, 900 (1963).

196. J.N. Van NieKerk and F.R.L. Schoening, Acta Cryst., 6, 227 (1953).

197. G.G. Cristoph and Y.B. Koh, Inorg.Chem., 18, 1122 (1979).

198. T.A. Mal'Kova, V.N. Shafrauskii and Yu.Ya.Kharitonov, Ko.ord.Khim., 3, 1747 (1977); Sov.J.Co-ord.Chem., 3, 1371 (1977).

199. V.N. Shafranskii and T.A. Mal'Kova, Zh.Obshch.Khim., 46, 1197 (1976); J.Gen.Chem.USSR, 46, 1181 (1976).

200. T.A. Stephenson, S.M. Morehouse, A.R. Powell, J.P. Heffer and G. Wilkinson, J.Chem.Soc., 3632 (1965).

201. L. Kitchens and J.L. Bear, J.Inorg.Nucl.Chem., 1969, 31, 2415.

202. Y.B. Koh and G.G. Cristoph, Inorg.Chem., 17, 2590 (1978).

203. L. Dubicki and R.L. Martin, Inorg.Chem., 9, 673 (1970).

204. Y.B. Koh, Ph.D. Thesis, The Ohio State University, 1979.

205. R.S. Drago, S.P. Tanner, R.M. Rickman and J.R. Long, J.Am.Chem.Soc., 101, 2897 (1979).

206. K. Das, K.M. Kadish and J.L. Bear, Inorg.Chem., 17, 930 (1978).

207. T.A. Mal'Kova and V.N. Shafrauskii, Zh.Obshch.Khim., 45, 631 (1975); J.Gen.Chem.USSR, 45, 618 (1975).

208. K. Das, E.L. Simmons and J.L. Bear, Inorg.Chem., 16, 1268 (1977).

209. L.A. Nazarova and A.G. Maiorova, Zh.Neorg.Khim., 21, 1070 (1976); Russ.J.Inorg.Chem., 21, 583 (1976).

210. T.A. Vateva and V.N. Shafrauskii, Zh.Obshch.Khim., 49, 488 (1979); J.Gen.Chem.USSR, 49, 428 (1979).

211. V.N. Shafrauskii, T.A. Mal'Kova and Yu.Ya.Kharitokov, J.Struct.Chem., 16, 195 (1975).

212. G. Preumakakis and N. Hadjiliadia, J.Chem.Soc., Dalton Trans., 596 (1979).

213. G. Winkhaus and P. Zieglar, Z.anorg.allg.Chem., 350, 51 (1967).

214. K. Aoki and H. Yamazaki, J.Chem.Soc.,Chem.Commun., 186 (1980).

215. R.S. Drago, J.R. Long and R. Cosmano, Inorg.Chem., 20, 2920 (1981).

216. F.A. Cotton, D.G. DeBeer, M.D. La Prade, J.R. Pipal and D.A. Ucko, J.Am.Chem.Soc., 92, 2926 (1970).

217. G.G. Cristoph and Y.B. Koh, J.Am.Chem.Soc., 101, 1422 (1979).

218. T. Kawamura, K. Fukamachi, T. Sowa, S. Hayashida and T. Yonezawa, J.Am.Chem.Soc., 103, 364 (1981).

219. G.G. Cristoph, J. Halpern, G.P. Khare, Y.B. Koh and C. Romanowski, Inorg.Chem., 20, 3029 (1981).

220. F.A. Cotton, T.R. Felthouse and S. Klein, Inorg. Chem., 20, 3037 (1981).

221. F.A. Cotton and T.R. Felthouse, Inorg.Chem., 19, 2347 (1980).

222. A. Holder, unpublished work.

223. L.A. Nazarova, I.I. Chernyaev and A. Morozova, Zh.Neorg.Khim., 10, 539 (1965); Russ.J.Inorg.Chem., 11, 1387 (1966).

224. F.A. Cotton and T.R. Felthouse, Inorg.Chem., 20, 600 (1981).

225. T.P. Zhu, M.Q. Ahsan, T. Malinski, K.M. Kadish and J.L. Bear, Inorg.Chem., 23, 1 (1984).

226. S.I. Ginzburg, N.N. Chalisova and O.N. Evstaf'eva, Zh.Neorg.Khim., 11, 742 (1966); Russ.J.Inorg.Chem., 11, 404 (1966).

227. F.R. Cotton and T.R. Felthouse, Inorg.Chem., 19, 320 (1980).

228. I.B. Baranovskii, S.S. Abdullaev and R.N. Shchelokov, Zh.Neorg.Khim., 24, 3149 (1979); Russ.J.Inorg.Chem., 24, 1753 (1979).

229. F.A. Cotton and T.R. Felthouse, Inorg.Chem., 20, 584 (1981).

230. K.G. Caulton and F.A. Cotton, J.Am.Chem.Soc., 93, 1914 (1971).

231. S.M. Peng and V.L. Goedken, unpublished work.

232. P.H. Davis, K.L. White and R.L. Bedford, Inorg.Chem., 14, 1753 (1975).

233. R.N. Icke, B.B. Wisegarver and G.A. Alles in 'Organic Synthesis', Wiley, New York, 1955, Collected Volumes III, p.723.

234. A.B. Brignole and F.A. Cotton, Inorg.Synth., 13, 90 (1972).

235. F.A. Cotton and J.G. Norman, Jr., J.Co-ord.Chem., 1, 161 (1971).

236. J.V. Brenck and F.A. Cotton, Inorg.Chem., 8, 7 (1969).

237. J.V. Brenck, I. Leban and P. Segedin, Z.anorg.allg. Chem., 427, 85 (1976).

238. A.R. Bowen and H. Taube, Inorg.Chem., 13, 2245 (1974).

239. F.A. Cotton and T.R. Webb, Inorg.Chem., 15, 68 (1976).

240. A.R. Bowen and H. Taube, J.Am.Chem.Soc., 93, 3287 (1971).

241. S.A. Best, T.J. Smith and R.A. Walton, Inorg.Chem., 17, 99 (1978).

242. J. San Fillipo, Jnr., H.J. Sniodoch and R.L. Grayson, Inorg.Chem., 13, 2121 (1974).

243. A.J. Lindsay and G. Wilkinson, J.Chem.Soc.,Dalton Trans., 2321 (1985).

244. V.L. Goedken and J.A. Ladd, J.Chem.Soc.,Chem.Commun., 142 (1982).

245. F.A. Cotton and J.L. Thompson, Inorg.Chim.Acta, 44, L247 (1980).

246. P.A. Agaskar, F.A. Cotton, K.R. Dunbar, L.R. Falvello, S.M. Tetrick and R.A. Walton, Inorg.Chem., 23, 4567 (1984).

247. A. Bino, F.A. Cotton and P.E. Fenwick, 18, 3558 (1979).

248. L.G. Bell and J.C. Dabrowiak, J.Chem.Soc.,Chem. Commun., 512 (1975).

249. V.L. Goedken, J.J. Pluth, S.M. Peng and B.Burnsten, J.Am.Chem.Soc., 98, 8014 (1976).

250. M.C. Weiss, B.Burnsten, S.M. Peng and V.L. Goedken, J.Am.Chem.Soc., 98, 8021 (1976).

251. V.L. Goedken and J.A. Ladd, J.Chem.Soc., Chem.Commun., 142 (1982).

252. K.M. Kadish, L.A. Bottomley, D. Sheeper, M. Tsutsui and R.L. Bobsein, Inorg.Chim.Acta, 36, 219 (1979).

253. (a) J.V. Brencic and F.A. Cotton, Inorg.Chem., 9, 351 (1970);

(b) A.B. Brignole and F.A. Cotton, Inorg.Synth, 13, 90 (1972).

254. R.W. Mitchell, A. Spencer and G. Wilkinson, J.Chem.Soc., Dalton Trans., 846 (1973).

255. V.L. Goedken and M.C. Weiss, Inorganic Synthesis, 20, 115 (1980).

256. T. Behling, G. Wilkinson, T.A. Stephenson, D.A. Tocher and M.D. Walkinshaw, J.Chem.Soc.,Dalton Trans., 2109 (1983).

257. J.L. Barltrop, C.G. Richards, D.M. Russel and G. Ryback, J.Chem.Soc., 1132 (1959).

Abbreviations

BM	Bohr Magneton
^{n}Bu	normal butyl
Bz	benzyl
DBU	1,8 diazabicyclo[5.4.0]undec-7-ene
dmf	dimethylformamide
DMG^{-}	dimethylglyoximate
dmso	dimethyl sulphoxide
e.s.d.	estimated standard deviation
e.s.r.	electron spin resonance
Et	ethyl
f.a.b.	fast atom bombardment
Hz	Hertz
MHz	Mega Hertz
MNT^{2-}	maleonitriledithiolate
Me	methyl
MeCN	acetonitrile
M	molecular weight
NHE	normal hydrogen electrode
n.m.r.	nuclear magnetic resonance
Ph	phenyl
p.p.m.	parts per million
^{n}Pr	normal propyl
$TBAPF_6$	tetra-^{n}butyl ammonium hexafluorophosphate
THF	tetrahydrofuran
ttn	trithianonane

List of Courses Attended

'Aspects of Structural Chemistry' by Dr. C. Glidewell.

'Organometallic Chemistry' by Dr. M. Schroder.

'Current Topics in Inorganic Chemistry' by Dr. M. Schroder Dr. G.A. Heath, Dr. A.J. Welch and Professor E.A.V. Ebsworth.

'Modern Inorganic Chemistry' by Dr. S. Craddock and Professor E.A.V. Ebsworth.

'Nuclear Magnetic Resonance' by Dr. I.H. Sadler.

'Recent Developments in Electrochemistry' by Dr. G.A. Heath and Dr. H. Girault.

'Molecular Electronics' by Dr. R.W. Munn and Dr. J.O. Williams.

University of Strathclyde Inorganic Club Conferences 1984, 1985, 1986.

2nd International Platinum Metals Conference, Edinburgh 1984.

3rd European Symposium on Macrocyclic Compounds, Stirling 1984.